Petrology of the Morrison Formation in the Colorado Plateau Region

GEOLOGICAL SURVEY PROFESSIONAL PAPER 556

Prepared on behalf of the
U.S. Atomic Energy Commission

Petrology of the Morrison Formation in the Colorado Plateau Region

By ROBERT A. CADIGAN

GEOLOGICAL SURVEY PROFESSIONAL PAPER 556

Prepared on behalf of the
U.S. Atomic Energy Commission

Interpretation of regional compositional and textural trends in sandstone strata in a major uranium-ore-bearing formation which was deposited in a subsiding continental basin in Late Jurassic time

UNITED STATES GOVERNMENT PRINTING OFFICE, WASHINGTON : 1967

UNITED STATES DEPARTMENT OF THE INTERIOR

STEWART L. UDALL, *Secretary*

GEOLOGICAL SURVEY

William T. Pecora, *Director*

Library of Congress catalog-card No. GS 67-155

For sale by the Superintendent of Documents, U.S. Government Printing Office
Washington, D.C. 20402 - Price $1.25 (paper cover)

CONTENTS

ILLUSTRATIONS

TABLES

PETROLOGY OF THE MORRISON FORMATION IN THE COLORADO PLATEAU REGION

By Robert A. Cadigan

ABSTRACT

The sandstone strata of the Morrison Formation of Late Jurassic age in the Colorado Plateau region contain the major part of the uranium ore reserves in the United States. For this reason, an investigation of the stratigraphy and lithology of the Morrison Formation in this region was undertaken. This report covers the petrologic part of the investigation.

Stratigraphic relations of the Morrison Formation vary from locality to locality in the region of study. The Morrison in some parts of the region disconformably overlies various formations of Late Jurassic age, although the contacts between lithologically similar strata in other parts of the region appear to be conformable. The Morrison is generally conformably overlain by formations of Early Cretaceous age, but near the south and west borders of the region of study it is disconformably overlain by the Dakota Sandstone of Late Cretaceous age.

The Morrison Formation in the region of study is divided into four members, which differ in areal extent. Where the members overlap, in the Four Corners area, the layered sequence from bottom to top is Salt Wash Member, Recapture Member, Westwater Canyon Member, and Brushy Basin Member. The Salt Wash is present in the northern two-thirds of the region; the Recapture and Westwater Canyon are both present in the southern half of the region; and the Brushy Basin is present throughout the region except where it was removed by pre-Dakota erosion.

Previous investigators of the Rocky Mountains and Great Plains regions concluded that the Morrison Formation was deposited in a continental fluviatile environment in which drainage was generally to the east and north from mountainous sources to the west and south. Morrison strata in the Colorado Plateau were interpreted to be closer to source areas than the strata in the Rocky Mountains and Great Plains areas of Colorado. The sequence of major tectonic events which preceded and accompanied deposition of the Morrison sediments was interpreted to have affected much of the Western Interior of the United States. Previous petrographic work established the presence of volcanic material in Morrison strata, particularly in the finer grained upper part, and suggested regional variation in composition of the sandstones.

For this study, samples were collected from the strata of the Morrison Formation at 96 localities. Most of the rocks sampled were sandstone, but some were siltstone, claystone, mudstone, or limestone. Petrographic data were obtained from various groups of samples by grain-size analysis, thin-section modal analysis, mineral grain counts, mineral grain shape studies, and rock classification studies. Regional variation and trends in compositional and textural data were studied and tested through the use of maps, statistical procedures, and trend-surface analysis.

Rock types which make up the Morrison Formation in the Colorado Plateau region are classified according to a binary logic scheme, based on proportions of 5 major rock component groups which are subdivided into 19 mineral and mineral-aggregate groups. The major components are related to the five rock classification groups: chemical rocks, orthoquartzites, arkoses, graywackes, and tuffs. Assignment of the mineral groups is based partly on thin-section study of probable effects of diagenesis on the original sediments. Major diagenetic changes appear to have occurred in the glassy volcanic sediments and in the montmorillonite clay minerals derived from them.

Diagenetic change of original detrital particles of sedimentary components altered the character of the particle-size distributions as well as the composition of the original sediments. The detrital components most affected were volcanic ash, pumice, glassy tuff fragments, and feldspars. Fine ash was altered almost entirely to finer textured clay; much of the glass in pumice and tuffaceous fragments was altered to clay minerals; and there is evidence that both albite and orthoclase were replaced by clay minerals. Sandstones, siltstones, or claystones which were composed of such detritus now have a finer average grain size as the result of the alteration of coarser particles to finer particles, and the sandstone and mudstone, at least, are now more poorly sorted than the original sediments.

The members of the Morrison Formation are continental sedimentary units characterized by thick-bedded resistant lensing cross-stratified ledge-forming sandstone strata and thick-bedded poorly resistant bench- or convex slope-forming mudstone, siltstone, and claystone strata. The rocks consist of varieties of orthoquartzites, arkoses, and tuffs. Detrital mineral components present include grains of quartz, chert, chalcedony, albite, oligoclase, orthoclase, and sanidine, fragments of quartzite, granite, and altered rock of unknown classification, and altered fragments of silicified devitrified felsite and tuff. Present in smaller proportions are flakes of biotite, muscovite, and chlorite, grains of zircon, tourmaline, garnet, staurolite, rutile, apatite, epidote, magnetite, ilmenite, and leucoxene, and miscellaneous minerals of much lower quantitative significance. Interstitial cementing components include authigenic quartz in the form of overgrowths on quartz grains, and authigenic chert and zoned chalcedony, calcite, dolomite, barite, gypsum, anatase, and some authigenic orthoclase in the form of overgrowths on detrital particles of orthoclase and albite. Iron oxides, alone or mixed with clay, are a common cementing component. Clay minerals include mica clays, montmorillonite, kaolinite, chlorite, and various mixed-layer montmorillonite, mica, and chlorite clay mineral aggregates.

Mineral components vary in kind and proportion from sample to sample, from locality to locality, and from member to member. This produces a similar degree of variation in rock classification. Mineral components also tend to vary with texture. Orthoquartzitic sandstones show an inverse relationship between grain size and feldspar content. Arkoses tend to show either no relationship or a positive relationship between grain size and feldspar content. Silicified-rock fragments tend to increase in proportion with increase in grain size. Clay minerals are present in larger proportions in the more poorly sorted sandstones, siltstones, and mudstones, although clay- and silt-sized material also contains substantial quantities of finely ground quartz and feldspar. Clay minerals are of major quantitative significance in the Brushy Basin Member; about 90 percent of this unit consists of siltstone, claystone, and mudstone strata composed of clay minerals derived from detrital glassy volcanic debris, detrital and authigenic quartz and chert, detrital feldspar, and silicified tuff and pumice fragments. The remaining 10 percent of the member consists of sandstone and conglomerate strata. The Westwater Canyon Member is approximately 80 percent sandstone and conglomerate and 20 percent siltstone, claystone, and mudstone; the Recapture Member is approximately 75 percent sandstone and conglomerate and 25 percent siltstone, claystone, and mudstone; and the Salt Wash Member is approximately 60 percent sandstone, 39 percent siltstone, claystone, and mudstone, and 1 percent limestone and miscellaneous rocks.

The sandstones of the Morrison Formation are generally fine grained and moderately well sorted, with moderately skewed highly peaked grain-size distributions. Sandstones of the lower part of the formation are slightly finer and better sorted than those of the upper part. The siltstones and claystones are of two general types: the coarser, slightly reworked mudstones such as those of the Salt Wash Member, whose average median particle size is that of medium silt, and the finer, unreworked mudstones such as those of the Brushy Basin Member, whose average median particle size is that of fine silt. True claystones (80 percent or more clay) are relatively scarce, but the finer, poorly sorted mudstones of the Brushy Basin Member contain higher proportions of clay than those of the Salt Wash Member. The original sedimentary volcanic debris which resulted in the mudstone strata was probably significantly coarser than it is now. Diagenetic change reduced most fine-textured glassy particles in the original sediments to even finer clay.

Regional variation in mineral composition, grain-size distribution measures, detrital heavy- and light-mineral grain-count data, and grain-sphericity values were tested by trend-surface analysis. Prior to trend-surface analysis, sample data for the Salt Wash and Recapture Members were combined and treated as representing the lower part of the Morrison, and sample data for the Westwater Canyon and Brushy Basin Members were combined and treated as representing the upper part of the Morrison. Compositional and textural trends were determined almost exclusively from sandstone sample data.

Interpretation of trends in terms of movement of sediment from source areas is based on the assumption of general paleoalluvial drainage across the southwestern continental interior from southwest to northeast; normal fluctuations probably occurred in direction of movement, ranging from about north to east-southeast, as might be expected where tributary streams are flowing across an aggrading area of deposition. The assumed orientation is based on sedimentary-structure orientations measured in the region of study. Mean distance to sources is estimated to be about 400 miles from the center of the plateau region (lat 38 N., long 109 W.), on the basis of average distances to probable orogenic areas. Directions of source indicated by trend-analysis results are similar for the upper and lower parts of the Morrison, a fact which is interpreted to mean that the suggested systematic regional variations are significant in both the mathematical and the geological senses.

Relatively high proportions of each mineral component tested were found to be present in Morrison sediments in one or more marginal areas of the Colorado Plateau region. These highs were interpreted as the effects of sources located in certain directions from the center of the region. These interpreted source directions describe a continuous arc, from southeast to west-northwest, that passes around the southwest edge of the region, but the sources themselves are not necessarily arranged in this manner.

Regional linear trends and significant variation of composition of sandstones determined by trend-surface analysis suggest the presence of a major source of dominantly potassic feldspar to the south and a minor source of dominantly sodic feldspar west of the region. The suggested major source of chert, silicified limestone, and unclassified silicified-rock fragments was west of the region. Regional linear trends of statistical measures of grain-size distributions of the sandstones showed grain size decreasing from southwest to northeast, sorting improving from southwest to northeast, and skewness and kurtosis decreasing from south to north.

Previous investigations and present petrologic evidence suggest that the Morrison Formation in this region was deposited on an aggrading partly eroded depositional plain that subsided at a rate which varied from low to high. Moderately well sorted fine-grained sandstones of the Salt Wash Member represent sediment deposited under conditions of slow subsidence. Poorly sorted mudstones of the Brushy Basin Member represent sediment deposited under conditions of moderately rapid subsidence. Source areas of various composition were subject to tectonic uplift at a low to moderate rate.

Previous work in the southwestern part of the United States suggests that the tectonic conditions prerequisite for erosion of source areas of the Morrison Formation could have been satisfied by rising positive areas in the Basin and Range province of Utah, Nevada, Arizona, and New Mexico. Deposition of the Morrison and uplift of western Basin and Range source areas may have coincided with the beginning of the Sierra Nevada orogeny.

INTRODUCTION

Stratigraphic studies of uranium-ore-bearing formations in the Colorado Plateau region were begun in July 1947 by the U.S. Geological Survey on behalf of the Atomic Energy Commission. The three general objectives of the program were (1) to determine the paleogeography of known uranium-bearing formations in the Colorado Plateau region to discover the possible or probable sources of the uranium, the means by which the uranium was transported to the area of deposition, and the controlling factors in uranium concentration and deposition in present-day ore bodies; (2) to determine criteria for the selection of other formations to be explored for uranium-ore deposits; and (3) to provide a sound foundation for stratigraphic nomenclature within the Colorado Plateau region, for use in present and future geologic mapping and mineral-exploration programs.

The first stratigraphic study dealt with the Morrison Formation, of Late Jurassic age, the major uranium-ore-producing formation in the Colorado Plateau region and in the United States. Fieldwork under the leadership of L. C. Craig was largely completed by 1952. Associated with Craig during this time were C. N. Holmes, V. L. Freeman, T. E. Mullens, G. W. Weir, and the author of this report. Subsequent work in the field, office, and laboratory was carried on intermittently from 1952 to 1960 by Craig, Mullens, and the author. The geologic investigation of the Morrison Formation in the Colorado Plateau region was divided into four parts, as follows: (1) A regional study of the stratigraphy of the Morrison and underlying and overlying formations, including the lithologic definition, regional extent, and facies changes of the formations and their component members; (2) a petrologic laboratory study of the sedimentary rocks which make up the formation; (3) a lithofacies (torrential versus quiet-water deposition) study; and (4) a study of the orientation of sedimentary structures in the formation.

This report presents the data and conclusions obtained in the petrologic study of the Morrison Formation, with major emphasis on studies of the sandstone strata in the formation for the reasons given on page 6. The conclusions are based on petrographic evidence, but evidence from the field studies has also been considered. A brief summary of the stratigraphy provides historical background for the study and a lithologic setting for the sample data. Basic sample data—including statistical measures of the phi grain-size distributions, mineral ratios, and miscellaneous data obtained from grain-size and mineralogical studies—have been tabulated and placed in open file (Cadigan, 1967). These tables are available for public inspection at the Geological Survey libraries in Washington, D.C., Denver, Colo., and Menlo Park, Calif. They may be purchased through the Geological Survey library in Denver, Colo.

GEOGRAPHIC AND GEOLOGIC SETTING

The Colorado Plateau region includes western Colorado, the northwest quarter of New Mexico, most of the east half of Utah, and the northeast quarter of Arizona (fig. 1). The elevation of the region ranges generally from 4,000 to 8,000 feet above sea level, averaging about 6,000 feet. Minimum elevations are

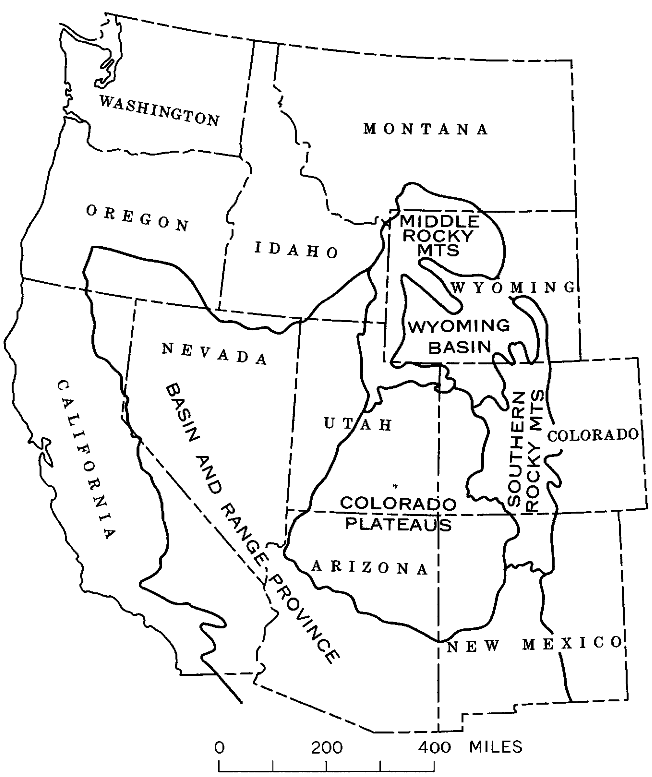

FIGURE 1.—Location of Colorado Plateaus and adjoining physiographic provinces. After Fenneman (1931).

along the Colorado River, which drops from about 5,700 feet at Glenwood Springs, Colo., near the northeast edge of the region, to about 3,100 feet at Glen Canyon, where the river crosses the Utah-Arizona border in the west-central part of the region. Maximum elevations of 12,000–13,000 feet along the west edge of the Southern Rocky Mountains and in the La Sal Mountains, 20 miles southeast of Moab, Utah.

The climate is semiarid to arid in most of the region. Vegetation is sparse or almost absent in the lower elevations and increases in abundance with increase in elevation in response to lower mean temperatures and significant increases in total precipitation.

Regionwide geologic structures form the boundaries of the Colorado Plateau but are generally absent in the central part. Sedimentary beds are flat lying or gently warped in roughly four-fifths of the area; in the remainder, the beds reflect the tectonic disturbances of rising salt anticlines, major faulting at depth which has resulted in sharp monoclinal folds, and intrusion by laccoliths and volcanic plugs.

The rocks exposed in the region range in age from Precambrian to Recent. Newman (1962, figs. 42–68) published small-scale outcrop and subsurface isopach maps for various stratigraphic subdivisions. Rocks of Precambrian age are mostly granitic igneous and metamorphic. Those of Paleozoic age are marine carbonate and quartzitic clastic rocks in the lower part, and marginal-marine and continental evaporites and quartzitic-feldspathic clastic rocks in the upper part. Rocks of Mesozoic age, the most widely exposed in the Plateau, include dominantly terrestrial quartzitic-feldspathic-tuffaceous clastic rocks interlayed with minor marginal-marine rocks of similar composition. Rocks of Cenozoic age are mostly continental quartzitic-feldspathic-tuffaceous clastic rocks with minor amounts of intrusive and extrusive igneous rocks in the form of laccoliths, plugs, dikes, and flows.

The dry climate, combined with the relatively undisturbed resistant quartzitic sandstone in the sedimentary strata, yields excellent rock exposures both in the steep-walled canyons of the major streams and in the canyons and valley slopes of the minor and intermittent streams. In most areas, outcropping formations and their members can be traced in continuous exposures over many miles without interruption.

PREVIOUS AND CONTEMPORARY WORK

The name Morrison Formation was applied to beds of variegated shale and sandstone near Morrison, Colo., in the eastern foothills of the Front Range of the Rocky Mountains, by G. H. Eldridge (Emmons and others, 1896, p. 60). The name had been published earlier, however, with credit to Eldridge, by C. W. Cross (1894, p. 2). The strata to which the name Morrison Formation was applied were later correlated with similar beds in New Mexico and southwestern Colorado by Lee (1902; 1917, p. 172, 213) and became the object of study of many other geologists in the Rocky Mountain area.

The name was extended to beds on the west side of the Rocky Mountains and on the Colorado Plateau by various authors, but especially by Baker, Dane, and Reeside (1936, p. 9–10, 32–43), who traced the formation throughout much of the Colorado Plateau region.

Correlation of the Morrison Formation throughout the Western Interior of the United States and the conclusions as to its continental origin by most early investigators were based on various features: the persistent variegated banded siltstones and shales and crossbedded lensing sandstone ledges, the fairly abundant fossil saurian bones, the fossil land-plant remains, and the physical continuity and stratigraphic relations of the rocks. The Morrison was found to be present in the Rocky Mountains, the Western Great Plains, the Wyoming basins, and the Colorado Plateau region. Darton (1904, p. 442) noted, "As the western portion of the Great Plains is explored, it has been found that the Morrison formation is very extensive in its distribution. * * * The character of the formation is strikingly uniform throughout, * * *." Mook (1916, map) estimated that the Morrison had been recognized over an area of about 600,000 square miles in the United States.

The lack of a good guide to the age of the formation resulted in many years of controversy (Osborn, 1915) on the question of whether the Morrison was Jurassic or Cretaceous in age, or both. The U.S. Geological Survey has placed the Morrison in the Lower Cretaceous(?), in the Jurassic, and since 1936 (Baker and others, 1936, p. 10), in the Upper Jurassic.

Stratigraphic relations of the Morrison Formation to underlying rocks, which include a wide variety of units, are conformable in some localities and unconformable in others. Gilbert (1897, p. 2) mentioned that in the area of Pueblo, Colo., "* * * the deposits of the Morrison sea accumulated not only on the Fountain (Carboniferous age) sediments but on the ancient Archean rocks."

Darton (1904, p. 442) noted that the Morrison overlies the marine Jurassic Sundance Formation in extreme northern Colorado, and that in much of the rest of northern Colorado it overlies the Triassic Chugwater Formation. Lee (1915, p. 309) reported that the Morrison rests conformably on marine Jurassic in Wyoming and northern Utah, and unconformably on older rocks in western Colorado and on Triassic rocks in northern New Mexico and in eastern Colorado. Mook (1916, p. 111) interpreted a sharp but conformable contact between the continental Morrison and the marine Sundance in Montana as an erosional plane representing a short time break between the end of deposition of the Sundance and the beginning of deposition of the Morrison. He noted (p. 110) that the Morrison contact with underlying Jurassic rocks (La Plata Sandstone, a name that has since been abandoned) in western Colorado is apparently conformable. An erosional unconformity was reported at the base of the Morrison Formation in the eastern Utah area of the Colorado Plateau region by Emery (1918, p. 576) and Dake (1919, p. 646). Gilluly and Reeside (1928, p. 81) described the contact as an erosional angular unconformity in eastern and east-central Utah.

The Morrison was reported by Stanton (1905, p. 658) to be separated from the Dakota Sandstone of Late Cretaceous age, in most places in the Western Interior, by 100–200 feet of beds of Early Cretaceous age. A similar relationship exists in the Colorado Plateau region according to Stokes (1944), although the prominent sandstone facies of the Dakota are missing in some localities.

The Morrison was found to be generally conformable with the overlying beds. Stokes described the upper contact in the plateau region as uneven but showing no angular discordance; he described the contact as a surface of nondeposition rather than erosion. The differentiation of the Lower Cretaceous beds from the underlying Morrison in the Plateau region was made first on the basis of a lag conglomerate (Stokes, 1944) and later on the basis of structural and possible fossil evidence (Stokes and Phoenix, 1948). An erosional unconformity marking the Morrison-Dakota contact and representing much of Early Cretaceous time was recognized in the Western Interior by Stanton (1905, p. 658) and in the north-central part of the Colorado Plateau region by McKnight (1940, p. 110).

Lee (1915, p. 310–311) concluded that following withdrawal of the early Late Jurassic Sundance sea and a short period of nondeposition, the Morrison Formation accumulated as fluviatile deposits during slow regional subsidence. Similarly, Mook (1915, p. 319–322) inferred that the Morrison was deposited on a plain of low relief—the site of the present Colorado Plateau, Rocky Mountains, and adjacent regions—by several major streams flowing from mountainous sources to the west. The depositional plain contained paludal and lacustrine as well as fluviatile environments. Constant shifting of channels resulted in erosion and reworking of the resultant sediments to produce a series of deposits which were comparatively thin, with great lateral and vertical variation, but which presented the same characteristics over the whole area. Mook noted that the sediments in the southwestern areas (the Colorado Plateau region) were thicker and coarser textured than the sediments in the northeast (Western Great Plains). The Morrison Formation in the Colorado Plateau region was interpreted by Craig and others (1955) to consist of sediments from southern and southwestern sources, deposited by a regionwide stream system which flowed generally from southwest to northeast.

No regional petrologic work had been done on the Morrison Formation of the Colorado Plateau region when the present study was begun in 1948. Mook (1916, p. 119–125) included descriptive petrography of some samples from the Canon City, Colo., area in his regional study of the Morrison Formation. He recognized differences in cements in the sandstone, variation in the proportions of quartz and feldspar, and the presence of lava fragments. Coffin (1921, p. 92–95) and Stokes (1944, p. 963–964, 975) gave qualitative petrographic descriptions of the sandstones, emphasizing the quartzitic nature of the lower sandstone and alluding to the probable volcanic content of the upper variegated clays. Hess (1933, p. 463) suggested volcanic ash as the source material of the upper clays. Both he and Fischer (1942), however, were mainly concerned with petrographic relations between host rocks and ore deposits in the radium, vanadium, and uranium mining areas.

While the present study of the stratigraphy and petrology of the Morrison Formation was in progress, separate but cooperative petrographic investigations of the Morrison Formation were being carried on by other geologists and mineralogists employed by the U.S. Geological Survey and the U.S. Atomic Energy Commission. Weeks (1953) and Keller (1959, 1962) studied the mineralogy and petrography of the clays. Waters and Granger (1953) studied volcanic debris and its relation to the uranium ore deposits. Griffiths, Cochran, Hutta, and Steinmetz (1956) made a statistical study of petrographic features in ore and barren rock in part of the Salt Wash Member. Many other geologic investigations of the ore deposits in the Morrison Formation were made during the same period. For a comprehensive bibliography see Brown (1961).

ACKNOWLEDGMENTS

Indispensable help in the present petrologic study was received from L. C. Craig, Mary T. Finch, Alice D. Weeks, M. Eleanor Thompson, W. D. Keller, A. C. Walters, and A. T. Miesch, and from the late F. H. Spence, all of the U.S. Geological Survey, and from J. C. Griffiths of the Pennsylvania State University. Fieldwork and sampling were carried on under the guidance and supervision of Craig. Spence and Finch did most of the routine laboratory work connected with the grain-size analyses, loose grain studies, heavy mineral studies, and roundness and sphericity measurements, and contributed to the report by helping with the tabulation of data and with statistical calculations. Weeks, Thompson, and Keller provided guidance and information on the nature of the clay-mineral composition and structure, both in the field and in the laboratory. Waters stimulated the search for and recognition of the volcanic debris present in abundance in some sedimentary rocks of the Colorado Plateau region. Training and guidance in the use of thin section point-counting technique and statistical treatment of quantitative data were received from Griffiths. A. T. Miesch provided an introduction to trend-surface analysis techniques. I also thank Barbara V. Walker and Esther D. Renaud, U.S. Geological Survey, for help in preparation of the illustrations and tables.

PROBLEMS OF THE MORRISON STUDY

Investigation of the petrology of the Morrison Formation started with the uranium deposits as the focal point of sampling and study. Stratigraphic and petrographic evidence yielded by early work in the mining districts indicated that the uranium deposits were probably related to certain features of composition, texture, and structure of the host formation. To obtain a more complete knowledge of the host rocks, the investigation was expanded outward from the mineralized areas toward the regional limits of the formation. Consequently, sampling locations are denser in the mining areas.

Limitations of the study.—This report is concerned chiefly with the regional petrologic study of the sandstone strata and to a lesser extent with the siltstone, claystone, and mudstone strata of the Morrison Formation. Very little work was done on the coarse conglomerate and carbonate rock types. This limitation of the investigation was made for several reasons. The sandstones yield more geologic information than other rock types regarding their source areas, their areas of deposition, and their tectonic environment. The mineral constituents of mudstone and finer sediment are difficult to identify because of their fine texture. The clayey sediments contain much larger proportions of diagenetic mineral components than the sandy sediments and are thus generally less satisfactory for studies of origin and depositional process. Accessory detrital heavy minerals are almost absent from very fine grained clayey rocks and from very coarse grained conglomeratic rocks, or if present in the fine-grained sedimentary rocks, they may be indistinguishable from authigenic minerals (products of diagenesis or mineralization). Textural variation is more strongly influenced by diagenesis in fine-grained sedimentary rocks than in sandstone. Finally, and most importantly, the uranium deposits, the original motive for the study, are nearly all in sandstone host rocks.

The results of the study of the regional variation of size and composition of pebbles in the conglomeratic strata are to be presented in a subsequent professional paper on the stratigraphy of the Morrison.

Interpretations.—Regionwide, the Morrison is superficially and qualitatively homogeneous in bedding structure and in texture, but detailed studies of structure, texture, and composition indicate that the formation is quantitatively heterogeneous. The heterogeneity apparently reflects multiple sources of sediment and a variety of depositional processes, including shifts in the regional drainage system, that mixed the sediments over wide expanses of the area of deposition. The lithologic evidence of different source directions, differences in composition of sources, and differences in the texture of the derived sediments were thus reduced by the depositional processes to trends and patterns of varying strength.

The Morrison Formation has long been recognized as a fairly uniform predominantly fluviatile sedimentary unit deposited in a continental basin of at least 600,000 square miles. This basin, the sediment deposited in it, and the areas from which the sediment came were products of an even larger tectonic environment. Actual deposition took place on a basinwide continuous surface. The basinwide drainage system produced sedimentary structures and lithologic boundaries or trends which were oriented on this surface as depositional lineaments.

The Colorado Plateau region, which constitutes 10–20 percent of the area in which the Morrison was deposited, thus contains segments of major superregional depositional trends, as well as regional and local trends. To determine the location and composition of the source areas, almost all of which are outside the region of study, the observed trend segments must be analyzed and interpreted. Knowledge of the source areas in turn helps to define the even larger scale tectonic environment which controlled deposition of the Morrison Formation in the Western Interior.

Additional samples would add detailed information and probably alter the computed trends to some extent, but major trends in composition and texture, as now recognized, probably would not change significantly, nor would interpretations of tectonic environment be affected.

STRATIGRAPHY

The Morrison Formation in the Colorado Plateau region overlies several different formations of Late Jurassic age and is overlain by formations of Early and Late Cretaceous age.

The formations which underlie the Morrison (fig. 2) constitute the upper part of the San Rafael Group. The contact is apparently conformable in some areas of the Plateau and plainly disconformable in others. In the north half of the region the Morrison lies on the Summerville and Curtis Formations. The Summerville is mostly thin-bedded reddish-brown siltstone and very fine sandstone and generally is evenly bedded; it is a continental mud-flat type of deposit which contains bedded gypsum deposits in the San Rafael Swell-Green River Desert area (Gilluly and Reeside, 1928, p. 80; McKnight, 1940, p. 100). The Curtis Formation is the greenish-gray marine-fossil-bearing equivalent of the Summerville and intertongues with and replaces the Summerville to the north and northeast in the manner suggested diagrammatically by figure 2. In the south half of the region, the Morrison disconformably overlies medium-bedded "sandy" Sum-

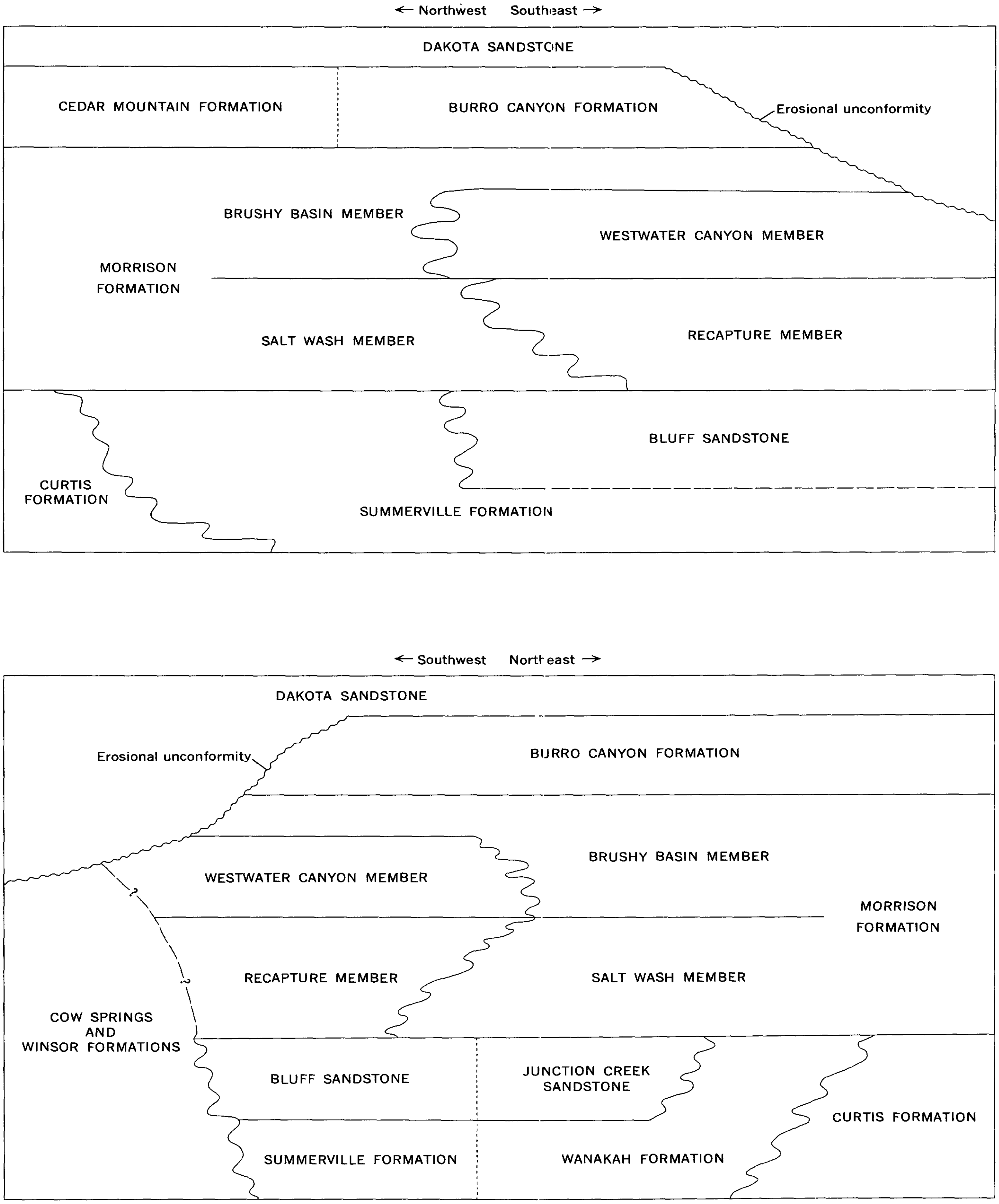

FIGURE 2.—Generalized stratigraphic relationships of the Morrison Formation in the Colorado Plateau region.

merville in some areas and various thick massive-bedded eolian sandstone equivalents in other areas. These equivalents are the Junction Creek Sandstone of southwestern Colorado, the Bluff Sandstone of northwestern New Mexico and southeastern Utah, the Cow Springs Sandstone of northeastern Arizona, and the Winsor Formation of south-central Utah. Where basal sandstone of the Morrison is in contact with sandstone of the Junction Creek or Bluff, a sharp erosional surface of moderate relief is present. Where siltstone is present at the contact in both the Morrison and underlying formation, there is a contrast in appearance, but the exact contact is not apparent. In the southern and southwestern parts of the region the Morrison contains sandstone strata similar in appearance to the Cow Springs and Winsor Formations, and the basal contact in many localities becomes a discontinuous parting which resembles similar partings above it. This disputed relationship may be a poorly defined contact which resulted from reworking of pre-Morrison Cow Springs sand by sluggish Morrison streams; or it may be a transition zone marked by intertonguing between equivalent Cow Springs and Morrison strata, the interpretation favored by Harshbarger, Repenning, and Irwin (1957, p. 48–57). In general throughout the plateau region, where strata of contrasting texture and structure are in contact the basal contact of the Morrison Formation is an erosional surface; where strata of similar texture and structure are in contact, the contact is either conformable or transitional. The Cow Springs Sandstone evidently was a significant intraregional source of the reworked sand in the Morrison Formation, and the Bluff and Junction Creek Sandstones were temporary local sources.

The formations overlying the Morrison resemble it in general appearance and include units with similar crossbedded lensing fluviatile sandstone and conglomerate ledges and variegated banded siltstones and shales. In western Colorado and eastern Utah the Morrison is conformably overlain by the Burro Canyon Formation of Early Cretaceous age. The Burro Canyon is a continental fluviatile unit of resistant ledge-forming grayish-white sandstone and conglomerate and pale-greenish-gray siltstone and shale. The sandstones and conglomerates contain a conspicuously greater proportion of black and gray pebbles and granules than do those of the Morrison, and the pale-green siltstones and shales contrast with the pale-red and purple shales and siltstones of the upper part of the Morrison Formation. The contact with the Morrison is set arbitrarily at the base of the lowest recognizable sandstone or siltstone having lithology typical of the Burro Canyon. In much of central Utah the Morrison is overlain conformably by the Cedar Mountain Formation of Early Cretaceous age. The Cedar Mountain includes strata equivalent to the Burro Canyon; it is dominantly a variegated siltstone unit which differs from the variegated siltstone in the top of the Morrison only by having a generally higher lime content and a higher proportion of white or bleached color banding in the variegated siltstone. Sandstones, where present, have the same distinguishing characteristics as the Burro Canyon. The recognition of a consistent Cedar Mountain–Morrison contact is easy in some localities but very difficult in others. In the northwestern New Mexico and northeastern Arizona areas and in west-central Utah, the Morrison is separated from the overlying Dakota Sandstone of Early and Late Cretaceous age by a regional angular unconformity. The slight angularity of the erosional contact can be observed in a few localities where exposures are continuous and clearly visible over a wide area. The discordant plane represents a cycle of erosion that removed some Morrison and Lower Cretaceous strata that accumulated prior to deposition of the Dakota. On the south and west margins of the region, erosion at this time removed all Morrison strata, so that basal Dakota is in contact with the San Rafael Group. The Dakota is a fluviatile-paludal unit consisting of pale-yellow to gray ledge-forming sandstone, and pebbly sandstone and nonresistant siltstone units which in most localities in the region contain thin coal seams, fragments of carbonized plant material, and carbonaceous shales. Dakota and Morrison strata are distinguished by differences in composition and structure. The Dakota is grayer and has a higher carbon content than the Morrison; pebbles in it are dominantly black and white in contrast with the green, red, white, and brown pebbles in the underlying Morrison.

The Morrison Formation in the Colorado Plateau region consists of mudstone, siltstone, claystone, sandstone, conglomerate, and minor limestone; it ranges in thickness from 500 to 1,000 feet. The sandstone and conglomerate are light colored (pale browns, oranges, yellows, and grays) and form conspicuous ledges. The mudstone, siltstone, and claystone are reddish brown, greenish gray, and purple; where they are thick to massive bedded, they form convex resistant slopes; where they are in thinner units, interbedded with the ledge-forming sandstone, they form poorly resistant concave slopes. Because of the relatively rapid erosion of these soft rocks, the sandstone ledges stand out in bold relief; the sandstones are gradually undermined and finally break off in large blocks which litter the slopes. Inconspicuous poorly resistant thin- to medium-bedded sandstone or, less commonly, limestone beds are interbedded with the mudstone strata. Much of the siltstone interbedded with the ledge-forming sandstone is limy; it grades laterally into very fine grained sandstone. Limestone and limy siltstone strata are most common in the basal part of the Morrison Formation and contain sparse microfossils (ostracodes, plant spores, algae). The most common fossil materials in the Morrison are fragments of wood, plants, and dinosaur bones; much less common are logs and complete skeletons. Also present but seldom found are fresh-water pelycepod shells.

The Morrison Formation in the Colorado Plateau region has been divided into four members (fig. 2). The Salt Wash Member (originally defined as part of the McElmo Formation (Lupton, 1914, p. 127)), shown in figure 3, is restricted in areal extent to the northern two-thirds of the Colorado Plateau region (fig. 4). The Recapture Member (Gregory, 1938, p. 59), shown in figure 5, overlies the Salt Wash in the Four Corners area and is restricted to the southern third of the region (fig. 4). The Westwater Canyon Member (Gregory, 1938), shown in figure 6, overlies the Recapture and is also restricted to the southern third of the region (fig. 4). The Brushy Basin Member (Gregory, 1938, p. 59), shown in figure 7, is the uppermost unit and extends throughout most of the region except the southwest corner (fig. 4). Gregory included both Salt Wash and Recapture in his type Recapture in the Four Corners area, but Stokes (1944, p. 963–964) traced the Salt Wash Member throughout southeastern Utah and separated it from the Recapture in the Four Corners area, where both are present. Harshbarger, Repenning, and Jackson (1951, p. 98) recognized and extended the Recapture throughout northeastern Arizona and northwestern New Mexico.

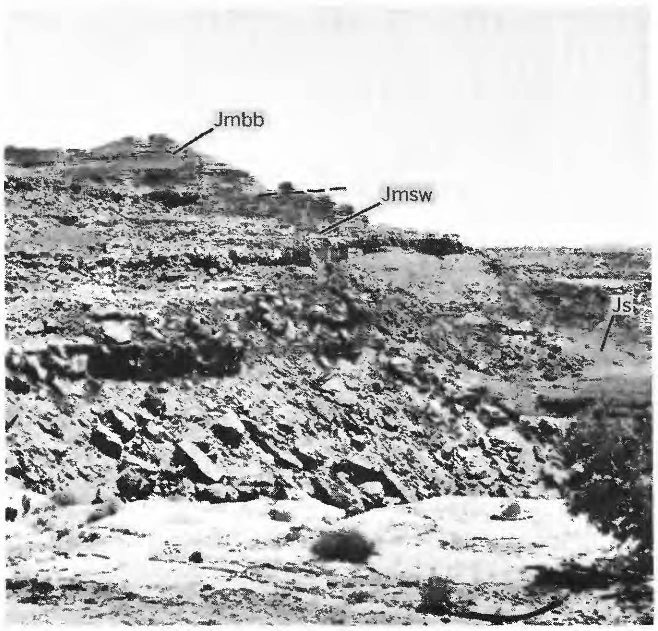

FIGURE 3.—Exposure at type locality of the Salt Wash Member of the Morrison Formation, Duma Point, near Salt Wash, Grand County, Utah. Jmbb, Brushy Basin Member; Jmsw, Salt Wash Member; Js, Summerville Formation. The Salt Wash Member is about 240 feet thick.

The present-day western and southern limits of the members of the Morrison Formation along the margin of the Colorado Plateau resulted primarily from erosion prior to deposition of the Dakota Sandstone; originally, at least, some members extended farther west and south. The southwestern limits are controlled in part by the gradation of Morrison strata into the Cow Springs Sandstone (Harshbarger, Repenning, and Jackson, 1951, p. 97, 98) in northeastern Arizona. The northern and eastern limits of the members generally represent the limits of recognition and differentiation of the members owing to lateral changes of facies and possible depositional pinchouts.

The estimated volume of the Morrison Formation in the Colorado Plateau region, prior to recent erosion, as calculated from sections measured by Craig, Holmes, and others (Craig, 1959) was at least 9,200 cubic miles. This volume of sedimentary material was divided among the four stratigraphic members and three general groups of rock types as shown in table 1

TABLE 1.—*Proportional composition of the Morrison Formation in terms of its four members and of the major textural rock types*

Members	Volume	Major rock types		
		Sandstone and conglomerate	Mudstone, siltstone, and claystone	Limestone and miscellaneous
Brushy Basin	34	3	31	(1)
Westwater Canyon	12	10	2	(2)
Recapture	15	11	4	(2)
Salt Wash	39	24	14	1
Total	100	48	51	1

[1] Probably about 1 percent, but not separated from mudstone, etc., in measurement of sections.
[2] Volumetrically insignificant.

PETROLOGIC METHODS

Laboratory analytical procedures, with the exception of the treatment of thin sections, were similar to those described by Krumbein and Pettijohn (1938). The schedule of procedures followed is shown in table 2. In addition to geographic and stratigraphic locations recorded for all samples, data compiled for selected groups of samples included (1) petrographic volumetric modal thin section analysis; (2) statistical

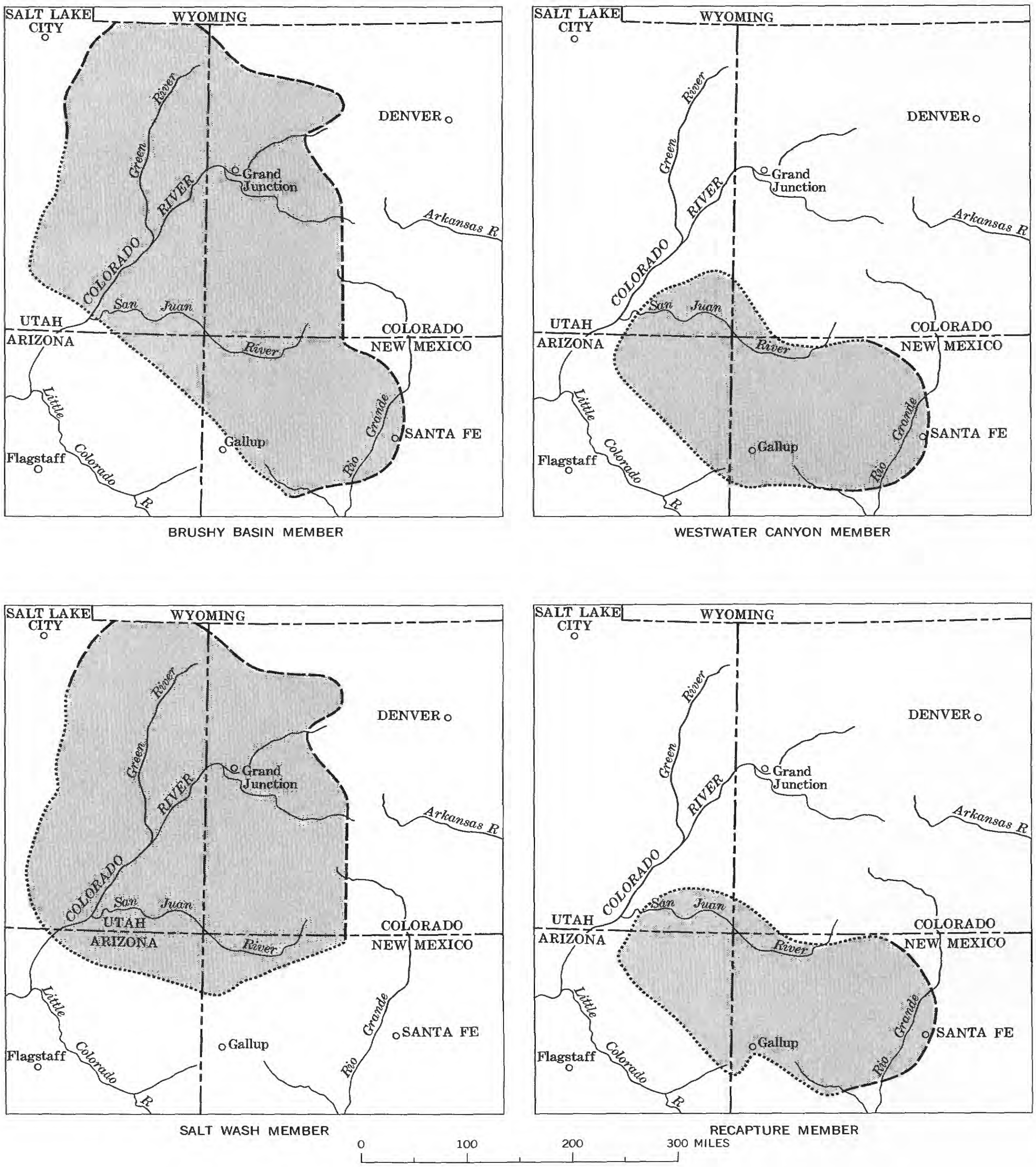

FIGURE 4.—Areal extent of the members of the Morrison Formation in the Colorado Plateau region and adjacent areas. Dotted line indicates approximate margin resulting from pinchout, facies change, or erosional cutoff; dashed line indicates approximate margin and limit of study. From Craig and others (1955) and Craig (written commun., 1965).

FIGURE 5.—Exposure at type locality of the Recapture Member of the Morrison Formation north of the mouth of Recapture Creek, San Juan County, Utah. Jmwc, Westwater Canyon Member; Jmsw, Salt Wash Member. The Recapture Member, Jmr, is about 150 feet thick.

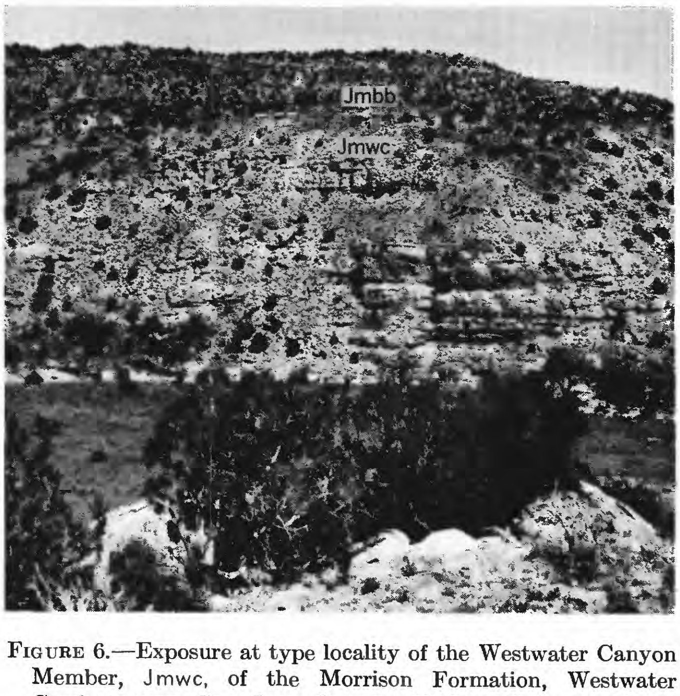

FIGURE 6.—Exposure at type locality of the Westwater Canyon Member, Jmwc, of the Morrison Formation, Westwater Creek canyon, San Juan County, Utah, and the overlying Brushy Basin Member, Jmbb. Only about 175 feet of strata is exposed in this outcrop; however, the Westwater Canyon Member is approximately 200 feet thick.

FIGURE 7.—Brushy Basin Member of the Morrison Formation at type locality, Brushy Basin Canyon, San Juan County, Utah. Knob on skyline at right is Burro Canyon Formation, possibly in a large slide block. White rough-textured strata at lower left are possibly Westwater Canyon equivalent. Thickness shown is approximately 300 feet.

measures of the grain-size distribution; (3) percentage acid-soluble material in the rock; (4) heavy-mineral ratios (the proportions of certain heavy detrital minerals within a suite of selected minerals); (5) light-mineral ratios (the proportions of certain light detrital minerals in certain particle-size classes); and (6) measurements of the roundness and sphericity of a representative number of light-mineral grains in certain particle-size classes.

Sampling.—Most of the sampling and other fieldwork was done during 1948–52. The Salt Wash Member, at that time the principal source of uranium ore in the Morrison, was the first unit studied and in general received more attention than the other members. All field localities used in the project were numbered, but not all were sampled. Table 3 lists the sample localities, the number of samples taken from each member, and the approximate geographic position. Plate 1 shows the sample localities.

A total of 483 samples were collected from 96 localities as follows: Salt Wash Member, 79 localities and 294 samples; Brushy Basin Member, 36 localities and 70 samples; Recapture Member, 22 localities and 60

TABLE 2.—*Flow sheet showing steps in laboratory study of samples*

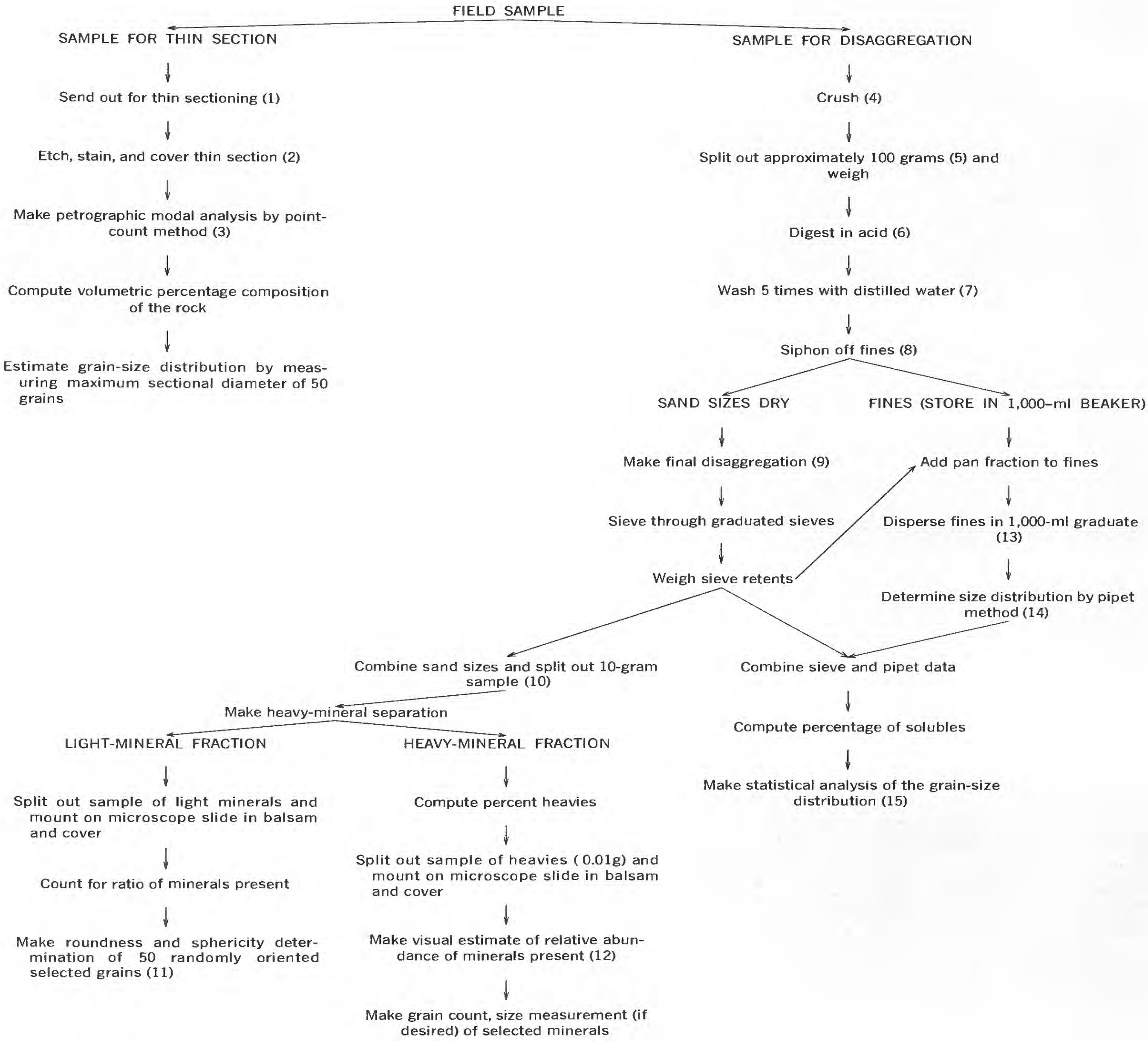

KEY TO NUMBERS IN PARENTHESES

(1) Request thin sections without cover glasses.
(2) Etch with hydrofluoric acid fumes for 1 minute; stain in sodium cobaltinitrite solution for 2 minutes to aid identification of feldspars (Keith, 1939; Gabriel and Cox, 1929).
(3) Chayes (1949, 1956).
(4) To pass through U.S. No. 5 sieve if nonpebbly.
(5) 100 grams for sandstone; 50 to 20 grams for medium to fine siltstones or claystones.
(6) Boil in 400 ml of 20-percent citric acid, cool, add 20 ml concentrated hydrochloric acid. Add additional increments of cold concentrated hydrochloric acid if undissolved calcite or curds of calcium citrate are present.
(7) Allow to settle 24 hours or longer between washings; siphon off supernatant liquid.
(8) Put poorly disaggregated claystone and medium and fine siltstone in a homogenizer for 1 minute.
(9) Hand crush aggregate with a rubber bulb or porcelain pestle on brown wrapping paper.
(10) More may be required if there are few heavy minerals.
(11) Krumbein (1941); Rittenhouse (1943); Wadell (1932, 1935).
(12) Record minerals in order of abundance.
(13) Disperse with sodium oxalate (N/100 concentration).
(14) Krumbein and Pettijohn (1938, p. 166–168).
(15) Krumbein and Pettijohn (1938, p. 239–253).

TABLE 3.—*Index of sample localities*

[Thicknesses from Craig (1959)]

Locality									Member sampled		Number of samples
No.[1] (pl. 1)	Name	State	County	Lat N.	Long W.	Sec.	T.	R.	Name	Thickness (ft)	
2	Almont	Colo	Gunnison	38.68°	106.83°	22	51 N.	1 E.	Salt Wash	32.0	3
3	Animas River	do	LaPlata	37.31°	107.88°	17	35 N.	9 W.	do	27	3
7	Beclabito Dome	N. Mex	San Juan	36.80°	109.01°	18	30 N.	20 W.	Brushy Basin	88	2
									Westwater Canyon	165	2
									Salt Wash	185	3
									Recapture	220	2
8	Bilk Creek	Colo	San Miguel	37.97°	107.92°	25, 36	43 N.	10 W.	Salt Wash	315.2	1
12	Black Ridge	do	Mesa	39.08°	108.82°	18	11 S.	102 W.	do	296	3
19	Bridgeport	do	Delta	38.82°	108.38°	20	14 S.	98 W.	do	229.4	2
24	Buckhorn Flat	Utah	Emery	39.20°	110.79°	4	19 S.	10 E.	Brushy Basin	308.8	1
									Salt Wash	126.8	3
25	Buckhorn Reservoir	do	do	39.21°	110.73°	20, 21, 36	18 S.	10 E.	Salt Wash	126.8	4
27	Burns	Colo	Eagle	39.88°	106.91°	21	2 S.	85 W.	do	79	1
28	Butler Wash	Utah	San Juan	37.46°	109.62°	28	38 S.	21 E.	Brushy Basin	213.2	1
									Westwater Canyon	279.2	3
									Recapture	163	1
									Salt Wash	71.2	2
29	Caineville	do	Wayne	38.38°	111.01°	15	28 S.	8 E.	Salt Wash	243.3	4
30	Calamity Flats	Ariz	Navajo	36.47°	110.59°				Westwater Canyon	48.3	1
31	Cane Spring	Utah	San Juan	38.40°	109.42°	7	28 S.	23 E.	Brushy Basin	373.8	4
						12	28 S.	22 E.	Salt Wash	339.9	5
37	Church Rock	do	do	38.05°	109.30°	29, 30	31 S.	24 E.	Brushy Basin	334.2	1
									Salt Wash	361.7	3
40	Collett Creek	do	Kane	37.56°	111.36°	5	38 S.	5 E.	Salt Wash	220.3	6
45	Crescent Creek	do	Garfield	38.08°	110.67°				do	Unknown	4
49	Cuchillo Arroyo	N. Mex	Sandoval	35.66°	106.90°	33, 34, 35, 36	17 N.	1 W.	Westwater Canyon	171.3	3
									Recapture	276.4	3
56	Dolores Group	Colo	Montrose	38.41°	108.74°	19, 20, 29, 30	48 N.	17 W.	Brushy Basin	365.8	4
									Salt Wash	334.9	8
59	Drunk Man's Point	Utah	Emery	38.96°	111.04°	31	21 S.	8 E.	Brushy Basin	324.7	1
									Salt Wash	188.8	3
61	Dry Creek anticline	Colo	Montrose	38.19°	108.63°	33, 34	46 N.	16 W.	Brushy Basin	478.1	4
									Salt Wash	377	5
64	Duma Point	Utah	Grand	38.81°	109.95°	24	23 S.	17 E.	Brushy Basin	294.5	4
						19	23 S.	18 E.	Salt Wash	216.1	6
67	Unaweep Canyon	Colo	Mesa	38.87°	108.53°	1, 2	14 S.	100 W.	Brushy Basin	298	1
						36	13 S.	100 W.	Salt Wash	279	1
71	Escalante	Utah	Garfield	37.81°	111.62°	6, 7	35 S.	3 E.	Brushy Basin	60.5	2
									Salt Wash	210.6	2
72	Escalante Forks	Colo	Delta	38.70°	108.29°	9, 10	51 N.	13 W.	Brushy Basin	339	1
									Salt Wash	303	4
73	Factory Butte	Utah	Emery	38.52°	110.93°	33	26 S.	9 E.	Brushy Basin	345.4	1
									Salt Wash	292.8	3
75	Flattop Buttes	do	do	38.52°	110.49°	27	26 S.	13 E.	Salt Wash	4.5	4
78	Fort Defiance	N. Mex	McKinley	35.75°	109.00°				Westwater Canyon	266.3	3
									Recapture	355.2	3
79	Fort Wingate	do	do	35.54°	108.56°	4, 8	15 N.	16 W.	Westwater Canyon	218	2
									Recapture	60	4
81	Garden Ranch	Utah	Sevier	38.55°	111.41°	18	26 S.	5 E.	Salt Wash	26	3
83	Ghost Ranch	N. Mex	Rio Arriba	36.35°	106.48°	2	24 N.	4 E.	Westwater Canyon	96.8	3
						35	25 N.	4 E.	Recapture	210.5	3
86	Halls Creek	Utah	Garfield	37.83°	110.94°	24	34 S.	8 E.	Brushy Basin	142.3	1
									Salt Wash	323.6	4
88	Hanksville	do	Wayne	38.39°	110.74°	18	28 S.	11 E.	Brushy Basin	262.6	1
						13	28 S.	10 E.	SaltWash	266.0	5
90	Hart Draw	do	San Juan	38.01°	109.42°	17, 18	32 S.	23 E.		14.6	3
92	Haystack Butte	N. Mex	McKinley	35.36°	107.92°	18, 19	13 N.	10 W.	Westwater Canyon	151.9	3
									Recapture	188.0	3
93	Head of Blue Canyon	Colo	Mesa	38.61°	108.75°	6	49 N.	17 W.	Salt Wash	328.4	3
						29, 30, 31	50 N.	17 W.			
99	Horseshoe Group	do	San Miguel	37.94°	108.76°	6	42 N.	17 W.	Brushy Basin	321.6	1
						1	42 N.	18 W.	Salt Wash	321.1	8
105	LaSal Creek	Utah	San Juan	38.35°	109.07°	28, 33	28 S.	26 E.	Brushy Basin	345.4	1
									Salt Wash	363.7	12
107	Last Chance Creek	do	Sevier	38.67°	111.28°	6	25 S.	6 E.	Salt Wash	10.3	3
						12	25 S.	5 E.			
112	Little Grand	do	Emery	38.97°	110.14°	29, 33	21 S.	16 E.	Brushy Basin	261.9	2
									Salt Wash	270.4	3
114	Lohali Point	Ariz	Apache	36.17°	109.74°				Westwater Canyon	161.0	1
									Recapture	480.1	4
115	Loma	Colo	Mesa	39.19°	108.82°	8	1 N.	3 W.	Brushy Basin	263.0	2
									Salt Wash	185.5	5
118	Longhouse Valley	Ariz	Navajo	36.57°	110.50°				Westwater Canyon	41.1	3
									Recapture	222.0	3
121	Los Pinos River	Colo	LaPlata	37.35°	107.61°	35	36 N.	7 W.	Salt Wash	Unknown	3
124	Lower McElmo Canyon	do	Montezuma	37.35°	108.85°	21, 23, 30, 32	36 N.	18 W.	Westwater Canyon	79.0	3
									Salt Wash	100.9	3
									Recapture	117.1	3
125	Lower Piedra River	do	Archuleta	37.26°	107.35°	5	34 N.	4 W.	Salt Wash	252.0	3
128	Lupton	N. Mex	McKinley	35.37°	109.06°	27	13 N.	21 W.	Westwater Canyon	94.4	2
		Ariz	Apache			4	22 N.	31 E.	Recapture	104.4	2
130	McIntyre Canyon	Colo	San Miguel	38.10°	109.00°	1, 12	44 N.	20 W.	Brushy Basin	415.6	1
									Salt Wash	334.1	3
133	Mancos Jim Butte	Utah	San Juan	37.75°	109.60°	21, 22	35 S.	21 E.	Salt Wash	276.7	1
135	Marsh Pass	Ariz	Navajo	36.64°	110.41°				Westwater Canyon	160.1	1
									Salt Wash	105.1	1
									Recapture	335.9	1
136-A	Calamity Mesa	Colo	Mesa	38.64°	108.82°	16, 17	50 N.	18 W.	Salt Wash	350.6	3
136-B	Maverick Canyon	do	do	38.62°	108.88°	16, 17	50 N.	18 W.	Brushy Basin	368.4	1
									Salt Wash	350.6	4
138	Meeker	do	Rio Blanco	39.97°	107.71°	19, 20	1 S.	92 W.	Salt Wash	148.0	1
140	Mesa Gigante	N. Mex	Valencia	35.02°	107.25°	2	9 N.	4 W.	Westwater Canyon	58.5	1
									Recapture	31.1	1

See footnotes at end of table.

TABLE 3.—*Index of sample localities*—Continued

Locality									Member sampled		Number of samples
No.[1] (pl. 1)	Name	State	County	Lat N.	Long W.	Sec.	T.	R.	Name	Thickness (ft)	
142	Monitor Creek	Colo	Montrose	38.61°	108.22°	9	50 N.	12 W.	Brushy Basin	305.0	1
									Salt Wash	309.0	4
146	Mounds	Utah	Carbon and Emery.	39.40°	110.56°	27	16 S.	12 E.	Brushy Basin	268.3	2
									Salt Wash	222.7	3
148	Navajo Point	do	Kane	37.26°	111.01°	--	--	--	Salt Wash	616.0	6
150	North Sinbad Valley	Colo	Mesa	38.58°	109.00°	30, 31	50 N.	19 W.	Salt Wash	281.4	3
151	Oak Creek	N. Mex	San Juan	36.72°	109.04°	13	29 N.	21 W.	Westwater Canyon	243.5	4
									Salt Wash	220.0	4 (2[2])
									Recapture	191.6	3 (1[2])
159	Pine Creek	Utah	Garfield	37.90°	111.64°	19	34 S.	3 E.	Brushy Basin	63.1	2
						24	34 S.	2 E.	Salt Wash	168.2	6
160	Piñon	Colo	Montrose	38.27°	108.36°	13	46 N.	14 W.	Salt Wash	326.4	4
161	Polar Mesa	Utah	Grand	38.68°	109.13°	27	24 S.	25 E.	Brushy Basin	323.1	1
						3	25 S.	25 E.	Salt Wash	356.2	4
162	Rattlesnake Mines	Ariz	Apache	36.91°	109.28°	4	13 N.	7 W.	Salt Wash	[3] 180.0	3
163	Recapture Creek	Utah	San Juan	37.32°	109.43°	18	40 S.	23 E.	Westwater Canyon	228.0	2
									Salt Wash	34.1	2
									Recapture	183.4	3
165	Red Canyon	Colo	Montrose	38.30°	108.18°	33	47 N.	12 W.	Salt Wash	437.0	1
171	Roubideau	Colo	Montrose	38.55°	108.19°	3	49 N.	12 W.	Salt Wash	414.0	1
172	Salina Trading Post	Ariz	Apache	36.03°	109.85°	--	--	--	Westwater Canyon	295.0	3
									Recapture	168.4	2
173	Salt Valley	Utah	Grand	38.88°	109.71°	29, 30, 31, 32	22 S.	20 E.	Brushy Basin	379.1	2
						5	23 S.	20 E.	Salt Wash	235.2	2
174	Salt Wash	Utah	Grand	38.83°	109.98°	12, 13	23 S.	17 E.	Brushy Basin	Unknown	10
									Salt Wash	Unknown	14
175	Sanastee Wash	N. Mex	San Juan	36.49°	109.01°	--	--	--	Westwater Canyon	283.6	4
									Salt Wash	52.4	2
									Recapture	472.2	4
177	San Miguel Canyon	Colo	San Miguel	38.05°	108.10°	29	44 N.	11 W.	Brushy Basin	390.0	2
									Salt Wash	380.6	4
178	San Rafael	Utah	Emery	38.87°	110.35°	26, 27	22 S.	14 E.	Brushy Basin	317.0	1
									Salt Wash	191.0	7
179	Sapinero	Colo	Gunnison	38.50°	107.25°	23	49 N.	4 W.	Salt Wash	183.2	4
181	Shootering Point	Utah	Garfield	37.70°	110.74°	31	35 S.	11 E.	Brushy Basin	164.3	1
						6	36 S.	11 E.	Salt Wash	512.3	3
182	Skein Mesa	Colo	Montrose	38.29°	108.85°	9, 16	46 N.	18 W.	Salt Wash	374.1	5
184	Slick Rock-Joe Davis Canyon.	Colo	San Miguel	38.05°	108.89°	27, 28, 30, 33	44 N.	18 W.	Salt Wash	400.6	2
						25	44 N.	19 W.			
189	Spring Canyon	Utah	Garfield	38.05°	111.07°	8, 17	32 S.	8 E.	Brushy Basin	160.2	2
									Salt Wash	243.7	5
194	State Line, Colo. Utah	Colo	Mesa	39.13°	109.06°	6	11 S.	104 W.	Salt Wash	230.8	1
195	Steamboat	Ariz	Apache	35.79°	109.77°	--	--	--	Westwater Canyon	110.0	2
									Recapture	128.0	1
197	Stoner	Colo	Montezuma	37.60°	108.25°	3	38 N.	13 W.	Salt Wash	Unknown	3
199	Summerville Draw	Utah	Emery	39.25°	110.45°	12, 21, 22, 23	18 S.	13 E.	Brushy Basin	239.6	1
									Salt Wash	192.4	4
200	Summit Point	Colo	San Miguel	38.00°	108.98°	8, 9, 16	43 N.	19 W.	Salt Wash	302.3	6
201	Tabeguache Creek	Colo	Montrose	38.39°	108.47°	34	48 N.	15 W.	Salt Wash	364.0	3
203	Tenderfoot Mesa	Colo	Mesa	38.68°	108.89°	17, 20	51 N.	18 W.	Salt Wash	331.5	5
207	Thoreau	N. Mex	McKinley	35.43°	108.17°	13	14 N.	13 W.	Westwater Canyon	181.0	3
									Recapture	208.8	3
208	Tidwell Ranch	Utah	Emery	38.98°	110.34°	21, 27, 28	21 S.	14 E.	Brushy Basin	416.3	2
									Salt Wash	260.0	3
209	Toadlena	N. Mex	San Juan	36.23°	108.89°	17	23 N.	19 W.	Westwater Canyon	259.0	2
									Recapture	418.5	3
210	Todilto Park	N. Mex	McKinley	35.96°	108.96°	13	20 N.	20 W.	Westwater Canyon	330.6	3
									Recapture	230.2	2
214	Upper McElmo Canyon	Colo	Montezuma	37.37°	108.73°	20, 21, 29, 30	36 N.	17 W.	Brushy Basin	194.1	3
									Salt Wash	269.6	4
215	Upper Montezuma Canyon.	Utah	San Juan	37.82°	109.28°	21, 22	34 S.	24 E.	Westwater Canyon	167.9	3
									Salt Wash	399.9	4
221	Vernal	Utah	Uintah	40.60°	109.47°	7	3 S.	22 E.	Brushy Basin	473.0	1
222	Wahweap Creek	Utah	Kane	37.04°	111.50°	17	43 S.	4 E.	Salt Wash	Unknown	3
228	Woodside anticline	Utah	Emery	39.20°	110.38°	5	19 S.	14 E.	Brushy Basin	Unknown	2
									Salt Wash	Unknown	2
230	Yale Point	Ariz	Apache	36.37°	109.76°	--	--	--	Westwater Canyon	147.6	2
									Recapture	680.4	6
231	Yellow Cat	Utah	Grand	38.84°	109.52°	12	23 S.	21 E.	Salt Wash	250.1	8
233	Legin group	Colo	San Miguel	37.95°	108.92°	29	43 N.	19 W.	Salt Wash [2]	Unknown	3
234	McPhee (Dolores River)	Colo	Montezuma	37.50°	108.52°	5	37 N.	15 W.	Salt Wash	Unknown	2

[1] Number sequence omits field locations not sampled. [2] Thin section data only. [3] J. D. Strobell (oral commun., 1964).

samples; Westwater Canyon Member, 24 localities and 59 samples.

Mechanical analysis.—Sandstone samples received initial coarse crushing by a power-driven jaw crusher. Disaggregated material was sieved through a set of twenty-five 8-inch-diameter brass sieves with openings graduated at one-half phi intervals from $-3\ \phi$ to $0\ \phi$ (8–1 mm) and at one-quarter phi intervals from $0\ \phi$ to $4.5\ \phi$ (1–0.44 mm). The phi scale is explained in a textbook by Krumbein and Pettijohn (1938, p. 84–85) and in an article by Krumbein (1936, p. 36–38). Sieves with openings of 0.125 mm or coarser were mechanically shaken for 15 minutes; sieves with finer openings were shaken for 20 minutes. Gross samples were weighed to 0.01 gram; refined samples (heavy minerals, clay decrements), to 0.1 milligram.

Modal analysis.—Petrographic volumetric modal analysis of the rocks was made from thin sections in the manner described by Chayes (1949, p. 2–4). To facilitate rapid mineral identification of the potassic feldspars, uncovered thin sections were etched with hydrofluoric acid fumes and treated with sodium cobaltinitrite (Gabriel and Cox, 1929; Keith, 1939). A resulting canary-yellow stain effectively delineates potassic feldspar detrital grains, and potassic feldspar crystals in fragments of granite, perthite, felsite, and crystal and lithic tuffs, and serves to identify altered potassic vitric tuff. This stain, if properly applied, does not interfere with the optical properties beyond changing the surface color of the grains. As the etching process is more rapid on weathered than on fresh grains of feldspar, the weathered grains absorb more of the stain and become brighter yellow. The etching also affects the sodic feldspars, tending slightly to accentuate the dull milky-white appearance of the grains, especially the weathered ones, between crossed nicols. Sanidine absorbs much less stain than other potassic feldspars, probably because of its high content of sodium. After staining, each thin section was covered with uncooked balsam and a glass slip and allowed to dry for a month or more. To avoid injury to the thin sections, neither heat nor solvents such as xylene were used in the procedures.

After staining, modal analysis (determination of the relative volumetric proportion of each rock-forming constituent) was made by the point-count method and use of a petrographic microscope and modified mechanical stage. By this method, the mineral composition is determined at intersections on an imaginary grid. This procedure leads to a computation of the percentage area of the thin section occupied by each constituent—an estimate of the volumetric modal composition of the rock. Chayes (1956, p. 4–15) proved mathematically the validity of the relationship of points to area to volume.

Ideally, a 10×50 intersection-point grid (10 traverses of 50 counts) was used to yield 500 identifications on each thin section. For siltstones with detrital grains obscured by iron oxide-impregnated clay and carbonate minerals, the composition was estimated on the basis of only 100 counts (2 traverses of 50 counts each).

Heavy-mineral separation and count.—A study was made of the regional variation in the ratios of several nonopaque detrital minerals of specific gravity greater than 2.90—those known as heavy minerals. The minerals selected for the study were apatite, epidote, garnet, rutile, staurolite, tourmaline, and zircon. Other nonopaque minerals—brookite, spinel, biotite, and muscovite—were observed in some of the slides, but because of their scarcity were not used in the study of regional variation. Barite, anatase, dahlite, and hematite also were not used, as they were considered to be authigenic. In determinations of ratios, the opaque varieties of heavy minerals—mostly ilmenite, magnetite, and leucoxene—were lumped together for counting because of difficulties in identification.

Correlation coefficients used in this study are values of Pearson and Lee's r (Snedecor, 1956, p. 160); as used with heavy-mineral ratios or percentages which add up to a constant sum, the coefficients are subject to the limitations discussed by Chayes (1960, p. 4187).

The heavy minerals in fine-grained and very fine grained sandstone were separated from the size fraction retained between the U.S. No. 325 (44-micron openings) sieve and the U.S. No. 250 (62-micron openings) sieve. Fractions retained on the U.S. No. 250 or the No. 200 (74-micron openings) sieve were included for medium- and coarse-grained sandstone because of a lack of material in the finer sizes. The separation of the heavy minerals was made in tetrabromoethane in the manner described by Krumbein and Pettijohn (1938, p. 335). The heavy-mineral grains, after being washed with alcohol and dried, were weighed to determine the proportion of heavies in the size fraction used, and the whole crop or a split of it was mounted on a glass slide. The microscopic study of the heavy minerals consisted of (1) a rapid microscopic reconnaissance of all the grain mounts to identify each mineral variety and to estimate its relative abundance, and (2) a routine count of the selected minerals. Both opaque and nonopaque minerals were counted. Regularly spaced horizontal traverses were made across the slides, and each grain touched by the intersecting crosshairs was counted, until a total of 100 nonopaque mineral grains was reached. In a few instances the proportion of opaque minerals was very high, and the count was arbitrarily halted at 500 grains, which included less than the desired 100 nonopaque grains. The results of the routine count were used in the regional study.

As a basis for computing the heavy-mineral content of the detrital fraction of the rock, 16 samples (4 from each member of the Morrison) were investigated. The particle sizes used in the heavy-mineral separations contained about half the total heavy minerals in the rock, and this figure was used to compute the heavy-mineral content of the detrital fraction in all samples. The figure so obtained was corrected for authigenic heavy minerals to determine the detrital heavy-mineral content. Among the authigenic heavy minerals, barite is of principal concern, because its entire substance seems to have been introduced into the rock since deposition and also because it is relatively abundant. No deductions were made for authigenic titanium minerals because chemical analysis of plateau rocks in various states of alteration (Newman, 1962, table 7, p. 398) shows approximately constant proportions of titanium, and the authigenic titanium minerals are therefore probably alteration products of allogenic detrital titanium minerals. Other authigenic minerals were ignored because most are probably alteration products and all are of very little quantitative significance. The heavy-mineral fractions with a "flood" of barite were considered to be only 25 percent detrital; fractions with "dominant" barite were considered to be 70 percent detrital; fractions with "abundant" barite, 90 percent detrital; and fractions with "common" or less barite, 100 percent detrital.

Light-mineral separation and count.—A study of the light-mineral grains (<2.90 specific gravity) was made to determine regional variations in composition and to study the relations of composition to grain size. The study was similar to one made on Mississippi River sands by Russell (1936), who concluded that the composition of the light minerals varied with the grain size, and that percentage determinations could be made by analyzing a single grade size, provided that the grade chosen was representative of the whole sample and came from near the central part of the grain-size distribution. The size fraction used for the light-mineral study of Morrison Formation sandstone consisted of the combined retents in the two sieves finer than the sieve containing the modal grain size. (For example, if the sieve containing the mode was the one with 2.25 ϕ openings, the material used for the composition determination was taken from the sieves with 2.50 and 2.75 ϕ openings). The retents chosen were considered representative of the samples for two reasons: (1) feldspars were observed to be more plentiful in the finer size-fractions of the samples, which suggested that sand slightly finer than modal size would be more representative of feldspar content; and (2) most of the grain-size distributions were skewed to the fine side, which indicated that with reference to the modal size, the samples tended to consist of more fine material than coarse material by weight. A split was taken from the combined retents for each sample; the heavy minerals were removed by means of tetrabromoethane, and a small amount (about 1,000 grains) of the light-mineral crop was obtained with a microsplitter and mounted on a glass slide.

A count of 200 grains was made on each grain mount. Grains were classified as quartz (including quartzite), feldspar (with an index of refraction less than that of Canada balsam), silicified rock (including chert and silicified tuff), and miscellaneous (collophane, shale, etc.). The proportions of mineral grains counted were recorded as an estimate of the percentage composition of the light-grain fraction for each sample. Chemical analyses, by the flame photometer method, of 60 samples of disaggregated grains from various parts of region (15 samples from each member of the Morrison) indicated that the calcium content of the feldspars is low. Theoretical anorthite content of the samples, calculated from the calcium, averages less than 1 percent (Cadigan, 1956).

Acid-soluble fraction.—The acid-soluble fraction of each sample disaggregated for the study was measured in percent by weight. Carbonates, certain iron oxides, gypsum in some samples, and small amounts of other minerals and trace elements were taken into solution during the digestion process (table 2). The data served as a check on the volumetric modal analysis and was used in statistical studies such as that of Cadigan and Miesch (1958) on the distribution of elements in sandstone.

Roundness and sphericity determination.—The investigation of shape of the sand grains composing the sandstone of the Morrison Formation was limited to a study of roundness and sphericity. Visual estimates of roundness and sphericity were made of detrital grains on the light-mineral mounts using Krumbein's (1941) method and chart for roundness and Rittenhouse's (1943) method and chart for sphericity. For comparison, sphericity was also determined for many samples by measurement of camera-lucida projections with a polar planimeter, and determination of the nominal diameter following the method described by Wadell (1935). Thirty successive grains along one horizontal traverse on each grain mount were used for the first few determinations, but wide variations of sphericity within single samples made it necessary to increase the number of grains to 50, which number was used for most of the determinations.

Trend-surface analysis.—A method for mathematical analysis of regional petrographic data, called trend-surface analysis—one relatively new to petrologists—was defined by Krumbein (1959, p. 823) as "* * * a procedure for separating the relatively large-scale systematic changes in mapped data from essentially nonsystematic small-scale variations due to local effects."

Trend-surface analysis was applied to the Morrison Formation data to determine regional trends and to appraise the evidence of regional variation of petrographic parameters mathematically, prior to interpretation.

A computed surface (three dimensional) is the mathematical integral of a computed curve (two dimensional). A computed curve is the result of mathematically fitting a line or curve to a series of points, in one plane, which have the variable coordinates X and Y such as in a scatter diagram, utilizing the principle of least squares or computed polynomials. A computed surface is the result of mathematically fitting a planar or curved surface to a series of points in two or more parallel planes, which have the variable coordinates X, Y, and Z, utilizing the principle of least squares or computed polynomials. (See Davies and Yoder, 1941, p. 236; Snedecor, 1956, p. 461; De Lury, 1950; Krumbein, 1956, 1959.) The coordinate systems in both instances are based on mutually perpendicular axes.

Some of the terms commonly used in trend-surface analysis are as follows:

Degree of trend surface, increasing capability of flexure of the computed surface: first degree, second degree, and third degree, or linear, quadratic, and cubic, and so forth (Krumbein, 1956, p. 2173).

Linear (1°) surface, a computed planar surface which slopes according to the regional slope of the data. The mathematical relation for irregularly spaced data points is of the form

$$X_c=b_0+b_1U+b_2V+R_1$$

where X_c is the computed value of a regionally distributed parameter, U and V are the regional coordinates, R_1 is the residual or deviation from the linear surface, b_0 is a constant, and b_1 and b_2 are coefficients of U and V for a plane surface. The X axis lies in a vertical plane perpendicular to the horizontal plane containing the U and V axes. The three axes are mutually perpendicular. (See Allen and Krumbein, 1962, p. 517–522.)

Observed data (Xo), values of the regionally varying parameter, which are used in the computation of a trend surface.

Computed data (Xc), values of the regionally varying parameter which define a computed surface.

Residuals, values of the respective differences between individual sets of observed and computed data for the same points on a specific computed surface, otherwise known as deviations from the computed surface.

Residual surface, a hypothetical surface formed by the residuals or deviations from a single computed surface; it is illustrated by contouring on the residual values.

Sum of squares of residuals (SS_R), the result of squaring the residuals and then summing the squares.

Total sum of squares (SS_X), the sum of the squares of the deviations of the individual observed values (X_o) from the mean of the observed values ($\overline{X}$); it may also be computed from the formula

$$SS_X=\Sigma X^2-\frac{(\Sigma X)^2}{N}$$

where N equals the number of observed values.

Percent reduction of sum of squares (E_R), the difference between total sum of squares (SS_X) and sum of squares of residuals (SS_R) in terms of percent of SS_X, or

$$E_R=\frac{SS_X-SS_R}{SS_X}\times 100$$

Computations were made by the U.S. Geological Survey using its General Regional Gradients Program (No. 9114) and a Burroughs 220 computer. The X variable was the value of the parameter being studied, such as percent feldspar or phi median grain size; in some analyses U and V variables were coded values of the geographic coordinates of the data points read out in degrees and hundredths. Latitude was coded by subtracting 37.00° and longitude by subtracting 109.00°, in effect placing the origin at lat 37° N., long 109° W. Thus the U and V values consisted of small positive and negative numbers. As pointed out by Mandelbaum (1963, p. 507), the use of large U and V numbers in the input of a computer results in the generation of very large products in the computer, particularly for cubic and higher surfaces, which exceed the computer's digit capacity and are rounded off, resulting in a loss of significant figures and the calculation of surfaces which bear decreasing relationship to the data.

A nonorthogonal least-squares computation method was used throughout, although both regularly and irregularly spaced data points were used. First-degree through fifth-degree surfaces were computed for many experiments, although only the linear (1°) surfaces are discussed in the report. Sums of squares of the residuals were tested for significance by analysis of variance in the manner described by Allen and Krumbein (1962, p. 521–524).

The output data for each surface computed consisted of a recapitulation of the U and V coordinates and the observed data together with the computed data and the residuals. Also furnished were the total sum of squares, sum of squares of the residuals for each surface, mean and standard deviation of the observed data, and the standard error of estimate. Computed trend-surface and residual-surface data were plotted on maps and contoured for study.

An ordinary isopleth or contour map is one constructed over a horizontal reference plane which generally coincides with the plane of X=0. A computed linear (plane) surface or least-squares surface is generally a sloping reference plane which passes through the moment center of the three-dimensional *X* values. The *X* values may be thought of as points suspended in space. The linear residual surface may be shown by an isopleth map with positive and negative values, which is constructed with reference to the computed linear surface. Zero values would represent points of intersection with the linear surface. Thus high or positive areas on a linear residual map rise above the computed linear surface, and low or negative areas lie below the computed linear surface. Experience indicates (Allen and Krumbein, 1962) that linear residual surfaces may reflect many local and regional effects stripped of the major regional linear trend, and thus may furnish valuable evidence for interpretation of details of local effects of sources, and patterns of transportation and deposition.

The strength of regional linear trends was determined by calculating the percent reduction of the total sum of squares by the linear surface. Roughly, for the range of number of data points used in this report, a reduction of 10 percent is considered a weak trend; 25 percent, a strong trend; and 50 percent, an extremely strong trend. Reduction of total sum of squares by 80 percent or more is considered a significant fit of the surface to the data for purposes of prediction, according to Allen and Krumbein (1962, p. 521).

Confirming the experience of Whitten (1959, p. 844), locality data based on averages of two or more samples at each locality were found to yield better trends than locality data based on a single sample at each locality; averaging reduces the range of variation. A decrease in the effect of local variation was also obtained by using only one point per degree square in the manner of increasing cell size recommended by Krumbein (1956, p. 2177); the variations eliminated by this technique were the effects of clusters of points which tend to outweigh isolated points in the computation of trend surfaces. The method of using only one point per degree square was found to produce even spacing, but not regular spacing. In some instances, decrease in local variation was obtained by interpolating grid data points from an ordinary contour map of the observed data, using the intersection points of the geographic (degree) coordinates; this method yielded regularly spaced data points. The smoothest trend surfaces were obtained by using combined interpolated and moving-average data computed from the *X* values at the interpolated points in the manner illustrated by figure 8. Although averaging provides smoother trends, residual maps obtained from locality data are probably more critical to geologic interpretation, as indicated by Whitten (1959).

Symbols					Numbers				
a	b	c	d		8	4	4	6	
e	f	g	h		3	2	2	6	
	i	j	k	l		6	2	6	5
	m	n	o	p		9	0	5	7
	q	r	s	t	u	0	6	3	9	7
	v	w	x	y	z	9	3	6	5	6

INTERPOLATED DATA

a	b′	c′	d		8.0	5.3	4.7	6.0	
e	f″	g″	h′		3.0	3.2	3.0	6.0	
	i′	j″	k″	l		5.7	3.0	5.0	5.0
	m′	n″	o″	p′		5.0	3.7	4.3	7.0
	q′	r″	s″	t″	u	6.0	3.0	5.3	6.7	7.0
	v	w′	x′	y′	z	9.0	6.0	4.7	5.7	6.0

AVERAGED DATA

FIGURE 8.—Method of obtaining three-point moving averages of interpolated grid (*U*, *V*) data for trend-surface analysis. Symbols are used as follows: Letter—grid value interpolated from ordinary contour map; letter with single prime—three point average value, obtained by averaging grid value and two horizontally or vertically adjacent grid values (whichever are available); letter with double prime—average of grid value (used twice) and both horizontally and vertically adjacent grid values; the central value is used twice to weight the average toward that value.

Which preparation technique is best suited to the data can be determined only by experimentation. If the aim is to compute a surface which is as close a fit to the data as possible, a moving average or other "smoothing" treatment of the data may be used. If the aim is to construct a residual map which "pinpoints" local deviations in the data, locality data should be used. Locality data can be improved without loss of significant detail by eliminating clusters of data points through random selection of a certain number of the points per unit area from those available, or if clusters are small and tight, by combining the data for any locality points that lie within relatively small areas to yield one data point. Methods may be combined; for instance, moving-average data may be used to obtain major regional trend and residual surfaces, and locality data may be used to obtain more localized residual surfaces. For a more detailed discussion see Krumbein (1952; 1956, p. 2165–2167) and Allen and Krumbein (1962, p. 521–522).

For this report, many trend analyses were made on untreated averages of sample locality data or on sample locality data which were "declustered" by combining (averaging together) data from any samples collected within the same 80-square-mile circle (10-mile diameter). This declustering reduced the number of data points but greatly improved their spacing without omitting any sample data.

PETROLOGIC CLASSIFICATION

The investigative methods described were applied to the samples of sedimentary rocks of the Morrison Formation in the Colorado Plateau region. Information obtained consisted generally of data on the petrologic parameters of the rocks, measures obtained from statistical analyses of the data, and computed analyses of regional variations of some parameters and statistical measures. To simplify description, comparison, and interpretation, appropriate classification systems were applied to properties of the rock samples.

COMPOSITION

The petrographic modal analysis of the sandstone strata revealed a relatively wide range of composition based on the proportions of minerals present in the cement, grains, and matrix of the rocks.

The cementing materials of the sandstone consist dominantly of calcite and of optically continuous quartz overgrowths on detrital quartz grains. Other volumetrically significant cementing material includes iron oxides (mostly limonite, hematite, goethite), dolomite, barite, gypsum, microcrystalline authigenic quartz and silica minerals in the form of chert (microgranulitic), banded chalcedony (fibrous), and equidimensional or fan-shaped patches of opaline chalcedony (fibrous with radiating structure and flamboyant extinction under crossed nicols). In some clayey sandstone the matrix combines with the cements to form an impregnated interstitial material, usually brown or reddish brown, which acts as a cement and disguises the quantity and quality of the cementing minerals. Other precipitated material which, although of minor volumetric significance, contributes to the cementing of some rocks includes anatase in both euhedral and anhedral forms, epidote in clusters of subhedral microcrystals suspended in interstitial clay, orthoclase feldspar overgrowths or rims which fill interstices of some feldspar-rich (tuffaceous?) arkoses, and various vanadium, uranium, and copper ore minerals.

The sand grains of the sandstones, and also granules and pebbles, consist of both monomineralic and mineral aggregate particles. Quartz is volumetrically the chief monomineralic particle. It generally exceeds in volume all the others combined, including feldspars, micas, and heavy minerals. Potassic feldspars are orthoclase, microcline, and minor sanidine. Sodic feldspars are albite or albite-oligoclase. No significant quantity of calcic feldspar was detected. Muscovite and biotite, together with their alteration products chlorite or vermiculite, constitute the micas. Heavy minerals constitute the smallest proportion of the persistent monomineralic particles; those commonly present include zircon, tourmaline, rutile, staurolite, garnet, apatite, magnetite, ilmenite, leucoxene, spinel, and brookite.

The most widespread of the mineral-aggregate particles in the sandstones of the Morrison Formation is chert; others are fragments of silicified limestone, silicified rock of unknown petrogenesis, quartzite, granite, aplite, felsite, altered tuff and pumice, and phyllite or mica schist.

The matrix of the sandstone is composed of various clay minerals, ground-up quartz, and feldspar. The clay minerals (not investigated in detail) include montmorillonite, kaolinite, mica clay, and chlorite clay in both specific and group senses, and mixtures between montmorillonite and mica clay, montmorillonite and chlorite clay, and mica and chlorite clay. The clays have been described by Keller (1962). In many rocks the matrix contains microlites of the cementing mineral which vary in size and suggest incipient replacement of the matrix by the cement.

The physical arrangement of mineral constituents, known as microstructure, depends on the relative proportions of grains, matrix, and cement in a rock. A rock which consists of all or nearly all of one of these constituents has a homogeneous microstructure. A special type is the mosaic microstructure in sandstone, which consists of quartz grains cemented by optically oriented intergrown quartz overgrowths. A rock in which proportions of all constituents are relatively large has a heterogeneous microstructure. The rocks of the Morrison Formation contain representatives of nearly all types of microstructure; the sandstones and claystones tend to have relatively homogeneous microstructures; mudstones and calcareous rocks commonly tend to have heterogeneous microstructures. Arrangements of isolated grains suspended in calcite or other cement are referred to as a grain-and-cement microstructure (figs. 9, 10).

MINERAL AND MINERAL-AGGREGATE GROUPS

Approximately 100 rock-forming minerals were recognized as constituents of the sandstone, siltstone, and limestone samples from the Morrison Formation, but only about 30 of these normally compose more than

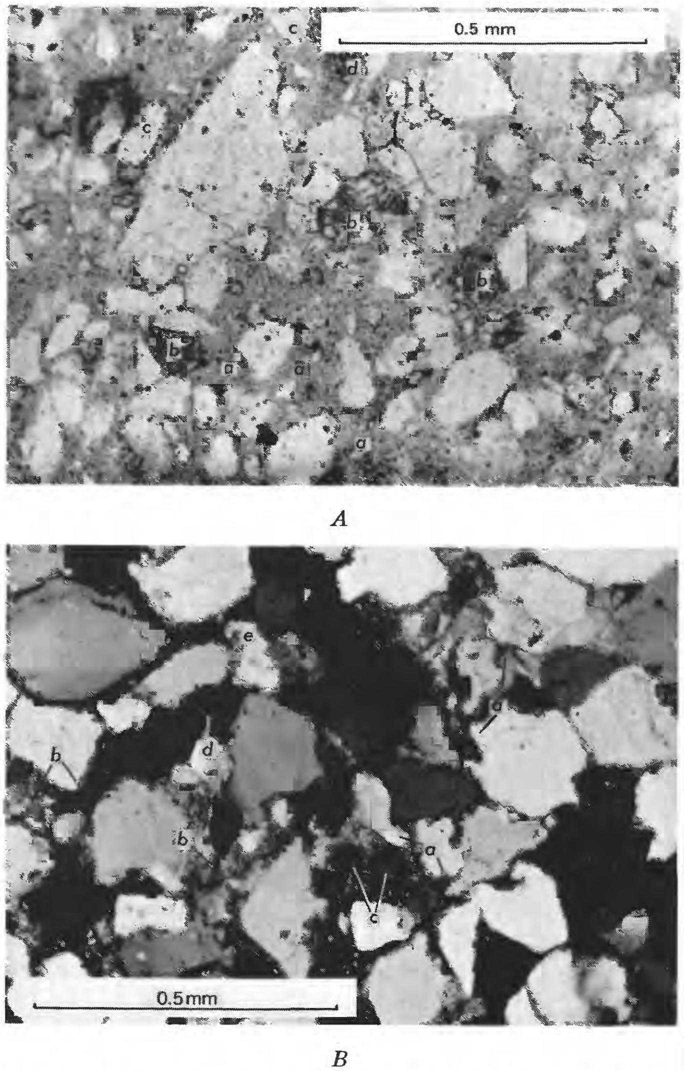

FIGURE 9.—Variation in arrangement of microstructural elements in the Salt Wash Member. *A*, Heterogeneous microstructure in sandy siltstone. Polarized light. Low degree of grain-to-grain contact; quartz grains seemingly suspended in an ashy-looking clay matrix consisting predominantly of mica-montmorillonite (hydrous mica?). Structural elements are *a*, mica-montmorillonite matrix; *b*, calcite microlitic clusters; *c*, grains of sodic plagioclase; *d*, pumice fragment which is nearly isotropic between crossed nicols; sample L456. *B*, Homogeneous microstructure in sandstone. Crossed nicols. A high degree of grain-to-grain contact augmented by the filling of interstices by optically oriented overgrowths on the quartz grains. Structure elements are *a*, overgrowths on quartz grains; *b*, calcite cement; *c*, ghosts of potassic feldspar grains replaced by calcite; *d*, partly isotropic silicified-rock fragment, probably tuff; *e*, penetration and replacement of quartz grain by calcite; sample L50.

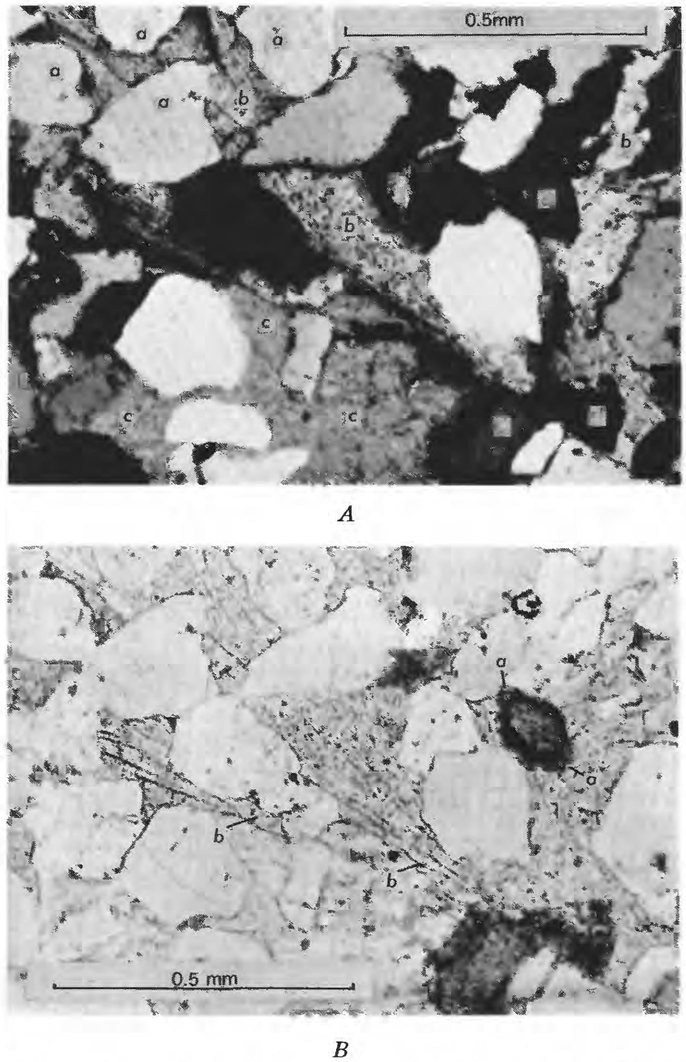

FIGURE 10.—Grain-and-cement microstructure in the Westwater Canyon Member, sample L792. *A*, Crossed nicols. Grains, some with overgrowths, are in contact or appear suspended in the minerals which form the cement. Structural elements are *a*, typical grains of quartz; *b*, barite in radial crystalline structure functioning as a cement; *c*, megacrystalline calcite functioning as a cement; *d*, potassic feldspar grains. *B*, Polarized light. Structural elements are *a*, overgrowths on a potassic feldspar grain; *b*, detail of contact between calcite (below) and barite (above).

0.2 percent of any of the rocks. For the Salt Wash Member, an average of all modal analyses indicates that 20 minerals compose 97 percent of the rock.

To decide which mineral constituents should be counted individually and which should be grouped for modal analysis, four factors were considered: (1) precision—possibility of good and consistent petrographic identifications; (2) speed—the rapidity with which particular mineral constituents could be identified and counted; (3) importance of detail—the particular minerals or rock fragments whose quantitative occurrence must be recorded if the objectives of study are to be realized; and (4) similarities in properties or occurrence that might cause misidentification or confusion. To study the variation in the major constituents and at the same time obtain data on the minor constituents, rock-forming minerals and mineral aggregates were classified in 19 mineral groups. These groups and the rock-forming constituents assigned to them are listed in table 4. The organization of table 4 anticipates the sections on rock classification which follow. Figures 11–16 illustrate the table.

TABLE 4.—*Classification of rock-forming constituents, Morrison Formation*

Mineral group	*Constituents*
Carbonates and sulfates	Calcite, dolomite, barite, gypsum (fig. 10).
Red iron oxides	Limonite, hematite, goethite, and other red, brown, and orange iron minerals.
Quartz grains and overgrowths.	Detrital quartz of any variety and optically continuous overgrowths (fig. 9).
Quartzite fragments	Fragments of metaquartzite, orthoquartzite, quartz schist, quartzose shale.
Chert, detrital	Grains of microcrystalline quartz with aggregate polarization; no isotropic areas.
Chert, authigenic	Authigenic microcrystalline quartz, present as interstitial fillings or replacements in the form of chert, chalcedony, or fibrous opaline chalcedony.
Mica	Flakes and books of biotite, muscovite, chlorite, vermiculite.
Chlorite and mica clays	Well-crystallized mica clay, mica-montmorillonite and chlorite clays, and glauconite (fig. 11).
Micaceous and mafic rock fragments.	Fragments of mica schist, micaceous phyllite, shale, basalt.
Heavy minerals (nonopaque).	Nonopaque minerals of specific gravity >2.90 (zircon, tourmaline, garnet).
Miscellaneous	Opaque interstitial material, unidentified minerals or mineral aggregates.
Tuff and felsite fragments	Grains of altered vitric, crystal, or lithic tuff; felsitic lava fragments; shards and pumice fragments (devitrified and now composed of microcrystalline quartz or calcite) (figs. 12, 13).
Silicified-limestone fragments.	Fragments of microcrystalline quartz containing silicified microfossils or other mineral or structural evidence of organic origin (fig. 14).
Silicified-rock fragments	Fragments of rocks of unknown petrogenesis consisting principally of microcrystalline quartz but containing areas of nearly isotropic silica, as well as clay, mica, or mafic mineral inclusions, either as original constituents or alteration products. The fine texture is suggestive of older volcanic or fine-grained metamorphic rocks. These source rocks were apparently silisified prior to erosion.

TABLE 4.—*Classification of rock-forming constituents, Morrison Formation*—Continued

Mineral group	*Constituents*
Potassic feldspar	Orthoclase, microcline, sanidine.
Plagioclase feldspar	Albite, oligoclase.
Kaolinitic clays	Kaolinite group of clays (fig. 15).
Montmorillonitic clays	Montmorillonite, poorly crystallized montmorillonite-mica, montmorillonite-chlorite, and chlorite-montmorillonite clays.
Altered ash	Heterogeneous mixtures of altered fine-textured volcanic debris including microcrystalline quartz and various clayey alteration products, vague shard structures, disintegrated tuff particles (fig. 16).

This grouping was devised to give the modal analysis data that are most meaningful petrologically and geologically, with greatest reliability in least time. It serves a special purpose in the analysis of sedimentary rocks such as those of the Morrison Formation, which, because they are composed of complex and widely divergent mixtures of mineral and rock fragments and clay matrices, are not amenable to the neat mineralogic and petrologic classifications applicable to many other kinds of rocks. Sulfates and carbonogic relationship, but for the following reasons: (1) ates are grouped, for example, not because of mineralthey are in general present as cementing components

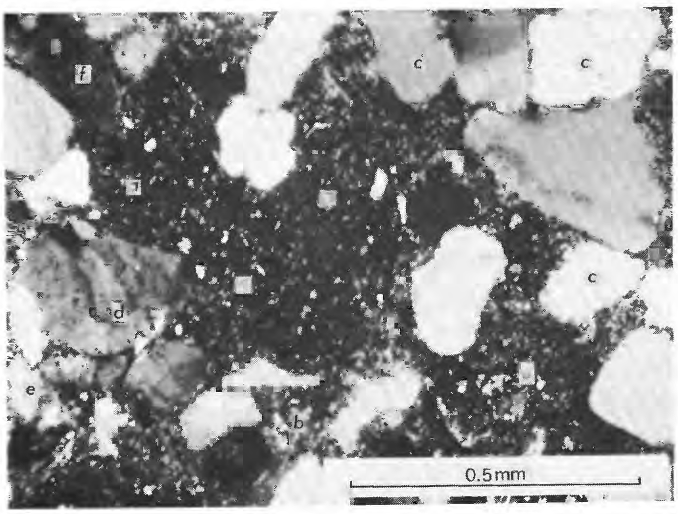

FIGURE 11.—Sandstone typical of the Morrison Formation. Crossed nicols. Structural elements are *a*, mica-montmorillonite clay; *b*, authigenic chert as an interstitial cement; *c*, quartz grains; *d*, fragments of quartzite; *e*, albitized grain of either sodic sanidine or sodic tuff; *f*, potassic feldspar. Contrast between *a* and *b* seems poor, but is characteristically so; there is no color difference. Salt Wash Member, sample L615.

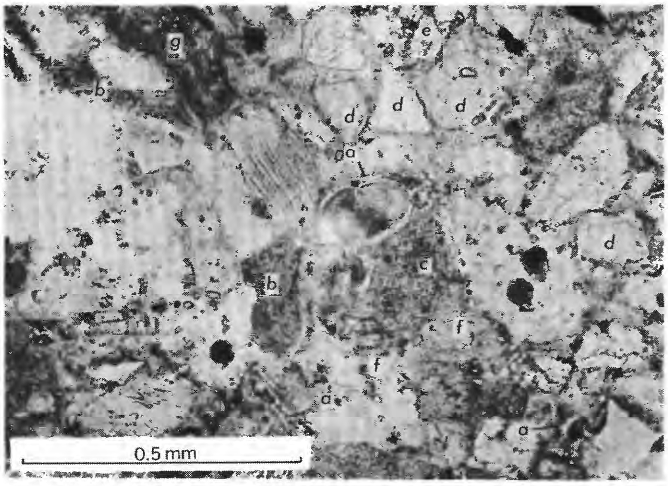

FIGURE 12.—Sedimentary tuff composed of altered shards, pumice fragments, glassy grains, and ashy matrix, together with quartz and feldspar fragments, Brushy Basin Member, sample L370. Polarized light. Structural elements are *a*, shards in which glass has altered to poorly crystallized nearly isotropic microcrystalline quartz; *b*, ashy matrix above and former vitric tuff fragment (resembling a mud pellet) altered to chlorite clay below; *c*, glassy fragment altered to poorly crystallized albite; *d*, quartz fragments probably of detrital origin; *e*, anhedral calcite crystal; *f*, sanidine; *g*, chloritized pumice fragment.

of the sandstones; (2) they are mostly secondary or authigenic; (3) as with calcite and dolomite, some are difficult to distinguish reliably in thin section; and (4) they are of little special diagnostic value in the interpretation of sources and depositional patterns of the sediments that became the Morrison Formation. In contrast, silicified-rock fragments and cherts, although perhaps almost identical mineralogically, are subdivided in as much detail as possible because they supply information on both provenance and distribution patterns. Similarly, volcanic components are also divided in detail.

ROCK-FORMING COMPONENTS

The mineral and mineral-aggregate groups just discussed are in turn grouped for purposes of rock classification into five major rock-forming components. These components and the rocks characteristic of them are listed in table 5. The assignment of kaolinite to the feldspathic components is based partly on the conclusions of Ross and Kerr (1931, p. 171–174), who named feldspars as the major source of kaolinite, and partly on work done for this report which confirms the strong association between kaolinite and highly feldspathic rocks. Montmorillonite is assigned to the volcanic components because much of the Morrison Formation is bentonitic, and because montmorillonite clay is associated with recognizable volcanic debris. Bentonites are generally regarded as alteration products of volcanic glass (Hewett, 1917; Ross and Hendricks, 1945, p. 64–68).

TABLE 5.—*Major rock-component groups*

Rock components	*Rock classification equivalents*
I. Chemical (cementing) components except silica.	I. Chemical and chemiclastic rocks.
a. Carbonates and sulfates	
b. Red iron oxides	
II. Siliceous components	II. Orthoquartzites.
a. Quartz grains	
b. Quartzite fragments	
c. Chert, detrital	
d. Chert, authigenic	
e. Silicified-rock fragments	
f. Silicified-limestone fragments	
III. Feldspathic components	III. Arkoses.
a. Potassic feldspar	
b. Plagioclase feldspar	
c. Kaolinitic clays	
IV. Dark mineral and mica components.	IV. Graywackes.
a. Mica flakes and books	
b. Chlorite and mica clays	
c. Micaceous and mafic rock fragments	
d. Heavy minerals (nonopaque)	
e. Miscellaneous	
V. Volcanic components	V. Tuffaceous rocks.
a. Tuff and felsite fragments	
b. Montmorillonitic clays	
c. Altered ash	

From thin-section data, rocks were classified according to a binary-logic design illustrated in figure 17. In general, the rock terminology follows Pettijohn (1949, p. 227) and Krynine (1948), but the treatment of the modifying terms and the clay may be original in this paper. As here used, and in accord with a suggestion of Pettijohn (1957, p. 381, footnote), limestone contains a minimum of 75 percent carbonates. The treatment of tuffaceous material follows that by Cadigan (1959, p. 534–536).

CLASSIFICATION PROCEDURE

Data from modal analysis of a sedimentary rock are applied directly to the classification procedure outlined in figure 17 without preliminary classification on the basis of texture or composition. Classification is based on composition only, to minimize the influence of genetic concepts which, as noted by Pettijohn (1957, p. 238), are the main source of conflict among proposed systems of sedimentary-rock classification. For greatest simplicity, the classification system represented by figure 17 "strains out" rock compositions in the order "chemical" rocks, sedimentary tuff series, graywacke series, akrose series, chert arenites, porcelanites, ortho-

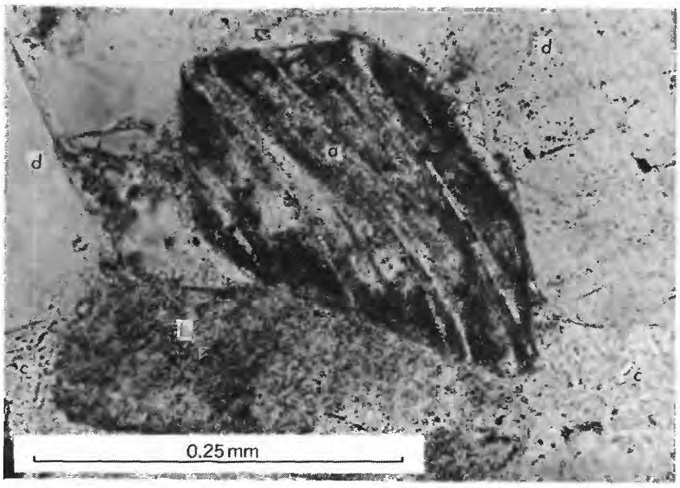

A

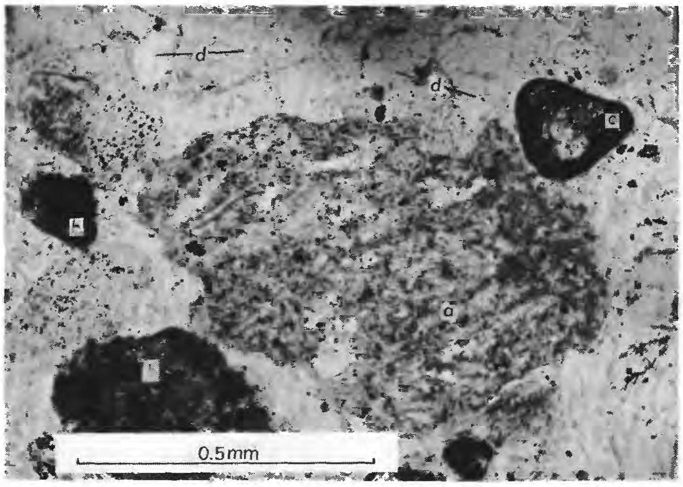

B

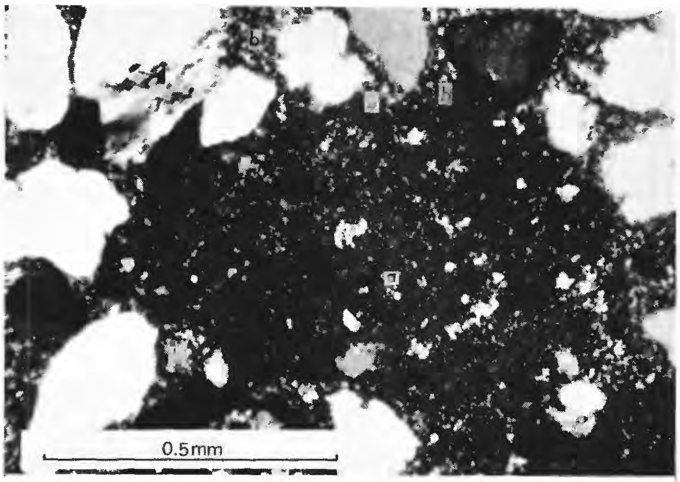

C

Figure 13.—Volcanic rock fragments in the Morrison Formation. *A*, Detrital grains in the Westwater Canyon Member, sample L197. Polarized light. Structural elements are *a*, devitrified rounded pumice fragment containing tubular vesicular structures which are now filled with poorly crystallized chert; *b*, detrital fragment of potassic feldspar; *c*, interstitial kaolinite clay; *d*, quartz grains. *B*, Detrital fragment of volcanic rock in the Salt Wash Member, sample L615. Polarized light. Structural elements are *a*, devitrified altered pumice fragment with elongated vesicular structures and crystal inclusions; *b* and *c*, rounded potassic feldspar grains; *d*, quartz grains. *C*, Pumice fragment of *B*. Crossed nicols. Structural elements are *a*, altered pumice fragment, nearly isotropic, composed partly of poorly crystallized quartz (chert) and montmorillonitic clay; *b*, interstitial chert cement, which shows better crystallization (more birefringence) than the altered pumice fragment.

quartzite series, and miscellaneous sedimentary rocks. These major compositions, except the sedimentary tuffs, are those of Krynine (1948), and the impure orthoquarzites and miscellaneous sedimentary rocks of the present report correspond to Krynine's "impure sandstones" and other rock types not covered by the classification system.

The binary system used here (fig. 17) is constructed to accomodate most sedimentary rocks under study on the Colorado Plateau, but it can readily be expanded to accommodate other kinds of rocks. The main principle of such a system of logic is that each decision (yes or no) limits the further possibilities to be considered. The classification of a rock—like many other things—is determined by negative as well as positive components; that is, by what the rock does not contain as well as by what it does contain. Thus, according to figure 17, a member of the graywacke series is a sedimentary rock that does not contain more than 74 percent of the components classed as Ia, or more than 49 percent of components Ib, or more than 24 percent components V, or more than 74 percent IVb, but does contain more than 24 percent of components of group IV. The last (group IV) are the essential components of a graywacke.

The names of rock types used here are those of common usage, which is not always consistent. The terms "orthoquartzite," "arkose," "graywacke," and "tuff" are used here in a purely compositional sense, in contrast with textural and structural terms such as sandstone, siltstone, claystone, and shale. A sandstone may have the composition of any one of the four rock types above, or may have some other composition, as of calcite. Following recent practice, orthoquartzite is used here in a compositional sense for rocks consisting principally of detrital quartz or other siliceous grains. It should not be confused with the old field term "quartzite," which, used in contradistinction to

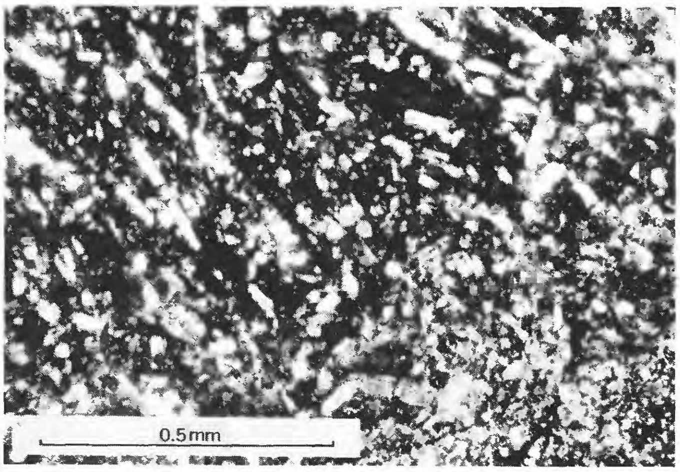

A

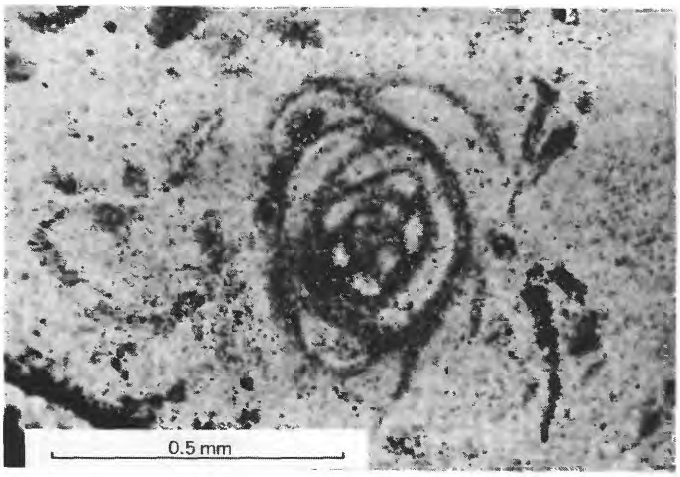

B

FIGURE 14.—Microfossils in silicified limestone fragments from the Salt Wash Member. *A*, Casts of filamentous algae(?) showing filaments with cell partings in a granule-size fragment of silicified limestone derived from some older sedimentary rock. Crossed nicols. Identified by E. B. Leopold (oral commun., 1961). Sample L614. *B*, Section of a foraminifera test present as a ghost structure in a pebble-size fragment of silicified limestone derived from an older sedimentary rock. Polarized light. Sample L614–2.

"sandstone," implies such thorough cementing that the rock breaks across the grains.[1]

In this paper, the term "orthoquartzite" is applied to sedimentary rocks containing more than 74 percent siliceous components, not more than 24 percent chemical components, not more than 24 percent dark-mineral and mica components, not more than 9 percent volcanic components, and not more than 9 percent feldspathic components. The siliceous components consist of at least 42 percent quartz and quartzite particles and overgrowths, and not more than 24 percent authigenic silica, nor more than 9 percent "chert" particles (groups IIc, e, f of classification). Using this definition, 12 samples from the Salt Wash Member are classified as orthoquartzites. Their mean composition is approximately 85 percent siliceous components, 7 percent chemical components, 5 percent feldspathic components, 1 percent dark-mineral and mica components, and 2 percent volcanic components.

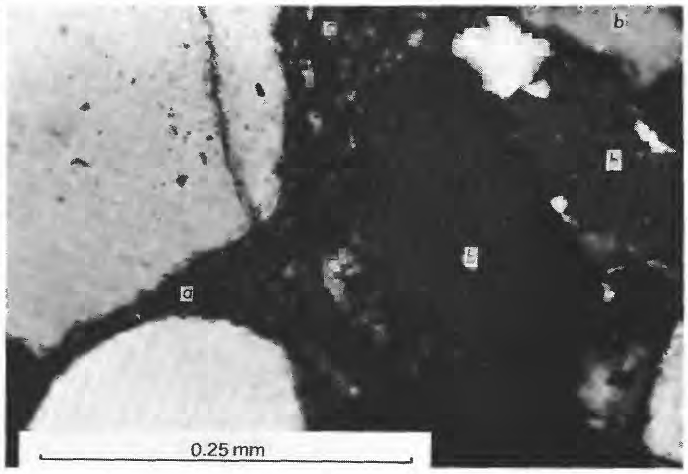

FIGURE 15.—Well-crystallized kaolinite clay, *a*, in sandstone of the Salt Wash Member. *b*, Quartz grains. Crossed nicols. Sample L826.

Although, as mentioned above, no genetic connotations are here attached to the compositional terms, the reader may, of course, make interpretations. The term "arkose" brings to mind as many associations of origin as does the term "granite." Most arkoses appear to result from the erosion of a rapidly rising granitic terrane, and the rapid accumulation of the derived sediments, mostly sandstone and conglomerates, in adjacent rapidly subsiding narrow basins. Tuffs, of course, imply volcanic activity. Most petrologists believe that orthoquartzites result mainly from slow deposition, reworking of quartzitic sediments, and effective weathering of the sediments prior to final burial.

[1] Unfortunately, the term "quartzite" has been used indiscriminately to classify both sedimentary and metamorphic rocks. Further confusion arises from the fact that many of the old "quartzites" such as the Shinumo Quartzite of Precambrian age (area of the Grand Canyon of the Colorado River) break across the grains, but have the composition of arkoses (more than 24 percent feldspathic components). A suitable solution may be the use of "orthoquartzite" to define the composition of a highly quartzitic sedimentary rock without regard to structure or hardness, the use of "metaquartzite" to define a highly quartzitic metamorphosed sedimentary rock, and the retention of "quartzite" as a field term referring to a very hard light-colored granular originally sedimentary rock of probably high quartz and silica content. Confusing the three quartzites does not introduce petrologic complications, in the opinion of the author, but calling an arkose a quartzite can produce highly erroneous petrologic interpretations or inferences.

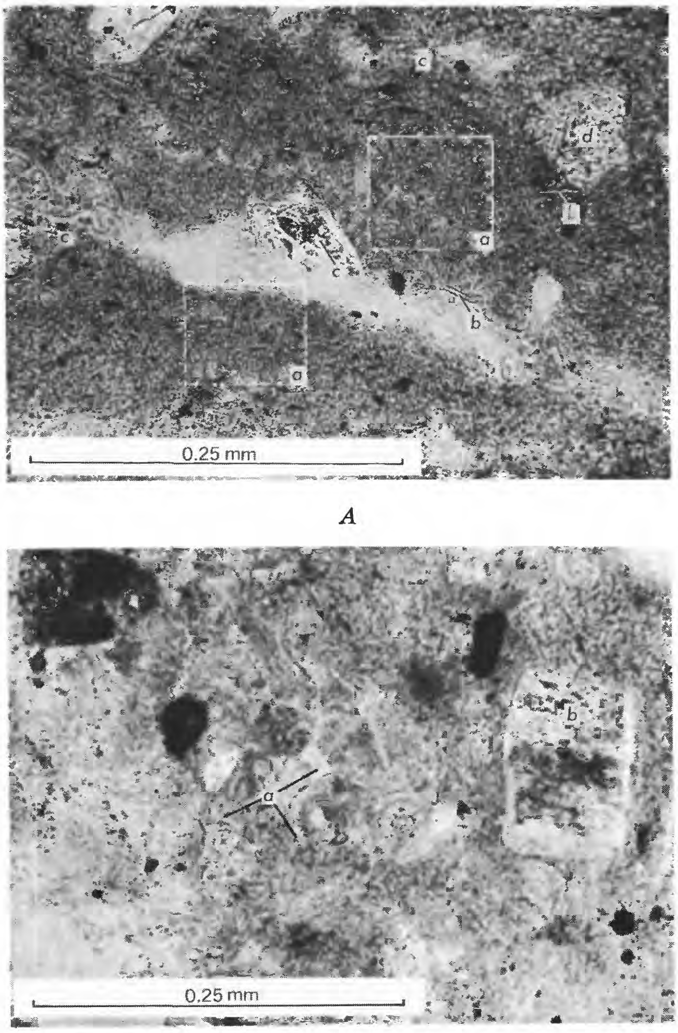

FIGURE 16.—Ash textures in mudstone. *A*, Salt Wash Member: *a*, felt-like structures, ghosts of fine glass shards which composed a fine volcanic ash now altered to montmorillonitic clay; *b*, cross sections of flakes of slightly altered biotite; *c*, sodic-feldspar fragments, slightly altered; *d*, fragment of albitized sodic pumice or tuff; sample L739. *B*, Bushy Basin Member: *a*, shard structure of ash particles that are now altered to montmorillonite-chlorite clay; *b*, subhedral particles of albite; sample L741.

LITHIFICATION AND DIAGENESIS

DIAGENETIC TRENDS

The term "diagenesis" is here used as defined by Sujkowski (1958, p. 2692) and Pettijohn (1957, p. 648, 649); it means all changes which occur in a sediment after deposition. No consistent diagenetic compositional trend in the Morrison Formation as a whole is discernible. The effects of lithification and diagenesis observed in some thin sections suggests the end product to be a quartzite composed of quartz grains with interlocking quartz overgrowths. In others, calcite has made such progress in filling interstices and replacing matrix and grains that a limestone could be the eventual product. In still others, chalcedony has replaced calcite and any remaining matrix to the extent that an arenaceous porcelanite is the end product. Arenaceous porcelanite, as used here, is a sedimentary rock consisting of sand or granules, and cement which is 25 percent or more authigenic chert or chalcedony. It may contain some calcite cement. On a fracture surface the cement is very hard and milky white (fig. 18).

Many other thin sections show no changes other than (1) alteration of the matrix from what was probably a glassy ash to a montmorillonitic clay, (2) slight alteration of sodic feldspar to small scalelike crystals of chlorite intergrown with the feldspar, (3) devitrification and alteration of tuff fragments, and (4) impregnation of the matrix with a small amount of authigenic chert. Thus, many kinds of diagenetic changes are evident, but no overall trend is readily apparent.

Cements are observed to replace all matrix materials, and in some thin sections they replace each other; but the matrix minerals show no evidence of being reconstituted from cementing material. Calcite replaces quartz overgrowths, and barite and chalcedony replace calcite. Iron oxide and other metallic oxides and sulfides can apparently replace everything. The greatest changes observed within the matrix are in the clay minerals, which are interpreted as principally products of diagenesis.

Diagenetic history of the montmorillonitic clays is generally as described by Ross and Hendricks (1945, p. 60–67). The trend of diagenesis seems to be from montmorillonite through the montmorillonite-mica clay mixtures to mica clay; or, in the presence of potassic feldspar or ash, through chlorite-montmorillonite to chlorite and kaolinite; or, in the absence or near absence of potassium and presence of abundant sodic feldspar or ash, to chlorite alone. Recrystallization of the clay minerals, possibly a continuing process, tends to obscure evidence of their origin.

ALLOGENIC AND AUTHIGENIC CONSTITUENTS

All thin sections of the sandstones contain evidence of diagnetic changes of various kinds. In the outline that follows, the principal original or allogenic detrital minerals of the rocks are listed first, according to grain size, and with each, the various diagnetic changes that have affected it. Next are the new or authigenic, chemically deposited, minerals resulting from diagenetic processes, and the changes that have in turn affected them. Many minerals are listed as both allogenic and

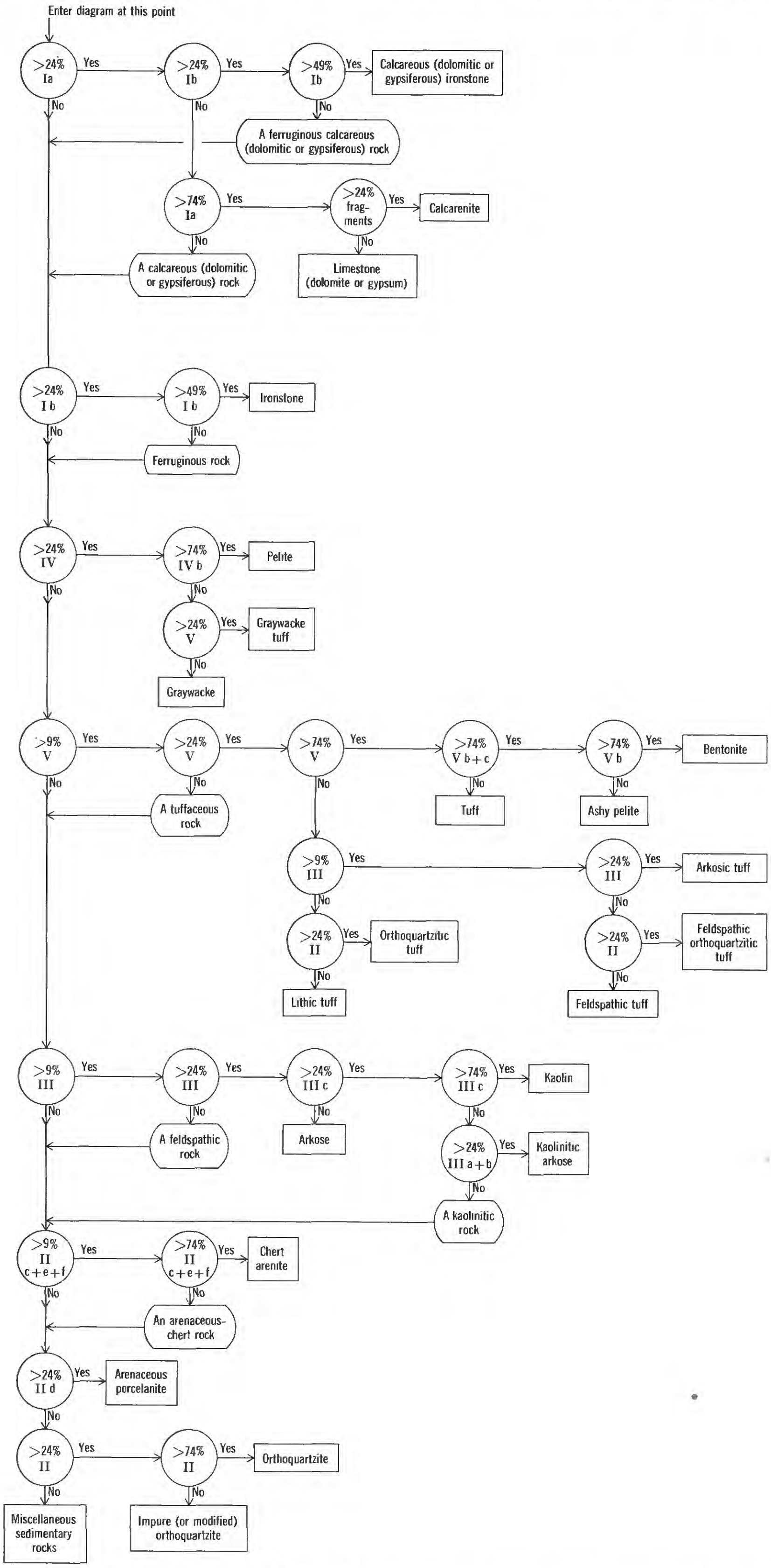

EXPLANATION

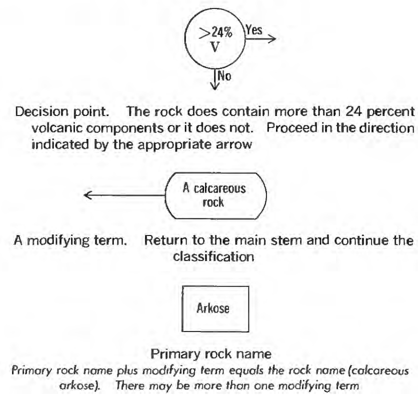

RECORDED ROCK COMPONENTS
(abstracted from table 5)

I. Cementing components except silica
   a. Carbonates and sulfates
   b. Red iron oxides
II. Siliceous components
   a. Quartz grains
   b. Quartzite fragments
   c. Chert, detrital
   d. Chert, authigenic
   e. Silicified-rock fragments
   f. Silicified-limestone fragments
III. Feldspathic components
   a. Potassic feldspar
   b. Plagioclase feldspar
   c. Kaolinitic clays
IV. Dark mineral and mica components
   a. Mica flakes and books
   b. Chlorite and mica clays
   c. Micaceous and mafic rock fragments
   d. Heavy minerals (nonopaque)
   e. Miscellaneous
V. Volcanic components
   a. Tuff and felsite fragments
   b. Montmorillonitic clays
   c. Altered ash

FIGURE 17.—Binary logic design of procedure for classifying sedimentary rocks of the Morrison Formation. Class limits taken from Pettijohn (1949, p. 227), P. D. Krynine (oral commun., 1952), and Cadigan (1959, p. 534–536).

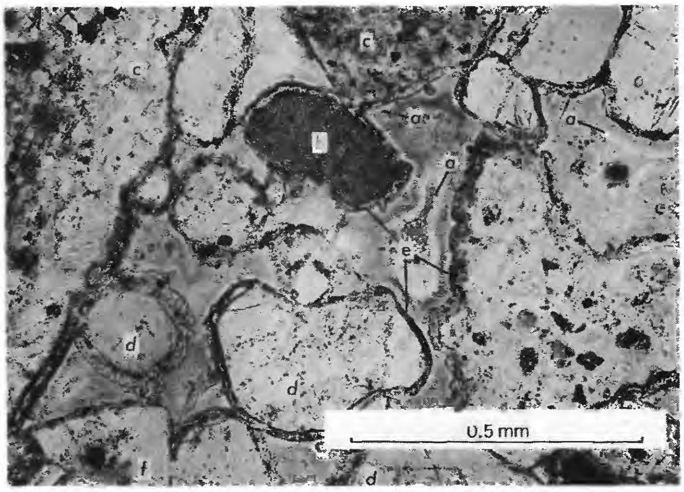

A

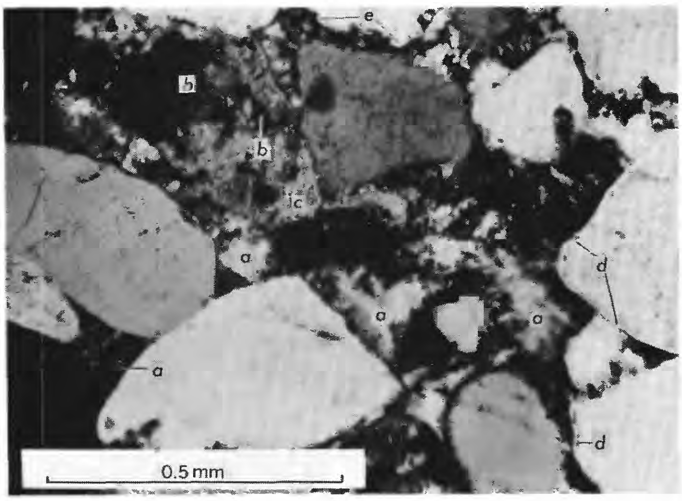

B

FIGURE 18.—Arenaceous porcelanite in the Brushy Basin Member. *A*, Rounded to subrounded fragments of quartz, chert, silicified limestone, and altered potassic vitric tuff, cemented with banded chalcedony; sample L686. Polarized light. *a*, Banded chalcedony forming interstitial cement; *b*, devitrified potassic tuff; *c*, silicified limestone; *d*, quartz; *e*, rims of chlorite-mica clay on detrital grains; *f*, chert. *B*, Rounded to subrounded fragments of quartz and feldspar, cemented with banded chalcedony; sample L225. Crossed nicols. *a*, Banded chalcedony forming interstitial cement—note fibrous or flamboyant extinction; *b*, dark spaces occupied by remnants of a feldspar grain almost totally replaced by calcite; *c*, calcite crystallized in the shape of the detrital feldspar grain; *d*, overgrowths on quartz grains; *e*, apparent destruction of overgrowths on quartz grain as well as corrosion of the grain itself, and replacement by interstitial chalcedony.

authigenic. In some rocks, evidence of allogenic or authigenic origin of many of the fine-grained minerals is clear cut, but in many others, the origin can be established only by inference based on experience. The term "replaced" is used in the physical sense only; it refers to the occupation by one mineral of an area in the thin section that microstructural relationships suggest was formerly occupied by another mineral.

Diagenetic changes affect texture as well as composition. The large-scale alteration of sand- and silt-size tuffaceous detritus to finer grained clay minerals results in a greatly increased proportion of clay- and silt-size particles in the tuff-bearing sediments. The alteration of feldspars to clay minerals produces similar effects. On the other hand, the replacement of clay minerals by chemically precipitated cements, the recrystallization of clays, and the addition of overgrowths to quartz grains all tend to increase grain size.

Outline of diagenetic changes

I. Allogenic constituents:
  A. Sand grains, granules, and pebbles:
    1. Quartz:
      a. Characterized by optically continuous overgrowths. In some rocks, overgrowth continued until the rock was completely cemented with quartz; in others, it stopped after formation of euhedral faces and terminations on the rounded grains, or formed only sawtoothed projections on the grains.
      b. Partly or completely replaced by calcite.
      c. Partly replaced by barite or metal oxides and sulfides.
    2. Chert, detrital:
      a. Partly replaced by calcite or, less commonly, by barite.
    3. Potassic feldspar:
      a. Partly or completely replaced by calcite or, less commonly, by barite.
      b. Etched, clouded, and partly removed by solution action.
      c. Characterized by optically nonoriented euhedral overgrowths (fig. 19).

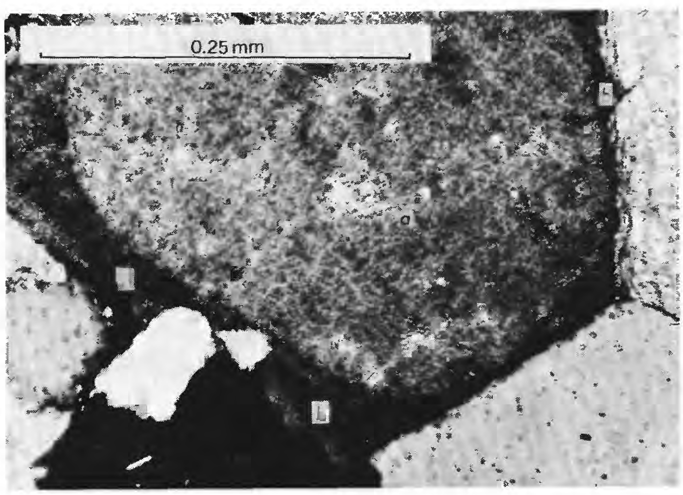

FIGURE 19.—Overgrowths on potassic feldspar in the Westwater Canyon Member, sample L792. Crossed nicols. *a*, Original rounded detrital grain; *b*, euhedral overgrowth, not in same optical orientation.

232-378 O - 67 - 3

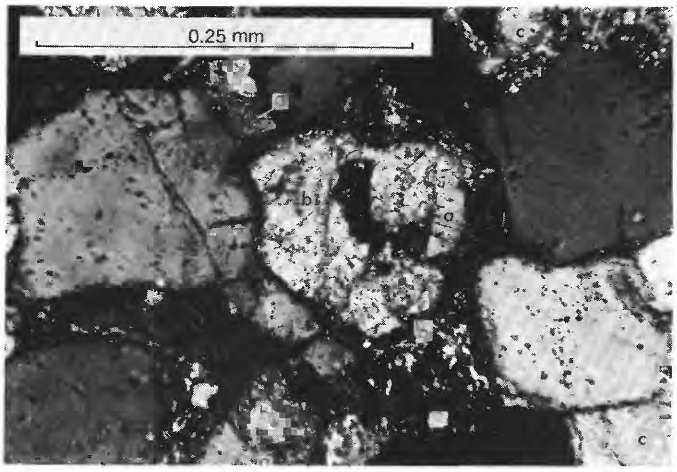

FIGURE 20.—Replacement of sodic feldspar by calcite in the Salt Wash Member, sample L626. Crossed nicols. *a*, Remnants of albite remaining in detrital grains that have been partly replaced by calcite although retaining the outward form of detrital grains; *b*, calcite that has replaced albite.

4. Sodic feldspar:
   a. Partly or completely replaced by calcite (fig. 20) or, less commonly, by barite.
   b. Partly altered to chlorite.
   c. Characterized by potassic-feldspar overgrowth (fig. 21).
   d. Etched, clouded, and partly removed by solution action.
5. Muscovite:
   a. Partly replaced by calcite.

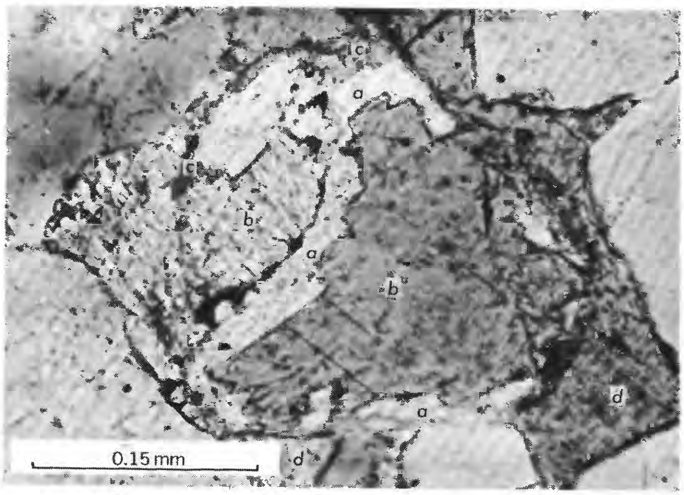

FIGURE 21.—Diagenetic changes in sodic feldspar in the Westwater Canyon Member, sample L792. Crossed nicols. *a*, Remnants of original detrital albite grain; *b*, calcite that has replaced part of feldspar grain; *c*, remnants of potassic-feldspar overgrowth shell around original grain; *d*, calcite outside boundary of the partly replaced detrital grain; this may be replaced potassic-feldspar overgrowth.

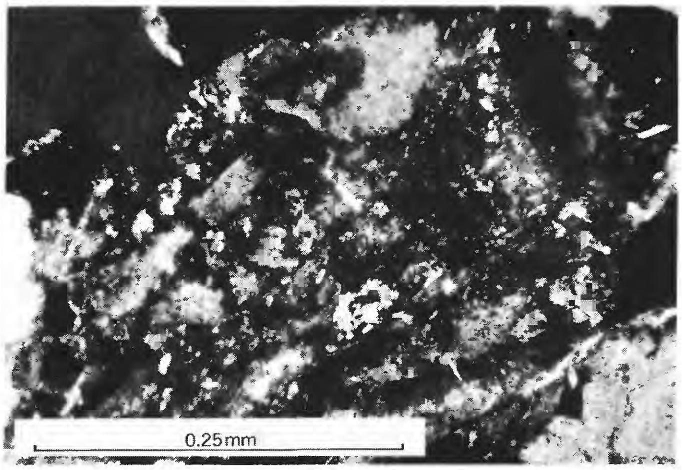

FIGURE 22.—Fragment of crystal tuff containing euhedral, anhedral, and almost indistinct crystals of potassic feldspar in a nearly isotropic groundmass of devitrified, silicified glass. Crossed nicols. Westwater Canyon Member, sample L750.

6. Biotite:
   a. Replaced by iron oxides.
   b. Altered to chlorite or vermiculite.
   c. Partly replaced by calcite.
7. Heavy minerals (for excellent descriptions and photographs, see Bowers and Shawe, 1961, p. 182–194):
   a. Ilmenite altered to leucoxene, anatase or red iron oxides.
   b. Magnetite altered to hematite or other iron oxides.
   c. Garnet and apatite etched by solutions.
   d. Some mafic minerals probably destroyed completely.
8. Potassic-tuff fragments:
   a. Devitrified, yielding an amorphous isotropic mixture shown by X-ray analysis to contain quartz and orthoclase, with preservation of flow structures, phenocrysts, and dust-like inclusions (fig. 22).
   b. Partly altered to montmorillonite or to a hydrous mica.
   c. Partly replaced by calcite or, less commonly, by barite.
9. Sodic-tuff fragments:
   a. Devitrified, yielding an apparently amorphous, nearly isotropic quartz matrix, with preservation of phenocrysts and other inclusions (fig. 23), or a poorly crystallized albite matrix.
   b. Partly altered to chlorite, chlorite-montmorillonite, montmorillonite, or a chlorite-hydrous mica clay.
   c. Partly or completely replaced by calcite or, less commonly, by barite.
10. Felsite fragments:
    a. Partly replaced by chlorite.
    b. Partly replaced by calcite.

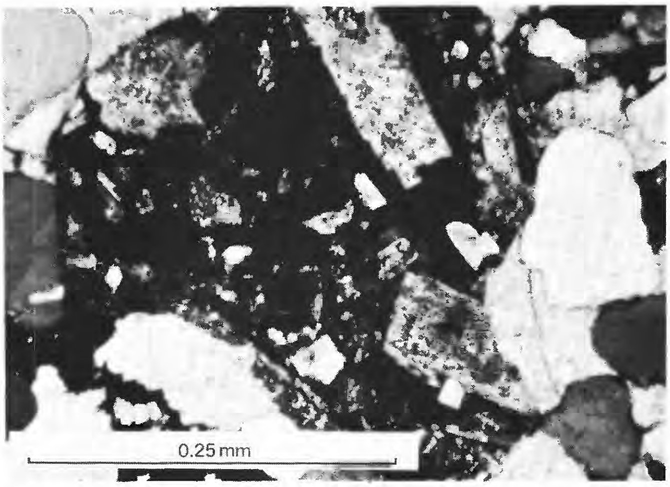

FIGURE 23.—Rounded fragment of crystal tuff consisting of mostly euhedral crystals of sodic feldspar in a nearly isotropic groundmass of devitrified silicified glass. Boundaries of lower part of fragment have been replaced by calcite cement. Crossed nicols. Brushy Basin Member, sample L3450.

11. Quartzite fragments:
    a. Partly or completely replaced by calcite or, less commonly, by barite.
12. Granite fragments:
    a. Feldspars and biotite differentially altered or replaced.
    b. Partly replaced by calcite.
13. Phyllite fragments:
    a. Partly replaced by calcite.
14. Silicified-limestone fragments:
    a. Partly replaced by calcite and possibly by chalcedony.
15. Silicified-rock fragments (some alteration predates deposition):
    a. Differentially altered and replaced because of heterogeneous composition.
    b. Partly replaced by calcite and possibly by chalcedony.

B. Clay-size fraction. (Note: All constituents of the clay-size fraction may have been replaced by cementing components such as calcite, quartz overgrowths, chalcedony, red iron oxides, or barite.):
1. Quartz:
    a. Partly or completely replaced by clay minerals.
    b. Removed by solution.
2. Potassic feldspar:
    a. Altered to, or replaced by, mica clay or kaolinite.
    b. Removed by solution.
3. Sodic feldspar:
    a. Altered to montmorillonite, montmorillonite-chlorite, or chlorite clays.
    b. Removed by solution.
4. Potassic volcanic ash:
    a. Altered to montmorillonite, hydrous mica group, or kaolinite clays.
    b. Devitrified and altered to chert with removal of potassium.
5. Sodic volcanic ash:
    a. Altered to montmorillonite, montmorillonite-chlorite, or chlorite clays (fig. 16).
    b. Devitrified and leached; silica precipitated as chert or chalcedony.
6. Mica clay and kaolinite:
    a. Recrystallized.
7. Montmorillonite:
    a. Recrystallized.
    b. Altered to mica-clay group (in the presence of potassium) or to kaolinite.
    c. Altered to montmorillonite-chlorite (in the presence of sodium and magnesium with potassium absent).
    d. Altered to a chlorite-mica clay mixture (in the presence of both sodium and potassium).
8. Chlorite:
    a. Recrystallized.
9. Mica-montmorillonite clay mixtures:
    a. Recrystallized.
    b. Altered to mica clay.
10. Mica-chlorite clay mixtures:
    a. Recrystallized.
11. Montmorillonite-chlorite clay mixtures:
    a. Altered to chlorite.

II. Authigenic constituents:

A. Mineral cements:
1. Calcite (and dolomite):
    a. Recrystallized.
    b. Replaced by chalcedony or barite (fig. 10).
2. Quartz overgrowths:
    a. Replaced by calcite or barite.
    b. Presumably rounded by solution action. Overgrowths on quartz grains cemented by chalcedony appear as thin rims without the usual conspicuous euhedral faces and crystal terminations; their outer surfaces parallel the surfaces of the quartz grains.
3. Barite (fig. 10):
    a. Replaced by chalcedony.
4. Iron oxides:
    a. Removed by solution.
    b. Recrystallized to clear crystals of hematite.
    c. Hydrolized.
5. Chalcedony:
    a. Recrystallized and banded (fig. 18).
6. Chert, authigenic (fig. 11):
    a. Recrystallized to resemble vein quartz.
    b. Replaced by calcite.
7. Leucoxene (interstitial):
    a. Recrystallized to anatase.
8. Anatase:
    a. Recrystallized to coarser euhedral crystals.
9. Epidote (interstitial):
    a. Recrystallized.

B. Clay minerals:
1. Kaolinite:
    a. Recrystallized to coarser euhedral octagonal plates and accordianlike crystal aggregates.

2. Mica clay:
   a. Recrystallized to form subhedral plates and highly birefringent fibrous rims on detrital particles.
3. Mica-montmorillonite clay mixtures:
   a. Altered to mica clay.
   b. Partially recrystallized to coarser grained mixtures.
4. Montmorillonite:
   a. Recrystallized to fibrous feltlike interstitial crystal aggregates.
   b. Altered to mica clay.
5. Chlorite:
   a. Recrystallized to more coarsely crystalline interstitial aggregates.
6. Montmorillonite-chlorite clay mixtures:
   a. Recrystallized.
   b. Altered to chlorite.
7. Mica-chlorite clay mixtures:
   a. Recrystallized and segregated in clusters.

TEXTURAL MEASURES

Particle size.—The study of the particle-size distributions in sandstone of the Morrison Formation consisted of mechanical analysis of rock samples as indicated in table 2, followed by calculations of the statistical measures for each sample. All samples were treated by the same procedures, unless otherwise noted; thus, the computed measures of the grain-size distributions are comparable. To determine the grain-size distributions of the samples, sand-size particles were divided into the conventional size classes by means of calibrated sieves. The size distribution by classes of silt and clay particles was determined by the pipet method described by Krumbein and Pettijohn (1938, p. 165–172). The pipet method is a sedimentation method which measures particle size in terms of settling velocity. The size classes used are those originally defined by Udden (1914, p. 657–658), revised by Wentworth (1922), and adopted with further refinements by the National Research Council (1947, p. 937). Table 6 lists the classification of Udden (1914), the classification adopted by the National Research Council, and the class limit value in millimeters and in the phi scale. The millimeter values of the class limits progress (increase) and regress (decrease) geometrically. The phi values, which progress and regress algebraically, are negative logarithms to the base of two ($-\log_2$) of the millimeter class limits. A millimeter-phi scale conversion table was published by Page (1955). Discussions of concepts of size of sedimentary particles may be found in the literature (Wadell, 1932, 1934; Pye, 1943; Pettijohn, 1949).

Statistical measures computed for grain-size distributions of all Morrison samples were given by Cadigan (1967).

TABLE 6.—*Systems of grain-size classification of sediments and their class limits, expressed in millimeters and phi scale equivalents*

Class limits (mm) [1] From	Class limits (mm) [1] To, but not including	Udden's classification (1914)	Krumbein's class limits phi scale (1934) [2]	National Research Council classification (1947)
*2048	4096		−12	Very large boulders.
*1024	2048		−11	Large boulders.
*512	1024		−10	Medium boulders.
*256	512		−9	Small boulders.
128	256	Large boulders	−8	Large cobbles.
64	128	Medium boulders	−7	Small cobbles.
32	64	Small boulders	−6	Very coarse gravel.
16	32	Very small boulders	−5	Coarse gravel.
8	16	Very coarse gravel	−4	Medium gravel.
4	8	Coarse gravel	−3	Fine gravel.
2	4	Gravel	−2	Very fine gravel.
1	2	Fine gravel	−1	Very coarse sand.
.5	1	Coarse sand	0	Coarse sand.
.25	.500	Medium sand	1	Medium sand.
.125	.250	Fine sand	2	Fine sand.
.0625	.125	Very fine sand	3	Very fine sand.
.031	.0625	Coarse silt	4	Coarse silt.
.016	.031	Medium silt	5	Medium silt.
.008	.016	Fine silt	6	Fine silt.
.004	.008	Very fine silt	7	Very fine silt.
.002	.004	Coarse clay	8	Coarse clay size.
.001	.002	Medium clay	9	Medium clay size.
.0005	.001	Fine clay	10	Fine clay size.
.00025	.0005		11	Very fine clay size.

[1] All limits except those starred (*) are from Udden (1914).
[2] Phi scale is arranged to show upper and lower class limits of each textural class. Thus, medium sand lies between 2 phi and 1 phi. Millimeter class limits are 0.250 and 0.500 mm.

The basic tabulation of the grain-size distribution of a sample is shown in table 7. All computations of statistical measures were concerned with the logarithmic (phi) grain-size distribution. Krumbein (1936, p. 37)

TABLE 7.—*Weight and percent of particles in each grain-size class in a sandstone sample, L338*

(1) Size-class limits (phi) [1]	(2) Class midpoint (phi)	(3) Weight (grams)	(4) Percent	(5) Cumulative percent
−1.000– −1.999	−1.500	3.65	3.86	3.86
.000– −.999	−.500	6.20	6.57	10.43
1.000– .001	.500	18.61	19.72	30.15
2.000– 1.001	1.500	47.91	50.76	80.91
3.000– 2.001	2.500	9.51	10.08	90.99
4.000– 3.001	3.500	1.88	1.99	92.98
5.003– 4.001	4.500	.85	.91	93.89
6.000– 5.001	5.500	.91	.96	94.85
7.000– 6.001	6.500	1.22	1.29	96.14
8.000– 7.001	7.500	1.25	1.32	97.46
9.000– 8.001	8.500	.79	.84	98.30
10.000– 9.001	9.500	1.60	1.70	100.00

[1] Millimeter equivalents and descriptive textural terms may be determined from table 6.

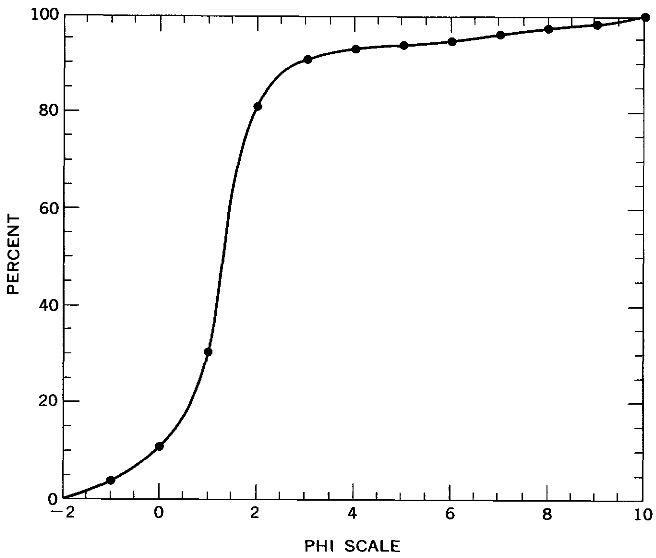

FIGURE 24.—Cumulative curve of the phi grain-size frequency distribution of sample L338, Brushy Basin Member. Frequency is given in percent by weight plotted over size in phi units. Data from table 7.

showed that particle-size distributions tend to be logarithmic and that arithmetic particle-size distributions are highly skewed. Computed measures for arithmetic distributions would be highly unrepresentative and of little use for either descriptive or interpretive purposes.

A cumulative curve (fig. 24) illustrates the logarithmic grain-size distribution of a sandstone. The curve represents the cumulative-frequency percentage data (table 7, col. 5) of a grain-size distribution plotted over the phi size scale.

The cumulative curve is useful for determining the percentage of grains that are of a given size or coarser. This size value is called a percentile. Percentile values may be determined by reading the phi size value directly below the intersection of the percent line and the cumulative curve. For example, in figure 24 the 30th percentile is approximately 1.0 ϕ, which is the $-\log_2$ of 0.5 mm. This signifies that 30 percent of the grains by weight are 0.5 mm or coarser in size.

The statistical measures obtained were (1) the mean, standard deviation, skewness and kurtosis of the logarithmic grain-size distribution, which were determined by moment computation; (2) the modal grain size estimated from the frequency distribution of the weights of sieve retents and pipet aliquots; and (3) the median size (ϕ_{50}), and the ϕ_2, ϕ_5, ϕ_{16}, ϕ_{84}, ϕ_{95}, and ϕ_{98} (phi) percentiles determined graphically from the cumulative-frequency curves. Computations of the first four moments and derivation of the mean, standard deviation, skewness, and kurtosis followed the method detailed by Krumbein and Pettijohn (1938, p. 250–252).

TABLE 8.—*Computed statistical measures of the phi grain-size distribution of sample L338*

Properties of the grain-size distribution	Phi units	Millimeters
Measures of the "average" grain size:		
Mean diameter	1. 600	0. 330
Modal diameter	1. 600	. 330
Median diameter	1. 433	. 370
Standard deviation	1. 874	
Skewness	1. 091	
Kurtosis	6. 487	
Percentiles:		
ϕ_2	−1. 20	
ϕ_5	−. 70	
ϕ_{16}	. 47	
ϕ_{50}	1. 43	
ϕ_{84}	2. 15	
ϕ_{95}	6. 20	
ϕ_{98}	8. 50	

The mean, modal, and median grain sizes are estimates of the "average" grain size. The mean is the computed average size. The modal size is the most plentiful, by weight; it more often coincides with the grain size estimated in the field than does the mean. The median size is the middle size of the distribution—half the grains by weight are finer, and half are coarser. The manner of reporting the statistical measures is shown in table 8. The listed percentile values are used in keeping a permanent record of the size distribution, after the suggestion of Inman (1952, p. 138).

Sorting.—The standard deviation, skewness, and kurtosis—computed measures of the grain-size distribution—were used as measures of average and internal sorting. Sorting is a geologic concept of the effect of the sorting process (described by Gilbert, 1914, p. 152) on a sediment. A medium of sediment transport, such as moving water or air, tends to exert a size-grading influence on the sedimentary material transported and deposited. The degree to which the grading action has been carried out prior to final deposition and burial of the sediment is the degree of sorting. The standard deviation of a grain-size distribution (table 9) is a good measure of the overall

TABLE 9.—*Classification of sorting of the grain-size distribution of sediments based on the phi standard deviation*

Degree of sorting	Standard deviation (phi distribution)	Spread of central 68 percent of distribution in grade-size units (phi)
Very well sorted	0. 000–0. 499	0. 00–0. 99
Well sorted	. 500– . 999	1. 00–1. 99
Moderately well sorted	1. 000–1. 499	2. 00–2. 99
Moderately sorted	1. 500–1. 999	3. 00–3. 99
Poorly sorted	2. 000–3. 999	4. 00–7. 99
Unsorted	≧4. 000	≧8. 00

average sorting of the sediment represented by a disaggregated sample (Krumbein, 1936, p. 43).

Skewness.—As discussed in another paper (Cadigan, 1961), the skewness is a measure of the contrast in internal sorting between the fine and coarse ends of the particle-size distribution (table 10); positive values indicate poorer sorting in the finer material; negative values indicate poorer sorting in the coarser material.

TABLE 10.—*Classification of relative skewness of the grain-size distribution of sediments based on the phi skewness*

Degree of skewness	Skewness coefficient (phi)
Negatively skewed	≦ −0. 100
Symmetrical	−. 099–0. 099
Slightly skewed	. 100– . 999
Moderately skewed	1. 000–1. 999
Highly skewed	≧2. 000

Kurtosis.—Kurtosis (peakedness) is a measure of the contrast in internal sorting between the average of the extremes of the size distribution and the center (table 11). Internal sorting differences are those occurring in different parts of the particle-size distribution of a sediment. A highly peaked size distribution is one in which the center part of the distribution is better sorted than the average of the extreme parts. (See Cadigan, 1961.) Skewness and kurtosis values represent the measure of deviations from the theoretically normal, or Gaussian, distribution. Thus, zero values for both would indicate that the particle sizes for a particular sediment were normally distributed, and that the degree of sorting in all parts of the particle-size distribution is about the same.

TABLE 11.—*Classification of relative peakedness of the grain-size distribution of sediments based on the phi kurtosis*

Degree of peakedness	Kurtosis
Flattened (platykurtic) distribution	≦ −1. 00
Normal (mesokurtic) distribution	−1. 00– . 99
Peaked (leptokurtic) distribution:	
Moderately peaked	1. 00– 9. 99
Highly peaked	10. 00–19. 99
Very highly peaked	≧20. 00

SALT WASH AND RECAPTURE MEMBERS OF THE MORRISON FORMATION

The Salt Wash Member (fig. 4) was deposited in the northern part of the region synchronously with the Recapture Member, which occupies the southern part of the region. The Recapture in part conformably overlies and in part intertongues with the Salt Wash in the Four Corners area, where both are present. Together they form the lower part of the Morrison Formation in the region of this study.

STRATIGRAPHIC RELATIONS AND CHARACTER

The stratigraphic, compositional, and textural relations of the Salt Wash and Recapture Members are such that for purposes of petrologic study it is convenient to treat them together as a single sedimentary unit. The two members form an alluvial-plain deposit consisting of two abutting and partly coalescing but separate alluvial fans, each of which tends to lean northward at the very irregular line of contact. The north edge of the Recapture is thus superposed on the south edge of the Salt Wash.

The Salt Wash and Recapture Members are both sedimentary units of continental origin. The Salt Wash is characterized by two general types of lithology: (1) white to pale-brown sandstone strata that are thick bedded to massive, ledge forming, resistant, lensing, and cross stratified or structureless, and (2) greenish-gray to dark-reddish-brown siltstone, mudstone, and minor claystone strata that are thick bedded, poorly resistant, and bench forming. The sandstone bedding structures show many scour surfaces which are associated with pebbles and clay galls, particularly at the base of ledge-forming sandstone beds.

The Recapture Member is similar to the Salt Wash but is characterized especially by thick-bedded white, pale-brown, or pale-reddish-brown sandstone that is structureless and ledge forming; and by thick-bedded poorly resistant bench-forming greenish-gray to gray-tinged, dark-reddish-brown siltstone and bentonitic mudstone and claystone. The unit has an overall brownish cast. The sandstone strata form either thick block-fractured irregular-sized ledges, or massive (in some places structureless) convex-weathered "slick-rim" type ledges. The block-shaped crossbedded ledges tend to contain or overlie truncation and scour surfaces that are associated with thin lensing festoon beds or laminae containing pebbles, granules, and pale-grayish-green or grayish-brown clay galls. Most of the convex-weathered beds, in contrast, are seemingly conformable with underlying and overlying strata; scour surfaces where present are obscured or appear as a stylolitic contact in an unindented thick to massive ledge.

SCOPE OF SAMPLING

Sample density for the Salt Wash Member is greater in the uranium-ore-producing mining districts than in the "barren" parts of the region. Sandstone samples were collected from the ledge-forming strata; samples of fine-textured rock were collected from the bench-forming strata between the ledges. Sampling was confined to the sandstones in most sample localities.

Sampling of the Recapture Member was done with appropriate spacing, but the general outcrop pattern does not permit adequate regional coverage. Almost all samples are of sandstone.

COMPOSITION OF SANDSTONES

The sandstone strata include rocks of the sedimentary orthoquartzite, tuff, and arkose series in the Salt Wash Member, and of the orthoquartzite and arkose series in the Recapture Member. The most common varieties are orthoquartzites, feldspathic orthoquartzites, and tuffaceous orthoquartzites. The sandstones are composed of grains, matrices, and cements which vary in kind and proportion from one part of the region to another.

The grains are particles of quartz, potassic and sodic feldspars, altered potassic and sodic tuffs, chert, quartzite, silicified limestone, and silicified metamorphic or igneous, possibly volcanic, rocks. Heavy-mineral grains (excluding high-density cement and ore minerals) represent less than 0.25 percent by weight, of most of the sandstones in the Salt Wash, and less than 0.50 percent in the Recapture. They consist largely of magnetite-ilmenite, leucoxene, and related titanium minerals, and zircon, tourmaline, garnet, staurolite, epidote, rutile apatite, and minor biotite and vermiculite. This assemblage of heavy minerals is also common to the sandstones of the other members of the Morrison Formation.

The matrix of the sandstone is composed of clay minerals that are dominantly in the mica-montmorillonite mixed clay series (fig. 11), and to a lesser extent in the mica, chlorite, kaolinite, and montmorillonite clay groups. Various other intermixtures of these minerals are also present.

The cement of the sandstones is composed dominantly of calcite and authigenic quartz with minor proportions of dolomite, barite, iron oxide, and gypsum.

Quartz and other silica minerals.—The dominant mineral in the Salt Wash and Recapture Members of the Morrison Formation is detrital quartz, most of which seems to have been derived from igneous and metamorphic rocks and contains minor inclusions of rutile, apatite, zircon, and dustlike material. The grains are rounded to subrounded in the coarser sizes and subrounded to angular in the finer sizes. Detrital quartz occurs also in the form of microcrystalline aggregates in subrounded chert grains and in angular to subangular silicified-rock fragments. Silicified-limestone fragments show replacement of the carbonate minerals and fossil shell fragments by microcrystalline quartz. Microcrystalline quartz and amorphous silica have replaced in various degrees the glassy matrix of vitrophyric extrusive igneous rock fragments, as well as various unclassified silicified-rock fragments.

Interstitial silica occurs as authigenic optically continuous overgrowths on detrital quartz grains, as fibrous opaline aggregates with flamboyant or radial optical extinction, as microcrystalline growths with aggregate polarization like chert, and, uncommonly, as interstitial banded chalcedony. In some rocks, overgrowth of authigenic quartz continued until nearly pure quartzites were produced. In these, detrital quartz grains are cemented tightly with quartz overgrowths to give a mosaic appearance between crossed nicols. In contrast, detrital quartz grains in many sandstones have only a thin skin of authigenic quartz over the abraded surfaces.

Feldspar.—Feldspar mineral grains include the potassic varieties orthoclase and microcline and the sodic varieties albite and oligoclase. The grains are at least as rounded as those of quartz and perhaps more rounded in the finer sizes. Microcline grains are the least altered, and albite grains the most altered. Albite evidently alters readily to chlorite and is the most readily replaced by carbonate minerals. Potassic feldspars are twice as plentiful as sodic feldspars in the average sandstone.

Tuffaceous fragments.—Tuffaceous fragments include particles of altered rhyolite; altered potassic and sodic vitric, crystal, and lithic tuffs; and vitrophyric rock and pumice fragments of probable silicic, alkalic volcanic origin (figs. 12, 13). All grains have probably been devitrified, but in many rocks the matrices of potassic vitric tuff particles still appear isotropic and show faint flow lines and vesicular structures; under the microscope, pumice cross sections appear as rounded particles containing shard structures surrounded by a clayey matrix. The devitrified crystal tuff and vitrophyric rock fragments, in some rocks partly altered to clay, contain feldspar phenocrysts in a nearly isotropic matrix; in other rocks, similar fragments are completely altered to montmorillonite, montmorillonite-mica, or chlorite clay. Lithic tuff grains are aggregates of quartz and feldspar crystals, microcrystalline quartz, mica, alteration products, and carbonate microlites. Grains in which microcrystalline quartz is dominant grade into those that are classed as silicified-rock fragments of unknown petrogenesis. In some sandstones of the Salt Wash Member, particularly the clayey ones, the matrix is composed of a montmorillonite-mica clay mixture, silt-size highly angular fragments of quartz and plagioclase, and silt-size aggregates of authigenic microcrystalline quartz. The contrast in angularity and relief between the brecciated silt-size quartz in the matrix and the more rounded sand-size quartz grains, the authigenic silica, and the character of the minerals suggest that the materials in this type of matrix are of volcanic origin. Clayey matrices in some sandy mudstones show feltlike structures, ghosts of fine glass shards which originally composed a fine valcanic ash and have altered to montmorillonite clay (fig. 16).

Clay minerals.—Mica clay, and mica-montmorillonite and montmorillonite-mica clay mixtures, occur respectively as micaceous-looking rims around grains and as composite continuous fibrous matrix or dull semiisotropic aggregates of platelets. In red claystone, mudstone, or sandstone, the mica and mica-montmorillonite clays are clouded owing to impregnation by very fine red iron oxide (hematite?) crystals. Montmorillonitic clays are nearly isotropic, but between crossed nicols they show a swirled structure of optically oriented microcrystals. Chlorite clay, when crystallized, is generally of the transparent bright scalelike pale-green pennine(?) or of the fibrous colorless clinochlore(?) varieties; in many rocks it is intermixed with other clay minerals; in the Recapture Member, especially, chlorite-montmorillonite-mica mixtures are common. Kaolinite is very common as a colorless well-crystallized interstitial clay of high relief (fig. 15). Any of these clays may be found together in the same rock. Pebbles, granules, and grains of clay, found very commonly in the sandstone, contain the same clay minerals as the sandstone.

Heavy minerals.—The most plentiful heavy minerals are those of the iron oxide–titanium oxide group. Magnetite, magnetite-ilmenite, and ilmenite occur as black to brown rounded to subangular opaque grains. Leucoxene occurs as white opaque well-rounded grains or as rims, halos, or seams in ilmenite and ilmenite-magnetite grains. Anatase occurs in pale-yellow cloudy amorphous-looking interstitial anhedral forms or in clear yellow to blue euhedral tabular crystals. The anatase is probably all authigenic. Based on semiquantitative spectrographic analyses of the heavy-mineral fraction, the titanium content of the heavy minerals appears to be relatively constant regardless of the variation of the proportions of dark opaque minerals to leucoxene or anatase (L. B. Riley, oral commun., 1951). Thus, the anatase, authigenic in its present form, was probably derived from detrital heavy minerals and does not represent a volumetric addition to the present suite of heavy minerals.

Zircon is of several varieties. Most common is the rounded clear colorless zircon; others are euhedral zircons in elongated dipyramidal prisms, rounded clouded metamict zircons, and rounded pink to light-purple clear zircons. Many of the euhedral zircons show zoning and crystal intergrowth, and many are pink.

Tourmaline is in rounded grains and in many pleochroic color combinations; the three main varieties, schorlite, elbaite, and dravite, occur in about equal proportions.

Garnet, variety grossularite(?), occurs as clear colorless to pink grains. Some grains show building-block forms (irregular arrangements of cubes) attributed to etching (Bowers and Shawe, 1961, p. 189); many grains are rounded and subrounded.

Staurolite occurs as angular to subangular or accordion- or splinter-shaped pale-golden grains; the accordion shape is attributed to probable solution action (Milner, 1952, p. 342). Epidote appears to be restricted to certain locations and occurs as subrounded lemon-yellow to greenish-yellow grains. Rutile occurs in well-rounded reddish-brown or golden-brown grains. Apatite is apparently restricted to certain strata; it may be abundant in one bed and sparse or absent in an adjacent bed. It occurs as colorless rounded oval grains, or, uncommonly, as euhedral or subhedral short prismatic or hexagonal grains.

Biotite and vermiculite occur in dark-brown, brown, and green contorted bundles or in flakes. Some flakes are almost colorless as a result of a loss of iron. Some of the mica is altered to chlorite, and some is altered to or replaced by iron oxide, which remains as pseudomorphs of the mica bundles.

Acid-soluble minerals.—Calcite, where present in relatively large proportions, forms continuous clear cement throughout a sandstone or appears in isolated subhedral patches. There is good evidence that calcite has replaced detrital feldspar grains. (See fig. 21.) Partly destroyed or skeletal feldspar grains are found in contact with calcite or engulfed by it, and optically anomalous grain-shaped ghosts are present in the calcite. (Some of these ghosts—those of potassic feldspar—absorb small patches of cobaltinitrite stain.) Calcite replaces both grains and matrix, as shown by the presence of corroded quartz grains suspended in calcite where matrix is almost totally absent. Calcite occurs in forms ranging from microlitic aggregates to the megascopic "sand crystals." It commonly appears to replace quartz overgrowths, but it is replaced in turn by fibrous flamboyant microcrystalline quartz.

Dolomite has been recognized in clay matrices or is associated with calcite as isolated rhombs; it commonly contains fine inclusions which give it a dusty appearance.

Barite occurs as colorless crystal aggregates that are interstitial, slightly radiating, bladed, and optically continuous. The aggregates appear to be paragenetically late; the barite tends to replace calcite, and as seen in thin section it has a higher average index of refraction than calcite (fig. 10).

Red iron oxides, although present in nearly all sandstones, are usually restricted to isolated interstitial patches; they impregnate clays to some extent in red rocks, and stain and impregnate carbonate rocks. Their role as cements is not significant.

Gypsum is common as a cement in the areas where beds of gypsum occur in the basal part of the Salt Wash Member. Some crystalline gypsum contains inclusions of silt-size euhedral authigenic quartz crystals.

Microstructure.—Thin sections of sandstone in the Salt Wash and Recapture Members show much variation in microstructure, which ranges from homogeneous to heterogeneous. The terms "homogeneous microstructure," for sandstones composed of grains in contact with others to a maximum extent (fig. 9*B*), and "heterogeneous microstructure," for sandstones composed of grains suspended in matrix with a minimum of intergranular contacts (fig. 9*A*), are used in an unrestricted sense. No attempt was made to divide the sandstones into separate populations on the basis of microstructure. In the examples shown in figure 9, the homogeneous sandstone is composed of 90 percent grains, 9 percent cement, and 1 percent matrix; the heterogeneous sandstone is composed of 65 percent grains, 0.5 percent cement, and 34.5 percent matrix. Obviously, many sandstones can be expected to have microstructures which lie between these extremes. Most ledge-forming sandstones tend to have homogeneous microstructures, but uranium ore mineralization tends to occur in ledge-forming sandstones whose microstructures are relatively heterogeneous.

COMPOSITION OF FINE-TEXTURED ROCKS

Fine-textured rocks in the lower part of the Morrison Formation contain the same general mineral components as the accompanying sandstones. Quartz, feldspar, and silicified-rock fragments are of silt size and are angular to subangular in shape. Feldspar and clay minerals, predominantly of the mica group with various proportions of intermixed montmorillonite, constitute a larger average proportion of the fine-textured rocks than of the sandstones. Calcite cement is more abundant than in the sandstones, particularly in the basal part of the Salt Wash Member, where mudstone is interbedded with silty limestone and grades into it. Thin sections of red and purple siltstone and mudstone show dustlike red iron oxide crystals impregnating the clay matrix. The thick mudstone strata of the Recapture Member, as observed in the field, tend to be more bentonitic and more reddish in hue than those of the Salt Wash Member.

ROCK CLASSIFICATION

Modal analyses were made of 52 thin sections of sandstone, 12 of fine-textured rocks, and 2 of carbonate rocks from the Salt Wash Member, and of 21 thin sections of sandstone and 1 of fine-textured rock from the Recapture Member. Results are summarized in tables 12 and 13. Of these samples, 71 belong to the orthoquartzite series, 4 to the arkose series, 4 to the graywacke series, and 6 to the tuff series; 1 is a modified porcelanite, and 2 are limestones. From the averages in table 12, it is evident that the average sandstone in the Salt Wash is an impure or modified orthoquartzite, the average siltstone is a tuffaceous feldspathic orthoquartzite, the average claystone is a bentonite, and the average mudstone is an orthoquartzitic tuff. Mudstone is the term applied to a fine-textured rock (median particle size <0.062 mm) which has a grain-size distribution standard deviation of 2.500 or larger. The averages in table 13 clearly show that the average sandstone in the Recapture is a feldspathic orthoquartzite; the siltstone is a graywacke, probably derived from a feldspathic orthoquartzitic tuff.

TEXTURAL MEASURES

Statistical analyses of the grain-size distributions were made for 267 sandstone samples collected from the Salt Wash Member and for 59 from the Recapture Member. The results are given in a tabular report by Cadigan (1967); the first page of that report is shown here (table 14) to illustrate the form in which the data are recorded. When the grain-size distribution classification systems of tables 6, 9, 10, and 11 are applied to the Salt Wash, the average sandstone is found to be fine grained with a moderately well sorted, moderately skewed, highly peaked (leptokurtic) grain-size distribution. The results of statistical analyses of the grain-size distributions in 22 samples of fine-textured rocks of the Salt Wash Member are also recorded by Cadigan (1967). Grain-size analyses were not made on fine-textured rock samples from the Recapture Member. By the same classification system, the average fine-textured rock in the Salt Wash Member is a poorly sorted medium-grained siltstone with a normally peaked, symmetrical grain-size distribution.

TABLE 12.—*Modes of rocks from the Salt Wash Member of the Morrison Formation*

[In percent by volume. Rock classification: O, orthoquartzite or orthoquartzitic; A, arkose or arkosic; C, calcareous; G, graywacke; T, tuff or tuffaceous; P, arenaceous procelanite; S, chert arenite or arenaceous chert; L, limestone; B, bentonite; I, impure; F, feldspathic. Samples are sandstone unless otherwise noted. Tuff fragments are dominantly potassic unless otherwise noted.]

	Colorado													
Locality (pl. 1) Sample	2 L657	27 L344	56 [1] L471	61 L50	67 [2] L456	115 [3] L3448	115 L3447	115 L3449	121 L607	124 L190	124 [1] L189	138 L343	142 L388	142 L389
I. Cementing components (except silica)														
a. Carbonates and sulfates (calcite)	0.8	15.0	5.2	7.0	3.6	91.4	33.0	31.0		16.2		12.8	7.8	17.6
b. Red interstitial iron oxides (in clay)							1.0	.2	0.6				.8	.4
Total	0.8	15.0	5.2	7.0	3.6	91.4	34.0	31.2	0.6	16.2	0.0	12.8	8.6	18.0
II. Siliceous components														
a. Quartz grains and overgrowths	80.2	68.2	55.8	83.8	36.8	2.4	41.6	41.6	92.4	70.4	46.6	68.8	84.4	70.8
b. Quartzite fragments		.2					.2			.2		.2		
c. Chert, detrital	1.0	2.0	1.2	.6	1.0		.4	.6	.2	.8	1.6	.2	.8	.2
d. Chert, authigenic														
e. Silicified-rock fragments	4.2	.6						.4				.8	1.2	.4
f. Silicified-limestone fragments	.8			.2									.2	
Total	86.2	71.0	57.0	84.6	37.8	2.4	42.2	42.6	92.6	71.4	48.2	70.0	86.6	71.4
III. Feldspathic components														
a. Potassic feldspar	0.0	8.6	1.0	5.6		0.4	10.2	6.4	2.4	4.4	12.8	10.8	0.8	4.2
b. Plagioclase feldspar	1.6	4.4	11.4	1.6	9.6	.4	4.0	3.0	.2	1.8	2.2	3.6	.4	1.6
c. Kaolinitic clays (alteration products)	.2			.2					3.4	3.0			2.6	4.4
Total	1.8	13.0	12.4	7.4	9.6	0.8	14.2	9.4	6.0	9.2	15.0	14.4	3.8	10.2
IV. Dark-mineral and mica components														
a. Mica flakes and books (biotite, chlorite [4])	0.4		1.0		0.2		0.2				0.4			
b. Chlorite and mica clays	1.4	0.2					.8			0.6		0.4	0.4	
c. Micaceous and mafic rock fragments	.2									.2		.2		
d. Heavy minerals (sp. gr. 2.90+)			.4							.2	.2			0.2
e. Miscellaneous (opaque and unidentified grains)			.2	.2	.2				.2	.6	1.0			
Total	2.0	0.2	1.6	0.2	0.4	0.0	1.0	0.0	0.2	1.6	1.6	0.6	0.4	0.2
V. Volcanic components														
a. Tuff and felsite fragment (silicified)		[5] 0.8	[6] 5.4	[5] 0.6			[5] 1.2	[5] 1.6	0.4	[5] 1.4	1.8	1.4		[6] 0.2
b. Montmorillonitic clays (alteration products)	9.2		10.0	.2	48.6	5.4	[3] 7.4	[3] 15.2	.2	.2	.2	.8	0.6	
c. Altered ash (chiefly shards, and clay)			8.4								[7] 33.2			
Total	9.2	0.8	23.8	0.8	48.6	5.4	8.6	16.8	0.6	1.6	35.2	2.2	0.6	0.2
Grand total	100	100	100	100	100	100	100	100	100	100	100	100	100	100
Rock classification	O	FO	TFO	O	FOT	L	CFO	CTO	O	IO	FOT	FO	O	FO

See footnotes at end of table.

TABLE 12.—*Modes of rocks from the Salt Wash Member of the Morrison Formation*—Continued

	Colorado—Continued									Utah					
Locality (pl. 1) Sample	142 L390	177 L350	214 L241	[8] 233 LE212	[8] 233 LE222	[8] 233 LE247	203 L28	234 [9] L802	234 L803	24 L484	25 [9] L2795	25 [1] L2796	25 [9] L2793	25 [1] L2794	40 L823
I. Cementing components (except silica)															
a. Carbonates and sulfates (calcite)	25.8	8.0	18.2	19.8	26.8	8.6	1.6			30.2	27.2	18.2	[10] 4.4	[10] 23.4	1.6
b. Red interstitial iron oxides (in clay)		1.2	3.0	.8	1.4	.8	.2	2.4	1.0		.2				.4
Total	25.8	9.2	21.2	20.6	28.2	9.4	1.8	2.4	1.0	30.2	27.4	18.2	4.4	23.4	2.0
II. Siliceous components															
a. Quartz grains and overgrowths	63.4	84.6	69.2	71.0	58.2	84.8	74.4	56.2	74.8	53.2	57.2	31.6	78.0	63.0	79.0
b. Quartzite fragments					.2										
c. Chert, detrital	2.0	1.8	.6	1.0	.2	1.2	.8	1.0	.8	1.6	.6	.2		.2	1.6
d. Chert, authigenic	.2			.4	.2		.2	5.6		.2	.2		.2		.2
e. Silicified rock fragments	.2						.4			.4					
f. Silicified limestone fragments		.4					.4		.4				1.0	.4	
Total	65.8	86.8	69.8	72.4	58.8	86.0	76.2	62.8	76.0	55.4	58.0	31.8	79.2	63.6	80.8
III. Feldspathic components															
a. Potassic feldspar	5.4		3.8	3.8	4.6	2.0	10.2			9.0	6.4	3.0	7.4	7.0	5.4
b. Plagioclase feldspar	1.0	0.6	.6	1.8	3.8	.8	1.4	2.8	1.6	4.0	6.4	2.8	2.4	5.0	1.8
c. Kaolinitic clays (alteration products)	.4		3.2		2.6	.4	2.6	20.2	14.4				.2		3.2
Total	6.8	0.6	7.6	5.6	11.0	3.2	14.2	23.0	16.0	13.0	12.8	5.8	10.0	12.0	10.4
IV. Dark-mineral and mica components															
a. Mica flakes and books (biotite, chlorite)								0.6	0.8	0.2	0.2			0.4	
b. Chlorite and mica clays		1.0	0.4	0.4	0.2	0.2	1.4		.6	.2		44.2	5.4		0.8
c. Micaceous and mafic rock fragments								.6							.6
d. Heavy minerals (sp. gr. 2.90+)				.2					.2	.4	.2		.4		
e. Miscellaneous (opaque and unidentified grains)							.2		.6	.4	.4		.2	.2	.2
Total	0.0	1.0	0.4	0.6	0.2	0.2	1.6	1.2	2.2	1.2	0.8	44.2	6.0	0.6	1.6
V. Volcanic components															
a. Tuff and felsite fragments (silicified)	1.4	[6] 2.4	1.0	0.8	1.8	1.2	1.6	[6] 1.4	[6] 1.8	0.2	1.0		0.4	0.4	[5] 4.0
b. Montmorillonitic clays (alteration products)	.2						4.6	9.2	3.0						1.2
c. Altered ash (chiefly shards, and clay)															
Total	1.6	2.4	1.0	0.8	1.8	1.2	6.2	10.6	4.8	0.2	1.0	0.0	0.4	0.4	5.2
Grand total	100	100	100	100	100	100	100	100	100	100	100	100	100	100	100
Rock classification	CO	O	IO	IO	CFO	O	FO	TFO	FO	CFO	CFO	G	FO	FO	FO

See footnotes at end of table.

TABLE 12.—*Modes of rocks from the Salt Wash Member of the Morrison Formation*—Continued

	Utah—Continued														
Locality (pl. 1) Sample	45 L808	64 L422	64 [3] L421	71 L2763	71 L2762	90 L488	90 L489	105 [1] L2808	105 [1] L2807	105 [1] L2810	105 L40	105 [1] L2809	105 L35	107 [3] L844	146 L626
I. Cementing components (except silica)															
a. Carbonates and sulfates (calcite)	38.0	34.4	2.0	18.8	39.6	4.4	15.6	31.4	2.6	26.6	7.8	17.6	8.8	78.4	19.6
b. Red interstitial iron oxides (in clay)			.4			.4	2.0	.2	2.0		.4	1.0	.2		
Total	38.0	34.4	2.4	18.8	39.6	4.8	17.6	31.6	4.6	26.6	8.2	18.6	9.0	78.4	19.6
II. Siliceous components															
a. Quartz grains and overgrowths	48.4	48.0	15.2	62.2	40.0	79.2	62.4	25.2	50.6	36.2	76.6	34.2	76.6	4.0	64.4
b. Quartzite fragments				.2										.2	
c. Chert, detrital	1.2	2.8	.2	1.8	.6	1.8	1.4	.4	.8	.6	1.0	.8	.4	10.8	4.8
d. Chert, authigenic						.2								.2	
e. Silicified rock fragments				.4	.2	.6	.8							2.4	1.0
f. Silicified limestone fragments	.8	3.4		2.2		.2								2.6	2.0
Total	50.4	54.2	15.4	66.8	40.8	82.0	64.6	25.6	51.4	36.8	77.6	35.0	77.0	20.2	72.2
III. Feldspathic components															
a. Potassic feldspar	7.6	6.8	5.4	6.4	9.2	6.0	6.2	15.2	23.2	17.6	6.8	9.6	6.6	0.8	
b. Plagioclase feldspar	1.4	3.0	.4	4.2	6.2	.4	3.4	2.8	6.2	8.0	2.4	.8	.8	.4	6.4
c. Kaolinitic clays (alteration products)				.2											
Total	9.0	9.8	5.8	10.8	15.4	6.4	9.6	18.0	29.4	25.6	9.2	10.4	7.4	1.2	6.4
IV. Dark-mineral and mica components															
a. Mica flakes and books (biotite, chlorite)	0.2	0.2							0.4						
b. Chlorite and mica clays					0.4	1.0	0.8	23.4	13.2	9.8	0.8	35.4	1.6		0.6
c. Micaceous and mafic rock fragments				0.2	.2									0.2	
d. Heavy minerals (sp. gr. 2.90+)			0.2		.2	.2		.2	.4	.4					.2
e. Miscellaneous (opaque and unidentified grains)			.8		.2	.2	.2	1.0	.6	.4	.4		.8		
Total	0.2	0.2	1.0	0.2	1.0	1.4	1.0	24.6	14.6	10.6	1.2	35.4	2.4	0.2	0.8
V. Volcanic components															
a. Tuff and felsite fragments (silicified)	1.8	0.8		3.4	3.2	5.4	2.6	0.2		0.4	[5] 3.2	0.6	3.8		[6] 1.0
b. Montmorillonitic clays (alteration-products)	.6	.6	75.4				3.0				.6		.4		
c. Altered ash (chiefly shards, and clay)							1.6								
Total	2.4	1.4	75.4	3.4	3.2	5.4	7.2	0.2	0.0	0.4	3.8	0.6	4.2	0.0	1.0
Grand total	100	100	100	100	100	100	100	100	100	100	100	100	100	100	100
Rock classification	CO	CFO	B	FO	CFO	O	FO	CG	A	CA	O	G	O	L	IO

See footnotes at end of table.

TABLE 12.—*Modes of rocks from the Salt Wash Member of the Morrison Formation*—Continued

	Utah—Continued														
Locality (pl. 1)	148	148	148	159	159	163	174	178	181	189	189	215	222	222	231
Sample	L825	L826	L828	L2955	L852	L312	[1] L450	L160	L615	L613	L614	L398	L831	L833	L268
I. Cementing components (except silica)															
a. Carbonates and sulfates (calcite)	21.0	6.6	20.0	24.2		23.2	8.6	20.2	0.2	24.8		0.2	8.0	0.2	
b. Red interstitial iron oxides (in clay)	.2	.4			1.0							.8			
Total	21.2	7.0	20.0	24.2	1.0	23.2	8.6	20.2	0.2	24.8	0.0	1.0	8.0	0.2	0.0
II. Siliceons components															
a. Quartz grains and overgrowths	67.8	81.8	64.6	60.0	75.4	67.2	39.2	63.4	52.0	46.0	5.2	86.4	66.2	76.0	62.8
b. Quartzite fragments				.2	.2				.4	.6	.4			.4	
c. Chert, detrital	.2	.4	2.2	1.8	7.6	2.6	.2	5.0	.2	1.8	22.8	.4	5.8	1.2	4.0
d. Chert, authigenic		.2	1.4				.2		25.5	.6			.6		
e. Silicified rock fragments	.4	.4	6.4	.4	2.2	1.0				6.0	27.8		5.8	.4	
f. Silicified limestone fragments	.2	.6	.4		.4	1.6		3.4	2.0	3.8	25.4		2.2	.4	2.2
Total	68.6	83.4	75.0	62.4	85.8	72.4	39.6	71.8	80.1	58.8	81.6	86.8	80.6	78.4	69.0
III. Feldspathic components															
a. Potassic feldspar	5.8	3.8	2.8	8.8	2.8	1.8		2.6	4.0	6.4	1.2	4.4	2.4	7.4	2.8
b. Plagioclase feldspar	.4	1.0	.2	1.2	.6	1.0	17.8	1.4	.4	.6	.2	.6	.4	2.0	2.4
c. Kaolinitic clays (alteration products)	.8	2.0	.6						3.5			2.2	1.4	2.6	
Total	7.0	6.8	3.6	10.0	3.4	2.8	17.8	4.0	7.9	7.0	1.4	7.2	4.2	12.0	5.2
IV. Dark-mineral and mica components															
a. Mica flakes and books (biotite, chlorite)						0.2	0.8		0.2			0.4			0.2
b. Chlorite and mica clays	0.6		0.4			.4	3.0			0.6		1.6	3.0	0.8	5.0
c. Micaceous and mafic rock fragments															
d. Heavy minerals (sp. gr. 2.90+)							.2		.2			.2			
e. Miscellaneous (opaque and unidentified grains)						.2	.4			.2		.4			
Total	0.6	0.0	0.4	0.0	0.0	0.8	4.4	0.0	0.4	0.8	0.0	2.6	3.0	0.8	5.2
V. Volcanic components															
a. Tuff and felsite fragments (silicified)	2.2	2.8	1.0	2.0	7.2	0.8	[6] 4.0	4.0	11.2	8.6	16.8	2.2	3.8	3.2	[6] 4.4
b. Montmorillonitic clays (alteration products)	.4			1.4	2.6		25.6		.2		.2	.2	.4	5.4	1.2
c. Altered ash (chiefly shards, and clay)															15.0
Total	2.6	2.8	1.0	3.4	9.8	0.8	29.6	4.0	11.4	8.6	17.0	2.4	4.2	8.6	20.6
Grand total	100	100	100	100	100	100	100	100	100	100	100	100	100	100	100
Rock classification	IO	O	O	FO	STO	IO	FOT	IO	TP	CSO	TS	O	SO	FO	TO

See footnotes at end of table.

TABLE 12.—*Modes of rocks from the Salt Wash Member of the Morrison Formation*—Continued

Locality (pl. 1)	Arizona		New Mexico					Average of sandstones (52 samples)	Average of siltstones (8 samples)	Average of claystones (2 samples)	Average of mudstones (2 samples)	Average of limestones (2 samples)
Sample	135 L321	162 L302	7 L358	7 L360	[8] 151 [11] L738	[8] 151 [11] L739	175 L744					
I. Cementing components (except silica)												
a. Carbonates and sulfates (calcite)	0.4	8.6	0.4	4.4	10.0		29.0	13.7	13.8	5.0	2.8	84.9
b. Red interstitial iron oxides (in clay)		.2		.2	.8	0.4		.4	.4	.6	.2	.0
Total	0.4	8.8	0.4	4.6	10.8	0.4	29.0	14.1	14.2	5.6	3.0	84.9
II. Siliceous components												
a. Quartz grains and overgrowths	77.6	69.6	84.8	86.2	10.0	10.4	57.2	66.9	39.9	10.2	26.0	3.2
b. Quartzite fragments								.1	.0	.0	.0	.1
c. Chert, detrital	1.2	.4	.6	.8				1.8	.7	.0	.6	5.4
d. Chert, authigenic			.2					.7	.0	.0	.0	.1
e. Silicified rock fragments	.2		2.2	.2				1.2	.0	.0	.0	1.2
f. Silicified limestone fragments								1.1	.0	.0	.0	1.3
Total	79.0	70.0	87.8	87.2	10.0	10.4	57.2	71.8	40.6	10.2	26.6	11.3
III. Feldspathic components												
a. Potassic feldspar	9.6	6.6	5.4	4.2			8.0	5.1	10.3	0.0	2.7	0.6
b. Plagioclase feldspar	1.2	5.0	2.4	2.2	2.8	3.6	2.2	2.1	6.5	3.2	5.0	.4
c. Kaolinitic clays (alteration products)								1.4	.0	.0	.0	.0
Total	10.8	11.6	7.8	6.4	2.8	3.6	10.2	8.6	16.8	3.2	7.7	1.0
IV. Dark-mineral and mica components												
a. Mica flakes and books (biotite, chlorite)	0.2		0.2			1.2		0.1	0.3	0.0	0.1	0.0
b. Chlorite and mica clays	4.6	0.4	.8					.7	16.1	.0	.0	.0
c. Micaceous and mafic rock fragments	.2						0.4	.1	.0	.0	.0	.1
d. Heavy minerals (sp. gr. 2.90+)								.1	.2	.0	.1	.0
e. Miscellaneous (opaque and unidentified grains)	.2		.4		1.2		.8	.1	.5	1.2	.5	.0
Total	5.2	0.4	1.4	0.0	1.2	1.2	1.2	1.1	17.1	1.2	0.7	0.1
V. Volcanic components												
a. Tuff and felsite fragments (silicified)	4.4	2.4	2.6	1.8	1.6	0.4	2.4	2.6	1.6	1.0	0.0	0.0
b. Montmorillonitic clays (alteration products)	.2	6.8			73.6	84.0		1.5	4.5	78.8	62.0	2.7
c. Altered ash (chiefly shards, and clay)								.3	5.2	.0	.0	.0
Total	4.6	9.2	2.6	1.8	75.2	84.4	2.4	4.4	11.3	79.8	62.0	2.7
Grand total	100	100	100	100	100	100	100	100	100	100	100	100
Rock classification	FO	FO	O	O	T	B	CFO	IO	TFO	B	OT	L

[1] Siltstone.
[2] Mudstone.
[3] Limestone.
[4] In the form of a detrital mica replacing biotite muscovite.
[5] Altered tuff fragments, potassic and sodic varieties equally abundant.
[6] Altered tuff fragments, sodic variety dominant.
[7] Mostly chlorite.
[8] Thin-section study only.
[9] Sandy siltstones arbitrarily treated as sandstones.
[10] Barite present as cement with calcite.
[11] Claystone.

TABLE 13.—*Modes of rocks from the Recapture Member of the Morrison Formation*

[In percent by volume. Rock classification: O, orthoquartzite; A, arkose; G, graywacke; T, tuffaceous; C, calcareous; F, feldspathic; I, impure. Samples are sandstone unless otherwise noted. Tuff fragments are dominantly potassic]

	Colorado			Utah	Arizona					
Locality (pl. 1)	124	124	124	163	118	118	128	172	230	230
Sample	L192	L193	L194	L206	L759	L760	L656	L753	L618	L620
I. Cementing components (except silica)										
a. Carbonates and sulfates (calcite)	5.6	1.6	[1] 3.8	1.6	16.2	4.8	1.0	0.8	----	0.2
b. Red interstitial iron oxides (in clay)	.8	----	.2	----	----	----	----	----	----	----
Total	6.4	1.6	4.0	1.6	16.2	4.8	1.0	0.8	0.0	0.2
II. Siliceous components										
a. Quartz grains and overgrowths	80.8	83.2	70.6	79.0	64.8	66.8	76.0	91.4	77.4	67.4
b. Quartzite fragments	----	----	.2	----	.2	.2	----	.2	----	----
c. Chert, detrital	.2	.4	.6	.4	----	.2	.2	.6	.6	.2
d. Chert, authigenic	----	.2	----	----	----	----	----	----	----	----
e. Silicified rock fragments	.2	----	----	----	----	----	----	.2	----	.4
f. Silicified limestone fragments	----	----	----	----	----	----	----	----	----	----
Total	81.2	83.8	71.4	79.4	65.0	67.2	76.2	92.4	78.0	68.0
III. Feldspathic components										
a. Potassic feldspar	6.0	8.2	8.0	10.4	11.2	12.2	8.2	1.8	8.0	12.8
b. Plagioclase feldspar	2.4	1.8	2.6	2.6	3.2	1.6	2.0	1.4	3.0	6.0
c. Kaolinitic clays (alteration products)	1.6	2.0	7.4	.6	.2	6.0	----	.4	.2	.4
Total	10.0	12.0	18.0	13.6	14.6	19.8	10.2	3.6	11.2	19.2
IV. Dark-mineral and mica components										
a. Mica flakes and books (biotite, chlorite [2])	----	----	0.4	----	----	0.2	0.2	----	----	----
b. Chlorite and mica clays	0.6	1.2	2.8	0.6	0.2	1.2	----	[3] 1.2	9.8	7.4
c. Micaceous and mafic rock fragments	----	----	----	----	----	----	----	----	----	----
d. Heavy minerals (sp. gr. 2.90+)	----	----	.4	----	.2	----	----	----	----	.4
e. Miscellaneous (opaque and unidentified grains)	.4	.2	.2	----	.4	.6	1.0	----	----	.2
Total	1.0	1.4	3.8	0.6	0.8	2.0	1.2	1.2	9.8	8.0
V. Volcanic components										
a. Tuff and felsite fragments (silicified)	1.2	1.0	2.8	3.8	2.4	6.0	2.8	2.0	1.0	4.0
b. Montmorillonitic clays (alteration products)	.2	.2	----	1.0	1.0	.2	8.6	----	----	.6
c. Altered ash (chiefly shards, and clay)	----	----	----	----	----	----	----	----	----	----
Total	1.4	1.2	2.8	4.8	3.4	6.2	11.4	2.0	1.0	4.6
Grand total	100	100	100	100	100	100	100	100	100	100
Rock classification	FO	FO	FO	FO	FO	FO	TFO	O	FO	FO

See footnotes at end of table.

TABLE 13.—*Modes of rocks from the Recapture Member of the Morrison Formation*—Continued

State	New Mexico												Average of siltstone (1 sample)	Average of sandstone (21 samples)
Locality (pl. 1)	7	7	49	79	83	92	92	92	140	[4] 151	175	210		
Sample	L565	L570	L838	L770	L789	L781	L782	L783	L722	[5] L740	L748	L742		
I. Cementing components (except silica)														
a. Carbonates and sulfates (calcite)			0.8	20.0	0.4	10.6	6.6	25.0	3.4	0.6	0.4		0.6	4.9
b. Red interstitial iron oxides (in clay)			.4							7.2		5.2	7.2	.3
Total	0.0	0.0	1.2	20.0	0.4	10.6	6.6	25.0	3.4	7.8	0.4	5.2	7.8	5.2
II. Siliceous components														
a. Quartz grains and overgrowths	79.2	84.6	60.0	66.8	64.6	75.0	67.8	53.4	51.0	27.2	71.4	56.2	27.2	70.8
b. Quartzite fragments					.4	.2	.2				.2		.0	.1
c. Chert, detrital	.8	.2		.8		1.4	1.0	.4		.8	.6	.2	.8	.4
d. Chert, authigenic							.4	.4	.2				.0	.1
e. Silicified rock fragments	1.0	.2	.2			1.8							.0	.2
f. Silicified limestone fragments													.0	.0
Total	81.0	85.0	60.2	67.6	65.0	78.4	69.4	54.2	51.2	28.0	72.2	56.4	28.0	71.6
III. Feldspathic components														
a. Potassic feldspar	4.6	8.8	14.2	7.0	18.4	6.0	7.8	5.2	16.6	4.0	11.8	9.0	4.0	9.3
b. Plagioclase feldspar	8.6	2.2	7.0	1.4	7.2	.2	1.2	4.8	9.0	10.0	3.6	5.8	10.0	3.7
c. Kaolinitic clays (alteration products)			1.4	1.0	.6	1.6			1.4			1.4	0.0	1.3
Total	13.2	11.0	22.6	9.4	26.2	7.8	9.0	10.0	27.0	14.0	15.4	16.2	14.0	14.3
IV. Dark-mineral and mica components														
a. Mica flakes and books (biotite, chlorite)			0.4		0.2			0.2	0.2	2.0	0.2	0.2	2.0	0.1
b. Chlorite and mica clays	1.6	0.8	6.2	0.8	3.6		11.2	6.6	[3] 5.2	45.6	[3] 6.4	[6] .2	45.6	3.2
c. Micaceous and mafic rock fragments						0.2							.0	.0
d. Heavy minerals (sp. gr. 2.90+)		.2							.2	.2		.2	.2	.1
e. Miscellaneous (opaque and unidentified grains)		.2	1.4		.4			.2	.4	.4		1.4	.4	.3
Total	1.6	1.2	8.0	0.8	4.2	0.2	11.2	7.0	6.0	48.2	6.6	2.0	48.2	3.7
V. Volcanic components														
a. Tuff and felsite fragements (silicified)	4.2	2.8	7.6	1.8	4.2	3.0	3.8	3.8	12.4	2.0	4.6	2.6	2.0	3.7
b. Montmorillonitic clays (alteration products)			.4	.4							.8	17.6	.0	1.5
c. Altered ash (chiefly shards, and clay)													.0	.0
Total	4.2	2.8	8.0	2.2	4.2	3.0	3.8	3.8	12.4	2.0	5.4	20.2	2.0	5.2
Grand total	100	100	100	100	100	100	100	100	100	100	100	100	100	100
Rock classification	FO	FO	FO	IO	A	O	IO	CFO	TA	G	FO	TFO	G	FO

[1] Barite present as cement with calcite (Ia).
[2] In the form of detrital mica replacing biotite or muscovite.
[3] Micaceous clay mostly chlorite (IVb).
[4] Thin-section study only.
[5] Siltstone.
[6] Black opaque interstitial (Ib).

TABLE 14.—*Record form used for statistical measures of the phi grain-size distribution of samples from the Morrison Formation*

[Excerpt from open-file report (Cadigan, 1967, table 1, "Statistical measures of the phi grain-size distributions of 267 sandstone samples from the Salt Wash Member of the Morrison Formation"). Data were obtained by mechanical grain-size analysis. Values in parentheses are locality averages (means). St. dev., standard deviation; Skew., skewness; Kurt., kurtosis. Percentiles in phi terms are shown as ϕ_2 (second percentile), ϕ_5 (fifth percentile), etc. Asterisk (*) indicates thin-section modal analysis of sample is given in this professional paper, table 12]

Locality (pl. 1)	Sample	Mode	Median	Mean	St. dev.	Skew.	Kurt.	ϕ_2	ϕ_5	ϕ_{16}	ϕ_{50}	ϕ_{84}	ϕ_{95}	ϕ_{98}
		millimeter		phi notation										
2	*L657	0.210	0.182	2.768	1.286	1.512	11.847	1.40	1.60	1.99	2.45	3.25	5.00	8.00
	L658	.125	.121	3.602	1.764	1.312	6.719	2.39	2.55	2.80	3.05	3.95	8.00	10.50
	L659	.210	.219	2.692	1.651	1.721	12.877	1.55	1.73	1.93	2.19	2.85	5.50	10.25
		(.182)	(.174)	(3.021)	(1.567)	(1.515)	(10.481)	(1.78)	(1.96)	(2.24)	(2.56)	(3.35)	(6.17)	(9.58)
3	L608	.148	.136	3.207	1.318	1.274	9.056	1.80	2.00	2.26	2.80	3.95	5.65	7.50
	L609	.125	.103	3.658	1.517	1.176	6.537	2.19	2.34	2.64	3.27	4.50	7.00	9.50
	L610	.138	.135	3.284	1.340	1.315	9.306	1.90	2.09	2.40	2.95	4.00	5.75	7.50
		(.137)	(.125)	(3.383)	(1.392)	(1.255)	(8.300)	(1.96)	(2.14)	(2.43)	(3.01)	(4.15)	(6.13)	(8.17)
7	*L358	.159	.165	2.700	.875	2.108	27.184	1.76	1.81	2.15	2.60	3.05	3.55	5.00
	L359	.125	.133	3.109	1.070	1.818	17.380	2.15	2.30	2.56	2.95	3.44	4.25	7.00
	*L360	.210	.222	2.289	.736	1.159	13.051	1.36	1.53	1.78	2.17	2.74	3.20	4.00
		(.165)	(.173)	(2.699)	(.894)	(1.695)	(19.204)	(1.76)	(1.88)	(2.16)	(2.57)	(3.08)	(3.67)	(5.33)
8	L368	.143	.122	3.364	1.414	1.450	10.464	2.00	2.18	2.45	3.05	3.91	6.00	9.00
12	L345	.210	.205	2.679	1.291	1.513	11.758	1.54	1.69	1.91	2.30	3.19	5.00	8.25
	L346	.126	.128	3.018	.758	1.817	22.327	2.31	2.44	2.63	2.87	3.36	3.70	4.25
	L347	.150	.161	2.765	.982	2.402	26.738	1.95	2.07	2.30	2.65	3.01	3.55	7.00
		(.162)	(.165)	(2.821)	(1.010)	(1.912)	(20.274)	(1.93)	(3.10)	(2.28)	(2.61)	(3.19)	(4.08)	(6.50)

Visual estimates of roundness (Krumbein, 1941) of 50 grains from each of 20 samples of sandstone from Salt Wash locality 56 and adjacent locality 182 (pl. 1) yielded a distribution of 1,000 roundness values with a mean of 0.447 and a standard deviation of 0.144. The distribution of these 1,000 values was found to be approximately normal. Visual estimates of the sphericity (Rittenhouse, 1943) of the same grains yielded a distribution of 1,000 sphericity values with a mean of 0.805 and a standard deviation of 0.071. This distribution was also found to be approximately normal. The average upper and lower limits of the sieve sizes of the sand grains used ranged from 0.129–0.182 mm. Estimates of sphericity were also made on 50 grains from each of 40 other samples of very fine grained sandstone from localities throughout the region. These values yielded a mean sphericity of 0.798, very similar to the mean of the 20 samples from the adjacent localities.

Visual estimates of roundness of 50 grains from each of 20 samples of sandstone from the Recapture at localities 7, 28, 78, 124, 128, 163, 209, and 210 in the Four Corners area and in northwestern New Mexico (pl. 1) yielded an approximately normal distribution of 1,000 values with a mean of 0.491 and a standard deviation of 0.130. The average upper and lower limits of the sieve sizes of the sand grains used ranged from 0.095 to 0.135 mm.

Visual estimates of sphericity on the same grains yielded an approximately normal distribution of 1,000 sphericity values with a mean of 0.798 and a standard deviation of 0.074. A possible regional trend in sphericity is discussed in the next section of the report; also discussed in the following section are regional variations of composition and texture, and interpretations of source and origin.

REGIONAL VARIATION, SOURCE, AND ORIGIN

FIELD STUDIES

From field studies of lithology, sedimentary structures, and distribution of rocks forming the lower part of the Morrison Formation, Craig and others (1955) concluded that the sediments of the Salt Wash Member were derived from sources southwest of the present Colorado Plateau and transported generally eastward or northeastward, and that sediments of the Recapture Member were derived from sources south of the present plateau and were transported generally northward. In the Morrison Formation as a whole, orientation of bedding structures indicates that the sediments moved across the Colorado Plateau area of deposition in directions ranging from north-northwest to southeast (table 15).

TABLE 15.—*Distribution of bedding-structure orientation resultants by azimuth classes (in degrees from north) for the members of the Morrison Formation in the Colorado Plateau region*

[Data furnished by L. C. Craig (written commun., 1964) from unpub. studies by G. W. Weir and G. A. Williams]

Azimuth classes [1] (degrees)	Salt Wash	Recapture	Westwater Canyon	Brushy Basin
1–15		2		
16–30	6		1	4
31–45	12	2	3	5
46–60	11		1	
61–75	11	2	1	
76–90	5	1	1	
91–105	10			
106–120	5			
121–135	3			
136–150	1			2
151–165	1			
166–180				
181–195	2			
196–270				
271–285			1	
286–300	1			
301–315				
316–330			1	
331–345	1			
346–360	1		1	
Total number of localities	70	7	10	11

[1] Mean azimuth of all resultants is approximately 61.5°.

A trend-surface analysis test of the locality orientation data for the lower part of the Morrison Formation indicates that there is neither regional convergence nor significant change in the orientation resultants in different parts of the region. This suggests that the resultant directions throughout the region of study are all part of the same statistical population. This in turn supports the interpretation that the major factors influencing streamflow orientations are supraregional—that sediment-bearing streams were flowing across the region without significant convergence.

An alluvial transport orientation diagram (fig. 25) illustrates the effect of varying transport directions from multiple sources lying outside the Colorado Plateau region.

Arrows in figure 25 represent directional axes of sediment flow from source areas assumed to lie 400 miles from the center of the region (the estimated average distance to the nearest orogenic areas). These arrows were constructed to converge slightly to represent the effect of vectors of fluctuation around the principal axes of movment. Thus, nearly all sediment moving directly from southwest of the center of the region would cross the region even though the direction of movement fluctuated widely. In contrast, sediment moving from areas south and west of the region would in part cross the Colorado Plateau and in part bypass it as the result of normal fluctuation in

232-378 O - 67 - 4

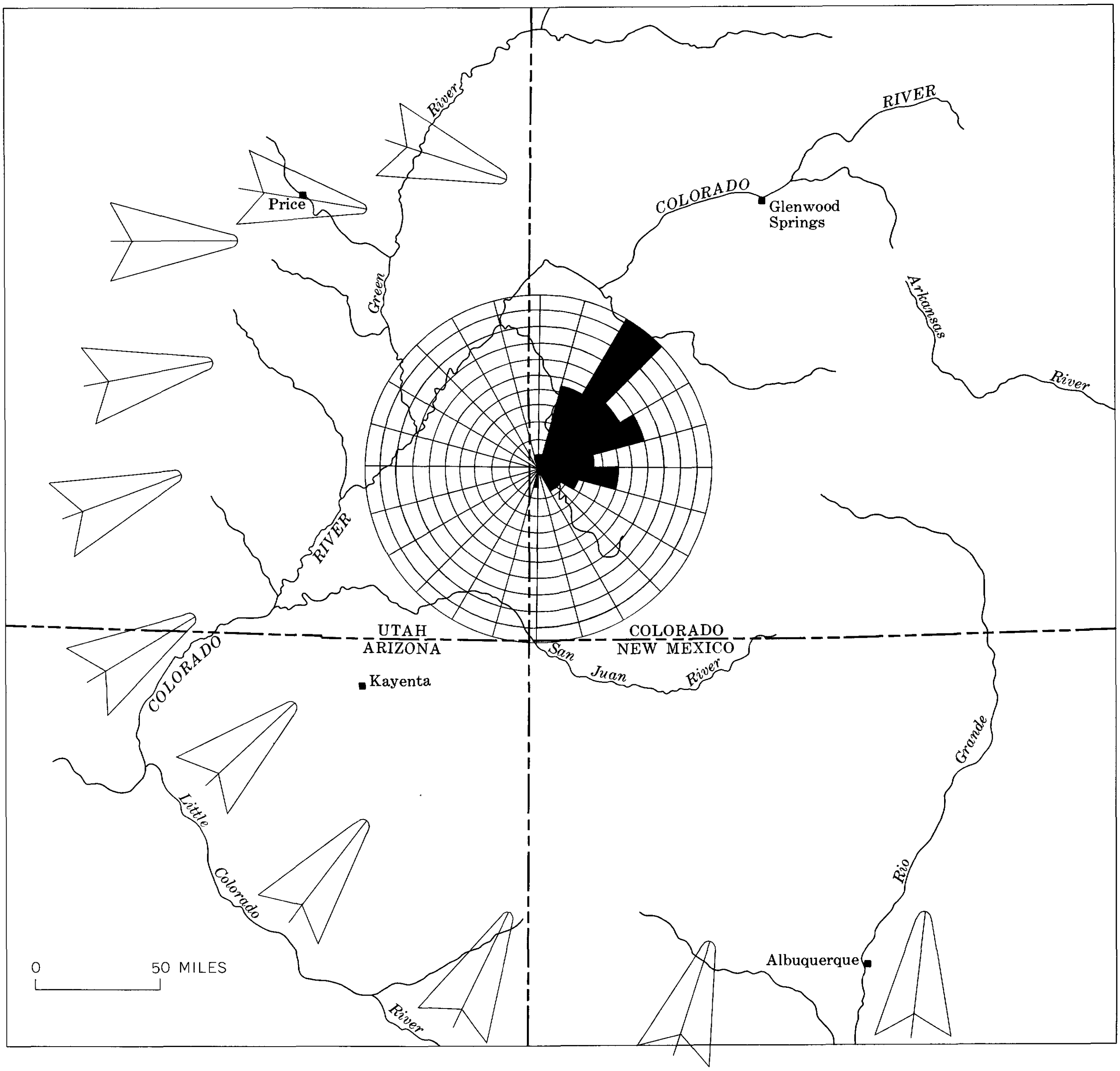

FIGURE 25.—Directions of movement of sediment into the Colorado Plateau region during deposition of the lower part of the Morrison Formation. Rose diagram shows sedimentary structure orientation. (See table 15.) As shown by large arrows, sediments from the southwest in general moved toward and across the center of the region, and sediments from the northwest and southeast moved across only parts of the region.

directions of flow about any designated axis of transport. Under these conditions, sediments of different composition moving in the same general direction might—and evidently did—retain recognizable difference in spite of the overall mixing action of alluvial transport and some differential subsidence in the area of deposition. The orientation data suggest that the Colorado Plateau was a major area of deposition but was not a focal point of deposition in the southwestern part of the Continental Interior basin.

PETROLOGIC STUDIES

In the following discussion, it is assumed that a directional pattern of progressive regional decrease in absolute quantities of a rock-forming component (as heavy minerals, for instance) is the effect of distance of transport from a source. With increased distance from source, the progressive effects of dilution and attrition tend to reduce the quantity of a component to the level of variation of "average" sediments in adjoining parts of the area of deposition. Mineral ratios may also be strongly affected by relative rates of attrition. A rapid rate of attrition of a heavy mineral *A* may result in a rapid increase in ratio of heavy mineral *B*. Under these conditions, mineral *A* has a strong regional trend which slopes away from the source, and mineral *B* has a strong regional trend which slopes toward the source.

Heavy-mineral ratios are used because variation in ratios is geologically more significant in this study than variation in absolute percentages in discerning variations of source effects. The total quantities of heavy minerals in samples of sandstone from the lower part of the Morrison Formation range from 2.25 to 0.01 percent, which suggests that the magnitude of the variations in quantity would obscure all other evidence of significant variation.

Attrition as here used is the apparent decrease in proportion of a mineral in a sedimentary rock with distance from source owing to loss or destruction of the mineral particles by weathering, abrasion, or other causes, or owing to preferential sedimentation. Heavy minerals, for example, settle closer to the source because of their high specific gravities (Pettijohn and Ridge, 1933). Like other minerals, they are reduced also by decomposition and removal by interstratal solutions after deposition (Russell, 1937, p. 1332–1348). In the sandstones of the Morrison Formation many particles of staurolite and garnet show surfaces that are apparently controlled by solution action rather than by abrasion. In contrast, zircon, rutile, tourmaline, and apatite generally display well-rounded forms or fracture surfaces resulting from abrasion or are euhedral to subhedral.

Significance of linear trends is estimated from percent reduction of total sum of squares, as described previously. It is assumed for this investigation that a weak trend (10 percent or less reduction) is not significant; a strong trend (25 percent reduction) is significant; an extremely strong trend (50 percent reduction) is highly significant; and a trend resulting in 80 percent or more reduction may be used for purposes of prediction. Uncertainties surrounding the above estimates of significance result from the use of locality averages instead of single samples, complicated by the fact that the "averages" are based on differing numbers of samples from different localities. Ideally, single sample values and evenly spaced localities should be used, but practically, the rock outcrops are not evenly spaced and variability between single samples tends to be too high to yield usable results for most geologic data. Using "averages" deliberately sacrifices reliable significance measures in order to obtain stronger trends and eliminate as much as possible the effects of minor variation not resulting from regional paleogeology.

ROCK TYPES

Sandstones and fine-textured and chemical rocks from the lower part of the Morrison include many different rock types as a result of variation in proportions of mineral or aggregate groups and rock components. A map of regional distribution of rock types (fig. 26) seems to show significant (nonrandom) regional variation of rock types. Orthoquartzites and feldspathic orthoquartzites, the most common types, are present in all parts of the region, as are the less common tuffaceous rocks. The uncommon sandstone arkoses are mostly restricted to the extreme southern part of the region, and the arenaceous-chert rocks are restricted to the extreme western parts.

FELDSPAR

As shown in figure 27, feldspar content of rocks of the lower part of the Morrison Formation is highest in the southeastern part of the region, thus suggesting significant (nonrandom) variation. The cumulative effects which led to delineation of the Recapture Member are being temporarily disregarded in order to study individual effects throughout the lower part of the Morrison. To evaluate regional variation in total feldspar, two different trend-surface analyses were run, one using the data for each location and the other using geographic-grid data by interpolation and extrapolation from figure 27. Because many of the finer siltstones contain a higher percentage of feldspar than associated sandstone, data from finer textured rock (median grain diameter 48 microns or less) were not used for the trend-surface analyses. Data from limestone were also omitted.

Input of the sample-locality-data trend-surface analysis consisted of coded geographic coordinates (U, V) of each of the 45 localities for which there were feldspar data, and the percentage or mean of the percentages of feldspar (X) at each of these localities. Because clusters of locality points adversely affect a trend-surface analysis, some pairs of adjacent localities (118 and 135, 24 and 25, and 71 and 159) were combined to yield single mean values for each pair. These modifications reduced the number of data points to 42.

Output of the feldspar locality trend-surface analysis consisted of calculated observations for each data

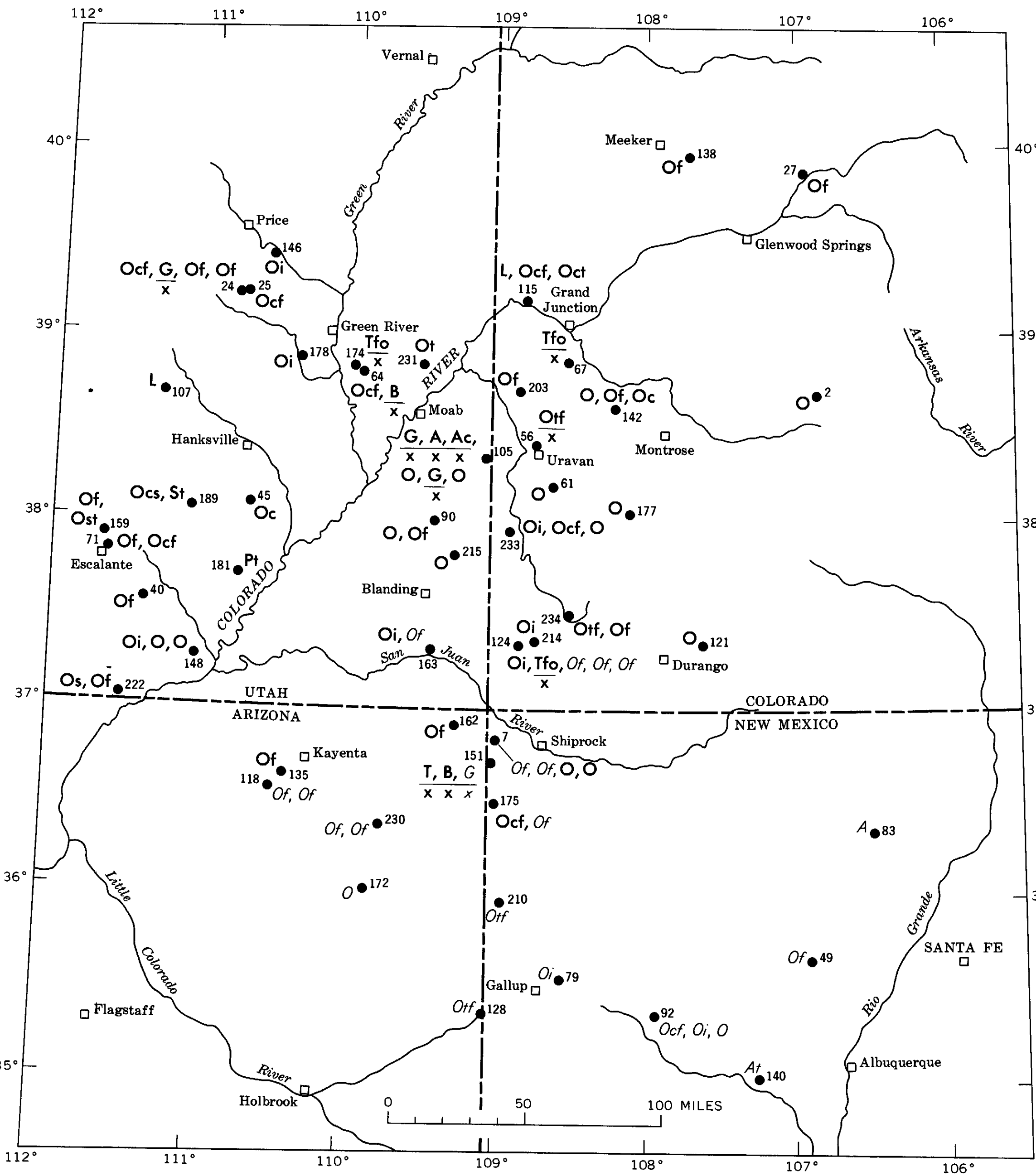

EXPLANATION

ROCK SYMBOL	MODIFYING TERM
O Orthoquartzite	o Orthoquartzitic
T Tuff	t Tuffaceous
A Arkose	s Arenaceous-chert
S Chert-arenite	c Calcareous
G Graywacke	f Feldspathic
L Limestone	i Impure
B Bentonite	
P Porcelanite	

Of — Salt Wash Member; *Of* — Recapture Member

Classification of a single sample of sandstone or limestone ("Feldspathic orthoquartzite")

G/x — Salt Wash Member; *G/x* — Recapture Member

Classification of a single sample of siltstone or mudstone ("Graywacke")

NOTE: Linear groups of symbols indicate several thin-sectioned samples from the same location. Arrangement within the group is not significant

FIGURE 26.—Rock classification symbols from tables 12 and 13 for the lower part of the Morrison Formation, distributed geographically according to appropriate localities. Based on 80 thin sections and 50 localities.

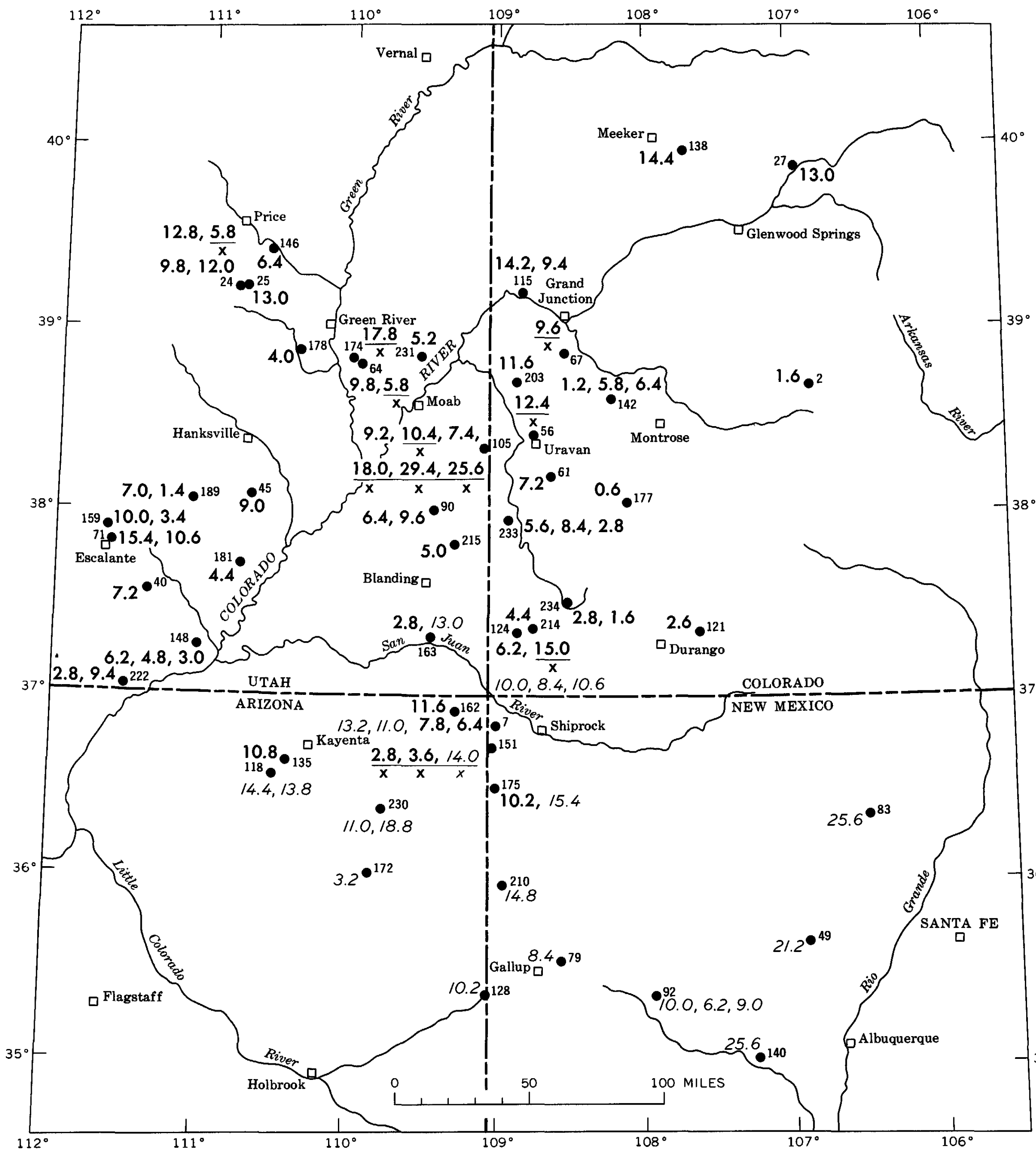

EXPLANATION

14.4 — Salt Wash Member; *14.8* — Recapture Member

Percentage of feldspar in one thin section of sandstone

11.6/x — Salt Wash Member; *10.2/x* — Recapture Member

Percentage of feldspar in one thin section of siltstone or mudstone

FIGURE 27.—Geographic distribution (in percent) of feldspar content in sandstone, mudstone, and siltstone of the lower part of the Morrison Formation, as measured in thin sections from 49 localities. Data from tables 11 and 12. Locality number refers to table 3.

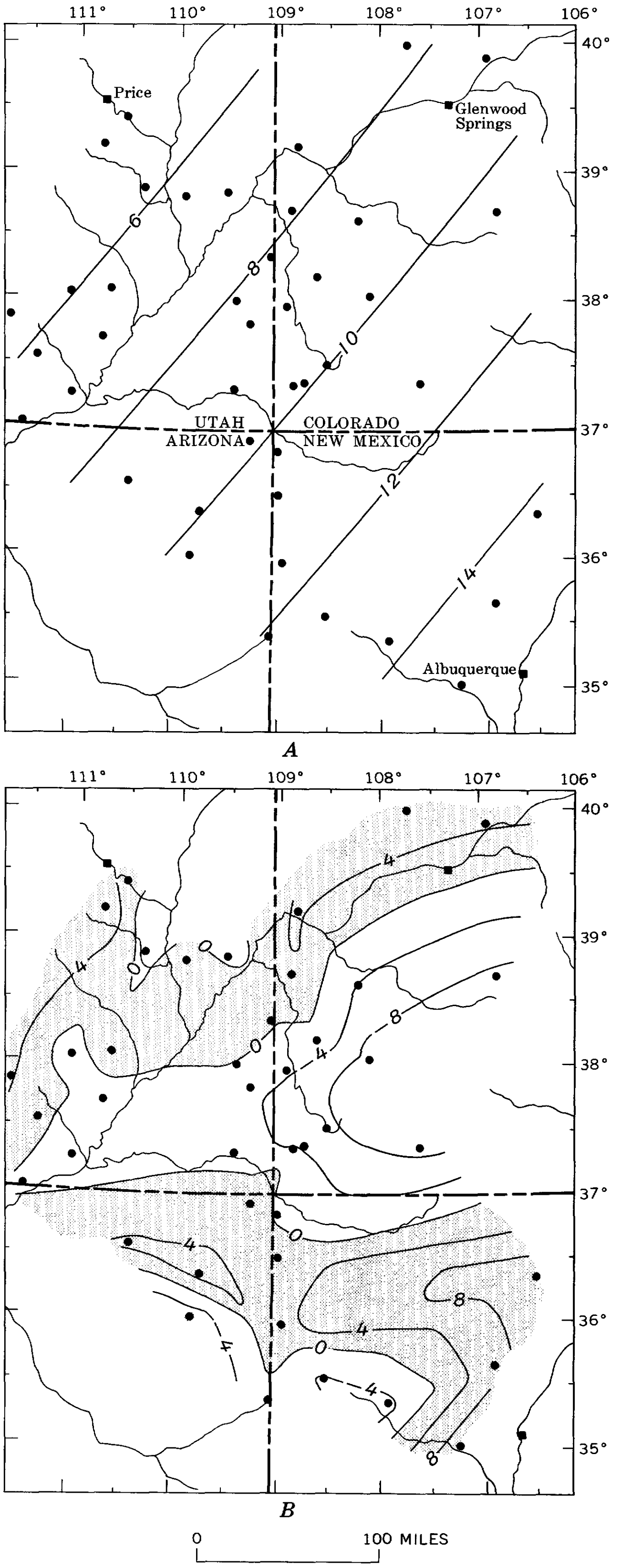

FIGURE 28.—Trend-surface analysis computed from modal feldspar data, lower part of the Morrison Formation. *A*, Linear surface; *B*, residual surface.

TABLE 16.—*Input and output values in trend-surface analysis of modal percent feldspar (sample locality means) in the lower part of the Morrison Formation.*

[*V*=longitude; *U*=latitude; *X*=percent feldspar]

Locality (pl. 1)	Input			Output	
	V (Coded)	*U* (Coded)	*X* (Observed)	*X* (Computed)	Residuals (from first-degree surface)
2	−2.17	1.68	1.6	10.6	−9.0
7	.01	−.20	9.6	10.3	−.7
24, 25	1.76	2.21	11.9	4.7	7.2
27	−2.09	2.88	13.0	8.8	4.2
40	2.36	.56	7.2	6.2	1.0
45	1.67	1.08	9.0	6.4	2.6
49	−2.10	−1.34	21.2	14.6	6.6
234	−.48	.50	2.2	10.0	−7.8
61	−.37	1.19	7.2	8.9	−1.7
64	.95	1.81	9.8	6.3	3.5
71, 159	2.63	.86	9.9	5.4	4.5
79	−.44	−1.46	8.4	12.6	−4.2
83	−2.52	−.65	25.6	14.2	11.4
90	.42	1.01	8.0	8.1	−.1
92	−1.08	−1.64	8.4	13.7	−5.3
105	.07	1.35	8.3	8.1	.2
115	−.18	2.19	11.8	7.3	4.5
118, 135	1.46	−.39	13.0	8.7	4.3
121	−1.39	.35	2.6	11.4	−8.8
124	−.15	.35	8.8	9.8	−1.0
128	.06	−1.63	10.2	12.2	−2.0
138	−1.29	2.97	14.4	7.7	6.7
140	−1.75	−1.98	25.6	15.0	10.6
142	−.78	1.61	4.5	8.9	−4.4
146	1.56	2.40	6.4	4.7	1.7
148	2.01	.26	4.7	7.1	−2.4
162	.28	−.09	11.6	9.8	1.8
163	.43	.32	7.9	9.0	−1.1
172	.85	−.97	-3.2	10.2	−7.0
175	.01	−.51	12.8	10.7	2.1
177	−.90	1.05	.6	9.8	−9.2
178	1.35	1.87	4.0	5.7	−1.7
181	1.74	.70	4.4	6.8	−2.4
189	2.07	1.05	4.2	5.9	−1.7
203	−.11	1.68	11.6	7.9	3.7
210	−.04	1.04	14.8	11.5	3.3
214	−.27	.37	4.4	9.9	−5.5
215	.28	.82	5.0	8.6	−3.6
222	2.50	.04	6.1	6.7	−.6
230	.76	−.63	14.9	9.9	5.0
231	.52	1.84	5.2	6.9	−1.7
233	−.08	.95	5.6	8.8	−3.2

Total sum of squares of deviations =1,319.3
Sum of squares of residuals (from linear surface) =1,038.0

Reduction in total sum of squares = 281.3=21.3 percent

point for the best fitting plane (linear) surface, and the residuals, or deviations from the linear surface for each sample locality. The linear and residual surfaces of regional distribution of feldspars in the lower part of the Morrison are illustrated in figure 28. Input and output values with respective locality numbers are shown as an example in table 16.

The computed regional linear surface for the 42-locality average values strikes N. 41° E. and dips northwestward; the surface reduces the sum of squares by 21.3 percent, evidence of a moderately strong regional trend of decreasing feldspar values from southeast to northwest. The residual surface contains two east-west elongated high areas (fig. 28*B*), one in the south having relatively high values and one in the north having much lower values. These highs signify areas of abnormally high feldspar because, as mentioned previously, the residual map tends to reflect the relative differences in a regional parameter, the effect of the overall regional trend being stripped out. Significant local variations, not evident in the linear regional trend, come into focus in the linear residual map.

For the geographic grid analysis, grid data were obtained by interpolating 26 values for the geographic-degree coordinate grid (fig. 29*A*) from figure 27 and averaging them in the manner previously described (fig. 8) to obtain the 26 moving average values shown in figure 29*B*. Input consisted of coded geographic coordinates and the averaged interpolated values of percent feldspar. Output consisted of computed grid values for the best fitting linear surface, and the grid residual values. Grid linear and residual surfaces are shown in figures 29*C* and *D*.

The computed linear surface for the 26 averaged interpolated values strikes N. 29° E. and dips northwest; the surface reduces the sum of squares by 24.4 percent, evidence of a strong regional trend of decreasing values from southeast to northwest. The residual surface is rather symmetrical, with a high area in the southeastern part of the region and one of lower value in the northwestern part.

A comparison of the results of the trend-surface analysis of the two sets of data (figs. 28, 29) shows a difference in strike between the two linear surfaces of only 12°. The dip of the locality data linear surface is steeper than that of the interpolated data. The linear residual surface of the locality data shows much more detail than the linear residual surface of the interpolated data. The surface of the interpolated data apparently shows only the major deviations from the regional trend in feldspar content of the rocks. The strength or significance of the trend of the two linear surfaces is about the same. The lower percent reduction of the sum of squares for the locality-data surface is more than compensated for by the fact that it is based on 30 percent more data points than the interpolated data surface. The slightly more uniform surfaces derived from the interpolated data do not compensate for the loss of detail as compared with the surfaces obtained from the locality data. Consequently, locality data are used wherever possible in preference to interpolated data in the following trend analyses.

Using the direction-component map (fig. 25) and the residual-surface map (fig. 28*B*) and assuming a distance to source areas of 400 miles from the center of the Colorado Plateau region (the estimated average distance to the nearest orogenic areas), a general direction from the center of the region to each of the high-feldspar source areas can be tentatively designated. Thus, contributions of high-feldspar sediments in the southeastern part of the Plateau region came from sources to the south; those in the southwestern part came from the southwest; those in the northwestern part came from the west-southwest to west-northwest; and those in the northern part came from west-northwest of the center of the region.

The relatively low feldspar sediments contributed to the south-central part could have been reworked from the Cow Springs Sandstone. Those extending from the central-western border into the central part show decreasing feldspar content northeastward. This may reflect the effect of attrition and dilution in sediments deposited along the main stem of the regional drainage. The low-feldspar sediments that were contributed to the north-northwest area suggest a low-feldspar source west-northwest of the region.

The ratios of potassic feldspar to sodic feldspar (R_1) are plotted in figure 30. Modal data on both sandstones and fine-textured rock, except limestone, were averaged for 49 localities, and the averages were used to compute linear and residual trend surfaces, shown in figures 31*A* and *B*. Linear and residual surfaces based on the theoretically reciprocal ratio sodic feldspar to potassic feldspar (R_2) are also shown in figure 31. The two ratios are not quite complementary because adjustments are made to eliminate ratios of infinity, and because the percentages used do not add up to a constant sum—that is, as can be seen by comparing the two sets of surface maps.

The ratio R_1 shows a relatively weak linear trend that strikes N. 34° W. and dips northeast. Reduction of the sum of squares by the computed linear surface is only 7.8 percent. The residual map from the linear surface shows high areas in the southeastern and northwestern parts of the region (fig. 31*B*), corresponding roughly with the high feldspar areas shown in figure 28*B*.

The ratio R_2 shows a slightly stronger linear trend that strikes N. 50° W. and dips southwest. Reduction of the sum of squares by the computed linear surface is 13.3 percent. The residual surface shows a high area in the northeastern part of the region. A much weaker high along the southwestern margin of the region is the result of computed zero and negative values on the edge of the southwestward-dipping linear surface, and it is therefore meaningless in the interpretation of sources.

The directions of feldspar sources which affect the R_1 and R_2 ratios should be the same as those for the total-feldspar sources, with the difference that R_1 highs would reflect relatively high proportions of potassic feldspar and R_2 highs would reflect relatively

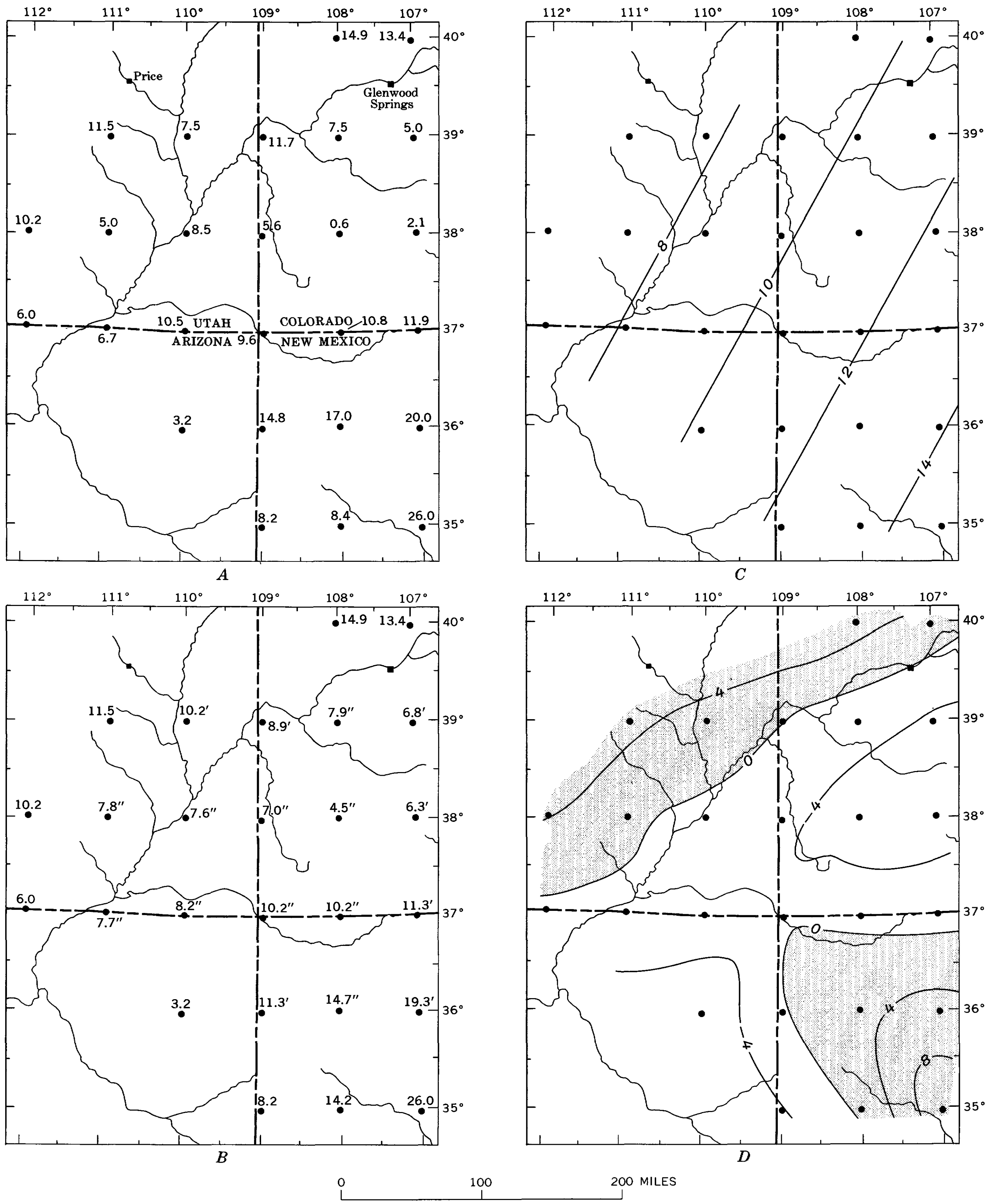

FIGURE 29.—Trend-surface analysis of interpolated feldspar data, lower part of the Morrison Formation. *A*, Interpolated grid data from modal feldspar data. *B*, Moving average grid of interpolated modal feldspar data using method of figure 8. *C*, Linear surface computed from moving average grid of interpolated modal feldspar data. *D*, Residual surface computed from *C*.

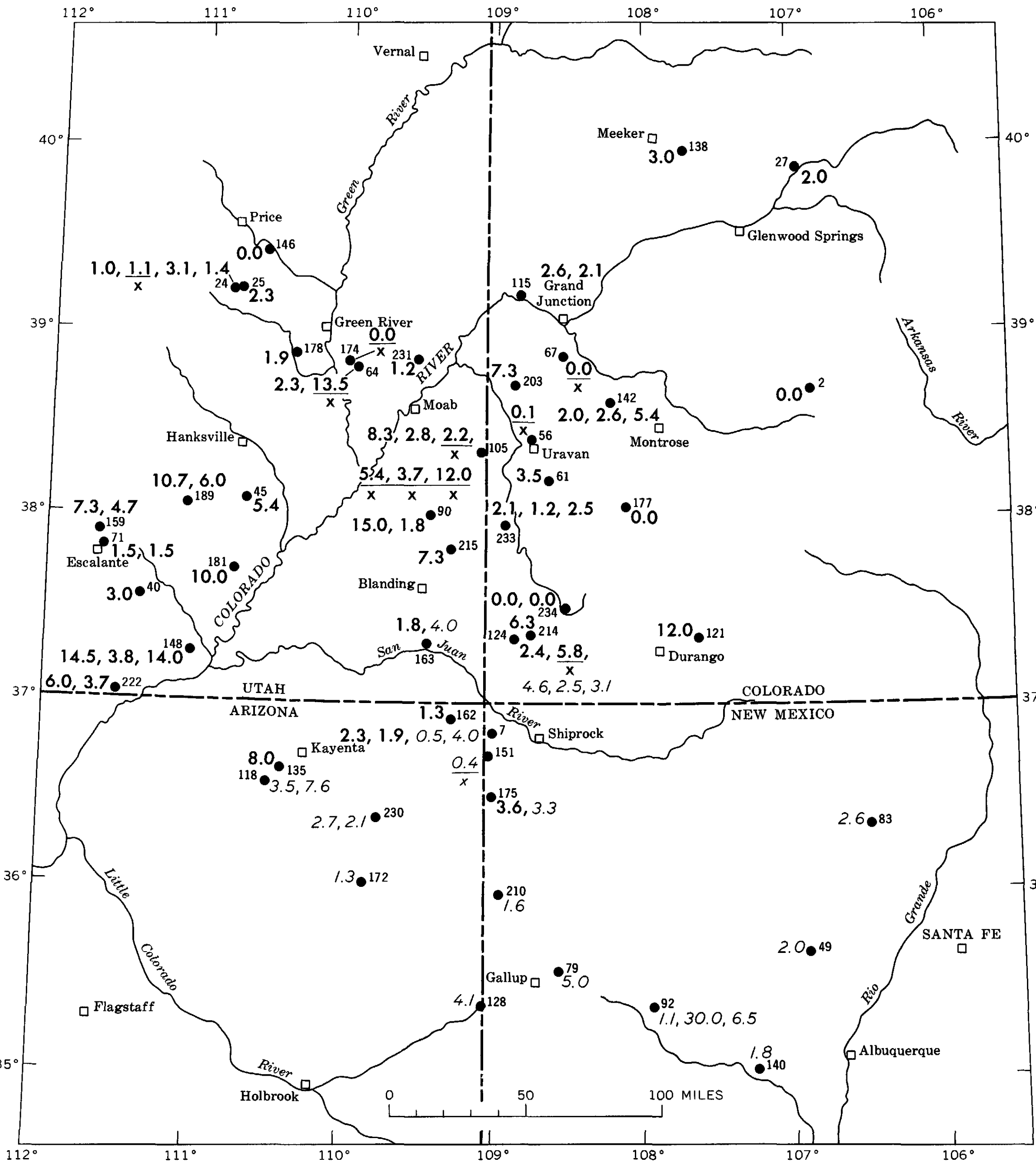

EXPLANATION

0.0 — *2.0*
Salt Wash Member — Recapture Member
R_1 for a single sample of sandstone

$\frac{0.0}{x}$ — $\frac{0.4}{x}$
Salt Wash Member — Recapture Member
R_1 for a single sample of siltstone

FIGURE 30.—Geographic distribution of ratio of potassic feldspar to sodic feldspar (R_1) in the sandstone and siltstone in the lower part of the Morrison Formation in 49 localities. Data from tables 12 and 13. Locality number refers to table 3.

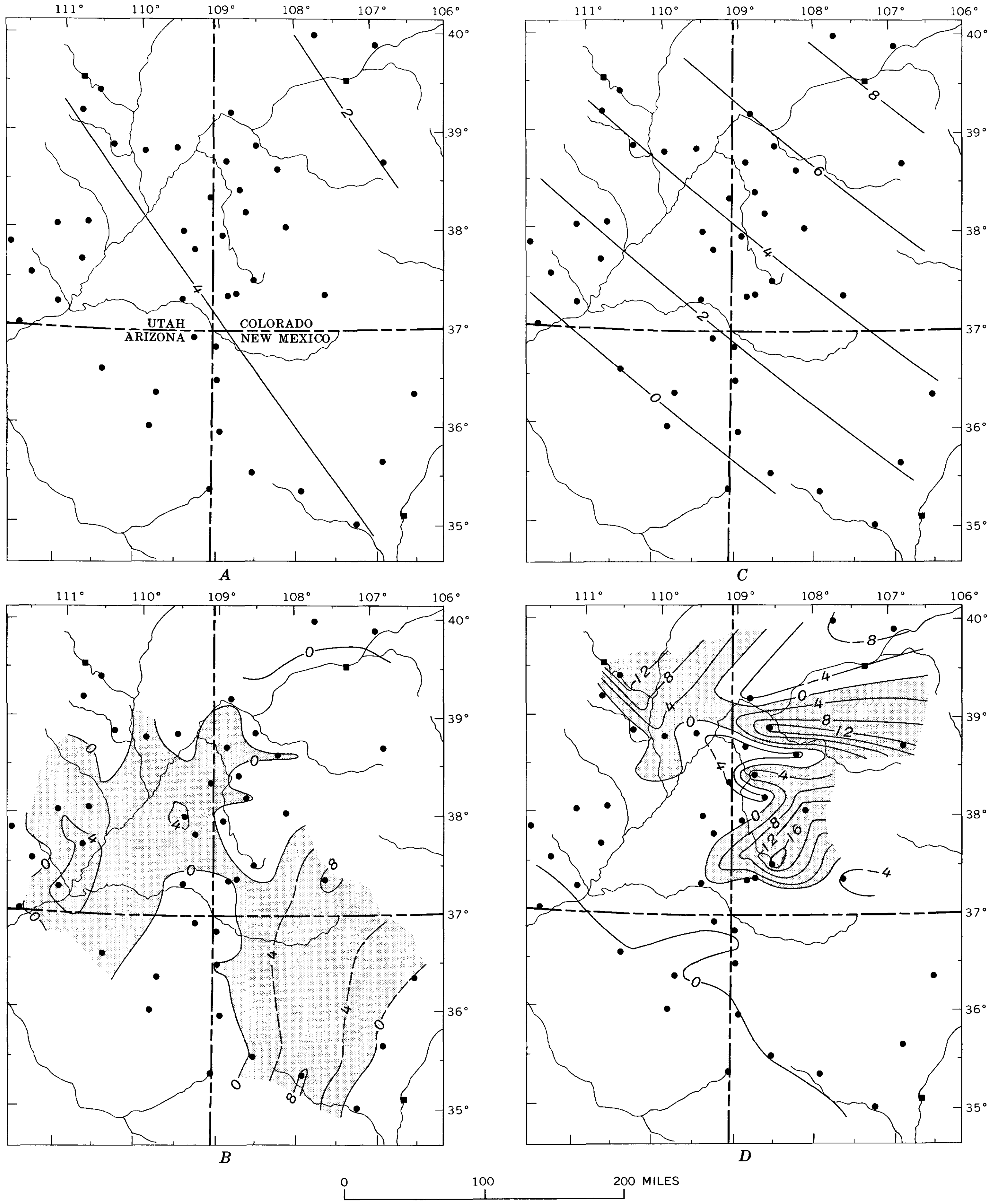

FIGURE 31.—Trend-surface analysis of potassic-sodic feldspar ratios, lower part of the Morrison Formation. *A*, Linear surface computed from R_1 locality data. *B*, Residual surface computed from *A*. *C*, Linear surface computed from R_2 locality data. *D*, Residual surface computed from *C*.

high proportions of sodic feldspar. The residual maps indicate that the sediments from southern and from southwestern-to-western feldspar sources had higher proportions of potassic feldspar than those from west-northwestern sources, which contained higher proportions of sodic feldspar.

TUFF AND FELSITE FRAGMENTS

Regional variation in percentages of tuff and felsite fragments (tables 12, 13) is plotted in figure 32. In the discussion to follow, these materials will be referred to simply as tuffaceous fragments. Quantitative data on proportions of sodic and potassic varieties of tuffaceous fragments are lacking, but a nonparametric differentiation of the two varieties was made in each thin section studied, leading to recognition of a northwest-southeast dividing line as indicated in figure 32. Samples containing dominantly sodic tuffaceous fragments are restricted to the northeastern part of the region, but samples containing dominantly potassic tuffaceous fragments occur throughout the region. Regional variation in the tuffaceous fragments was tested by trend-surface analysis. Observed data were taken from detrital rock samples with median particle size greater than 48 microns because there is a possible relationship between particle size and particle composition. Averaged data for each of the 42 data points were used, and the computed linear and residual surfaces are shown in figure 33.

The linear surface strikes N. 59° W. and dips northeastward. The computed trend surface is of moderate strength and reduces the total sum of squares by 15.1 percent. The residual surface shows high areas in the southeastern and northwestern parts of the region. According to the concept of sediment movement of figure 25, tuffaceous sediment appears to have been transported from sources south and south-southeast of the center of the region, and west-southwest and west-northwest of the center. The west-northwestern sources appear to have contributed a higher proportion of sodic tuffaceous material than did the others. The complicated relations in the northwest quadrant (fig. 33) suggest high variation in the amount of tuffaceous material in the sediments deposited there.

SILICIFIED-ROCK FRAGMENTS

As interpreted from the regional distribution of rock classification symbols (fig. 26), arenaceous-chert components seem to have significant regional variation. The definitive detrital components of the arenaceous-chert rocks are detrital chert, silicified-limestone fragments, and other silicified-rock fragments. For purposes of discussion, the percentages of these mineral groups from tables 12 and 13 are combined and referred to as silicified-rock fragments. Figure 34 illustrates the regional distribution of percentages of silicified-rock fragments in thin sections of samples from the lower part of the Morrison. To obtain a trend-surface analysis, averaged data were taken from 43 data points (fig. 34), using only samples in the median detrital particle size of more than 48 microns, because of a possible relationship between particle size and particle composition. The samples used include the limestone at locality 107, sample L844. Computed linear and residual surfaces are shown in figure 35.

The computed linear trend is of moderate strength; the linear surface reduces the total sum of squares by 17.9 percent. The surface strikes N. 23° E. and dips east. The residual surface shows a strikingly high area west of the center of the region, and smaller ones north-northwest and west-southwest of the center. A high area on the east is principally the effect of computed zero and negative values in the linear surface and has no interpretive significance.

The direction of the major sources of silicified-rock fragments, from figure 25, appears to be west and west-southwest of the center of the region. The significance of the minor highs is in some doubt; however, they may have received sediments from these same sources.

HEAVY MINERALS

Heavy-mineral separations were made on 313 samples of sandstone from the lower part of the Morrison. Grain counts made on prepared slide mounts supplied mineral-ratio data for both heavy and light-mineral fractions (Cadigan, 1967).

Table 17 illustrates the form in which heavy-and light-mineral ratios were recorded. To facilitate the study of regional variation in heavy-mineral ratios, in samples that vary widely, a regional grid was established covering the area of study. Heavy-mineral ratios in terms of grains per hundred for all samples in each grid square and for each mineral class studied were averaged together to produce a grid-average value (fig. 36). These grid-average values include the proportion of nonopaque heavy minerals, and the ratio of occurrence of each mineral within a selected heavy-mineral suite consisting of zircon, tourmaline, garnet, staurolite, rutile, apatite, and epidote.

Regional variation in the distribution of heavy minerals was analyzed first by means of a nonparametric chi-square test. For each mineral, grid-square values were divided into two groups—below average (median) and above average. The proportion of above

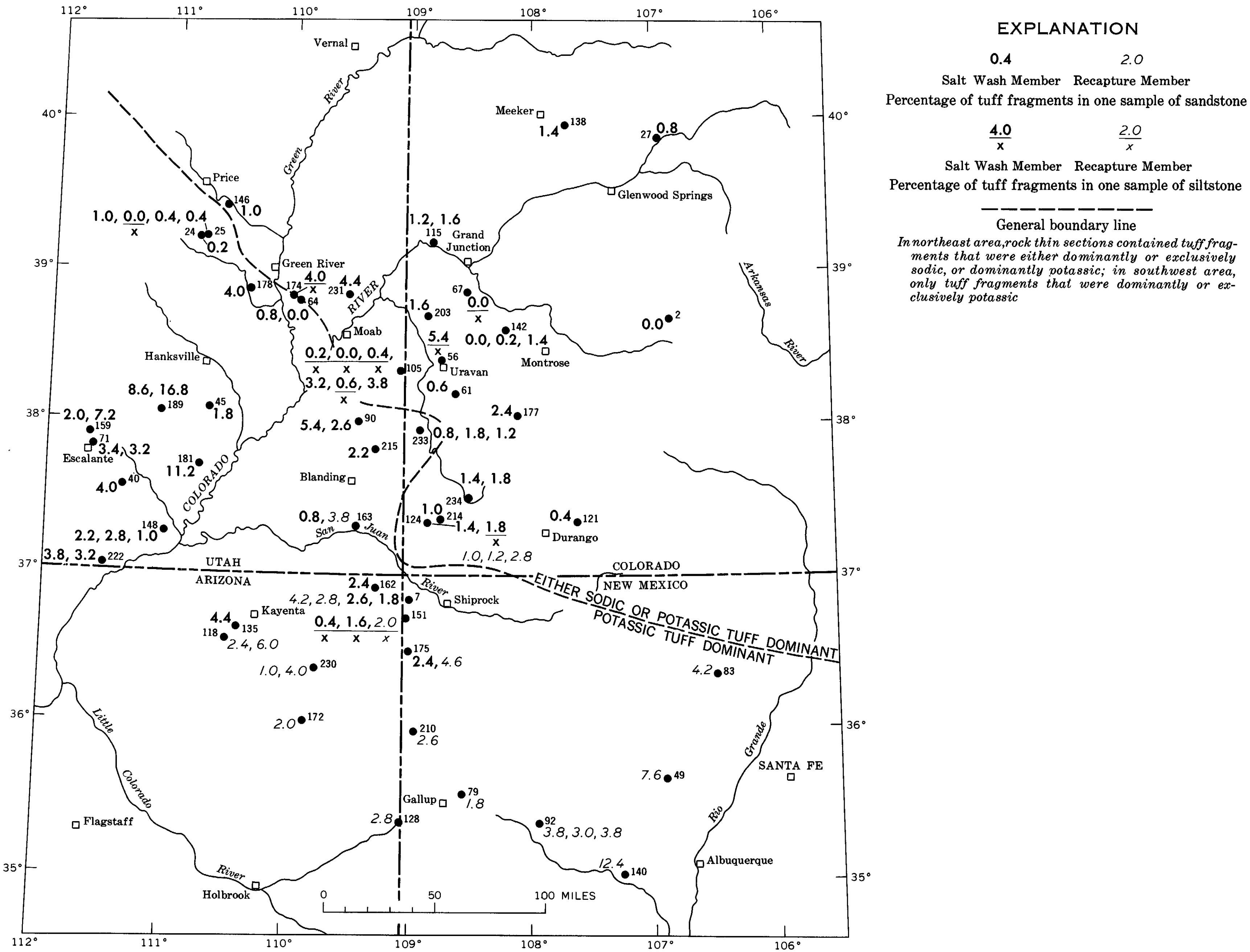

FIGURE 32.—Geographic distribution (in percent) of tuffaceous fragments and of major varieties of tuff in sandstone and siltstone from the lower part of the Morrison Formation, as determined by thin-section point-count analysis in samples from 49 localities. Data from tables 12 and 13. Locality number refers to table 3.

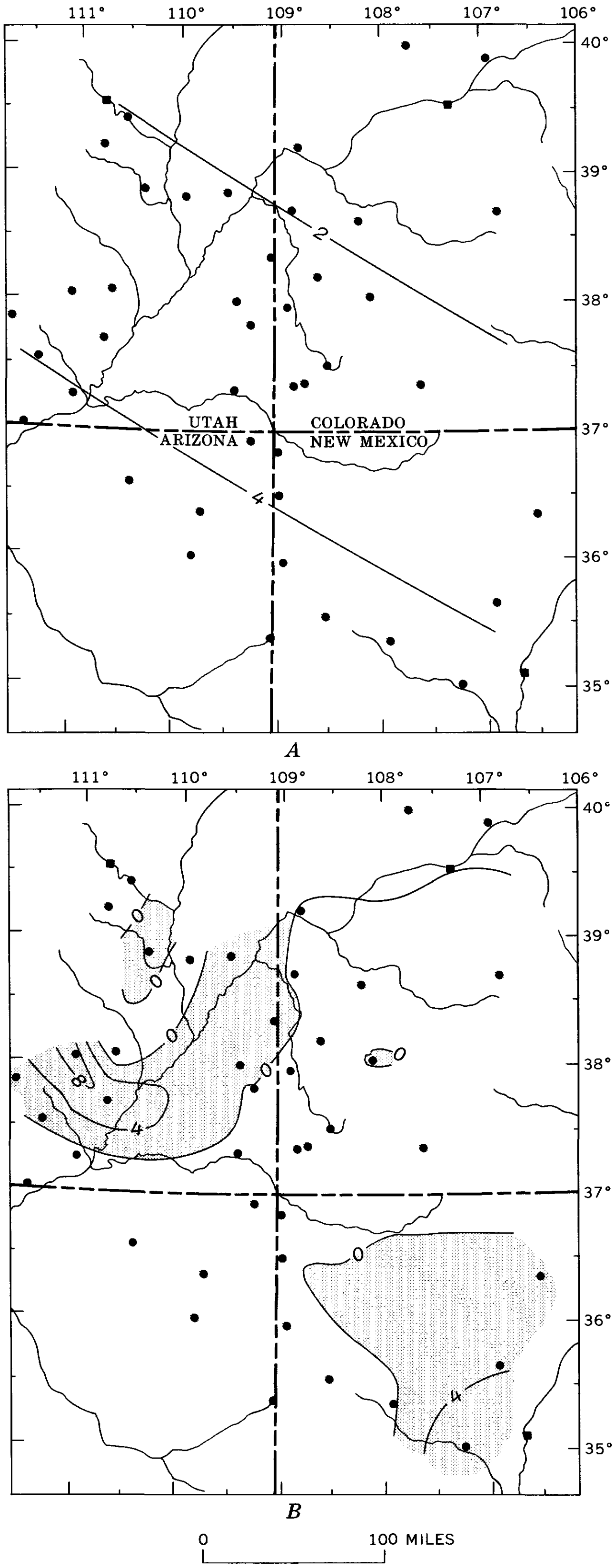

FIGURE 33.—Trend-surface analysis of tuffaceous fragment data, lower part of the Morrison Formation. *A*, Linear surface computed from modal data on tuffaceous fragments. *B*, Residual surface from *A*.

average and below average grid-square values in each of the four quadrants formed by the Four Corners was tested for departure from random. Finally, the probability of the combined distributions in the four quadrants together was tested for departure from random. The tests gave values of P_1, P_2, P_3, *and* P_4, probabilities of random distribution of the mineral ratios in each of the respective quadrants, and P_r, probability of randomness in the region as a whole. (*P* stands for probability of randomness; 1, 2, 3, 4, and *r* designate the four quadrants and the region.) A more detailed description of the method was published earlier (Cadigan, 1962a). The computed probabilities of randomness for the respective minerals are shown in figure 36. A value $P = 0.05$ or less is considered to be evidence of significant (nonrandom) regional variation.

The second means of study was by trend-surface analysis utilizing the grid-square values as input (*X*) values and the grid squares themselves as coordinate (*U*, *V*) values. The southwest corner of the regional grid was used as the origin of the coordinate system for nonopaque minerals and zircon. Coded grid coordinates were used for the other minerals; the origin was set at four squares to the east and six squares to the north of the southwest corner, permitting the use of smaller (*U*, *V*) numbers.

Before the regional distribution of separate parts of the heavy-mineral suite was studied, a trend-surface analysis was made of the regional distribution of the mean approximate percentage of total heavy minerals at each sample locality (Cadigan, 1967) which were recorded as in table 18. The input included heavy-mineral content, in average percent, for 90 localities, and coded geographic coordinates as used for the modal data. Figures 37*A* and *B* show the computed linear and linear residual surfaces. The computed regional linear-trend surface strikes N. 46° E. and dips northwestward. The reduction of total sum of squares by the linear surface of 19.9 percent suggests that the linear trend is moderately strong. The residual surface is very irregular and spotty but shows isolated high areas in a zone trending northwest across the region. The isolated high areas in the southeastern and central parts of the region are evidence of high variability in the regional distribution.

To reduce the effect of the high variability of the heavy-mineral data on trend-surface analysis results, and to obtain information on the major trends, the 90 data points were reduced to 28. These 28 points consisted of one sample locality selected randomly from each geographic degree quadrangle plus any points on the margins of the region not included in the degree

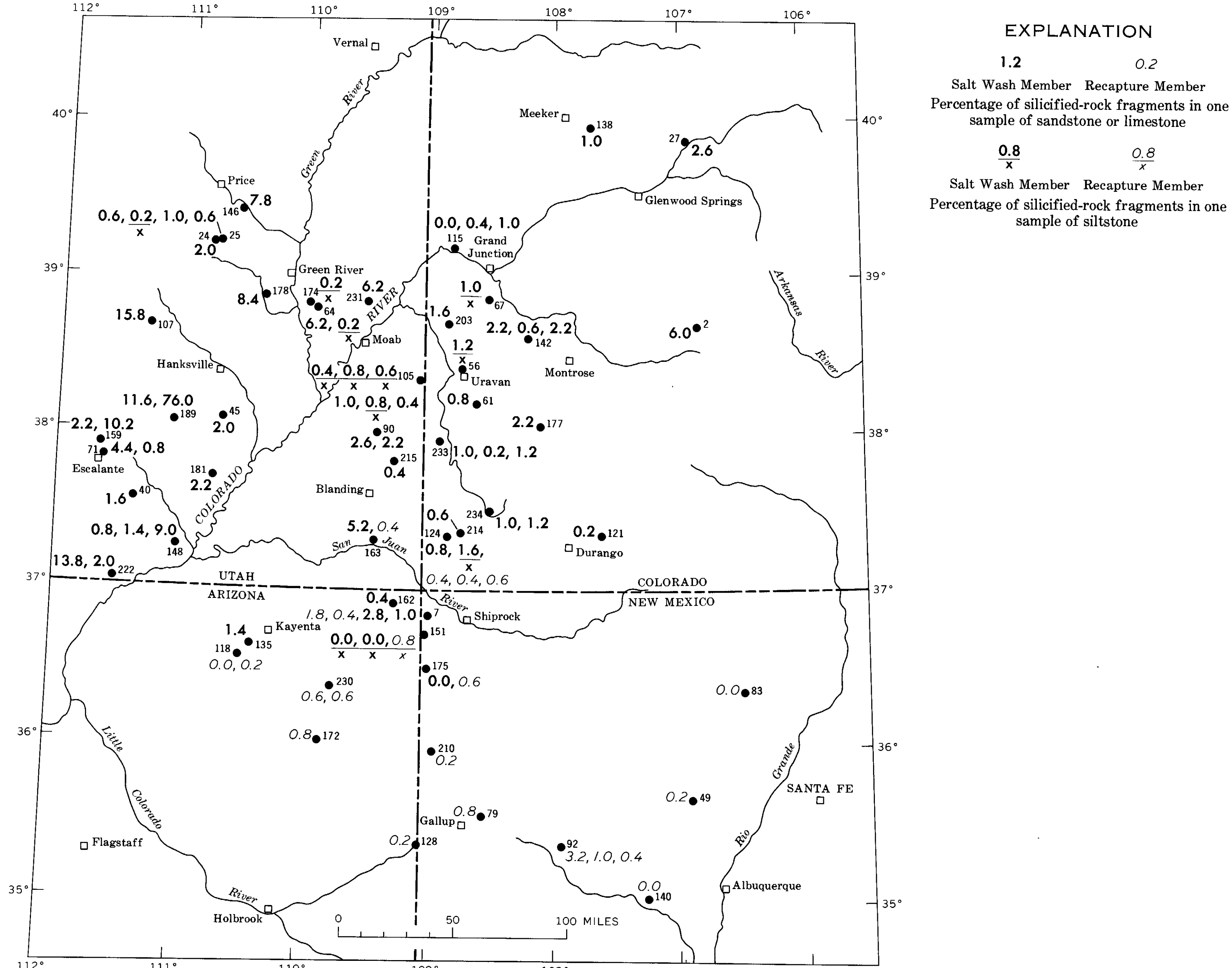

FIGURE 34.—Geographic distribution (in percent) of detrital fragments of chert, silicified limestone, and silicified rock of unknown origin in samples of sandstone, mudstone, siltstone, and limestone from the lower part of the Morrison Formation in 50 localities. Data from tables 12 and 13. Locality number refers to table 3.

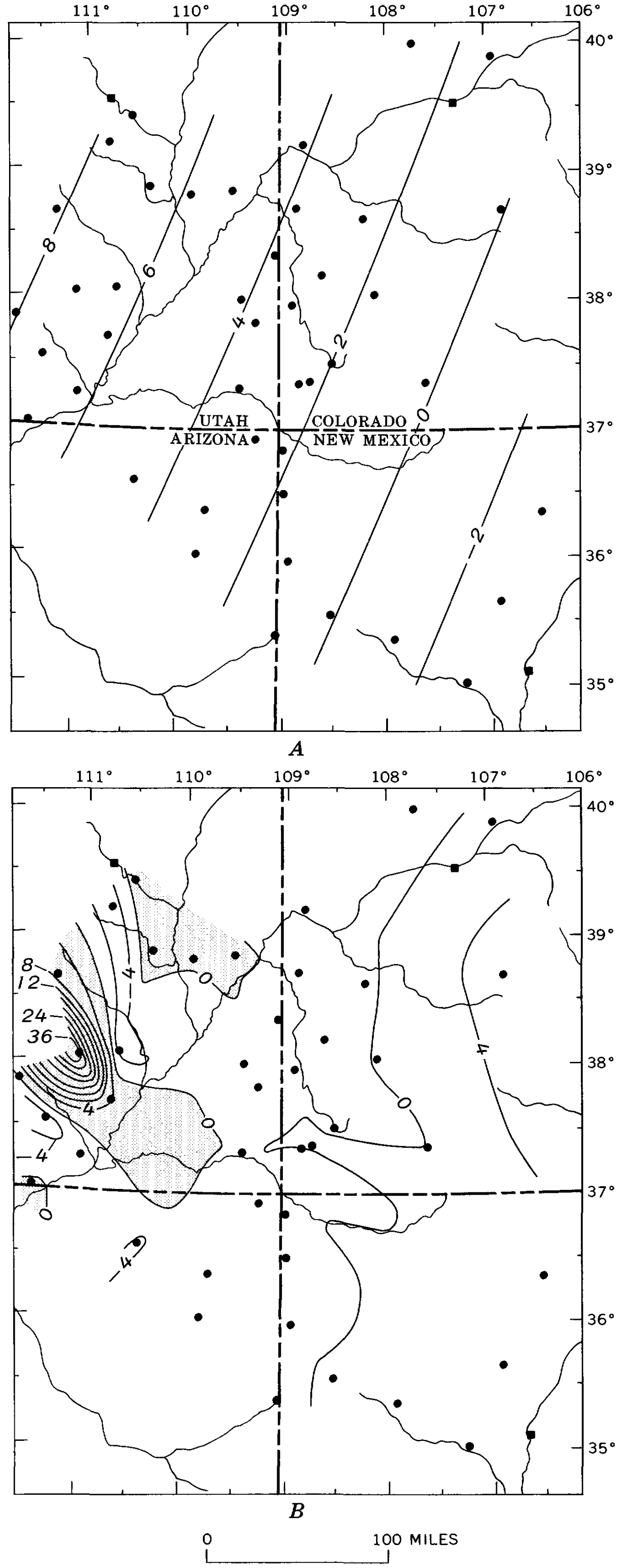

FIGURE 35.—Trend-surface analysis of silicified-rock fragment data, lower part of the Morrison Formation. *A*, Linear surface computed from modal data on silicified-rock fragments. *B*, Residual surface from *A*.

quadrangle category. Trend analysis of the data from the 28 points yielded the linear and residual surfaces shown in figures 37*C* and *D*. The linear surface strikes N. 50° E. and dips northwestward, about the same as for the 90-point surface. The data give a very strong linear trend; the total sum of squares is reduced 39.7 percent by the linear surface. The residual surface is similar to but much simpler than the 90-point surface, showing major highs in the southeast corner of the region and in the Four Corners area. The apparent high values shown by the residual map along the northwest margin of the region are mostly effects of the hypothetical zero and negative values of the computed linear surface and have no geological significance.

The regional distribution of the average percentage ratios of nonopaque heavy minerals in the opaque plus nonopaque heavy-mineral suite is shown in figure 36. Because there is a direct inverse relationship between the percent nonopaque and percent opaque fractions in the suite, the regional distribution of opaque minerals is also apparent from this figure.

The probability (P) that the observed regional (r) distribution of the nonopaque minerals occurs by chance, (P_r), is less than 0.05 but greater than 0.02. The probabilities of randomness of the nonopaque distribution, in individual quadrants, show probable nonrandom distribution in the northwestern (P_1) and southwestern (P_3) quadrants, and probable randomness in the northeastern (P_2) and southeastern (P_4) quadrants.

Trend-surface analysis of the regional distribution of nonpaque minerals yielded linear and residual surfaces shown in figures 38*A* and *B*. The computed linear surface, based on 48 grid control points, strikes N. 67° E. and dips southeastward; the surface reduces the total sum of squares by 48.0 percent, suggesting a very strong linear trend with proportions of nonopaque heavy minerals decreasing from northwest to southeast. The residual surface indicates low values in an irregular northwest-trending central area or corridor, and high values in irregular belts on each side. Because the two proportions (percent opaques and percent nonopaques) add up to a constant sum, the computed surfaces for the nonopaque minerals are complementary to those which would be obtained from trend analysis of proportions of opaque heavy minerals. Since the nonopaque trend is also opposite to the total heavy-mineral trend (fig. 37), the linear trend surfaces for the opaque heavy mineral agrees somewhat with the strike and slope of the linear trend surface of the percent total heavy minerals. This fact suggests a positive correlation between proportions of opaque heavy minerals and percent total detrital heavy minerals.

TABLE 17.—*Record form used for light- and heavy-mineral ratios in sandstone samples from the Morrison Formation*

[Excerpt from open-file report (Cadigan, 1967, table 5, "Mineral ratios obtained in the disaggregated light-grain and heavy-mineral studies of 253 sandstone samples from the Salt Wash Member of the Morrison Formation"). Q, quartz; F, potassic and sodic feldspar; SRF, silicified-rock fragments including tuff; M. miscellaneous; O, opaques; NO, nonopaques; Z, zircon; T, tourmaline; G, garnet; S, staurolite; R, rutile; A, apatite; E, epidote. Values in parentheses are locality averages (means)]

Locality (pl. 1)	Sample	Light-grain study				Heavy-mineral study, ratios given in percent								
		Q	F	SRF	M	All heavies		Nonopaque heavies						
						O	NO	Z	T	G	S	R	A	E
2	L657	97	0	3	0	37.6	62.4	87.1	11.9	0	0	1.0	0	0
	L658	98	0	2	0	41.5	58.5	68.7	21.8	0	0	9.5	0	0
	L659	92	0	8	0	69.4	30.6	79.8	17.0	0	0	3.2	0	0
		(96)	(0)	(4)	(0)	(49.5)	(50.5)	(78.5)	(16.9)	(0)	(0)	(4.6)	(0)	(0)
3	L608	94	2	4	0	47.3	52.7	70.9	29.1	0	0	0	0	0
	L609	92	6	2	0	42.0	58.0	65.5	33.3	0	0	1.2	0	0
	L610	91	7	2	0	39.7	60.3	70.2	28.7	0	0	1.1	0	0
		(92)	(5)	(3)	(0)	(43.0)	(57.0)	(68.8)	(30.4)	(0)	(0)	(0.8)	(0)	(0)
7	L358	88	7	5	0	43.7	56.3	57.9	23.9	16.4	0.6	1.2	0	0
	L359	87	12	1	0	25.1	74.9	67.1	15.1	13.7	0	4.1	0	0
	L360	81	12	7	0	74.0	26.0	48.2	34.8	14.3	0	2.7	0	0
		(86)	(10)	(4)	(0)	(47.6)	(52.7)	(24.6)	(14.8)	(14.8)	(0.2)	(2.7)	(0)	(0)
8	L368	(96)	(0)	(4)	(0)	(30.7)	(69.3)	(70.7)	(24.5)	(.5)	(0)	(4.3)	(0)	(0)
12	L345	70	15	15	0	39.8	60.2	71.5	19.5	5.0	2.0	2.0	0	0
	L346	84	14	2	0	34.7	65.3	74.9	8.7	11.1	2.9	2.4	0	0
	L347	81	15	4	0	44.2	55.8	57.0	18.6	21.5	2.3	.6	0	0
		(78)	(15)	(7)	(0)	(39.6)	(60.4)	(67.8)	(15.6)	(12.5)	(2.4)	(1.7)	(0)	(0)

TABLE 18.—*Record form used for total heavy-mineral content and other data from Morrison Formation rock samples*

[Excerpt from open-file report (Cadigan, 1967, table 13, "Miscellaneous data obtained from the grain-size and mineralogical studies of 266 sandstone samples from the Salt Wash Member of the Morrison Formation"). Values in parentheses are locality averages (means). In barite column symbols indicate proportion of barite in heavy-mineral suite: 0, absent, or <1 percent; C, common, about 1–5 percent; A, abundant, about 5–20 percent; D, dominant, more than any other mineral, about 20–50 percent; F, flood, more than all other minerals, about 50–100 percent]

Locality (pl. 1)	Sample	Components (percent by weight)			Barite	Total heavy minerals in percent of detrital fraction (excluding barite)
		Acid solubles	Sand	Fines		
2	L657	1.7	92.70	7.30	F	0.22
	L658	2.7	84.73	15.27	F	.20
	L659	1.6	92.00	8.00	F	.05
						(.16)
3	L608	5.0	84.80	15.20	0	.10
	L609	6.2	77.10	22.90	C	.09
	L610	6.5	84.30	15.70	0	.07
						(.09)
7	L358	4.0	96.90	3.10	0	.04
	L359	6.2	93.80	6.20	0	.17
	L360	6.6	98.30	1.70	0	.08
						(.10)
8	L368	12.4	85.60	14.40	F	(.05)
12	L345	14.9	93.12	6.88	F	.13
	L346	21.9	97.90	2.10	0	.10
	L347	5.1	96.54	3.46	0	.15
						(.13)
19	L332	15.8	94.30	5.70	F	.04
	L333	18.9	93.20	6.80	A	.10
						(.07)
24	L482	17.1	92.25	7.75	0	.19
	L483	12.6	91.80	8.20	0	.06
	L484	30.4	70.20	29.80	A	.23
						(.16)
27	L344	13.9	93.80	6.20	A	.38

The sediment in the northwest half of the region has higher proportions of nonopaque to opaque minerals than sediment in the southeast half; however, sediments in the southeast half of the region contain generally larger total amounts of heavy minerals and therefore probably larger total amounts of nonopaque as well as opaque minerals.

As is generally true where a very strong linear trend surface is present (Allen and Krumbein, 1962, p. 521, 522), the residual surface from the nonopaque linear surface shows high areas in roughly circular arrangement around low areas, and the opportunities for specific interpretation are thus reduced. Especially high areas exist in the southeastern and central-western parts of the region; these suggest incoming sediments with relatively high ratios of nonopaque to opaque heavy minerals. The low areas, which in fact represent areas of high proportions of opaque minerals extend generally south-southeastward through the center of the region. They are lowest, however, at the north and south margins, suggesting that incoming sediments in those areas were relatively high in ratios of opaque to nonopaque heavy minerals.

The nonopaque heavy mineral zircon (fig. 36) has a highly nonrandom regional distribution. Distribution is nonrandom also in the northeast, southwest, and northwest quadrants, as measured by P_2, P_3, and P_1. Samples in the northeast quadrant apparently tend to have higher than average proportions of zircon. Samples in the other two quadrants tend to have lower than average proportions of zircon. Trend-surface analysis of the regional distribution of zircon, using grid values, yields a computed linear surface (fig. 38*C*) which strikes N. 34° W. and dips southwestward.

Reduction of the total sum of squares by the linear surface is 24 percent, suggesting a strong trend with proportions of zircon increasing from southwest to northeast. This trend suggests the effects of downstream attrition in the sediments—that is, enrichment in zircon, a highly resistant mineral—by destruction or removal of less resistant materials. The residual surface (fig. 38*D*) shows an irregular high zone trending east-northeastward across the central part of the region and another high zone at the southeast margin.

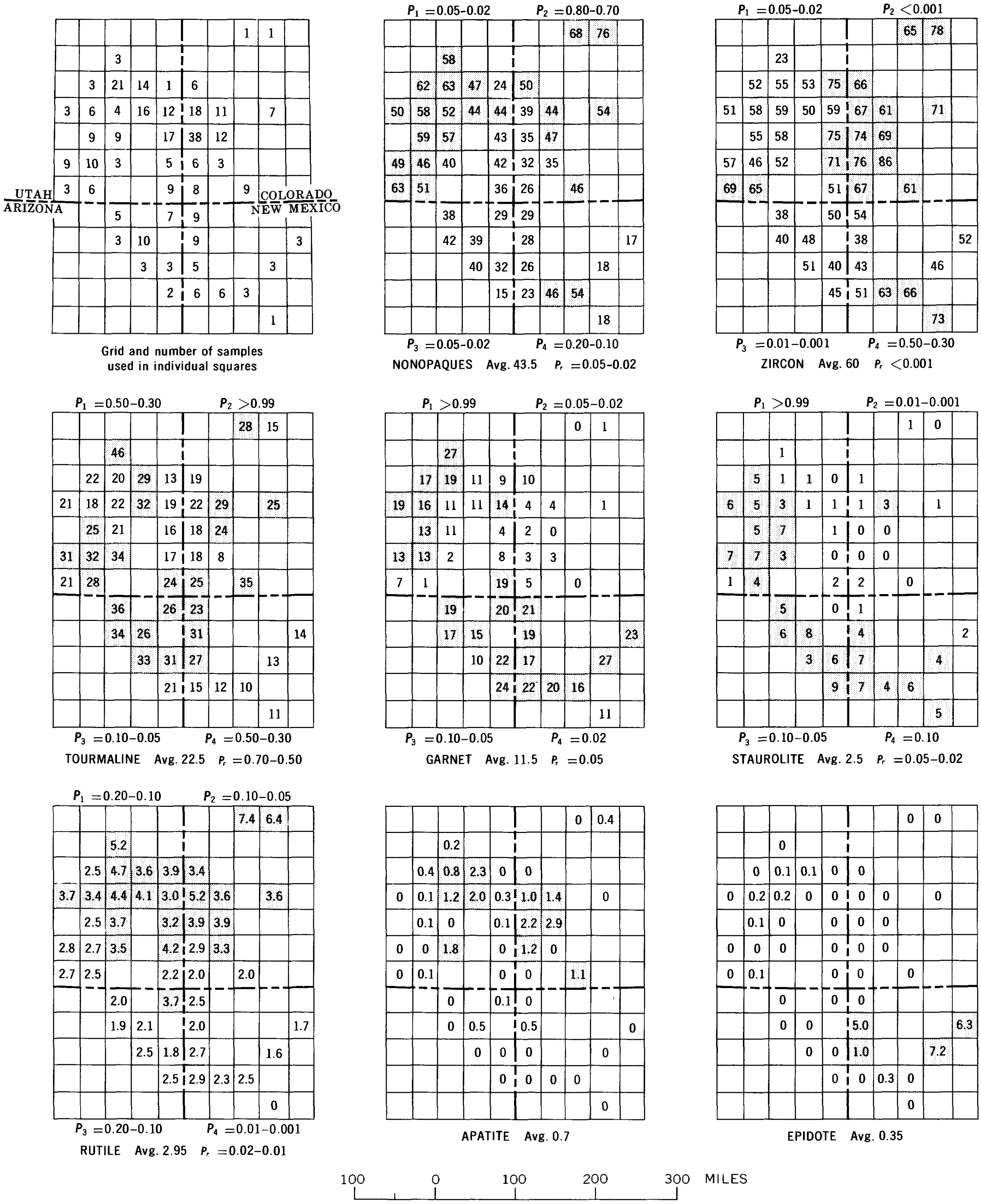

FIGURE 36.—Heavy-mineral grid ratios (in percent), lower part of the Morrison Formation. Probability of randomness for each quadrant and for the region is indicated in each mineral-ratio map by P_1, P_2, P_3, P_4, and P_r values, respectively. Average (median) ratio value (avg.) is given for each mineral. Stippling in square indicates above average proportion; number in clear square indicates below average proportion.

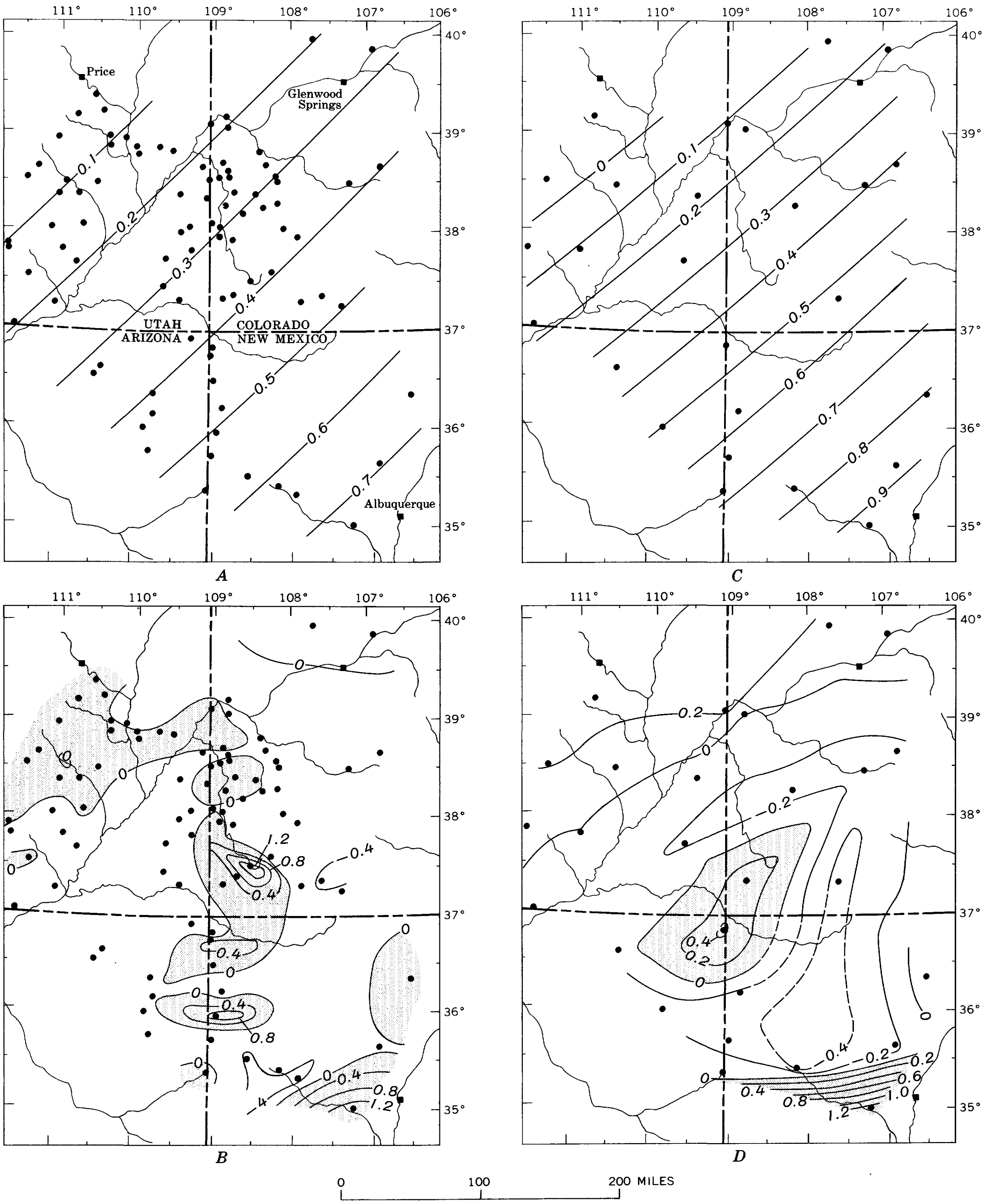

FIGURE 37.—Trend-surface analysis of total heavy-mineral data, lower part of the Morrison Formation. *A*, Linear surface computed from locality data and average total heavy-mineral content. *B*, Residual surface computed from *A*. *C*, Linear surface computed from selected locality data and average total heavy-mineral content. *D*, Residual surface computed from *C*.

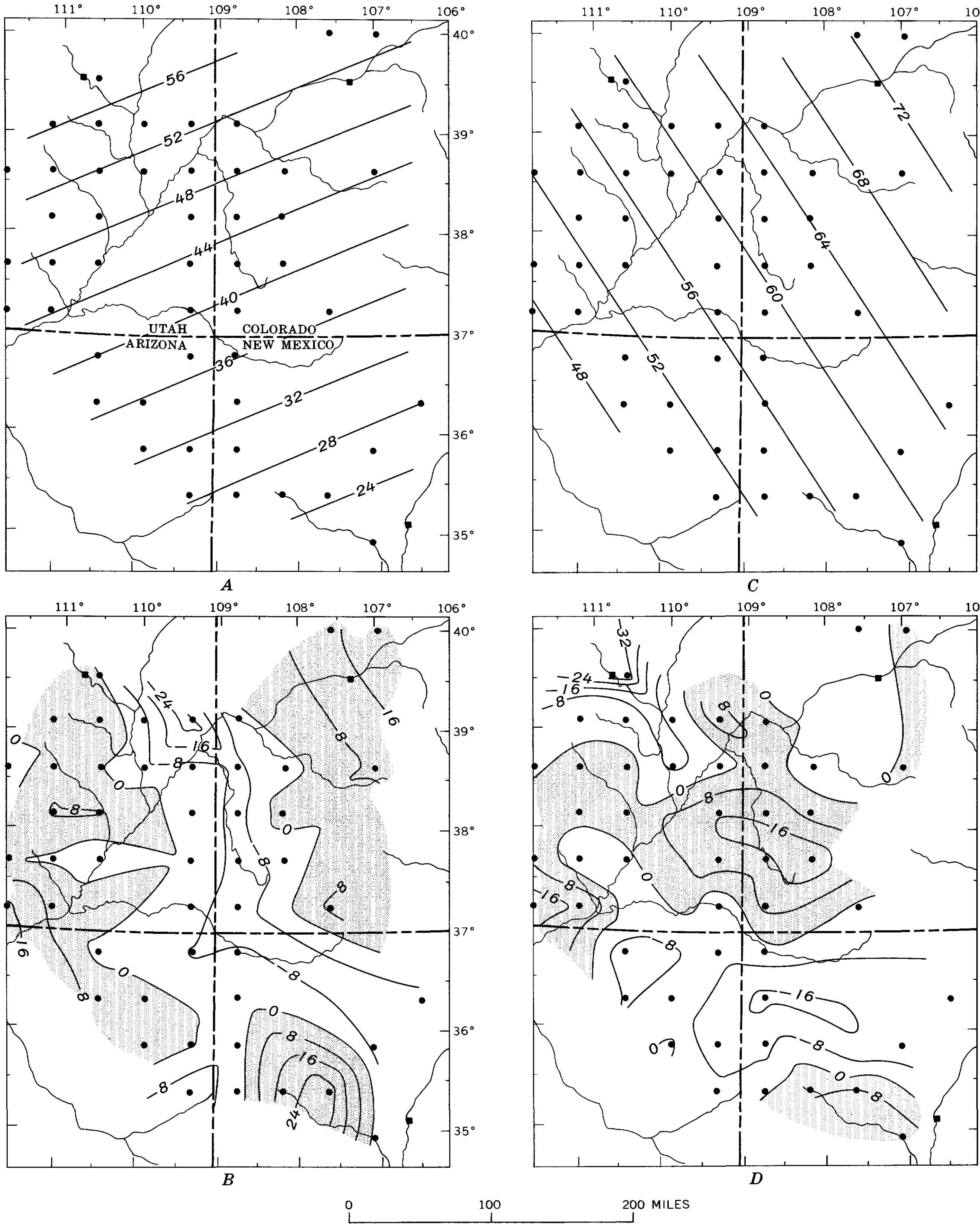

FIGURE 38.—Trend-surface analysis of nonopaque minerals and zircon data, lower part of the Morrison Formation. *A*, Linear surface computed from nonopaque heavy-mineral grid ratios. *B*, Residual surface computed from *A*. *C*, Linear surface computed from zircon grid ratios. *D*, Residual surface computed from *C*.

The heavy mineral tourmaline (fig. 36) has an apparently random regional distribution as indicated by a P_r of less than 0.70 and greater than 0.50. The probability of randomness is lowest for the southwest quadrant, but is above the conventional level of significance, 0.05. Trend-surface analysis was made (fig. 39*A*) on the basis of 48 grid-square values and coded grid coordinates. The linear surface strikes N. 7° E. and dips eastward; it reduces the sum of squares by 17.5 percent, suggesting a moderate trend with proportions of tourmaline decreasing from west to east. The residual surface (fig. 39*B*) shows a wide irregular but arcuate high zone crossing the south- and west-central parts of the region, and another high area near the northeastern margin. High residuals are on the north-northwestern and southwestern margins, in general conformance with the computed west-east linear trend, but the apparent randomness of the grid data makes regional interpretations uncertain.

The heavy mineral garnet (fig. 36) has a nonrandom regional distribution as indicated by P_r of 0.05. The southeast and northeast quadrants show nonrandom distributions. The probability of randomness for the southwest quadrant is also very low. Trend-surface analysis yields a computed linear surface (fig. 39*C*) which strikes N. 57° W. and dips northeastward. The lineary surface reduces the total sum of squares by 26.5 percent, suggesting a strong trend with proportions of garnet decreasing northeastward. The residual surface (fig. 39*D*) is high in irregular zones in the southern and northwestern parts of the region. Sands in these two areas appear to be affected by southern and western sources, respectively. The northeast dip of the regional trend surface evidently reflects progressive downstream losses of garnet by attrition.

The heavy mineral staurolite (fig. 36) has a nonrandom regional distribution as indicated by the P_r of 0.05—0.02. Only the northeast quadrant shows evidence of nonrandom distribution, although the probability of randomness for the southwest and the southeast quadrants is very low. Trend-surface analysis (fig. 40*A*) yields a linear surface that strikes N. 48° W. and dips northeastward; the surface reduces the total sum of squares by 46.5 percent, suggesting a very strong regional trend with proportions of staurolite decreasing from southwest to northeast. The residual surface (fig. 40*B*) shows highs in the northwestern, southern, and southeastern parts of the region. These may be validly interpreted as effects of southwestern sources. A high in the northeastern area is the result of computed zero and negative values in the strong steeply dipping linear trend surface. The eastward dip of the trend surface suggests downstream loss of staurolite by attrition.

The heavy mineral rutile (fig. 36) has a nonrandom regional distribution as indicated by the P_r of 0.02–0.01. Of the individual quadrants, only the southeastern one has a nonrandom distribution, although the northeast quadrant has a low probability of randomness. Trend-surface analysis (fig. 40) yields a computed linear surface that strikes N. 76° W. and dips southwestward; the surface reduces the total sum of squares by 62 percent, suggesting a very strong regional trend with proportions of rutile increasing from southwest to northeast. The residual surface (fig. 40) shows irregular high areas in the west-central and northern parts of the region. As mentioned previously, if the linear surface is very efficient—that is, if it accounts for a large percentage of the sum of squares, as in the present instance—the residual surface is likely to be subject to local sample variation and to show little response to regional factors. Thus, the residual surface loses much of its interpretational significance. This is true for the rutile residual surface. As for zircon, the rutile linear surface dips "upstream" and may be affected by differential attrition of garnet and staurolite. The grid map (fig. 36) suggests a western source of rutile for incoming sediment in the northwestern part of the region.

The heavy mineral apatite is erratically distributed as shown in figure 36, and no probabilities of randomness were computed. Trend-surface analysis yields a computed linear surface (fig. 41*A*) that strikes N. 69° W. and dips southwestward. The surface reduces the sum of squares by only 11.6 percent, suggesting a weak regional trend with proportions of apatite decreasing from northeast to southwest. The residual surface (fig. 41*B*) contains an irregular U-shaped high in the center of the region. This high does not aid interpretations of transport pattern except to confirm that apatite is more abundant in the northern part of the region, and thus that a source relatively rich in apatite existed to the west of the northern part of the region.

Like apatite, the heavy mineral epidote (fig. 36) has limited and erratic distribution. No probabilities of randomness were computed, and no trend-surface analysis was made. Samples with relatively high proportions of epidote are concentrated in the southeast quadrant in a zone which extends from the east-southeast margin into the south-central part of the region. The distribution suggests a southern source for most of the epidote.

In summary, total percent heavy minerals in the detrital fraction of sandstones in the lower part of the Morrison Formation seems to be highest in the southeastern part of the region, which is occupied mostly by the Recapture Member. Nonopaque minerals constitute a higher proportion of the heavy-mineral suite in the northwest half of the region.

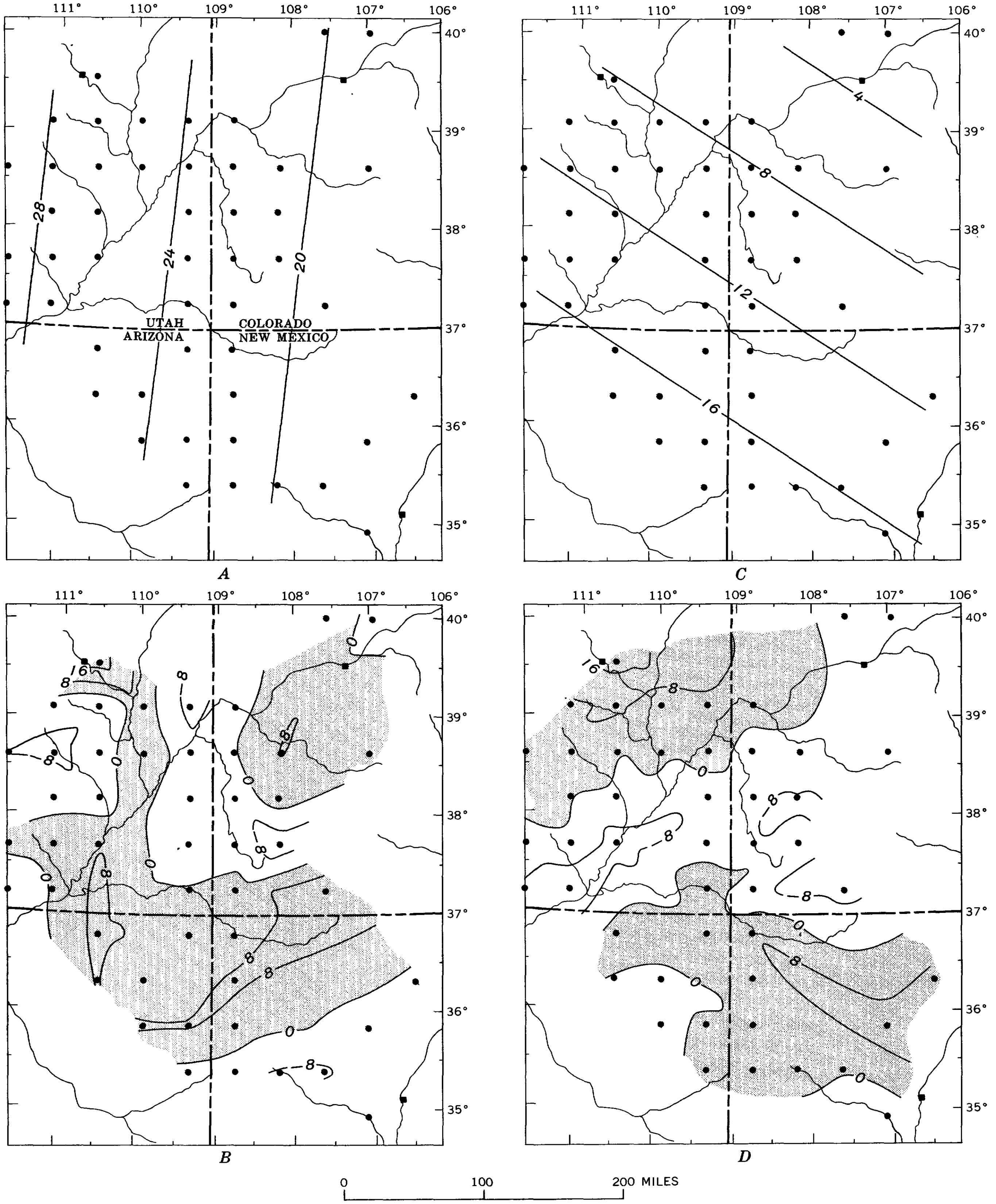

FIGURE 39.—Trend-surface analysis of tourmaline and garnet data, lower part of the Morrison Formation. *A*, Linear surface computed from tourmaline grid ratio data. *B*, Residual surface computed from *A*. *C*, Linear surface computed from garnet grid ratio data. *D*, Residual surface computed from *C*.

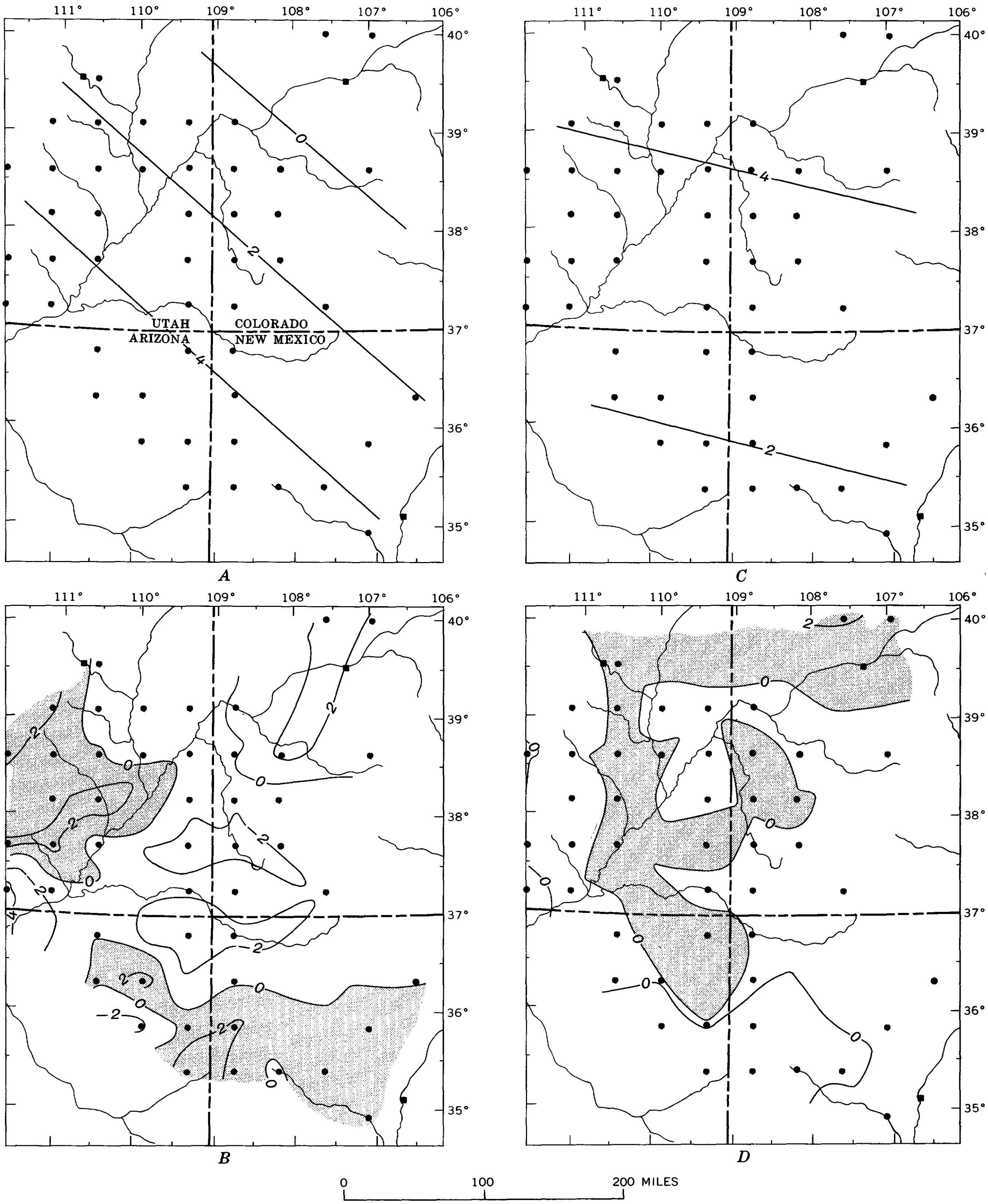

FIGURE 40.—Trend-surface analysis of staurolite and rutile data, lower part of the Morrison Formation. *A*, Linear surface computed from staurolite grid ratio data. *B*, Residual surface computed from *A*. *C*, Linear surface computed from rutile grid ratio data. *D*, Residual surface computed from *C*.

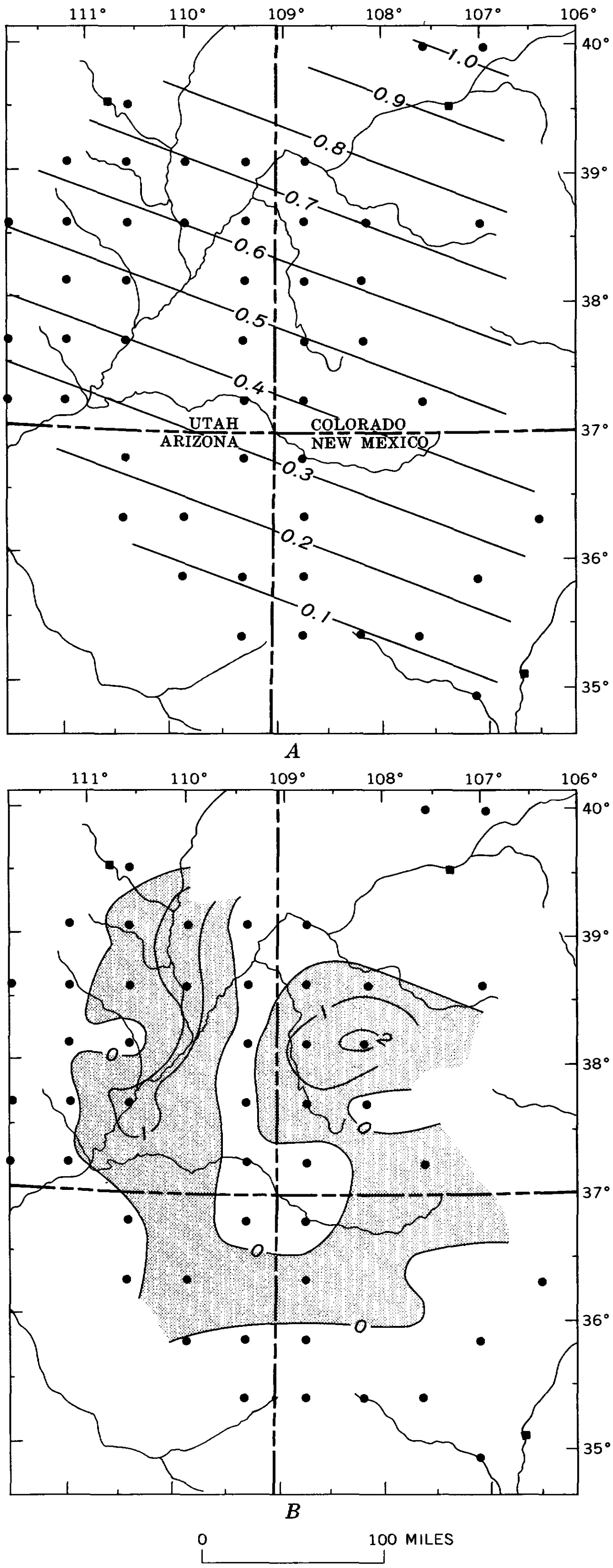

FIGURE 41.—Trend-surface analysis of apatite data, lower part of the Morrison Formation. *A*, Linear surface computed from grid ratios. *B*, Residual surface computed from *A*.

Zircon increases in proportion generally from southwest to northeast. Tourmaline regional variation appears to be random and yields vague evidence of high areas on the northwest, west and south-southwest margins. Garnet decreases in proportion generally from southwest to northeast in highly significant negative correlation ($r=-0.756$) with the proportion of zircon. Staurolite decreases in proportion generally from southwest to northeast in highly significant negative correlation ($r=-0.500$) with the proportion of zircon. Rutile increases in proportion generally from south-southwest to north-northeast, probably owing to the loss by attrition of other nonopaque minerals such as garnet and staurolite (with which it has highly significant negative correlations of $r=-0.368$ and -0.449, respectively). Apatite proportions show a trend similar to that of rutile, but much weaker. Epidote occurs in relatively high proportion, but erratically, in southeastern and west-northwestern parts of the region.

The suggested directions of movement of heavy minerals from source areas to margins of the area of deposition are summarized in figure 42. The directional arrows follow the theory of sediment transport proposed in figure 25. The marginal areas indicated by the arrows are those which show the statistical effects of detrital mineral influx revealed by the grid maps on the linear trend and residual maps of the regional distribution of heavy minerals.

LIGHT MINERALS

Light-mineral fractions from the 312 samples which supplied the heavy minerals were studied for composition by grain-count method; the results were presented (Cadigan, 1967) as percentage ratios in terms of the classes quartz, feldspar, silicified-rock fragments, and miscellaneous. The regional variation of these ratios was found to be complicated by size-composition relationships within the samples. Thus, discussion of regional variation of sand-grain composition in the present report is postponed to a later section in which the relationships between particle size and composition within all members can be discussed. Regional variation in grain sphericity is discussed below.

Preliminary work on regional variations in sphericity values of sand grains yielded conflicting results. Sands with high mean sphericity were found in areas where there appeared to be an increase in the proportions of sand grains with low sphericity. A few samples of sandstones from Salt Wash and Recapture in the Four Corners area contained evidence of southern sources of low-sphericity sand, indicated by increased skewness to the low side of the sphericity value distributions. High variation obscures recognition of any

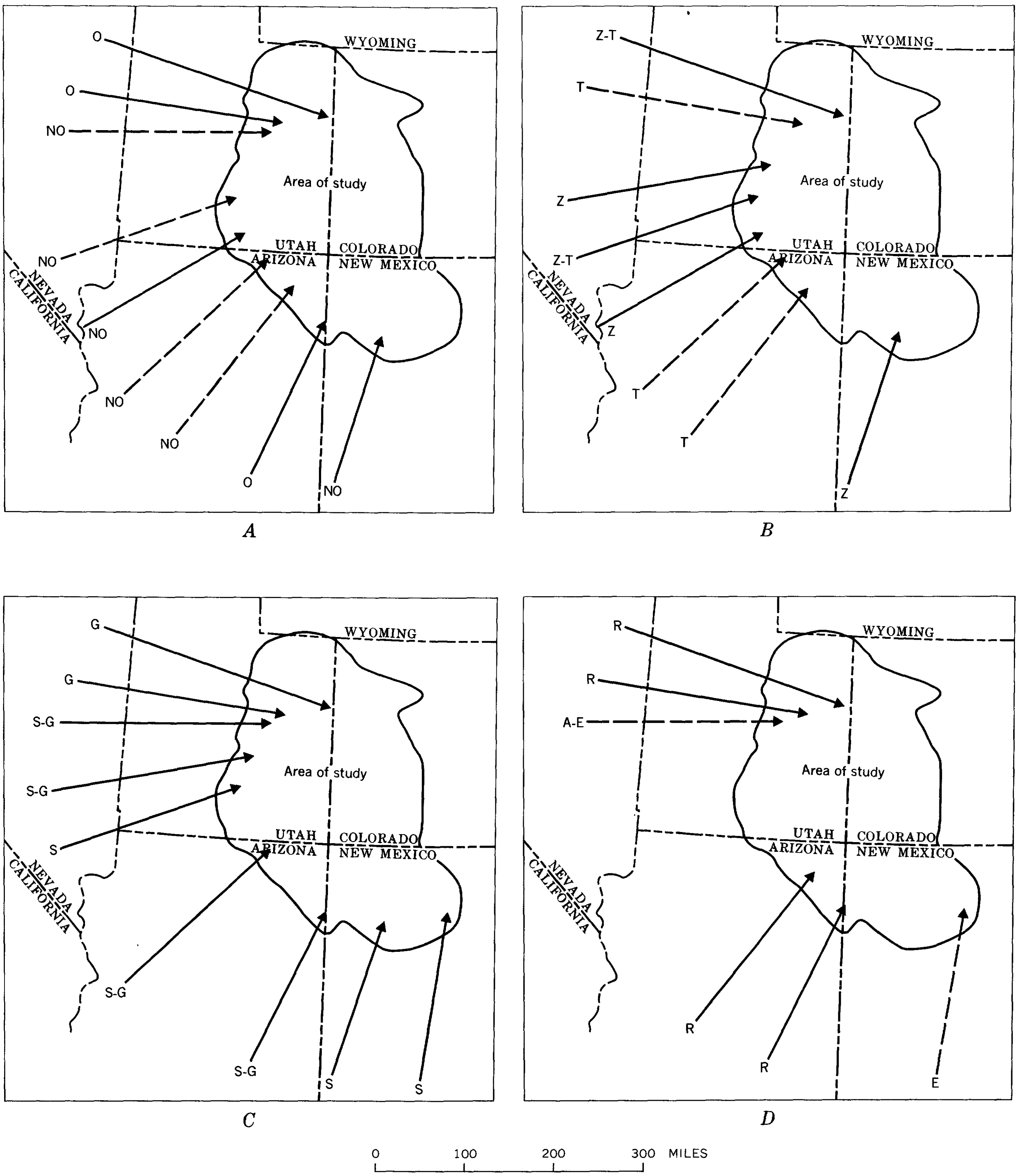

FIGURE 42.—Inferred directions of sediment transport during deposition of the lower part of the Morrison Formation as interpreted from the regional distribution of heavy minerals. *A*, Sediment having high proportions of opaque (O) and nonopaque (NO) heavy minerals. Origins of rays are possible approximate locations of source rocks. *B*, Sediment with high proportions of zircon (Z) and tourmaline (T). Note: All indicated directions for tourmaline are weak. *C*, Sediment with high proportions of garnet (G) and staurolite (S). *D*, Sediment with high proportions of rutile (R), apatite (A), and epidote (E). Heavy line, strongly indicated direction; dashed line, weakly indicated direction.

possible trend when histograms of the sphericity are studied visually. To further test for significant regional variation in sphericity, trend-surface analysis was tried.

Trend-surface analysis of the regional variation of the mean sphericity values was based on estimations made on 50 grains of very fine sand from single samples of sandstone from 56 localities (40 Salt Wash, 16 Recapture). Sphericity values were coded by subtracting 0.70 from each value. The computed linear surface (fig. 43*A*) strikes N. 45° E. and dips southeastward. The linear surface reduces the sum of squares by 19.6 percent, suggesting a moderately strong regional trend with sphericity increasing from southeast to northwest.

The residual map (fig. 43*B*) shows low values of sphericity in the southeastern and northwestern parts of the region, and high values in the central-western and northeastern parts. The north-central part of the region shows considerable variation.

A second sphericity value called subsphericity, which consists of the number of grains out of 50 that have a sphericity of less than 0.75, was taken from 56 samples as a measure of both the proportion of grains with low sphericity and an indication of skewness of the distributions toward the low side. Trend-surface analysis of subsphericity yielded a computed linear surface which strikes approximately N. 50° E. and dips northwestward (fig. 43*C*). The linear surface reduces the sum of squares by 20.6 percent, suggesting a moderately strong regional trend which decreases from southeast to northwest. The linear residual surface shows high values near the south and northwest margins of the region, and low values in the southwest and north. High values mixed with low are obtained from the central part of the region, and values are mostly low along the east edge.

The sphericity and subsphericity trends complement each other. The suspicion of a trend of combined high skewness and high sphericity is not supported by the trend-analysis results. The suspicion of low-sphericity sands in the southern part of the region is supported by the trend analysis, and unexpectedly, an area of low-sphericity sand is indicated in the northwestern part of the region. Regional variation in sphericity of sand grains of the same size is suggested by McEwen, Fessenden, and Rogers (1959) to be related to relative proportions of feldspar, quartz, and rock fragments. Sand grains consisting of higher proportions of feldspar fragments tend to be less spherical than sand grains consisting of higher proportions of quartz and (quartzitic?) rock fragments. The low sphericity of very fine sand grains in the southern part of the region (fig. 43) may well be attributed to the higher proportions of feldspar in the southeast. The low-sphericity area in the northwestern part of the region may be of similar origin.

GRAIN-SIZE STATISTICAL MEASURES

The effects of combined regional, local, and sample variation in the grain-size distributions of the sandstones of the lower part of the Morrison Formation are reflected in variations of averages of the median grain size ($Md\phi$), standard deviation ($\sigma\phi$), skewness ($Sk\phi$), and kurtosis ($K\phi$), determined for 90 sample localities. To test these averages mathematically for significant regional or local variation, trend-surface analysis procedures were used. To prepare the data, sample localities lying within 80-square-mile circles (approximately 10-mile diameter) were combined to reduce the effect of clustered data points. Combined localities include 7 and 151; 8 and 177; 12 and 115; 19 and 72; 29 and 73; 37 and 90; 64 and 174; 71 and 159; 93, 203, 136A and 136B; 112, 208, and 178; 114 and 172; 118 and 135; 124 and 214; 130, 184, and 200; 142 and 171; 150 and 161; and 173 and 231. (See pl. 1.) This process improved the spacing but reduced the number of data points from 90 to 69.

To study regional variation in average grain size, the phi median grain size (ϕ_{50}) was used in preference to the phi mean ($M\phi$) because the median is mathematically more independent of size-distribution characteristics which strongly affect the standard deviation, skewness, and kurtosis. Thus, regional variation of the median will tend to correlate with regional variation of any one of the other three measures only in response to geologic factors.

Interpretation of grain-size measures generally follows a discussion published previously (Cadigan, 1961).

Trend-surface analysis was made of the phi median grain size averages for the 69 data points. The computed linear surface (fig. 44*A*) strikes N. 10° W. and dips southwestward. The linear surface reduces the sum of squares by only 6.8 percent, evidence of a very weak regional trend of decreasing grain size from west-southwest to east-northeast (phi values increase as grain size decreases).

The residual linear map (fig. 44*B*) shows low phi median values (coarser sand) in the southeastern and northwest-north central parts of the region. High phi median areas are scattered along the west and north margins and occupy most of the south-central part of the region.

From the interpretation of direction of sediment movement (fig. 25), it is clear that coarser sands are associated with southern and west-southwestern to

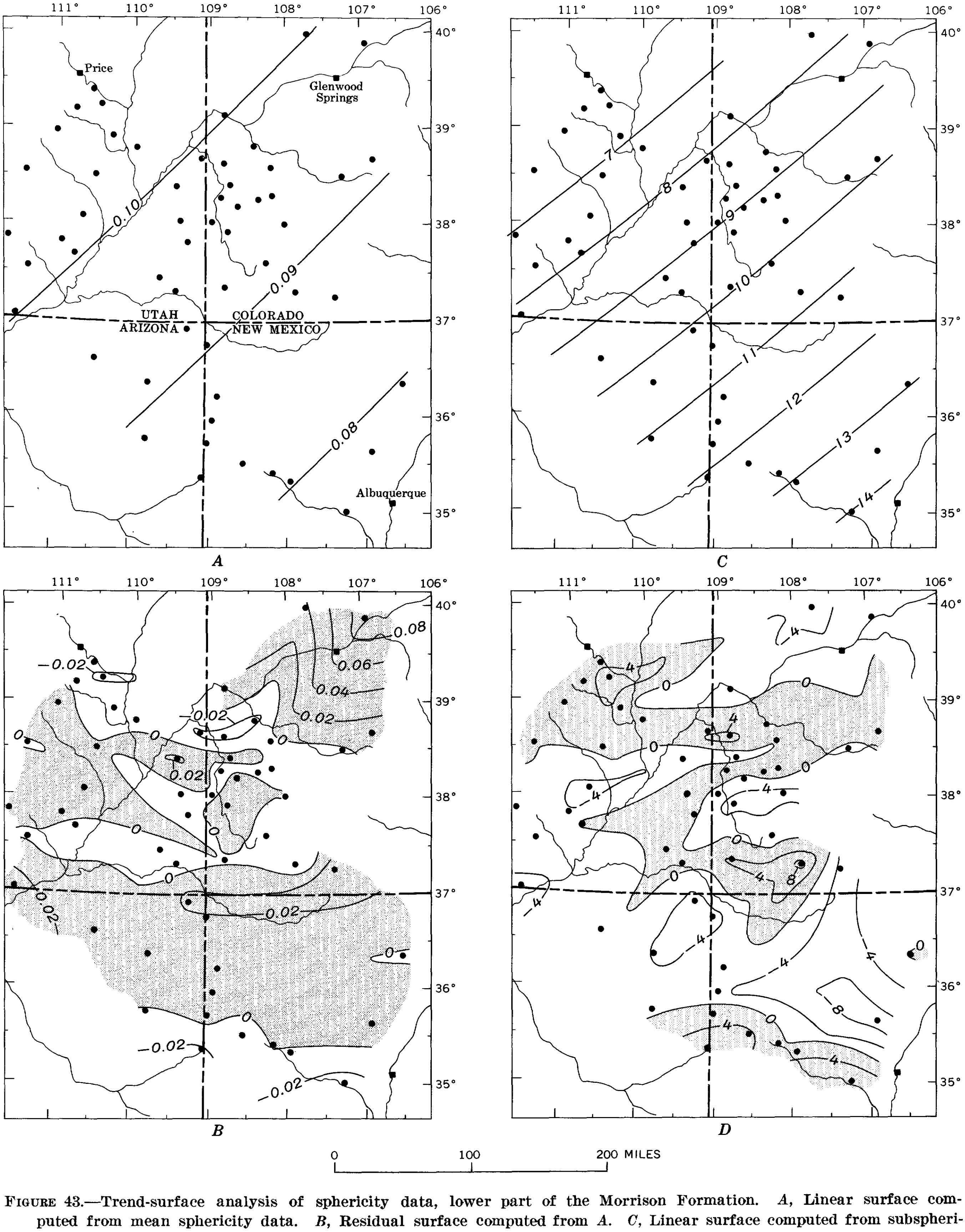

FIGURE 43.—Trend-surface analysis of sphericity data, lower part of the Morrison Formation. *A*, Linear surface computed from mean sphericity data. *B*, Residual surface computed from *A*. *C*, Linear surface computed from subsphericity data. *D*, Residual surface computed from *C*.

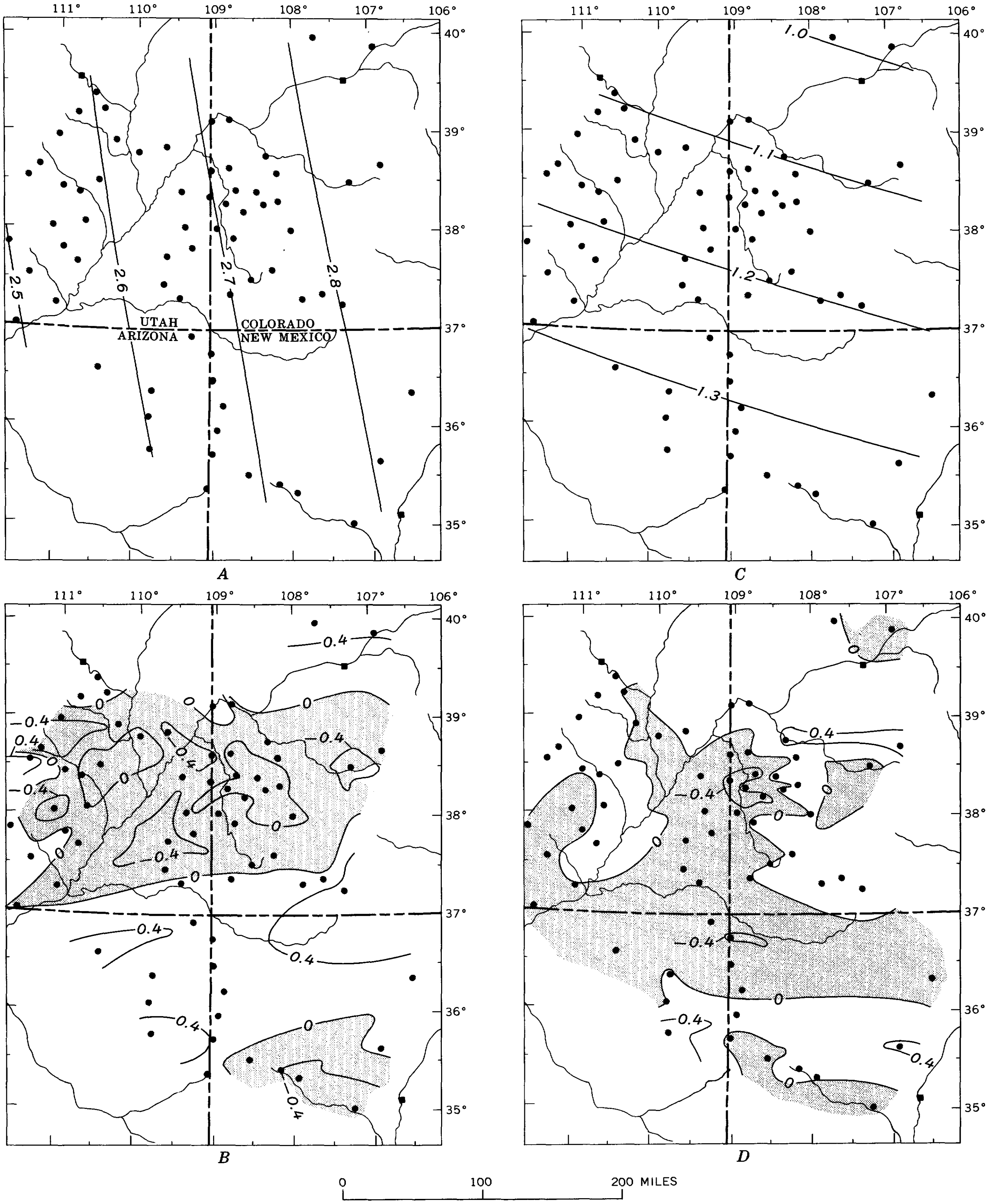

FIGURE 44.—Trend-surface analysis of phi median grain size and grain-size standard-deviation data, lower part of the Morrison Formation. *A*, Linear surface computed from phi median grain-size locality data. *B*, Residual surface computed from *A*. *C*, Linear surface computed from grain-size-distribution phi-standard-deviation locality data. *D*, Residual surface computed from *C*.

west-northwestern sources. Finer sands seem to be related predominantly to south-southwestern and southwestern sources, which probably included older Jurassic sandstones. (See p. 8.)

The rather spotty occurrences of residual-surface high areas on the west margin may be the result of high variation in the sand sizes contributed from the various sources.

Trend-surface analysis of regional variations of the standard deviations of the grain-size distributions ($\sigma\phi$) was based on the same 69 data points as the analysis of the median. The computed linear surface (fig. 44*C*) strikes N. 72° W. and dips northeastward. The linear surface reduces the sum of squares by 11.8 percent, evidence of a weak regional trend of improved sorting of sands from south-southwest to north-northeast. The linear residual map (fig. 44*D*) has low standard deviation values in the center of the region and in local areas near the south, southwest, west, and east margins.

Variation in sorting within a stratigraphic unit is evidently a function of relative amounts of reworking of a sediment, of the degree of contrast between mixtures of sediment from different tributary sources, and of tectonic changes in source or depositional areas during deposition of the sediment. In the lower part of the Morrison Formation, the observed variation seems to be due principally to differences in amount of reworking and to different sources. The large central area of low $\sigma\phi$ values (fig. 44*D*) is interpreted as the main stream channel area in which reworking would have been at a maximum. Variation in the marginal areas evidently reflects tributary streamways and the mixing of sediments of contrasting texture. Along the south margin of the region, for example, sands are better sorted to the east than they are to the west. Two sediments evidently are mixed in this area; one, a coarser sediment probably came from a distant igneous and feldspathic source; the other, a finer sediment, probably came from a nearer sedimentary source. Similar relationships may occur in the western and northwestern areas, although the specific sources are not as definite.

Trend-surface analysis of the regional variation in phi skewness of the grain-size distributions of sandstones in the lower part of the Morrison Formation was also made from the 69 data sets. The computed linear surface (fig. 45*A*) strikes N. 83° W. and dips northward. The linear surface reduces the sum of squares by 15.4 percent, evidence of a moderately strong regional trend of decreasing skewness from south to north.

The linear residual map (fig. 45*B*) has low skewness values in places along the southwest and northwest margins of the region and in a relatively small area near the center. The remainder of the region has high skewness values. Geologic interpretations of skewness values are not well established, but previous studies (Cadigan, 1961) suggest that skewness and standard deviation (sorting) values together are meaningful. High skewness values for the particle-size distribution of a sand are suggestive of considerable reworking of the sand or of the intermixture of two or more sands of different texture. Low skewness combined with good sorting (low standard deviation) values suggests a very highly reworked sediment. Low skewness combined with poor sorting (high standard deviation) values, a relation suggesting little reworking, is absent in most of the sandstone of the lower part of the Morrison in the region of study, and areas of high and low skewness may therefore be considered as respectively areas of moderately reworked and possibly intermixed sands, and of extensively reworked sands.

This interpretation, applied to the areas of low skewness mentioned above, suggests that sediment that moved into the region from the southwest and west was extensively reworked, a circumstance that in turn suggests that the sediment moved a considerable distance or that it was derived from older sediments, or both. Centrally located areas of low skewness suggest highly reworked sand and a stream-channel environment of deposition.

Trend-surface analysis of the phi kurtosis of the grain-size distributions of sandstones in the lower part of the Morrison Formation also was made from the 69 sets of data. The computed linear surface (fig. 45*C*) strikes N. 79° W. and dips northward. The linear surface reduces the sum of squares by 12.4 percent, evidence of a weak regional trend of decreasing kurtosis from south to north.

The linear residual map (fig. 45*D*) closely resembles that of skewness. Variation in kurtosis is interpreted in the same way as variation in skewness. Gradual decrease in kurtosis from south to north suggests, as for skewness, a gradual improvement in the internal sorting of the grain-size distributions of the sandstone in the general direction of regionwide sediment movement.

In summary, regional trends of grain-size distribution measurements are oriented generally from southwest to northeast. Grain size decreases from west to east, sorting improves from south to north, and skewness and kurtosis decrease from south to north. These trends are all compatible with the inferred directions of movement of the sediment across the Colorado Pla-

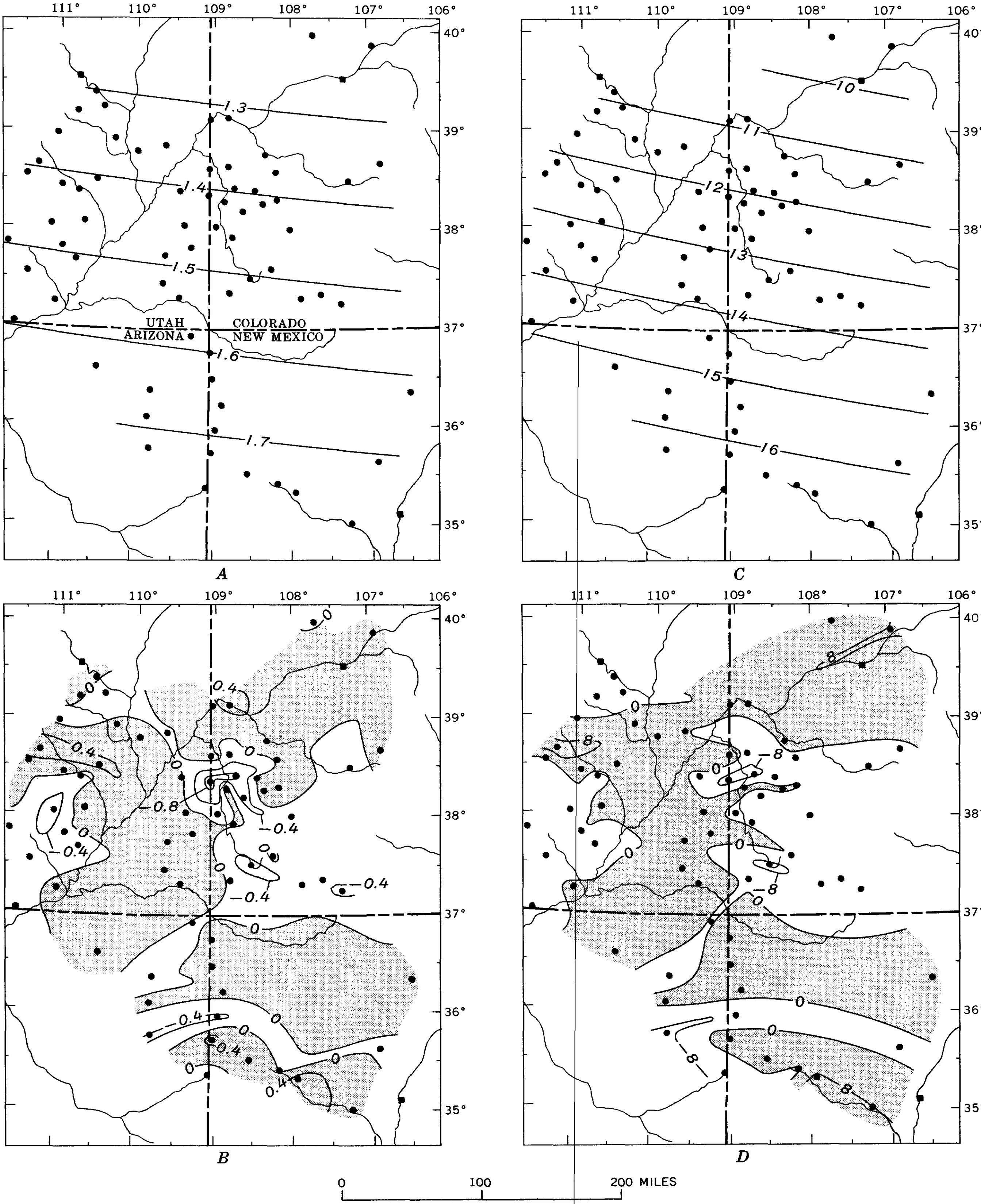

FIGURE 45.—Trend-surface analysis of grain-size skewness and kurtosis data, lower part of the Morrison Formation. *A*, Linear surface computed from grain-size-distribution phi-skewness locality data. *B*, Residual surface computed from *A*. *C*, Linear surface computed from grain-size-distribution kurtosis locality data. D, Residual surface computed from *C*.

teau region during deposition of the lower part of the Morrison Formation.

The trends are resultants of the effects of multiple sources. Inasmuch as these sources are not equally represented in the sediments, the regional trends of various parameters are influenced in different degrees by the different sources. The west-east orientation of the grain-size trend suggests that western and southwestern sources contributed on the average coarser material than the southern sources. On the other hand, the size and sorting characteristics of sediment from southern sources resulted in higher skewness and kurtosis values than did those from western sources. Such sediment may be the effect of contributions of eolian sands derived from the upper part of the San Rafael Group.

WESTWATER CANYON AND BRUSHY BASIN MEMBERS OF THE MORRISON FORMATION

The Westwater Canyon Member (fig. 4) conformably overlies the Recapture Member in the southern part of the region and in the Four Corners area. The Westwater Canyon intertongues northward with the Brushy Basin Member. The Brushy Basin Member conformably overlies the Salt Wash in the northern part of the region; its lower part intertongues with the Westwater Canyon in the southern part of the region and its upper part conformably overlies the Westwater Canyon. Together, the Brushy Basin and the Westwater Canyon form the upper part of the Morrison Formation.

STRATIGRAPHIC RELATIONS AND CHARACTER

The stratigraphic, compositional, and textural relations of the Westwater Canyon and Brushy Basin Members are such that for purposes of petrologic study it is convenient to treat them together as a single sedimentary unit. The Westwater Canyon is present only in the south half of the region; the Brushy Basin is present throughout most of the region. The predominantly silty Brushy Basin Member is interbedded with and generally overlies the predominantly sandy Westwater Canyon Member where both are present. Their relationship appears to be that of an alluvial-paludal-plain silt and sand deposit of regionwide extent (the Brushy Basin) enclosing a sandy alluvial-fan deposit of restricted areal extent (the Westwater Canyon).

The Westwater Canyon Member is characterized by (1) thick-bedded to massive, pale-yellowish-brown to pale-reddish-brown sandstone strata that are resistant, lensing, cross-stratified or structureless, and ledge forming; and (2) medium-bedded poorly resistant pale-yellowish-green siltstone, bentonitic mudstone, and claystone strata which form narrow benches between the sandstone strata. The effect of the rock colors is to give the unit an overall greenish cast in northernmost exposures and a yellowish-green cast in other areas. The sandstone strata form either thick block-fractured irregular ledges, or massive, in some cases structureless, convex-weathering "slick-rim" type continuous ledges. Most of the thick irregular block-shaped ledges are crossbedded and contain scour and truncation surfaces which are associated with thin beds or laminae containing pebbles, granules, and pale-yellowish-green clay galls. The convex-weathered beds tend also to be crossbedded but are seemingly more conformable with underlying and overlying strata.

The Brushy Basin Member is different in that it is characterized by massive pale-grayish-green, reddish-brown, and purple bentonitic mudstone, siltstone, and claystone that are poorly resistant and horizontally laminated; of secondary importance are thick-bedded pale-grayish-brown pebbly to conglomeratic sandstone strata that are resistant, lensing, ledge forming, and crossbedded. Typically, in outcrop, the thick resistant sandstone ledges tend to occur at the base of the member and to serve as a platform above which the variegated fine-textured rocks rise in convex weathered slopes. The fine-textured beds also include some thin beds of limestone and limy siltstone, smooth chert pebbles (gastroliths?) of many colors, red chert granules, and thin layers of pure bentonite (montmorillonite).

SCOPE OF SAMPLING

Samples from the Westwater Canyon Member were taken with appropriate spacing, but the general outcrop pattern does not permit adequate regional coverage. Samples were collected from the sandstone strata only. Most of the samples collected from the Brushy Basin Member were taken from the conspicuous ledge-forming sandstone strata in the lower part of the member throughout the region of study. Fine-textured rocks were sampled only in eastern Utah and southwestern Colorado to obtain representative rock types of that area.

COMPOSITION OF SANDSTONES

The sandstone strata of the Westwater Canyon Member of the Morrison Formation include rocks of the sedimentary arkose, tuff, and orthoquartzite series. The most common varieties are feldspathic orthoquartzites, arkoses, and tuffaceous feldspathic orthoquartzites. The sandstone strata of the Brushy Basin Member include rocks of the sedimentary orthoquartzite and tuff series. The most common varieties are siliceous orthoquartzites, orthoquartzites, feldspathic orthoquartzites, and feldspathic orthoquartzitic tuffs.

The strata of the two members are composed of grains, matrices, and cements almost identical with those of the Salt Wash and Recapture Members.

Detrital heavy-mineral grains in the sandstone represent less than 0.50 percent in the Westwater Canyon and less than 0.25 percent in the Brushy Basin.

The matrix of the sandstones of the Westwater Canyon is composed predominantly of clays of the kaolinite group and to a lesser extent of chlorite and clays of the mica and montmorillonite groups. That of the Brushy Basin is composed of clays that are dominantly of the montmorillonite group, and to a lesser extent of chlorite, and minerals of the kaolinite and mica-clay groups.

Cements in the Westwater Canyon vary from those of the other members only in that they include potassic feldspar overgrowths.

Quartz and other silica in sandstones of the Westwater Canyon and Brushy Basin are generally identical with those in sandstone in the lower part of the Morrison. Quartz overgrowths make up 10–15 percent of the sandstone in the Westwater Canyon, compared with 5–10 percent in the Brushy Basin.

Feldspar in the upper members is generally the same type as that in the lower members. Feldspars of the Salt Wash and Brushy Basin, and of the Recapture and Westwater Canyon Members, bear closer resemblances to each other, owing probably to regional effects. Unlike the other members, the Brushy Basin contains twice as much sodic feldspar as potassic feldspar. Feldspar is not usually considered a cement, but in some of the sandstones of the Westwater Canyon, potassic feldspar forms an interstitial crystalline cement consisting of optically continuous overgrowths on sodic feldspar and perthite (fig. 28); in some places it forms a fresh-looking shell around a weathered partly altered or replaced albite grain.

Heavy minerals in the Westwater Canyon and Brushy Basin Members are virtually the same as those described as present in the lower part of the formation. The calculated age of the zircons, $4.8 \times 10^8 \pm 5.5 \times 10^7$ years, was determined by T. W. Stern in 1959 by use of the lead-alpha method on a composite sample of zircons from sandstones in the Westwater Canyon Member (loc. 92, Haystack Mountain, Valencia County, N. Mex.). His results suggest that the zircons were either derived directly from Precambrian crystalline rocks or reworked from later (Paleozoic?) sediments. Significant contributions from contemporary Jurassic sources of fresh zircon are not probable.

Acid-soluble minerals in the sandstones in the upper part of the formation are the same as those already described as present in sandstones in the lower part.

Microstructural variations described as present in sandstones in the lower part of the formation are also present in the upper part. Some heterogeneous sandstone and most of the mudstone in the Brushy Basin Member probably derived its present matrix-rich microstructure from the alteration to clay of much of its original sand-size glassy volcanic debris.

COMPOSITION OF FINE-TEXTURED ROCKS

Fine-textured rocks in the Westwater Canyon Member were not studied. Fine-textured rocks in the Brushy Basin Member are, qualitatively, of the same general mineral composition as the interbedded sandstone. Quartz, feldspar, silicifed-rock fragments, and altered-tuff fragments range in size from fine silt to coarse sand and are rounded to angular in shape. Feldspar and altered tuff occur in greater proportion to quartz than in the sandstone. Clay minerals are of the montmorillonite group and include chlorite and intermixed hydrous mica-montmorillonite. Thin sections of red and purple "variegated shale" show dustlike red iron oxide (hematite?) crystals impregnating the clay matrix. The more clayey rocks are probably predominantly the products of diagenesis, the postdepositional alteration of glassy tuffaceous material and fine feldspathic constituents. Keller (1958, 1962) discussed extensively the clays in the Brushy Basin Member in terms of present composition and genesis. He reported them to be rich in montmorillonite which was derived from volcanic ash, as suggested by the presence of relict shards in some montmorillonitic layers. Hydrous mica and, locally, glauconite are associated with and were probably derived from the montmorillonite. He proposed that in rare instances ferric iron combined with the montmorillonite to produce glauconitic mica.

ROCK CLASSIFICATION

Modal analyses were made on 24 thin sections of sandstone from the Westwater Canyon Member and on 27 thin sections of sandstone and 2 thin sections of fine-textured rocks from the Brushy Basin Member. The measured amounts of different mineral and mineral aggregate groups and rock-forming components in the thin sections, together with the rock classifications according to figure 17, are summarized in tables 19 and 20.

Thirty-seven of the rocks represented by thin sections belong to the orthoquartzite (or modified orthoquartzite) series, eight to the arkose series, and four to the tuff series; three are chert arenites, and one is an arenaceous porcelanite. If averages of the components (tables 19, and 20) are taken, the average sandstone in the Westwater Canyon is a feldspathic orthoquartzite, the average sandstone in the Brushy Basin is a (tuffaceous?) arenaceous chert orthoquartzite, and the average fine-textured rock in the Brushy Basin is a bentonite.

TEXTURAL MEASURES

Statistical analyses of the grain-size distributions were made for 59 sandstone samples from the Westwater Canyon Member and for 53 from the Brushy Basin Member. The computed statistical measures are given by Cadigan (1967). If the grain-size distribution classification systems in tables 6, 9, 10, and 11 are applied, the average sandstone from the Westwater Canyon is found to be fine grained, with a moderately well sorted to moderately sorted, moderately skewed, highly peaked (leptokurtic) grain-size distribution. The average sandstone from the Brushy Basin is found to be fine grained to medium grained with a moderately well sorted, moderately skewed, highly peaked grain-size distribution.

No grain-sized analyses were made of fine-textured rock samples from the Westwater Canyon Member. Statistical analyses of the grain-size distributions were made for 18 samples of typical fine-textured rocks from the Brushy Basin Member (table 21). The average fine-textured rock in the Brushy Basin is estimated to be a poorly sorted fine-grained siltstone with a symmetrical normally peaked grain-size distribution.

Six samples (L442–447, inclusive) of prominently exposed and typical bentonitic Brushy Basin "variegated shales" were taken at the Salt Wash, Utah, locality (No. 174), and include samples studied by Weeks (1953). These poorly sorted "shales" contain, on the average, 60 percent silt, 30 percent clay,

TABLE 19.—*Modes of typical sandstones from the Westwater Canyon Member of the Morrison Formation*

[In percent by volume, 24 thin sections. Rock classification: O, orthoquartzite; FO, feldspathic orthoquartzite; A, arkose; T, tuffaceous]

	Colorado			Utah					Arizona				
Locality (pl. 1) Sample	124 L195	124 L196	124 L197	28 L372	28 L373	215 L395	215 L396	215 L397	118 L763	128 L654	172 L712	230 L705	230 L704
I. Cementing components (except silica)													
a. Carbonates and sulfates (calcite)	[1] 2.6	5.6	6.4	6.8	2.2	[1] 3.4	3.0	[1] 8.6	0.2				
b. Red interstitial iron oxides (in clay)	1.2	1.2	1.0			1.2		.2			1.4		0.6
Total	3.8	6.8	7.4	6.8	2.2	4.6	3.0	8.8	0.2	0.0	1.4	0.0	0.6
II. Siliceous components													
a. Quartz grains and overgrowths	81.8	72.2	54.6	75.6	79.2	66.0	54.4	78.8	84.4	77.6	71.8	68.4	71.4
b. Quartzite fragments			.2			.2		.4		.4	.2	.6	
c. Chert, detritel		.4	.6	1.0		2.0	.6	.4	.2	.4	.2	.8	.8
d. Chert, authigenic			.2				22.2						
e. Silicified-rock fragments	.4		.2			2.4	1.0		1.0				
f. Silicified-limestone fragments						.2							
Total	82.2	72.6	55.8	76.6	79.2	70.8	78.2	79.6	85.6	78.4	72.2	69.8	72.2
III. Feldspathic components													
a. Potassic feldspar	5.4	7.8	2.6	12.0	11.6	1.4	7.4	3.6	5.6	10.4	14.8	5.4	10.0
b. Plagioclase feldspar	.8	1.8	5.0	1.4	1.4	8.6	5.4	5.8	.6	5.0	4.0	1.4	1.0
c. Kaolinitic clays (alteration products)	4.8	4.8	17.4	.6	.6	5.2		.2	2.6		2.2	5.0	11.0
Total	11.0	14.4	25.0	14.0	13.6	15.2	12.8	9.6	8.8	15.4	21.0	11.8	22.0
IV. Dark-mineral and mica components													
a. Mica flakes and books (biotite, chlorite [2])						0.2				0.2	0.2		
b. Chlorite and mica clays	0.8	1.2	0.2		[3] 0.6	4.4	0.2	0.4	[3] 0.6	4.4	[3] 2.2		1.0
c. Micaceous and mafic rock fragments						.2							
d. Heavy minerals (sp. gr. 2.90+)	.2				.2								
e. Miscellaneous (opaque and unidentified grains)		.2	.6			.6			.2	.2			
Total	1.0	1.4	0.8	0.0	0.8	5.4	0.2	0.4	0.8	4.8	2.4	0.0	1.0
V. Volcanic components													
a. Tuff and felsite fragments (silicified)	[4] 1.6	[4] 4.0	[4] 10.8	[4] 2.6	[4] 4.2	[5] 3.8	[4] 3.8	[5] 1.6	[4] 4.6	[4] 1.0	[4] 2.6	[6] 7.6	[4] 1.6
b. Montmorillonitic clays (alteration products)	.4	.8	.2			.2	2.0			.4	.4	10.8	2.6
c. Altered ash (chiefly shards, and clay)													
Total	2.0	4.8	11.0	2.6	4.2	4.0	5.8	1.6	4.6	1.4	3.0	18.4	4.2
Grand total	100	100	100	100	100	100	100	100	100	100	100	100	100
Rock classification	FO	FO	TA	FO	FO	FO	FO	FO	O	FO	FO	TFO	FO

See footnotes at end of table.

TABLE 19.—*Modes of typical sandstones from the Westwater Canyon Member of the Morrison Formation*—Continued

	New Mexico											Average of (24 samples)
Locality (pl. 1)	7	7	49	79	83	92	92	92	140	175	210	
Sample	L 566	L 571	L 725	L 777	L 792	L 784	L 785	L 786	L 721	L 750	L 646	
I. Cementing components (except silica)												
a. Carbonates and sulfates (calcite)	0.4	0.6			[7] 21.6	0.2			12.6			3.1
b. Red interstitial iron oxides (in clay)	.6					.8	0.4	0.2			0.6	.4
Total	1.0	0.6	0.0	0.0	21.6	1.0	0.4	0.2	12.6	0.0	0.6	3.5
II. Siliceous components												
a. Quartz grains and overgrowths	63.4	74.8	62.6	62.2	59.8	47.0	45.2	60.2	41.8	63.4	50.0	65.3
b. Quartzite fragments		.2	.2	.6	.2		.4	.2	.2	.6		.2
c. Chert, detrital	.4			1.0		.4	.2	.6	.8	.2	.6	.5
d. Chert, authigenic	4.0											1.1
e. Silicified-rock fragments												.2
f. Silicified-limestone fragments					.2			.4				.0
Total	67.8	75.0	62.8	63.8	60.2	47.4	45.8	61.4	42.8	64.2	50.6	67.3
III. Feldspathic compouents												
a. Potassic feldspar	5.6	6.8	18.4	14.4	12.0	16.8	21.0	10.0	10.2	19.0	19.8	10.5
b. Plagioclase feldspar	13.8	8.4	11.0	6.4	4.0	14.0	17.8	12.4	17.4	6.4	1.2	6.5
c. Kaolinitic clays (alteration products)	3.4		1.4	3.4		3.6	3.6	7.4	8.0	.8	6.8	3.9
Total	22.8	15.2	30.8	24.2	16.0	34.4	42.4	29.8	35.6	26.2	27.8	20.9
IV. Dark-mineral and mica components												
a. Mica flakes and books (biotite, chlorite)		0.2	0.2	0.2	0.2	0.4			0.2			.1
b. Chlorite and mica clays	0.6	.2	1.2	.4	.4	2.0	1.6	0.6	[3] 6.0	[3] 1.8	[3] 15.2	1.9
c. Micaceous and mafic rock fragments										.2	.2	.0
d. Heavy minerals (sp. gr. 2.90+)			.2						.2			.0
e. Miscellaneous (opaque and unidentified grains)								.2				.1
Total	0.6	0.4	1.6	0.6	0.6	2.4	1.6	0.8	6.4	2.0	15.4	2.1
V. Volcanic components												
a. Tuff and felsite fragments (silicified)	[5] 6.8	[4] 8.2	[4] 4.8	[4] 11.2	[4] 1.6	[4] 14.6	[4] 9.8	[8] [4] 7.2	[4] 2.0	[4] 6.8	[4] 4.2	5.3
b. Montmorillonitic clays (alteration products)	1.0	.6		.2		.2		.6	.6	.8	.4	.9
c. Altered ash (chiefly shards, and clay)											1.0	.0
Total	7.8	8.8	4.8	11.4	1.6	14.8	9.8	7.8	2.6	7.6	5.6	6.2
Grand total	100	100	100	100	100	100	100	100	100	100	100	100
Rock classification	FO	FO	A	TFO	FO	TA	TA	A	A	A	A	FO

[1] Barite present as cement with calcite (Ia).
[2] In the form of detrital mica replacing biotite or muscovite.
[3] Contains chloritic clay (IVb).
[4] Altered tuff fragments, potassic variety dominant (Va).
[5] Altered tuff fragments, sodic variety dominant.
[6] Tuff fragments present altered to montmorillonitic clay.
[7] Contains 3 percent barite (Ia).
[8] Contains 1 percent or more white semiopaque grains with vitrophyric structure (Va).

and 10 percent sand. The coarsest of the six (L443) contains 44 percent silt, 11 percent clay, and 45 percent sand; the finest (L446) contains 45 percent silt, 50 percent clay, and 5 percent sand. The "shales" thus tend to be poorly sorted sandy siltstone. If a standard deviation of 2.500 ϕ or higher is used as the sorting definition of a mudstone, 2 of these 6 samples are mudstones and 8 of the 18 samples listed in table 21 are mudstones, an incidence of about one-third. The presence of this proportion of mudstones in the Brushy Basin Member, which is 90 percent fine-textured rocks and which constitutes 31 percent of the Morrison Formation, is of much importance to the interpretation of conditions of deposition of the member.

Visual estimates of roundness of 50 grains from each of 20 sandstone samples of the Westwater Canyon Member from localities 7, 78, 124, 128, 163, 209, 210, and 215 yielded an approximately normal distribution of 1,000 roundness values, with a mean of 0.495 and a standard deviation of 0.139. Visual estimates of the sphericity of the same grains yielded a nearly normal distribution of 1,000 sphericity values with a mean of 0.791 and a standard deviation of 0.074. The average upper and lower limits of the sieve sizes of the sand grains used are 0.134 and 0.187 mm.

Visual estimates of roundness of 50 grains from each of 20 sandstone samples of the Brushy Basin from localities 7, 28, 56, 61, 64, 174, 178, 208, and 214 (east-central Utah, southwestern Colorado, and the Four Corners area) yielded a nearly normal distribution of 1,000 roundness values with a mean of 0.468 and a standard deviation of 0.129. Visual estimates of the sphericity of the same grains yielded an approximately normal distribution of 1,000 values with a mean of 0.782 and a standard deviation of 0.070. The average upper and lower limits of the sieve sizes of the grains used are 0.101 and 0.143 mm.

A possible regional trend in sphericity is discussed in the section of the report on regional variations in the upper part of the Morrison Formation, as are regional variations of composition and texture, and interpretations of source and origin.

REGIONAL VARIATION, SOURCE, AND ORIGIN

FIELD STUDIES

From field studies of lithology, sedimentary structures, and distribution of rocks forming the upper part of the Morrison Formation, Craig and others (1955) concluded that the sediments of the Westwater Canyon Member were derived from south of the southeastern part of the Colorado Plateau, and that sediments of the Brushy Basin were probably derived from the same sources as the Salt Wash. Bedding orientation data are less plentiful for sandstone of the upper part of the Morrison but agree generally with those for sandstones of the lower part. (See table 15.) Thus the regional directions of transport of sediment into and

TABLE 20.—*Modes of typical sandstones and fine-textured rocks from the Brushy Basin Member of the Morrison Formation*

[In percent by volume, 29 thin sections. Rock classification: O, orthoquartzite or orthoquartzitic; F, feldspathic; C, calcareous; B, bentonite; S, chert arenite, or arenaceous chert; T, tuff, or tuffaceous; P, arenaceous porcelanite; IO, impure orthoquartzite. Samples are sandstone unless otherwise noted]

	Colorado								Utah					
Locality (pl. 1)	56	61	115	115	142	177	214	214	24	28	31	37	59	71
Sample	L89	L136	L3450	[1] L3451	L387	L528	L243	L244	L674	L370	L695	L698	L672	L3776
I. Cementing components (except silica)														
a. Carbonates and sulfates (calcite)	8.0	[2] 7.2	26.4		17.2	1.2	0.8	15.6	27.8	0.8	22.4	[2] 17.6	8.6	
b. Red interstitial iron oxides (in clay)	3.8				2.2	1.2	.8	2.8			.2	.2	1.4	
Total	11.8	7.2	26.4	0.0	19.4	2.4	1.6	18.4	27.8	0.8	22.6	17.8	10.0	0.0
II. Siliceous components														
a. Quartz grains and overgrowths	73.2	66.2	47.4	2.4	60.2	54.4	84.8	69.4	48.0	27.6	56.6	40.8	59.2	75.4
b. Quartzite fragments	.6		.6		.4						.2	1.0	.2	.2
c. Chert, detrital	1.2	1.4	6.8		5.2	1.4	.4	.2	14.0	.4	7.8	8.0	16.2	2.4
d. Chert, authigenic	.2		.2		.6				2.2		.2	.6	4.2	
e. Silicified-rock fragments	.2		4.4		4.2			.6	2.6		2.2	13.0	1.0	6.2
f. Silicified-limestone fragments	4.8		.8		3.2				.8		1.8	9.6	.2	2.4
Total	80.2	67.6	60.2	2.4	73.8	55.8	85.2	70.2	67.6	28.0	68.8	73.0	81.0	86.6
III. Feldspathic components														
a. Potassic feldspar	1.4			0.4	2.0		3.4	4.6	3.2	8.2	0.8	1.8		1.4
b. Plagioclase feldspar	1.2	16.2	5.8		1.0	15.8	1.4	2.2	1.0	6.4	.6	.8	4.2	.4
c. Kaolinitic clays (alteration products)	2.4				3.0	.4	6.0	2.8			2.6	1.4	2.4	2.2
Total	5.0	16.2	5.8	0.4	6.0	16.2	10.8	9.6	4.2	14.6	4.0	4.0	6.6	4.0
IV. Dark-mineral and mica components														
a. Mica flakes and books (biotite, chlorite [3])	0.2									1.6		0.2		
b. Chlorite and mica clays	.4	3.6			0.2			0.2					0.2	
c. Micaceous and mafic rock fragments													.2	
d. Heavy minerals (sp. gr. 2.90+)										.2				
e. Miscellaneous (opaque and unidentified grains)		.2	0.2			0.2				.8				0.2
Total	0.6	3.8	0.2	0.0	0.2	0.2	0.0	0.2	0.0	2.6	0.0	0.2	0.4	0.2
V. Volcanic components														
a. Tuff and felsite fragments (silicified)	[4] 2.2	[4] 5.2	[4] 7.2	0.4	[4] 0.4	[4] 7.8	[5] 1.0	[5] 1.2	[6] 0.2	[4] 43.4	[5] 4.4	[6] 4.6	[4] 1.0	[6] 9.0
b. Montmorillonitic clays (alteration products)	.2		.2	96.8	.2	.4	1.4	.4	.2	10.6	.2	.4	1.0	.2
c. Altered ash (chiefly shards, and clay)						17.2								
Total	2.4	5.2	7.4	97.2	0.6	25.4	2.4	1.6	0.4	54.0	4.6	5.0	2.0	9.2
Grand total	100	100	100	100	100	100	100	100	100	100	100	100	100	100
Rock classification	O	FO	CSO	B	SO	FOT	FO	FO	CSO	FOT	SO	S	SO	SO

See footnotes at end of table.

TABLE 20.—*Modes of typical sandstones and fine-textured rocks from the Brushy Basin Member of the Morrison Formation*—Continued

	Utah												New Mexico			Average of siltstone (2 samples)	Average of sandstone (27 samples)
Locality (pl. 1)	71	73	112	146	159	159	174	178	181	189	208	221	7	7	175		
Sample	L3777	L815	L678	L665	L734	L735	L211	L225	L688	L686	L409	L2317	L568	L569	[1]L741		
I. Cementing components (except silica)																	
a. Carbonates and sulfates (calcite)	0.2	33.6	16.2	20.4	7.4	0.6	------	2.6	17.4	23.2	11.8	------	0.2	17.4	0.2	0.1	11.3
b. Red interstitial iron oxides (in clay)	1.4	------	------	.2	1.2	.2	------	------	1.0	------	------	------	.2	------	------	.0	.6
Total	1.6	33.6	16.2	20.6	8.6	0.8	0	2.6	18.4	23.2	11.8	0	0.4	17.4	0.2	0.1	11.9
II. Siliceous components																	
a. Quartz grains and overgrowths	36.0	51.4	68.8	55.0	74.2	67.4	69.6	49.6	64.6	39.0	63.2	10.0	39.6	62.4	17.0	9.7	56.1
b. Quartzite fragments	------	------	------	------	------	------	------	------	.4	------	.6	------	------	------	------	.0	.2
c. Chert, detrital	13.6	1.2	2.6	8.4	.6	4.4	1.8	5.0	.8	11.8	5.2	71.4	------	.2	------	.0	7.1
d. Chert, authigenic	.2	------	------	------	3.2	.8	.2	32.2	------	------	1.0	------	------	------	------	.0	1.7
e. Silicified-rock fragments	22.0	------	.2	.6	2.0	3.8	------	.2	.6	3.8	4.0	2.6	------	------	------	.0	2.8
f. Silicified-limestone fragments	7.4	------	3.8	------	4.0	.4	.8	9.0	------	6.8	5.0	15.8	------	.4	------	.0	2.9
Total	79.2	52.6	75.4	64.0	84.0	76.8	72.4	96.0	66.4	61.4	79.0	99.8	39.6	63.0	17.0	9.7	70.8
III. Feldspathic components																	
a. Potassic feldspar	2.0	7.8	------	------	2.6	7.0	0.2	0.4	2.8	1.2	------	------	6.0	3.4	------	0.2	2.2
b. Plagioclase feldspar	------	4.8	3.6	12.8	.6	.6	4.8	.2	.4	.4	4.6	------	7.8	10.0	4.0	2.0	4.0
c. Kaolinitic clays (alteration products)	2.6	------	------	1.0	.8	2.6	------	.4	7.8	------	------	------	------	.2	------	.0	1.4
Total	4.6	12.6	3.6	13.8	4.0	10.2	5.0	1.0	11.0	1.6	4.6	0	13.8	13.6	4.0	2.2	7.6
IV. Dark-mineral and mica components																	
a. Mica flakes and books (biotite, chlorite [3])	------	------	------	------	------	------	------	------	------	0.2	------	------	0.2	------	0.2	0.1	.1 0.2
b. Chlorite and mica clays	------	------	------	------	------	0.2	------	------	------	------	1.4	------	------	------	------	.0	
c. Micaceous and mafic rock fragments	------	------	------	------	------	------	------	------	------	------	------	------	------	------	------	.0	.0 .0
d. Heavy minerals (sp. gr. 2.90+)	------	------	------	------	------	------	------	------	------	------	------	------	.2	------	------	.0	
e. Miscellaneous (opaque and unidentified grains)	0.2	------	------	0.6	------	------	------	------	0.2	------	------	------	.2	------	.4	.2	.1 — .4
Total	0.2	0	0	0.6	0	0.2	0	0	0.2	0.2	1.4	0	0.6	0	0.6	0.3	0
V. Volcanic components																	
a. Tuff and felsite fragments (silicified)	[6] 14.0	[5] 1.2	[4] 4.4	[4] 1.0	[6] 2.4	[6] 8.2	[4] 6.8	[4] 0.4	[7] 3.4	[6] 12.6	[4] 2.8	0.2	[5] 10.6	[5] 6.0	[4] 2.6	1.5	6.0
b. Montmorillonitic clays (alteration products)	.4	------	.4	------	1.0	3.8	15.8	------	.6	1.0	.4	------	35.0	------	75.6	86.2	2.7
c. Altered ash (chiefly shards, and clay)	------	------	------	------	------	------	------	------	------	------	------	------	------	------	------	.0	.6
Total	14.4	1.2	4.8	1.0	3.4	12.0	22.6	0.4	4.0	13.6	3.2	0.2	45.6	6.0	78.2	87.7	9.3
Grand total	100	100	100	100	100	100	100	100	100	100	100	100	100	100	100	100	100
Rock classification	TS	CFO	O	FO	O	TFO	TO	P	FO	TSO	SO	S	FOT	FO	B	------	------

[1] Siltstone.
[2] Barite present as cement with calcite (Ia).
[3] In the form of detrital mica replacing biotite or muscovite.
[4] Altered tuff fragments, sodic variety dominant (Va).
[5] Altered tuff fragments, potassic and sodic varieties dominant (Va).
[6] Altered tuff fragments, potassic variety dominant (Va).
[7] Potassic tuff of a nearly isotropic nature is the dominant grain of volcanic origin (Va).

across different parts of the Colorado Plateau suggested in this report for the lower part of the Morrison Formation (fig. 25) probably hold true also for sediments which formed the upper part of the formation.

As previously mentioned in description of the Salt Wash and Recapture Members, arrowheads in figure 25 represent directional axes of sediment flow from multiple source areas assumed to lie 400 miles from the center of the region. Convergence of the directions indicated by the arrowheads illustrates the effects of normal fluctuation of transport directions around the axes of regional drainage; the convergence is not meant to suggest that the Colorado Plateau was a focal point of deposition.

PETROLOGIC STUDIES

The indicated and assumed effects of attrition discussed previously in relation to the lower part of the formation also apply to sediments forming the upper part of the formation. The computation and interpretation of linear trends and residuals illustrated and used for analysis of petrologic parameters of Salt

TABLE 21.—*Statistical measures of the phi grain-size distributions of 18 siltstone and claystone samples from the Brushy Basin Member of the Morrison Formation*

[Values in parentheses are locality averages (means)]

Locality (pl. 1)	Sample No.	Mode	Median	Mean	Standard deviation	Skewness	Kurtosis	ϕ_2	ϕ_5	ϕ_{16}	ϕ_{50}	ϕ_{84}	ϕ_{95}	ϕ_{98}
		Millimeters		Phi notation										
31	L478	0.0004	0.001	9.599	1.943	−0.531	0.550	4.40	5.92	7.45	10.20	11.45	11.82	11.92
	L479	.004	.005	7.319	1.742	−.006	−.211	3.85	4.38	5.68	7.32	9.02	10.25	11.40
		(.0022)	(.003)	(8.459)	(1.843)	(−.269)	(.169)	(4.13)	(5.15)	(6.57)	(8.76)	(10.24)	(11.04)	(11.66)
56	L468	.088	.006	7.197	3.155	.002	−1.480	2.62	2.95	3.45	7.45	11.23	11.88	11.97
	L469	.031	.018	6.303	2.447	.275	−.435	2.45	3.10	3.98	5.77	9.20	11.45	11.85
	L470	.019	.015	6.426	1.922	.227	−.368	3.45	3.77	4.48	6.10	8.55	9.95	10.85
		(.046)	(.013)	(6.642)	(2.508)	(.168)	(−.761)	(2.84)	(3.27)	(3.97)	(6.44)	(9.66)	(11.09)	(11.56)
61	L464	.074	.021	5.957	2.721	.234	−.849	2.10	2.45	3.12	5.55	9.12	11.33	11.82
67	L455	.0003	.002	8.393	2.672	−.254	−.906	3.13	3.75	5.17	8.92	11.38	11.87	11.96
72	L460	.045	.022	6.319	2.599	.288	−.838	2.83	3.20	3.88	5.55	9.48	11.45	11.87
105	L474	.004	.004	7.735	2.274	−.132	−.425	3.12	3.65	5.47	7.87	9.98	11.70	11.93
115	[1] L3451	.004	.008	6.689	2.650	−.062	−1.139	2.10	2.39	3.44	6.94	10.03	10.70	10.88
174	L442	.022	.009	6.929	2.540	.002	−.257	1.95	3.08	4.63	6.72	9.80	11.55	11.88
	L443	.062	.052	4.503	2.698	.156	−.032	−.75	.25	1.88	4.30	7.18	9.62	10.85
	L444	.004	.004	7.802	1.791	−.092	.353	3.75	4.47	6.28	7.82	9.22	11.10	11.73
	L445	.062	.007	6.983	1.908	.011	−.320	3.65	3.82	5.25	6.98	8.95	9.98	11.45
	L446	.004	.004	7.819	2.080	−.236	.189	3.35	3.90	5.95	8.03	9.75	11.37	11.82
	L447	.004	.008	7.064	2.334	.031	−.751	2.95	3.35	4.45	7.05	9.55	11.17	11.70
		(.026)	(.014)	(6.850)	(2.225)	(−.021)	(−.136)	(2.48)	(3.15)	(4.74)	(6.82)	(9.08)	(10.80)	(11.57)
228	L535	.052	.003	7.542	2.729	−.224	−.933	2.40	2.78	4.07	8.30	10.10	11.55	11.85
	L536	.001	.002	8.131	2.421	−.280	−.407	2.95	3.65	5.48	8.65	10.65	11.73	11.88
		(.027)	(.003)	(7.837)	(2.575)	(−.252)	(−.670)	(2.68)	(3.22)	(4.78)	(8.48)	(10.38)	(11.64)	(11.87)
Approximate means			0.011	7.151	2.368	−0.033	−0.459							

[1] Thin-section modal-analysis data in table 20.

Wash and Recapture Members were also applied to petrologic parameters of rock samples from the Westwater Canyon and Brushy Basin Members.

ROCK TYPES

Variation in modal proportions of mineral and mineral-aggregate groups and rock components among samples from the upper part of the Morrison is sufficient to yield a variety of rock types. The areal distribution of these rock types, depicted in figure 46, suggests that significant (nonrandom) regional variation of rock types is probable. Feldspathic orthoquartzites, the most common rock types, are present in all parts of the region; arkoses are nearly all restricted to the southeastern part; and arenaceous-chert rocks are restricted to the northern and northwestern parts. Nearly all rock types include tuffaceous varieties.

FELDSPAR

Feldspar content of sandstone of the upper part of the Morrison Formation (fig. 47) is highest in the southeastern part of the Colorado Plateau. This fact suggests presence of significant (nonrandom) regional variation.

To prepare the data for trend-surface analysis, it was necessary to combine some of the more closely spaced data points in order to minimize the effects of clustering. Any two or more sampling localities within an 80-square-mile circle (10-mile diameter) were treated as one data point, and all samples in such localities were averaged to obtain one value. The localities so combined include 71 and 159, 124 and 214, and 178, 208, and 112. Locality 221 was not used because of its isolation from the other data points. The modifications reduced the number of data points to 31. These data points are also used in the trend analyses of all other modal components in samples from the upper part of the Morrison.

Trend-surface analysis of the regional variation of percent feldspar in the upper part of the Morrison produced a computed linear surface (fig. 48*A*) which strikes N. 55° E. and dips northwestward. The surface reduces the total sum of squares by 63.4 percent, suggesting a very strong regional trend with proportions of feldspar decreasing from southeast to northwest. The residual surface (fig. 48*B*) shows high values in south-southeast and northwest margin areas which may be interpreted as evidence of the effects of sources of feldspar to the south and to the west and west-northwest of the center of the region. The coincidence of the south-southeastern high with the very strong linear trend suggests that the southern source was the major source of feldspar-rich sediment during deposition of the upper part of the Morrison.

Study of the regional variation in the ratios between sodic and potassic feldspars was undertaken using two sets of ratios, R_1 and R_2 (see p. 49), calculated from data in tables 19 and 20.

Trend analysis of R_1 yielded a computed linear surface (fig. 49*A*) which strikes N. 40° W. and dips northeastward. The surface reduces the sum of squares by 31.3 percent, suggesting a strong regional trend with proportions of potassic feldspars to sodic feldspars decreasing from southwest to northeast. The residual map (fig. 49*B*) shows significantly high values in the western to south-southwestern marginal areas and just north of the southern marginal area. Minor highs are

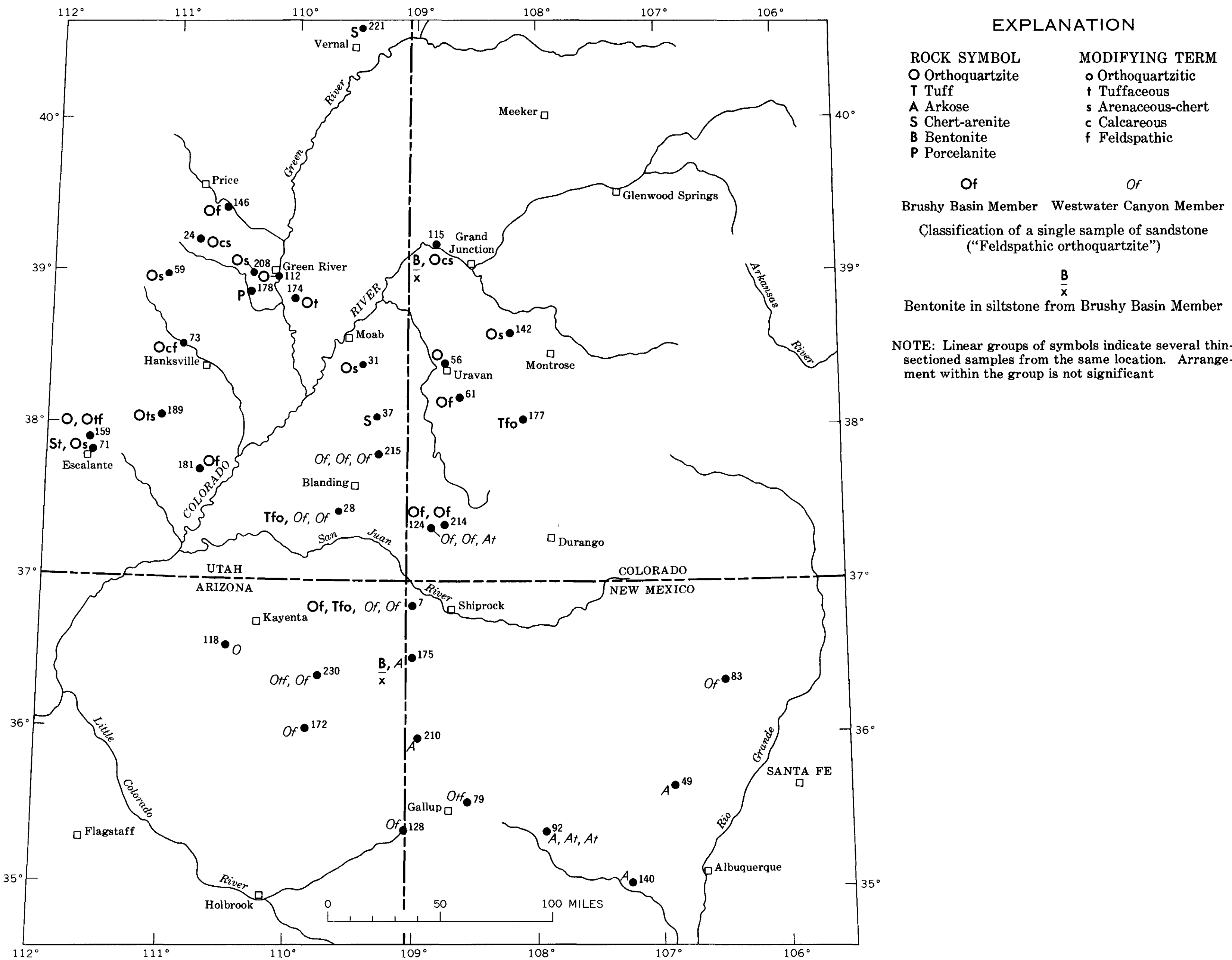

FIGURE 46.—Geographic distribution of rock types, upper part of Morrison Formation, as indicated by classification symbols (tables 19 and 20) of 53 samples from 36 localities. Locality number refers to table 3.

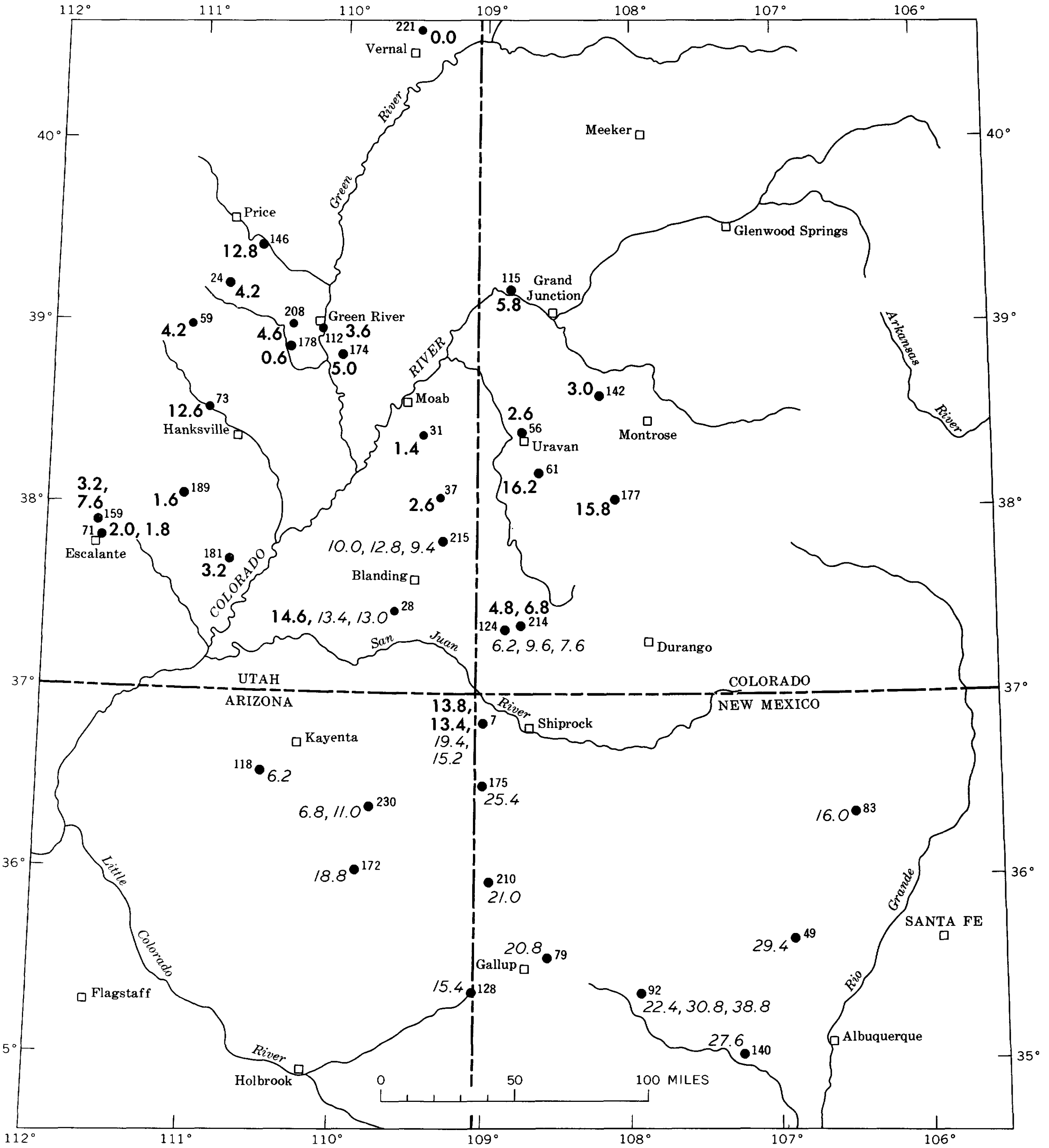

FIGURE 47.—Geographic distribution (in percent) of feldspar content in sandstone, mudstone, and siltstone of the upper part of the Morrison Formation, as measured in thin sections from 36 localities. Data from tables 19 and 20. Westwater Canyon Member data are in italics. Locality number refers to table 3.

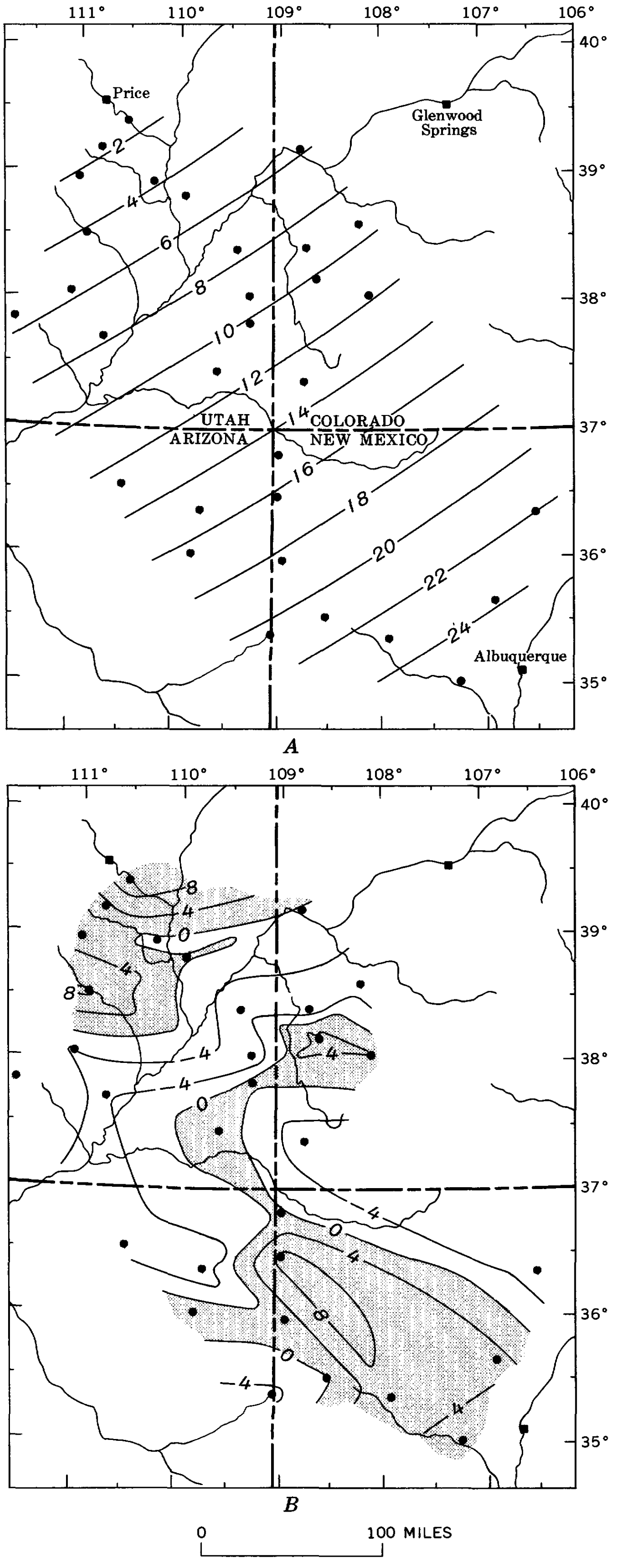

FIGURE 48.—Trend-surface analysis of feldspar data, upper part of the Morrison Formation. *A*, Linear surface com puted from modal-percent-feldspar locality data. *B*, Residual surface from *A*.

present in northwestern and northern to northeastern marginal areas. The highs in the northern to northeastern marginal area, however, were produced by the hypothetical computed zero values on the linear surface and are meaningless for interpretations of source. Interpretation of the significant highs suggests northeastward movement of sediment with a high R_1 ratio from sources west-southwest to southwest of the center of the region. The major source of feldspar to the south apparently supplied both potassic and sodic feldspar to the region.

Trend-surface analysis of R_2 yielded a computed linear surface (fig. 49*C*) which strikes N. 63° W. and dips southwestward. The surface reduces the sum of squares by 34.7 percent, suggesting a strong regional trend with proportions of sodic feldspars to potassic feldspars decreasing from north-northeast to south-southwest. The residual map (fig. 49*D*) contains significant highs in the west-northwestern to northern marginal areas and highs in the east-central part of the region. The highs in the south-southwestern to southeastern marginal areas are the effect of hypothetical computed zero and negative values on the linear surface. Interpretation of the significant highs suggests the movement into the region of sediment with high R_2 ratio from sources west-northwest of the center of the region.

The coincidence of R_2 highs with percent feldspar highs (p. 49) in the northwestern marginal area suggests that the west-northwestern feldspar sources were relatively high in proportion of sodic feldspar to potassic feldspar.

TUFF AND FELSITE FRAGMENTS

Percentages of tuff and felsite fragments (tables 19, 20) were plotted in figure 50. In the following discussion, these fragments will be referred to simply as tuffaceous fragments. Quantitative data on proportions of sodic and potassic varieties of tuffaceous fragments are lacking, but a nonparametric differentiation of the two varieties was made to determine which variety was dominant in each thin section studied. This differentiation led to recognition of the northwest oriented dashed lines shown in figure 50, dividing the region into sodic-tuff-dominant, potassic-tuff-dominant, and sodic- or potassic-tuff-dominant areas. The samples containing dominantly sodic tuffaceous fragments are restricted to the northern and northeastern parts of the region. Samples containing dominantly potassic tuffaceous fragments are restricted to the southern and southwestern parts of the region. Samples of intermixed dominancy are found in a diamond-shaped area near the center of the region between the sodic

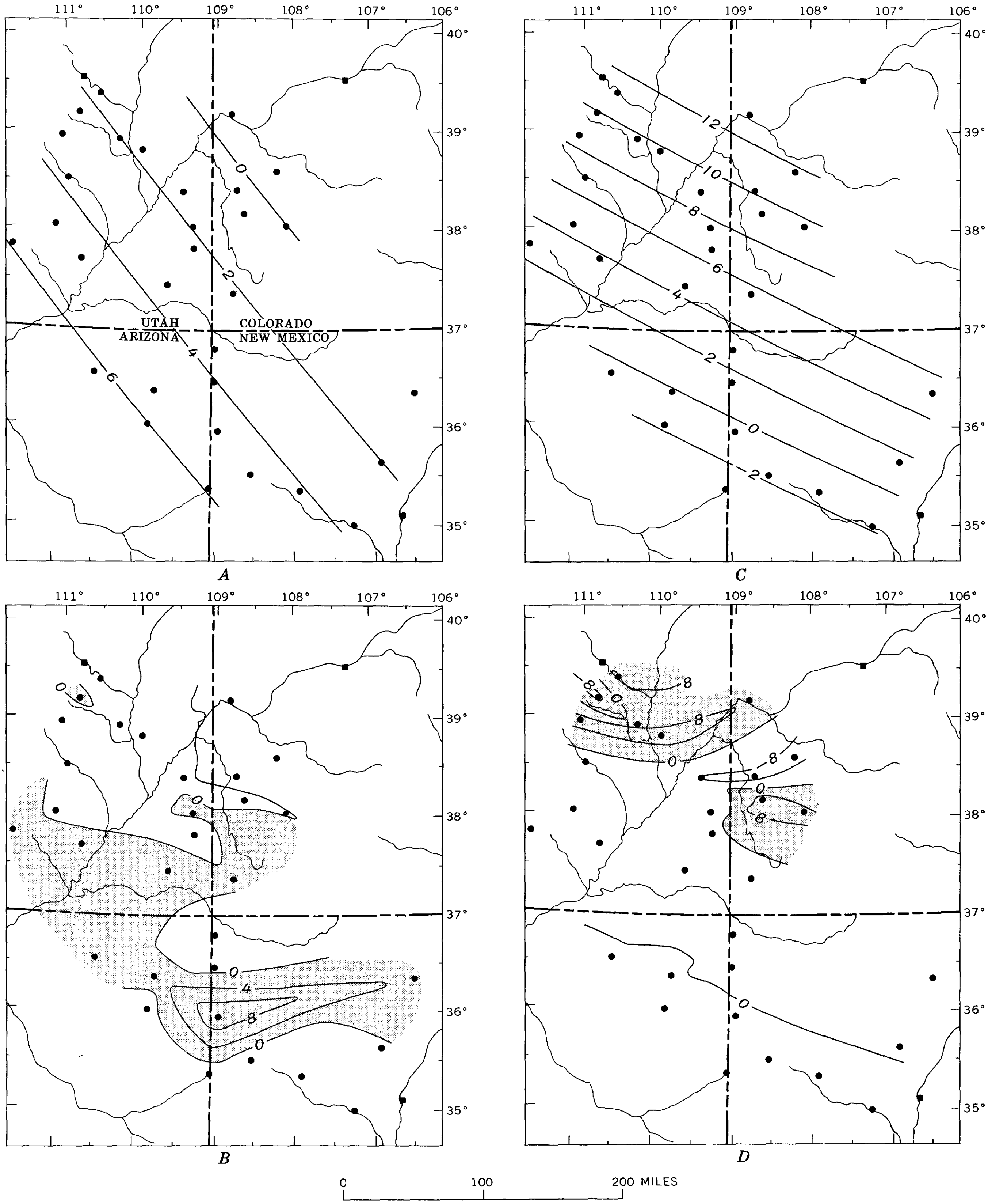

Figure 49.—Trend-surface analysis of potassic feldspar–sodic feldspar ratio data, upper part of the Morrison Formation. *A*, Linear surface computed from the R_1 feldspar ratio locality data. *B*, Residual surface from *A*. *C*, Linear surface computed from the R_2 feldspar ratio locality data. *D*, Residual data computed from *C*.

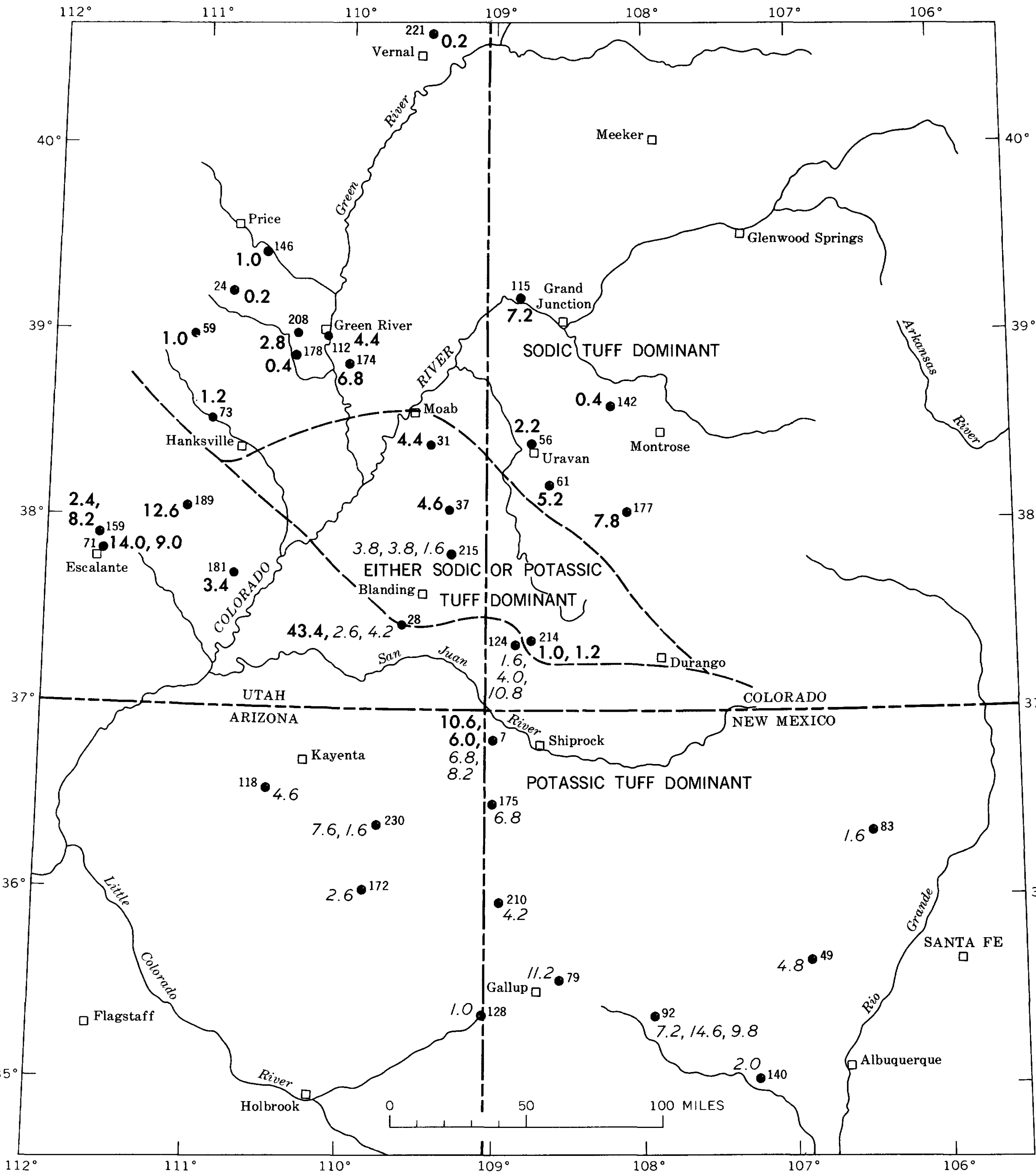

FIGURE 50.—Regional distribution (in percent) of tuffaceous fragments and of major varieties of tuff in samples of sandstone from the upper part of the Morrison Formation at 36 localities. Westwater Canyon Member data are in italics. Westwater Canyon samples, except at locality 215, are dominantly potassic tuff; Brushy Basin samples at locality 7 contain nearly equal proportions of sodic and potassic tuff. Data from tables 18 and 19. Locality number refers to table 3. Dotted line indicates estimated boundary line based on regional changes in relative proportions of potassic tuff to sodic tuff fragments as observed in thin section.

tuff dominant and potassic tuff dominant areas. Sodic tuff is abundant in the New Mexico samples but sparse in the Arizona and south-central Utah samples.

Trend-surface analysis of the regional variation of percent tuffaceous fragments in sandstone from the upper part of the Morrison, based on mean values at 32 data points, yielded a computed linear surface (fig. 51*A*) which strikes N. 54° W. and dips northeastward. The computed surface decreased the total sum of squares by 7.8 percent, suggesting a weak trend with percent tuffaceous fragments decreasing from southwest to northeast.

The linear residual surface (fig. 51*B*) has high values in south-southeastern, western, north-northwestern, and northern marginal areas. Sediments containing the highest proportions of tuffaceous fragments appear to have been transported from sources south and west-southwest of the center of the region. The source which contributed the sediment with the dominant proportions of sodic-tuff fragments is tentatively interpreted to have been west of the region. The high areas to the north and east may represent paths of the high-tuff sediment from west to east and southwest to northeast. Desirable detail is missing because data points are lacking.

SILICIFIED-ROCK FRAGMENTS

From the regional distribution of rock types (fig. 46), arenaceous-chert components appear to have significant regional variation. The definitive detrital components of the arenaceous-chert rocks are detrital chert, silicified-limestone fragments, and silicified-rock fragments. For purposes of discussion, the percentages of these mineral groups are combined from tables 19 and 20 and referred to as "silicified-rock fragments." Figure 52 illustrates the regional distribution of percentages of silicified-rock fragments in thin sections of samples of sandstone from the upper part of the Morrison Formation.

Trend-surface analysis of the regional variation of percent silicified-rock fragments in the sandstone of the upper part of the Morrison yielded a computed linear surface (fig. 53*A*), which strikes N. 63° E. and dips southeastward. The surface reduces the total sum of squares by 35.4 percent, suggesting a strong regional trend with proportions of silicified-rock fragments decreasing from northwest to southeast. The residual surface (fig. 53*B*) shows high values in western, northwestern, southern, and east-northeastern marginal areas. The highs in the western marginal area appear to be the most significant and extend into the center of the region. The high in the southern marginal area is the effect of hypothetical negative

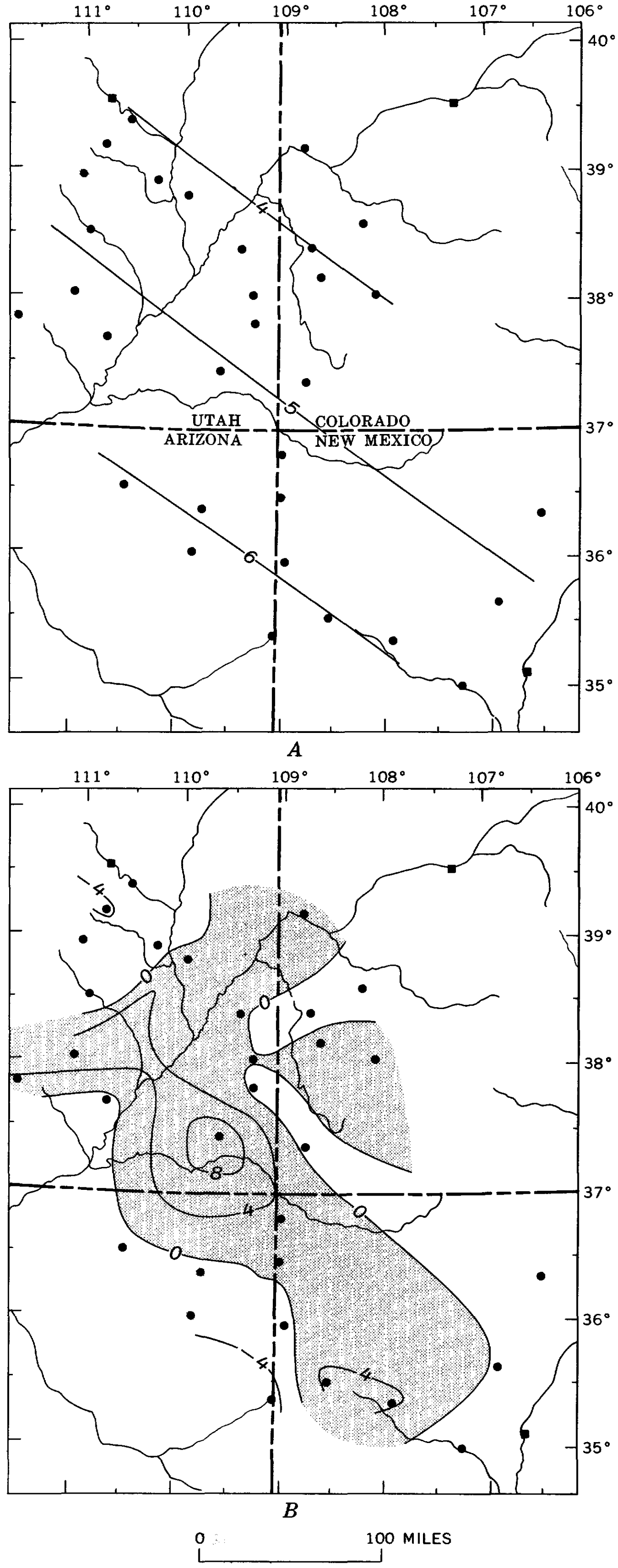

FIGURE 51.—Trend-surface analysis of tuffaceous-fragments data, upper part of the Morrison Formation. *A*, Linear surface computed from locality data on modal percent tuffaceous fragments. *B*, Residual surface computed from *A*.

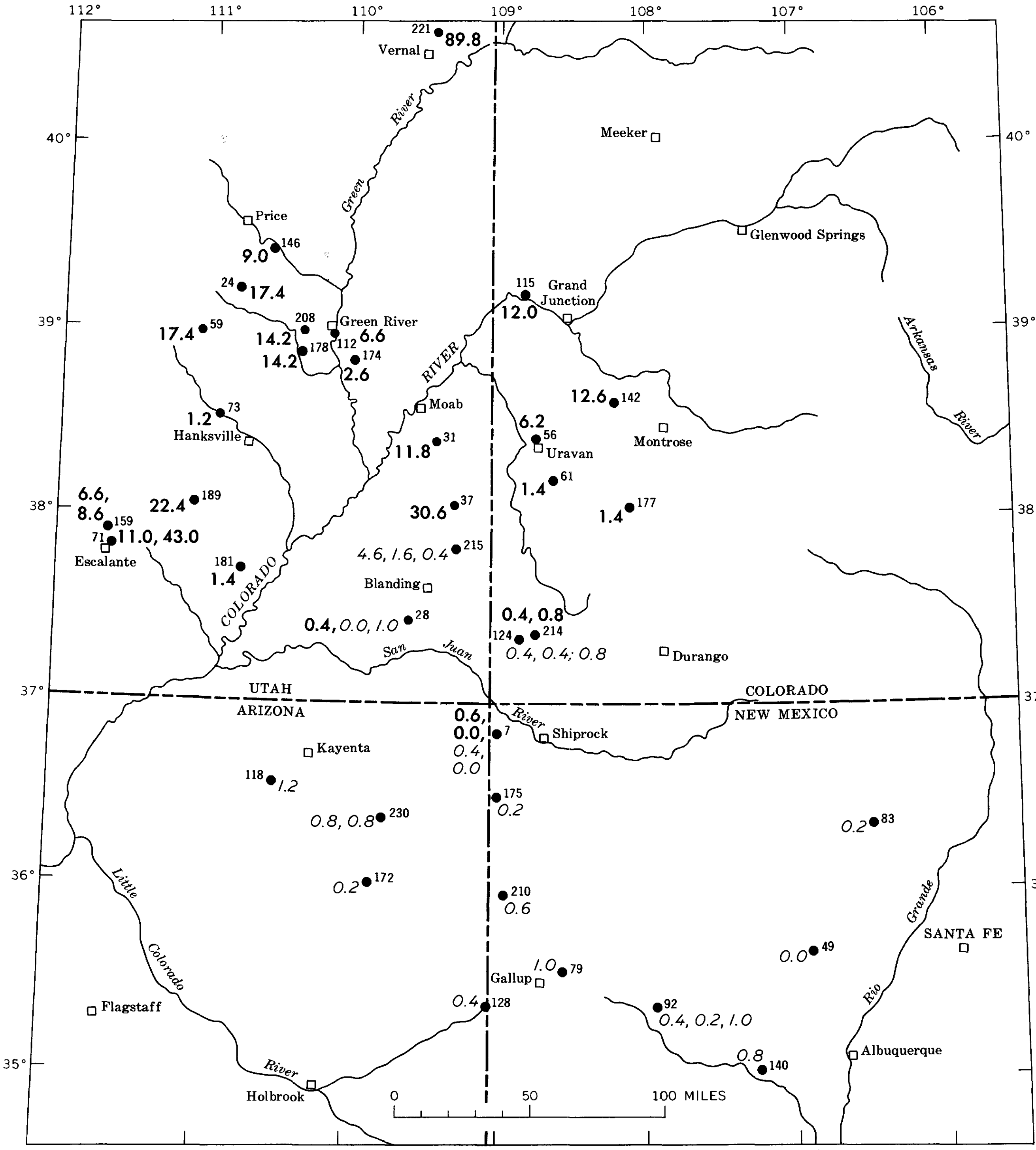

FIGURE 52.—Percentage of detrital fragments of chert, silicified limestone, and silicified rock of unknown origin in samples of sandstone from the upper part of the Morrison Formation at 36 localities. Westwater Canyon Member data are in italics. Data from tables 18 and 19 based on single samples. Locality number refers to table 3.

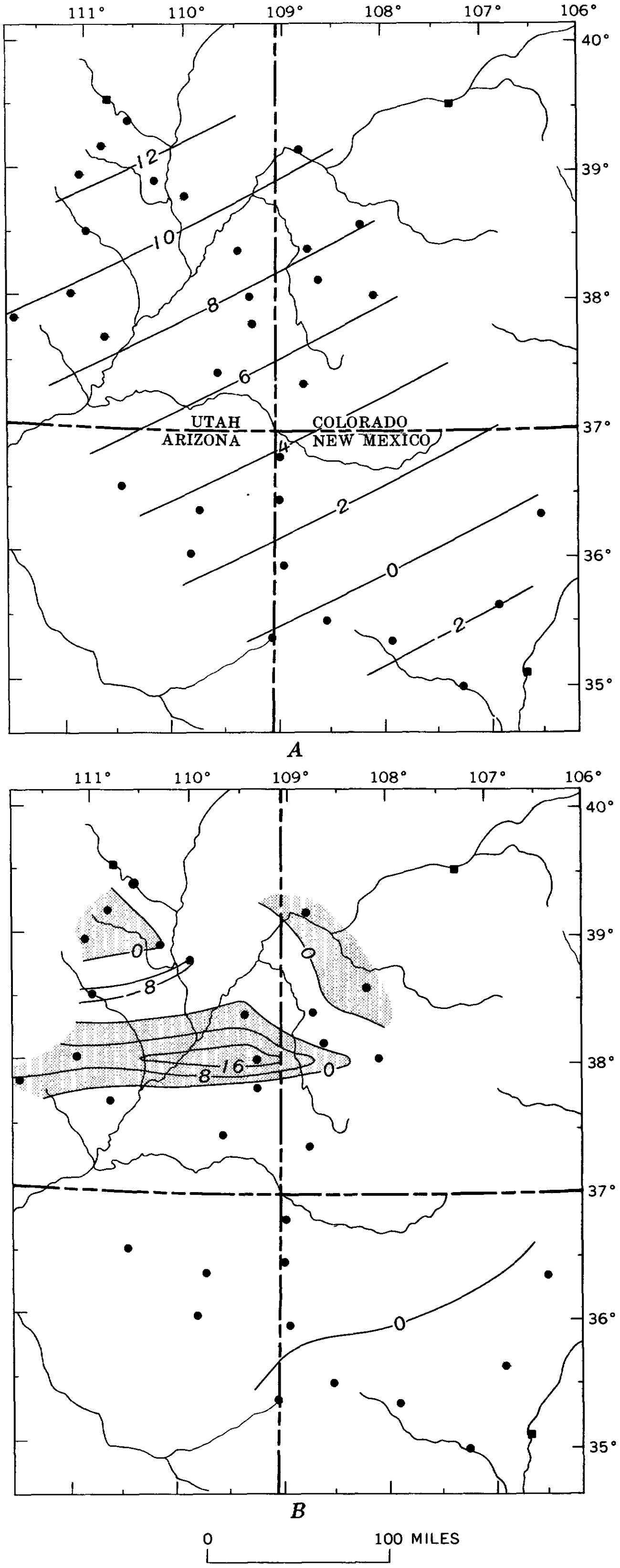

FIGURE 53.—Trend-surface analysis of silicified-rock-fragment data, upper part of the Morrison Formation. *A*, Linear surface computed from locality data and modal percent silicified-rock-fragment content. *B*, Residual surface computed from *A*.

values in the computed linear surface and has no interpretive significance. The northwestern and east-northeastern highs are related to the extreme high in the western marginal area. The effects suggest a source of silicified-rock fragments west of the center of the region. The coincidence of the northwestern high area with the strong regional trend suggests that the western source was the major source of silicified-rock fragments during deposition of the upper part of the Morrison.

HEAVY MINERALS

Heavy-mineral separations were made on 112 samples of sandstone from the upper part of the Morrison. Grain counts made on prepared slide mounts yielded mineral-ratio data for both heavy- and light-mineral fractions. Data are listed by Cadigan (1967) in the form illustrated in table 17.

To facilitate the study of regional variation in heavy-mineral ratios, and because of wide sample variation, a regional grid was established covering the area of study. Heavy-mineral ratios in terms of grains per hundred for all samples in each grid square, and for each mineral class studied, were averaged together to produce a grid-average value (fig. 54). These grid values include the proportion of nonapaque heavy minerals in the opaque-plus-nonopaque heavy-mineral suite, and the ratio of occurrence of each nonopaque mineral within a selected suite composed of zircon, tourmaline, garnet, staurolite, rutile, apatite, and epidote.

Randomness of regional variation in the distribution of heavy minerals was analyzed first by means of a nonparametric statistical test utilizing chi-square, as described with respect to the Salt Wash and Recapture Members. The computed probabilities of randomness are shown with their respective minerals in figure 54. A value of $P=0.05$ or less is considered evidence of significant (nonrandom) regional variation.

The second means of study was by trend-surface analysis, also as described with respect to the lower part of the Morrison Formation.

Before studying the grid data on individual minerals and mineral groups in the heavy-mineral suite, a trend-surface analysis was made of the regional distribution of the mean percentage of total heavy minerals at each sample locality, using data tabulated by Cadigan (1967). To improve the calculated trend surface by reducing the clustering of values, data from sample localities within the same 80-square-mile circle (10-mile diameter) were combined to yield one value (mean). The localities combined were 7 and 151; 30, 118, and 135; 64 and 174; 71 and 159; 112, 178, and

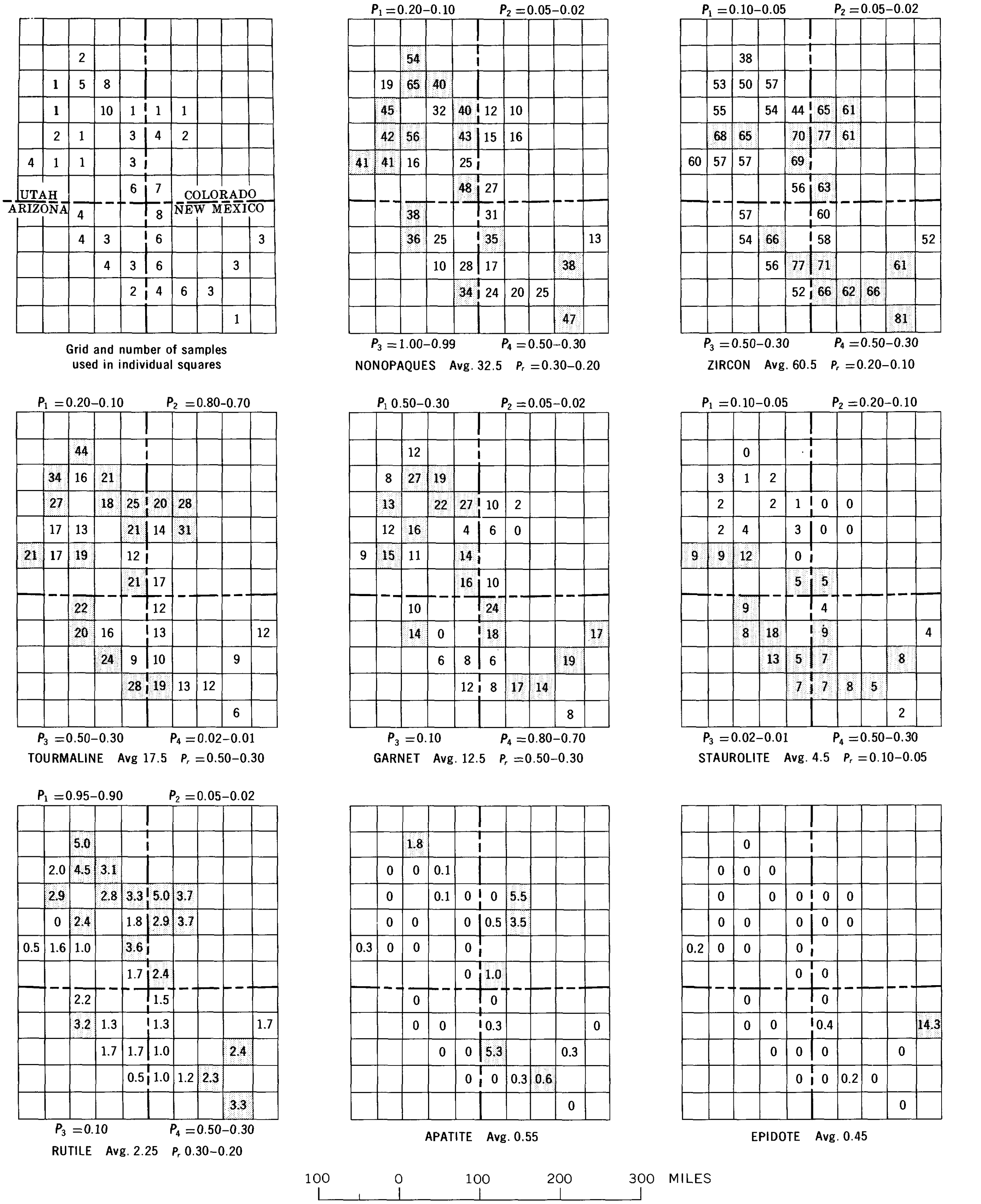

FIGURE 54.—Heavy-mineral grid ratios (in percent), upper part of the Morrison Formation. Probability of randomness for each quadrant and for the region is indicated in each mineral-ratio map by P_1, P_2, P_3, P_4, and P_r values, respectively. Average (median) ratio value, Avg., is given for each mineral. Stippling indicates above average proportion.

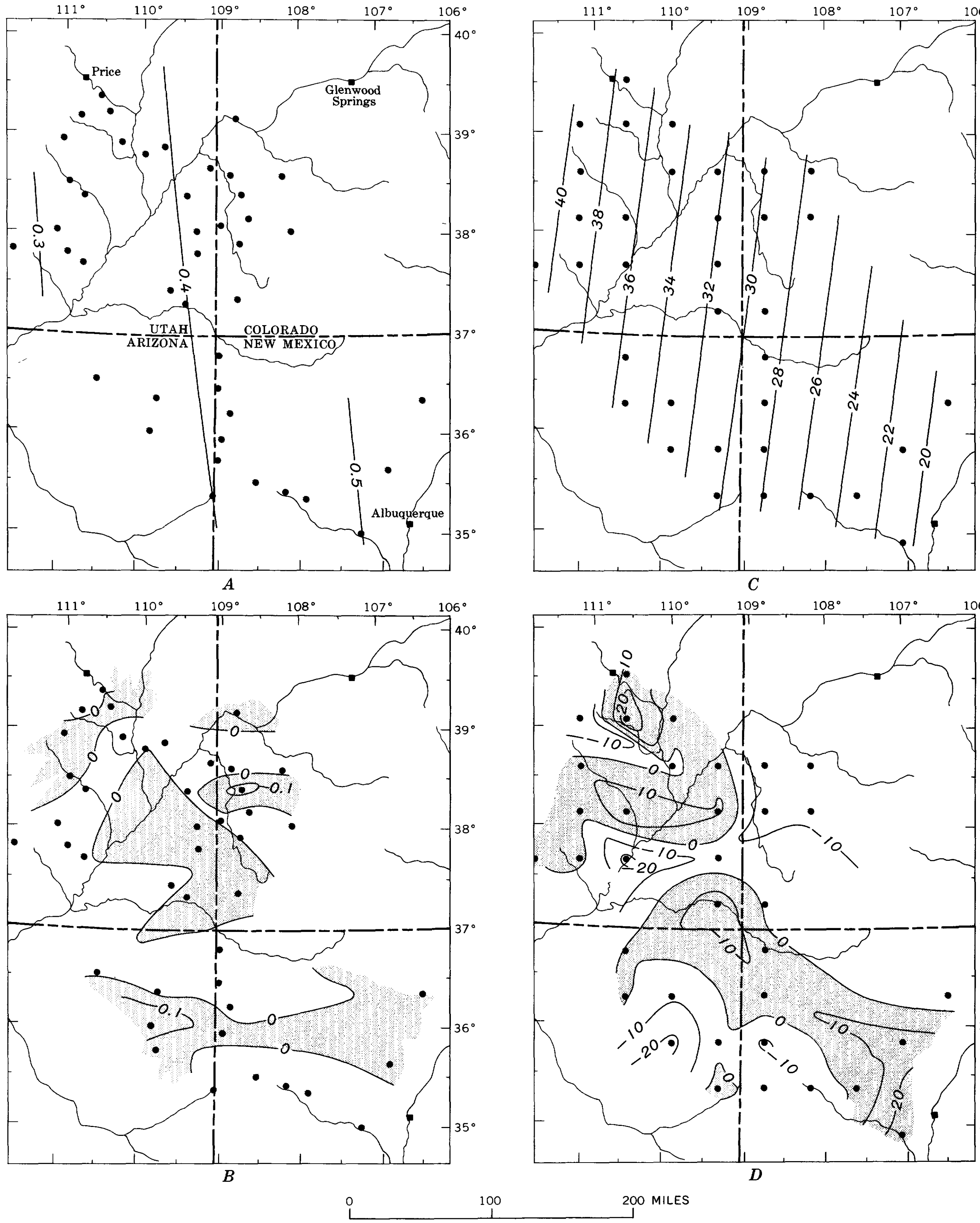

FIGURE 55.—Trend-surface analysis of heavy-mineral content and nonopaque heavy-mineral data, upper part of the Morrison Formation. *A*, Linear surface computed from locality data and approximate percent total heavy-mineral content. *B*, Residual surface from *A*. *C*, Linear surface computed from percentage proportion nonopaque heavy-mineral grid data. *D*, Residual surface from *C*.

208; 114 and 172; and 124 and 214. Locality 221 was not used because of its isolation from the other localities. Use of this isolated value would not appreciably influence the attitude of the trend surface or the significance (strength) of the trend, but it would complicate the contouring of the residual surface. Reduction of the effect of clustering and isolation reduced the locality data points to 44 in number.

The computed linear surface (fig. 55*A*) of the variation in percentage of heavy minerals strikes N. 7° W. and dips westward. The linear surface reduces the sum of squares by 1.38 percent, suggesting an extremely weak trend with heavy-mineral content decreasing from east to west. The linear residual surface (fig. 55*B*) shows a pattern of high and low areas that could well be due to random variation of locality values. The regional distribution of heavy-mineral content of sandstone samples from the upper part of the Morrison Formation appears to offer no definite basis for interpretation of source direction.

The regional grid distribution of proportions of nonopaque heavy minerals is shown in figure 54. Because of a direct inverse relationship (p. 57), the regional distribution of opaque minerals is evident from the data on the ratios of nonopaques.

The value of P_r=0.30–0.20 is evidence that the probability (P) of regional variation (r) in nonopaque grid values does not depart significantly from random. Only the probability value (0.05–0.02) for the northeast quadrant (P_2) suggests nonrandom variation.

Trend-surface analysis of regional variation of nonopaque ratios, based on 35 grid values, yielded a computed linear surface (fig. 55*C*) which strikes N. 8° E. and dips eastward. The surface reduces the sum of squares by 15.8 percent, suggesting a moderately strong regional trend of proportions of nonopaque grains of the heavy-mineral suite decreasing from west to east.

The linear residual map (fig. 55*D*) has high values in south-southeastern, western and northwestern marginal areas and in an interior zone connecting the southwestern and south-southeastern marginal areas. Low nonopaque values, which would also be high opaque values, are present in south-southwestern, western, and west-northwestern marginal areas and extend across the center of the region to occupy the northeast quadrant. Data are lacking for the west-southwestern marginal area.

Arrangement of the high and low areas suggests that there were sources of heavy minerals relatively high in proportions of nonopaque minerals to the south, west-southwest, and west-northwest of the center of the Colorado Plateau region, and sources of heavy minerals relatively high in proportions of opaque minerals south-southwest to west of the region during deposition of upper sediments of the Morrison.

The regional distribution of the nonopaque heavy mineral zircon (fig. 54) does not significantly depart from random except in the northeast quadrant, as indicated by the P values. In the northeast quadrant, significantly more of the higher-than-average ratio values occur than would be expected in a random distribution.

Trend-surface analysis of regional variation of zircon ratios produced a computed linear surface (fig. 56*A*), which strikes N. 54° E. and dips northwestward. The surface reduces the sum of squares by 18.0 percent, suggesting a moderately strong regional trend with proportions of zircon decreasing from southeast to northwest.

The linear residual map (fig. 56*B*) shows high values in the western marginal area extending into the north-central part of the region, and both high and low values in the southern and southeastern areas. The arrangement suggests that during deposition of the upper part of the Morrison sources of relatively high-zircon sediments lay west-southwest and south of the center of the region.

The regional distribution of the nonopaque heavy mineral tourmaline (fig. 54) does not significantly depart from random except in the southeast quadrant, as indicated by the P values. In the southeast quadrant tourmaline is less abundant than would be expected if variation were random.

Trend-surface analysis of regional variation of tourmaline ratios yields a computed linear surface (fig. 56) which strikes N. 60° E. and dips southeastward. The surface reduces the sum of squares by 33.9 percent, suggesting a strong regional trend with proportions of tourmaline in the heavy-mineral suite decreasing from northwest to southeast.

The linear residual map (fig. 56*D*) shows high values in southwestern to southeastern, northwestern, and northeastern marginal areas. These highs suggest the presence of sources of high-tourmaline sediments west to west-northwest and west-southwest to south of the center of the region during deposition of the upper part of the Morrison. The continuity of the areas of high and low values is an indication of low variation —despite the effects of a strong linear trend—and suggests that the differences illustrated are mathematically, and thus geologically, highly significant.

The regional distribution of the nonopaque heavy mineral garnet (fig. 54) does not significantly depart from random except in the northeast quadrant, where significantly less garnet is present than would be expected if variation were random.

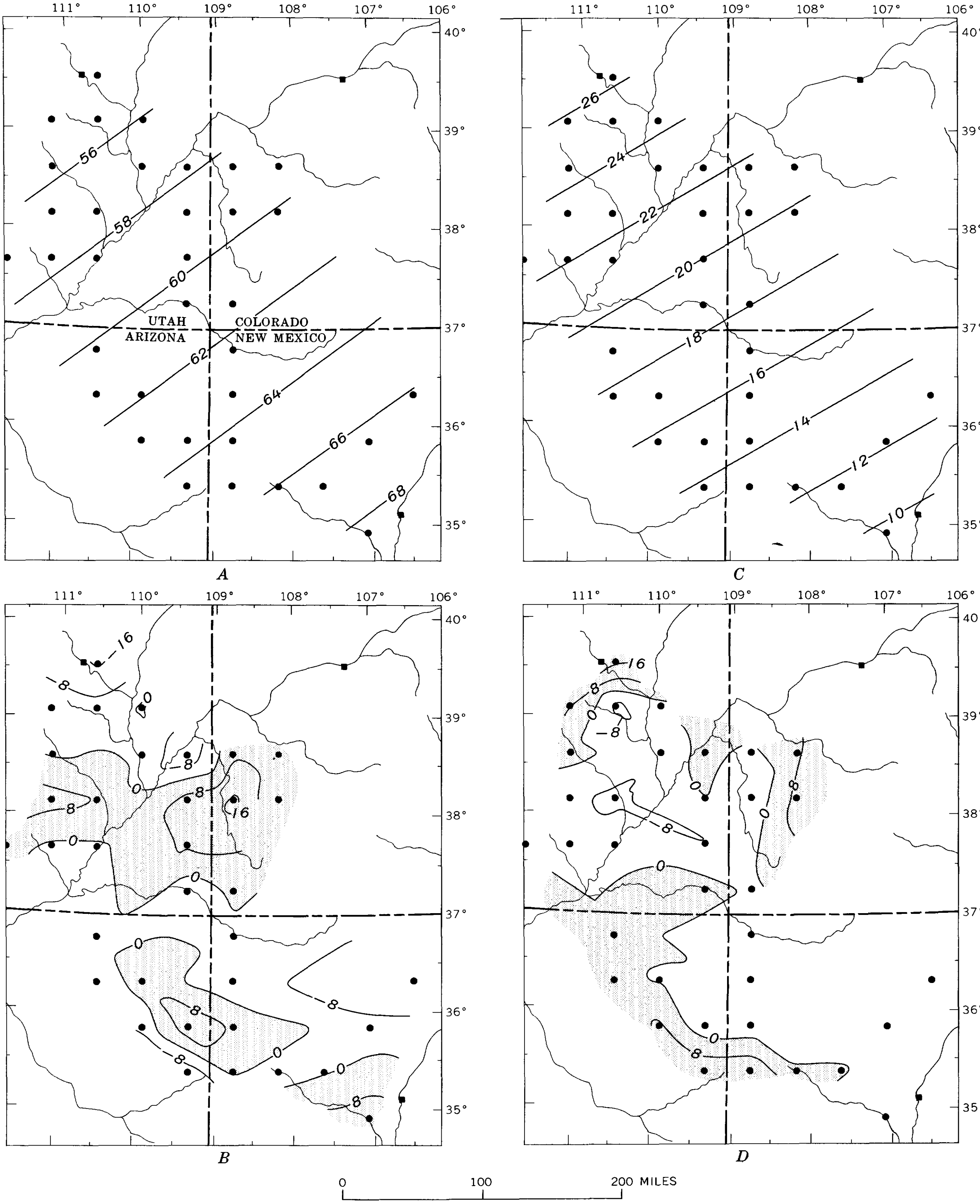

FIGURE 56.—Trend-surface analysis of zircon and tourmaline data, upper part of the Morrison Formation. *A*, Linear surface computed from zircon percentage-ratio grid data. *B*, Residual surface computed from *A*. *C*, Linear surface computed from tourmaline percentage-ratio grid data. *D*, Residual surface computed from *C*.

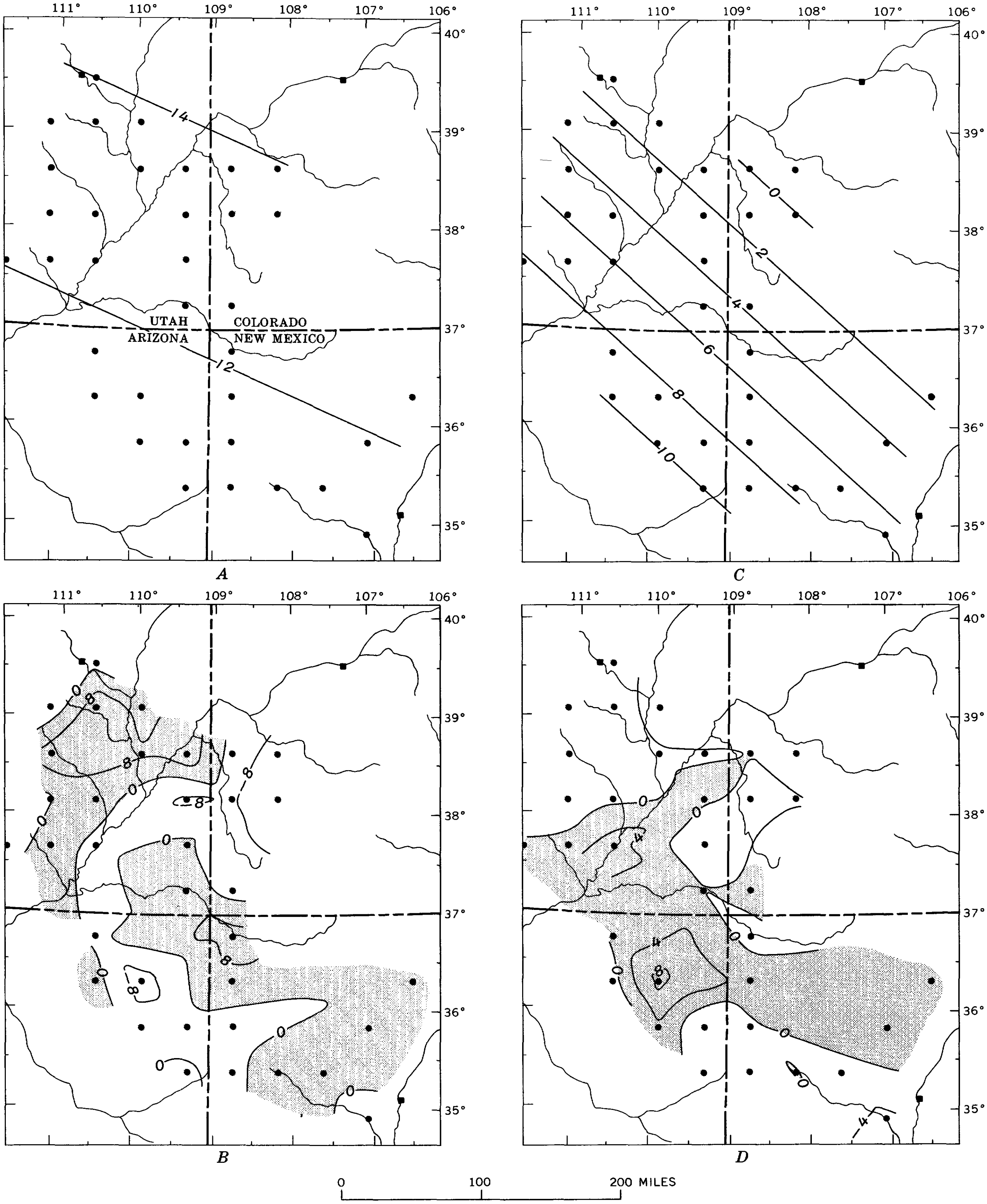

Figure 57.—Trend-surface analysis of garnet and staurolite data, upper part of the Morrison Formation. *A*, Linear surface computed from garnet percentage-ratio grid data. *B*, Residual surface from *A*. *C*, Linear surface computed from staurolite percentage-ratio grid data. *D*, Residual surface from *C*.

Trend-surface analysis of regional variation of proportions of garnet in the heavy-mineral suite produces a computed linear surface (fig. 57*A*) which strikes N. 66° W. and dips southwestward. The linear surface reduces the sum of squares by 2.2 percent, evidence of an extremely weak regional trend which shows proportions of garnet decreasing from northeast to southwest.

The linear residual map (fig. 57*B*) shows high values in the south-southeastern, southwestern and northwestern marginal areas, and in a central area. These patterns suggest the presence of sources of high-garnet sediment to the south and west-southwest to west-northwest of the region during deposition of the upper part of the Morrison Formation.

The regional distribution of the nonopaque heavy mineral staurolite (fig. 54) does not significantly depart from random except in the southwest quadrant, as suggested by the *P* values; however the P_r for the region, 0.10–0.05, is suspiciously low. In the southwest quadrant higher-than-average ratio values are significantly more numerous than would be expected in a random distribution.

Trend-surface analysis of regional variation of staurolite ratios yielded a computed linear surface (fig. 57*C*) which strikes N. 48° W. and dips northeastward. The surface reduces the total sum of squares by 57.5 percent, suggesting a very strong regional trend with proportions of staurolite decreasing from southwest to northeast. On the linear residual map (fig. 57*D*), very high staurolite values are present in the south-southwestern to west-southwestern marginal areas, and some of this variation is due possibly to the strong trend. Insignificant minor highs resulting from zero values on the computed surface are present in the northern marginal areas. The major sources of staurolite during deposition for the upper part of the Morrison Formation are interpreted as lying west-southwest to south-southwest of the center of the region.

The regional distribution of the nonopaque heavy mineral rutile (fig. 54) does not significantly depart from random except in the northeast quadrant, judging from the *P* values. In the northeast quadrant, significantly more of the higher-than-average values occur than would be expected if variation were random.

Trend-surface analysis of regional variation of rutile ratios produced a computed linear surface (fig. 58*A*) which strikes N. 50° W. and dips southwestward. The surface reduces the sum of squares by 44.8 percent, suggesting a strong to very strong trend with proportions of rutile decreasing from northeast to southwest.

The linear residual map (fig. 58*B*) shows high values in the south-southeastern, southern to west-southwestern, and northwestern to northern maginal areas. The highs are interpreted as representing the presence of possible sources of rutile south to west-southwest and west to west-northwest of the center of the region during deposition of the upper part of the Morrison Formation.

Regional distribution of the nonopaque heavy mineral apatite (fig. 54) is very erratic and was not tested for randomness because only 13 of the grid squares showed values larger than zero.

Trend-surface analysis, based on all 35 grid values, yielded a computed linear surface (fig. 58*C*) which strikes N. 29° W. and dips southwestward. The linear surface reduces the sum of squares by 12.1 percent, which suggests a weak regional trend with proportions of apatite decreasing from northeast to southwest.

The linear residual map (fig. 58*D*) shows high values in the southern to south-southeastern and northwestern marginal areas and in the north-central part of the region. The southwestern marginal high is the result of the calculated hypothetical negative values of the trend surface and has no interpretive significance. The highs in the south-southeastern and northwestern marginal areas suggest sources of high-apatite sediment to the south and to the west-northwest of the center of the region. The highs in the north-central part of the region are interpreted to be an effect of either the west-northwestern or the southern source.

Regional distribution of the heavy mineral epidote (fig. 54) is very limited and irregular. Most grains counted were in the southeast quadrant, and a trace was found in the northwest quadrant. No probabilities of randomness or trend surfaces were computed because the mineral was lacking in most sandstone samples studied. The relative abundance in the southeast quadrant suggests a generally southern source.

In summary, the percentage of total heavy minerals in the detrital fraction of sandstones in the upper part of the Morrison Formation shows no significant regional variation. This negative evidence suggests no significant trend of decrease in proportion of total heavy minerals in the detrital sediments by attrition from the direction of a single source; rather, it suggests that contributions from multiple sources tended to compensate for losses by attrition and obscure them.

The effects of attrition in garnet may be obscured and compensated for by the widely spaced effects of two different source areas. This would explain the lack of significant trend and apparent random regional distribution. On the other hand, attrition of staurolite combined with more locally concentrated source

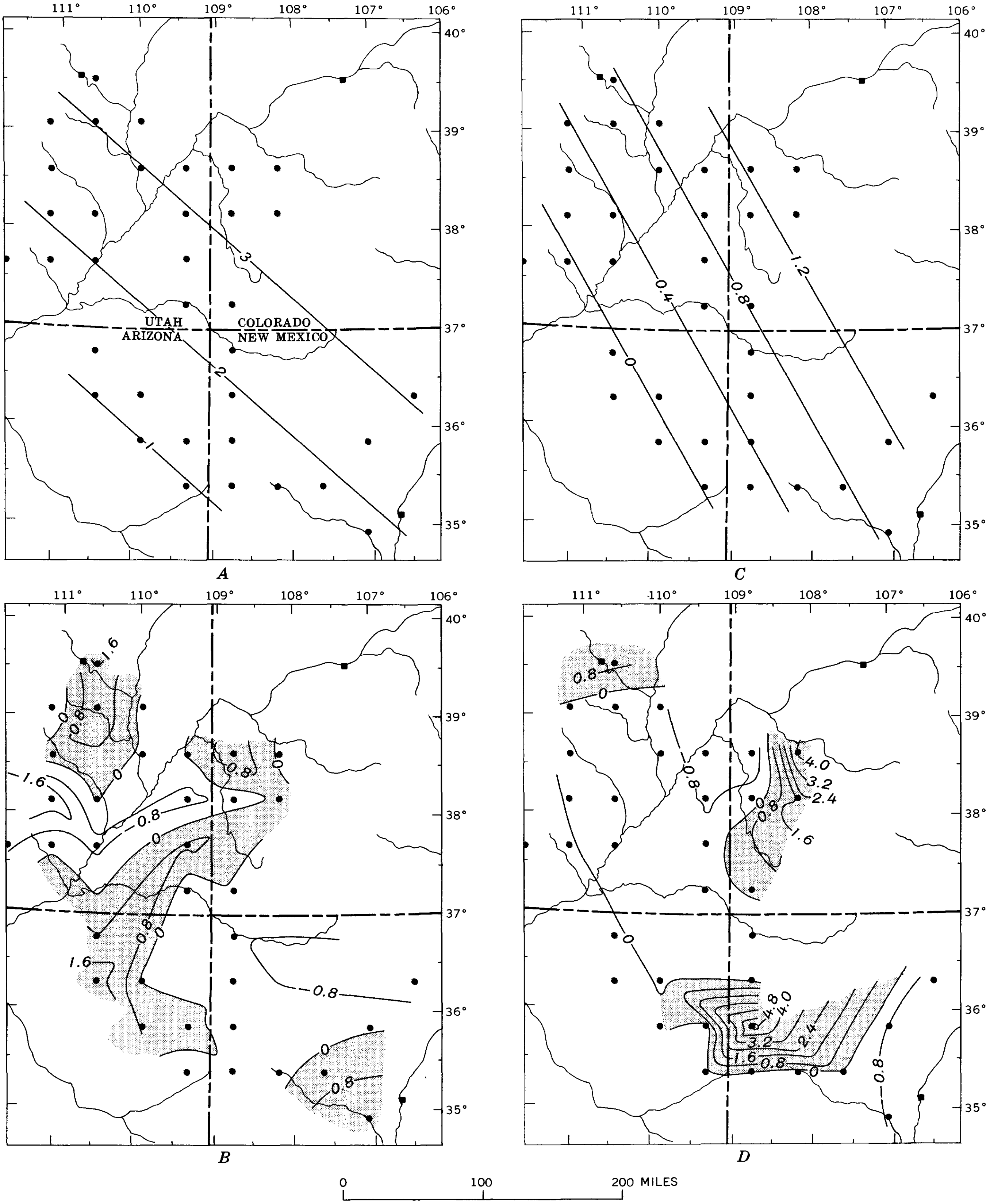

FIGURE 58.—Trend-surface analysis of rutile and apatite data, upper part of the Morrison Formation. *A*, Linear surface computed from rutile percentage-ratio grid data. *B*, Residual surface computed from *A*. *C*, Linear surface computed from apatite percentage-ratio grid data. *D*, Residual surface computed from *C*.

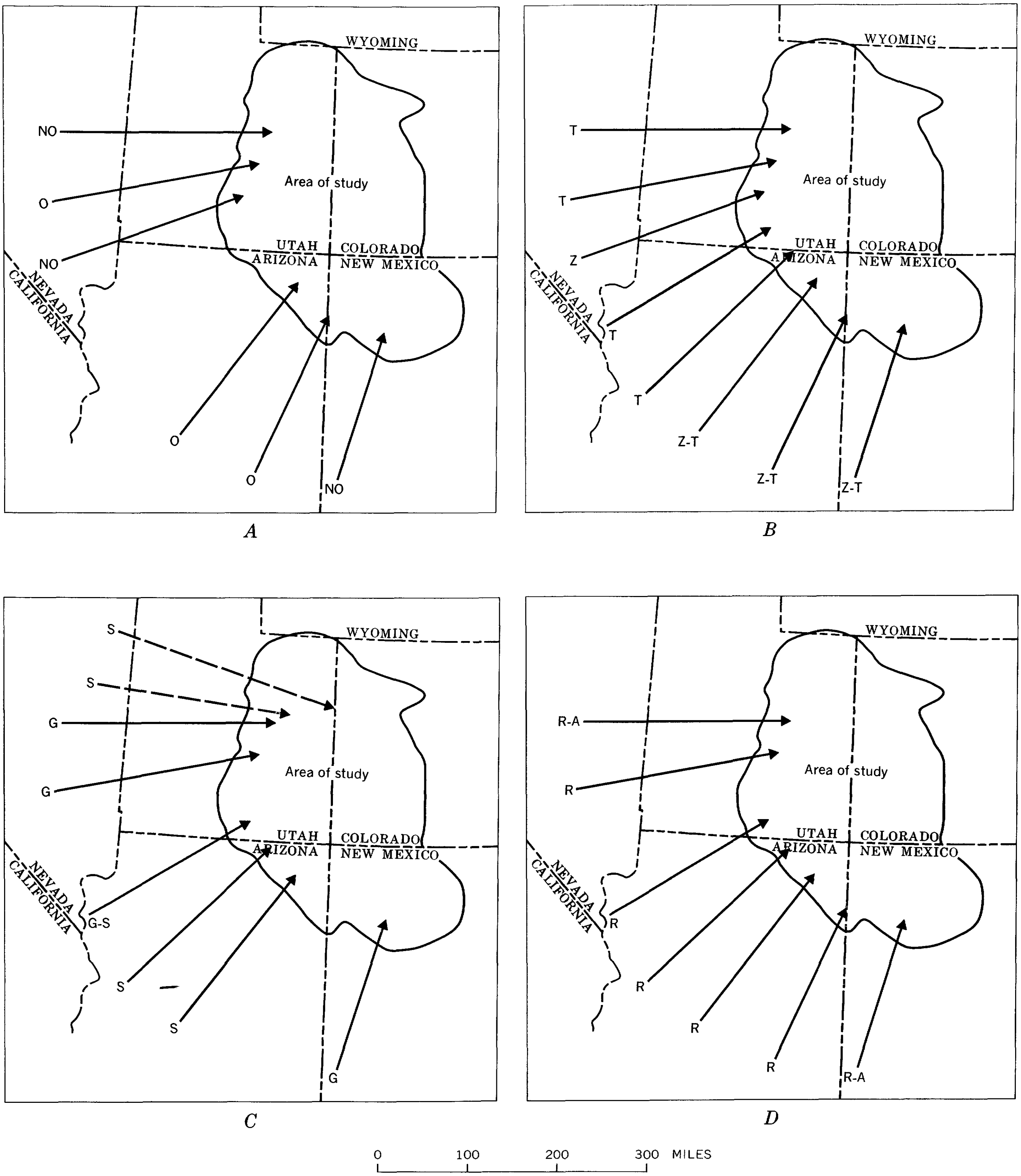

FIGURE 59.—Inferred directions of sediment transport during deposition of the upper part of the Morrison Formation as interpreted from the regional distribution of heavy minerals. *A*, Sediment with high proportions of opaque (O) and nonopaque (NO) heavy minerals. *B*, Sediment with high proportions of zircon (Z) and tourmaline (T). *C*, Sediment with high proportions of garnet (G) and staurolite (S). *D*, Sediment with high proportions of rutile (R) and apatite (A). Both indicated directions for apatite are weak. Heavy line, strongly indicated direction of transport. Dashed line, weakly indicated direction of transport.

effects produces a very strong trend which dips away from the source directions. The indication that garnet was lost by attrition is supported by a highly significant negative correlation between zircon and garnet ($r=-.340$).

Significant negative correlations also exist between zircon and staurolite, between rutile and staurolite, and between zircon and tourmaline. The last of these correlations is interpreted to be the effect of different sources and of mathematical dependency (Chayes, 1960). The first two correlations are interpreted to be due to attrition alone, because there is a relatively small proportion of staurolite in most samples. Rutile increases in proportion to other nonopaque heavy minerals from southwest to northeast, probably owing to both source effects and attrition of other minerals.

The suggested directions of movement of heavy minerals from source areas to marginal areas in the area of deposition are summarized in figure 59. The directional arrows follow the plan of sediment transport proposed in figure 25. Marginal areas indicated by the arrows are those which show the statistical effects of detrital mineral influx revealed by the grid maps or the linear trend and residual maps of the regional distribution of heavy minerals.

LIGHT MINERALS

Light-mineral fractions from 112 samples referred to on page 86 were studied for composition by grain-count method; the results are presented as percentage ratios in terms of the mineral classes quartz, feldspar, silicified-rock fragments, and miscellaneous (Cadigan, 1967). The regional variation of these ratios was found to be complicated by relationships between size and composition within the samples. Discussion of regional variation of sand-grain composition is postponed to a later section of the report in which the relationships between particle size and composition within all members can be discussed. Regional variation in grain sphericity based on studies of these light-mineral separates is discussed below.

The relationship of grain sphericity to composition (McEwen and others, 1959) suggests that interpretations based on sphericity alone are of doubtful significance unless the sedimentary unit studied is of uniform composition. Study of sphericity data from the lower part of the Morrison Formation tended to confirm this conclusion. The regional low sphericity values obtained from trend-surface analysis coincided approximately with the compositional effects of the sources of feldspar.

Trend-surface analysis of regional variation in measured sphericity in the upper part of the Morrison based on 15 locality points (4 Brushy Basin Member and 11 Westwater Canyon Member samples of very fine sand) yielded a computed linear surface that strikes N. 82° W. and dips southward. The surface reduced the total sum of squares by 4.4 percent, evidence of a very weak trend of decreasing sphericity from north to south.

The residual surface contained low areas in the southern and north-central parts of the region, but too few data are available and the trend is too weak to provide detail necesary for interpretation. The indicated regional trend is compatible with the thesis of McEwen, Fessenden, and Rogers (1959) in view of other evidence of a southern major source of feldspar (p. 78).

GRAIN-SIZE STATISTICAL MEASURES

The effects of combined regional, local, and sample variation in the grain-size distributions of the sandstones of the upper part of the Morrison Formation are reflected in the variations of the averages of the median grain size (Mdϕ), standard deviation ($\sigma\phi$), skewness (Skϕ) and kurtosis (Kϕ) for 54 sample localities. To test these averages mathematically for significant regional or local variation, trend-surface analysis was used. Preparation of the data consisted of combining sample localities which lie within an 80-square-mile circle (approximate 10-mile diameter) to reduce the effect of clustered data points. Combined localities include: 7 and 151; 30, 118, and 135; 64 and 174; 71 and 159; 112, 178, and 208; 114 and 172; and 124 and 214. Locality 221 was omitted because of its isolation from other localities. One result of these procedures was to reduce the number of data points from 54 to 44.

Trend-surface analysis of phi median grain size, based on the 44 data points, yielded a computed linear surface (fig. 60*A*) which strikes N. 90° E. and dips southward. The surface reduces the sum of squares by 2.8 percent, suggesting an extremely weak trend of decreasing median grain size (increasing phi values) from south to north.

The linear residual map (fig. 60*B*) shows low phi median (coarser sand) values in the south-southeastern and western marginal areas. High phi median (finer sand) values occupy the rest of the marginal areas and much of the central part of the region. Apparently, coarser sand invaded the region from sources south and west-southwest of the center of the region.

Trend-surface analysis of regional variation of the phi standard deviation of the grain-size distributions produced a computed linear surface (fig. 60*C*) which strikes N. 47° W. and dips northeastward. The surface reduces the sum of squares by 6.9 percent, suggesting a weak regional trend of decreasing standard

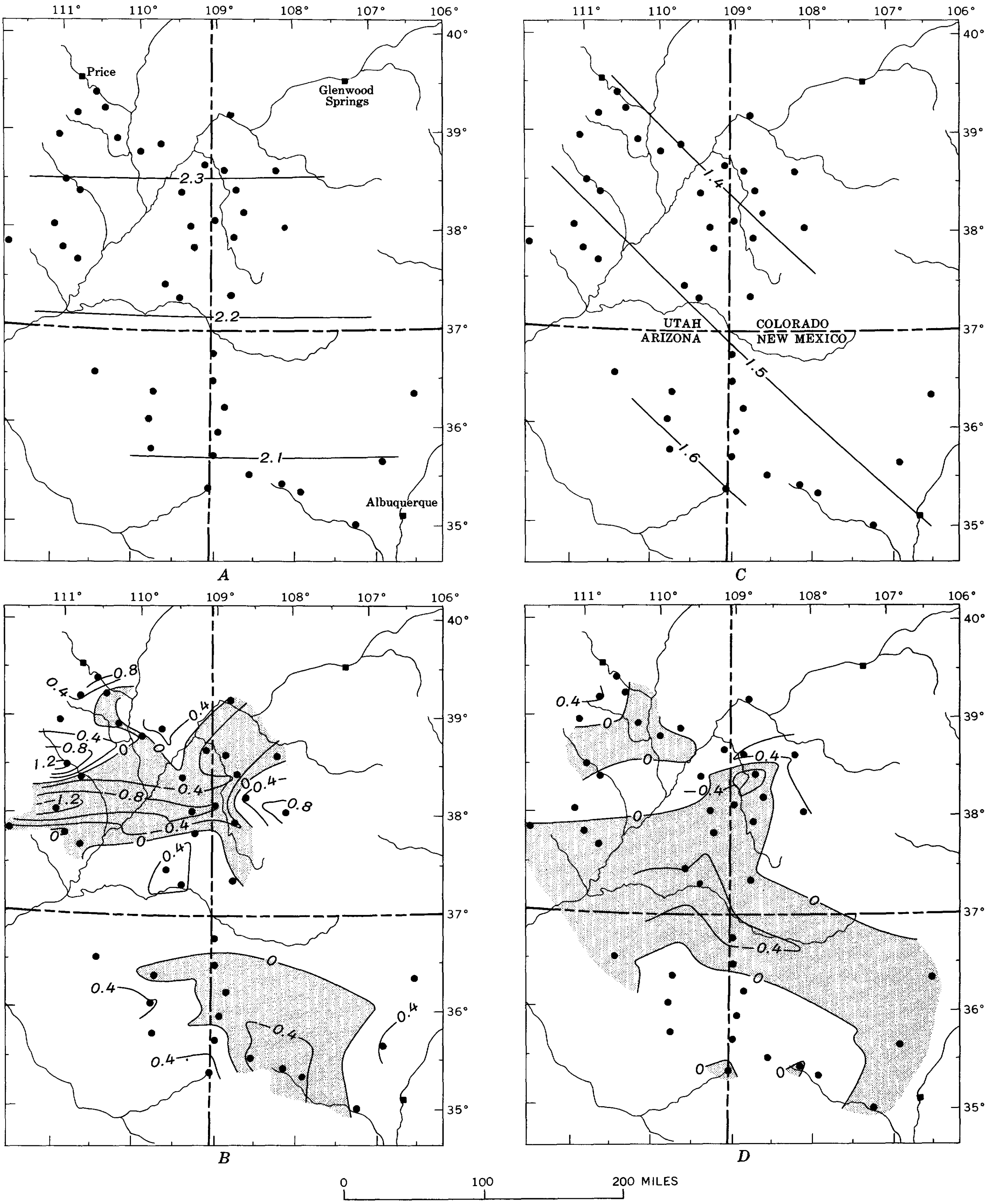

FIGURE 60.—Trend-surface analysis of median grain size and grain-size standard-deviation data, upper part of the Morrison Formation. *A*, Linear surface computed from locality averages of median grain size. *B*, Residual surface computed from *A*. *C*, Linear surface computed from locality averages of grain-size-distribution standard deviations. *D*, Residual surface computed from *C*.

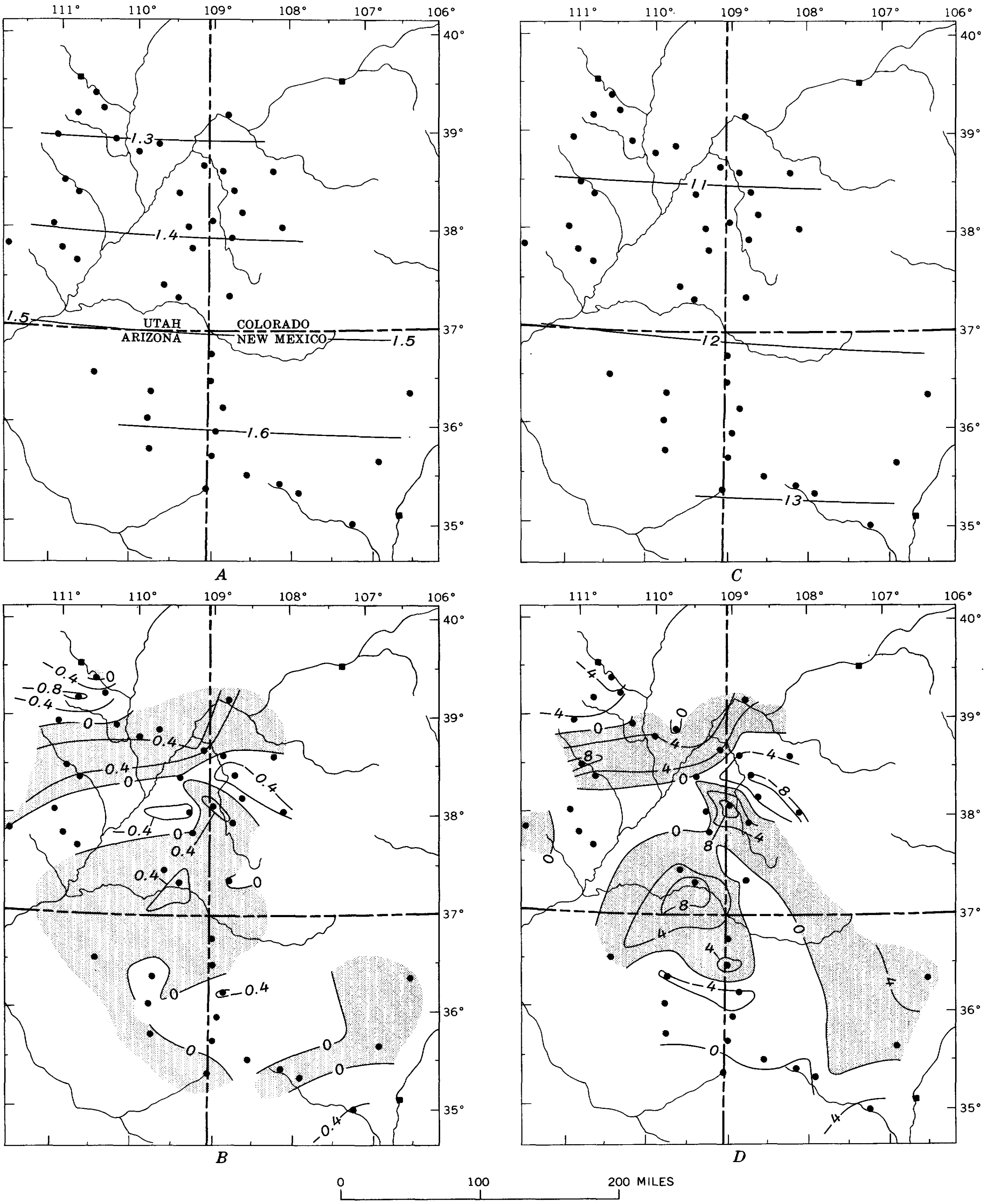

FIGURE 61.—Trend-surface analysis of grain-size skewness and kurtosis data, upper part of the Morrison Formation. *A*, Linear surface computed from locality averages of grain-size-distribution skewness. *B*, Residual surface computed from *A*. *C*, Linear surface computed from locality averages of grain-size-distribution kurtosis. *D*, Residual surface computed from *C*.

deviation (increasing degree of sorting) from southwest to northeast.

The residual surface (fig. 60*D*) contains low (better sorting) values in southwestern, northwestern, and southeastern marginal areas which extend from the southwest margin into the center of the region. The better sorted sand (stippled) is interpreted to have moved from areas west to southwest, and south-southeast of the center of the region. Poorer sorted sand moved from areas west-northwest, west-southwest, and south to southwest of the region.

The area of better sorted sand which crosses the southwest margin is interpreted as the main channelway. Other channelways along west to north-northwest, and south-southwest to southeast margins show the effects of intermixing of sediments from adjacent sources to produce areas of more poorly sorted sediment. (See discussion on p. 70.)

Trend-surface analysis of regional variation in the phi skewness of the grain-size distributions of sandstones yielded a computed linear surface (fig. 61*A*) which strikes N. 87° W. and dips northward. The surface reduces the total sum of squares by 11.8 percent, suggesting a weak regional trend with skewness decreasing from south to north.

The linear residual surface (fig. 61*B*) contains high values in southern, south-southwestern, southwestern, western, and northwestern to northern marginal areas. The rest of the marginal areas are low-value areas. With reference to the discussion of the interpretation of skewness on page 70, the best sorted and most highly reworked sands entered the region over western and west-southwestern marginal areas and over south-southeastern marginal areas; these areas contain sediment of low skewness combined with high degrees of sorting. The regional trends, weak as they are, are compatible with the idea of an increase in the degree of sorting and a decrease in skewness in the general direction of transportation.

Trend-surface analysis of the regional variation of phi kurtosis of the grain-size distributions yielded a computed linear surface (fig. 61*C*) which strikes N. 87° W. and dips northward. The surface reduces the sum of squares by 2.1 percent, evidence of a very weak trend of decreasing kurtosis from south to north.

The linear residual surface (fig. 61*D*) shows high values in southern, southwestern, western, and west-northwestern marginal areas. If kurtosis and skewness bear the same relationship to sorting, the linear residual surface for kurtosis indicates that the best sorted sand entered the region through west-southwestern and south-southeastern marginal areas.

In summary, regional trends of grain-size distribution measurements are oriented generally from south to north. More specifically, grain size decreases generally from south to north, sorting increases from southwest to northeast, and skewness and kurtosis decrease generally from south to north. These regional trends are compatible with the assumed directions of movement of sediment across the Colorado Plateau region.

In sandstones of the Morrison Formation, the effects of multiple sources on textural trends in the upper part as compared with those of the lower part are similar, with the exception of median grain size. The south-to-north trend in the upper part contrasts with the west-to-east trend in the lower part. The change in orientation suggests a proportional increased influx of coarser sediment from the south during deposition of the upper part.

PETROLOGIC CONTRASTS AND SIMILARITIES OF MEMBERS

Average composition and texture of sandstone strata within the Morrison Formation are summarized in tables that follow. Data on the finer textured sediments are available only to a limited extent for comparisons. Differences or similarities designated as stratigraphic refer to results of comparisons between stratigraphic units—that is, between the individual members, and between the upper and lower parts of the formation. Differences and similarities designated as geographic refer to results of comparisons between parts of the formation in different areas of the region.

COMPOSITION

Comparison of measured compositional features shows the presence of both stratigraphic and geographic similarities and differences. The results of thin-section modal analyses are summarized in table 22.

The sandstones of the Salt Wash Member have the highest average proportion of chemical and siliceous components and the lowest proportion of volcanic components. Sandstones of the Recapture Member have the highest proportion of dark mineral components. Sandstones of the Westwater Canyon Member have the highest average proportions of feldspathic and the lowest proportions of chemical and siliceous components. Sandstones of the Brushy Basin Member have the highest average proportions of volcanic components and the lowest of dark mineral and feldspathic components.

The coefficient of variation indicates the relative amount of variation of a component within the samples for each member and hence is a measure of the uniformity of occurrence of the component. Siliceous

TABLE 22.—*Summary of modal composition (in percent by volume) of rock components of sandstones from the Salt Wash, Recapture, Westwater Canyon, and Brushy Basin Members of the Morrison Formation*

[Data from tables 12, 13, 19, and 20. Symbols: S, standard deviation of the sample data in each member; CoV, coefficient of variation of the sample data in each member. Highest mean values are in italics]

Rock components	Salt Wash Member	Recapture Member	Westwater Canyon Member	Brushy Basin Member	Lower part of formation [1]	Upper part of formation [1]	Total [1]
I. Chemical:							
Mean	*14.1*	5.2	3.5	11.9	11.3	5.4	9.7
S	11.75	7.07	5.17	10.20			
CoV	83	136	147	86			
II. Siliceous:							
Mean	*71.8*	71.6	67.3	70.8	71.7	68.1	70.8
S	12.57	10.80	10.05	15.47			
CoV	18	15	15	22			
III. Feldspathic:							
Mean	8.6	14.3	*20.9*	7.6	10.4	17.8	12.0
S	4.26	6.1	9.15	5.09			
CoV	50	43	44	67			
IV. Dark mineral:							
Mean	1.1	*3.7*	2.1	0.4	1.9	1.7	1.9
S	1.32	3.43	3.28	.97			
CoV	120	93	156	242			
V. Volcanic:							
Mean	4.4	5.2	6.2	*9.3*	4.7	6.9	5.3
S	4.60	4.57	4.36	13.38			
CoV	105	88	70	144			

[1] Means weighted according to proportion by volume of total sandstone in formation represented by the individual members (table 1).

components show the lowest average coefficient of variation and are followed in ascending order by feldspathic, volcanic, chemical, and dark mineral components. In general, variation appears to be inversely correlated with proportional amount or percent.

Nonparametrically, the Recapture and Westwater Canyon Members have adjacent ranks for the proportions of chemical, feldspathic, dark mineral and volcanic components; and the Salt Wash and Brushy Basin Members are similarly paired except for volcanic components. In view of the regional distribution of the members, such pairing is interpreted as the effect of geographic differences in composition which are in turn related to the effects of different sources.

Stratigraphic differences in composition are minor, except that the sandstones of the upper part of the Morrison are more feldspathic and tuffaceous than those of the lower part. This difference may be interpreted as evidence of a significantly higher level of tectonic activity in the source areas during deposition of the upper part of the formation.

TEXTURE

Table 23 sumarizes the averages of the statistical measures of the grain-size distributions of sandstone samples from the Morrison Formation. The sandstones of the Brushy Basin Member show the average coarsest mean and median grain sizes, those of the Salt Wash Member show the best average sorting, and those of the Recapture Member show the highest skewness and kurtosis. The averages of grain size and sorting for the upper part of the Morrison as a whole, as well as for the Westwater Canyon and Brushy Basin separately, indicate that sandstone in the upper part of the Morrison is coarser grained and more poorly sorted than sandstone in the lower part. These are stratigraphic differences and are interpreted as the effects of different tectonic environments.

TABLE 23.—*Summary of average statistical measures of the grain-size distributions of sandstones in the Morrison Formation and its parts*

[Data from Cadigan (1967, tables 1–4). Highest average values are in italics]

Member	Median (mm)	Mean	Standard deviation	Skewness	Kurtosis
		Phi notation			
Brushy Basin Member	*0.240*	*2.51*	1.38	1.37	10.85
Westwater Canyon Member	.210	2.57	1.46	1.66	14.14
Recapture Member	.150	2.95	1.29	*1.81*	*17.67*
Salt Wash Member	.165	2.82	*1.11*	1.37	11.99
Upper part of formation [1]	.216	2.56	1.44	1.59	13.38
Lower part of formation [1]	.160	2.86	1.17	1.51	13.78
Whole formation [1]	.175	2.78	1.24	1.53	13.67

[1] Weighted according to proportion by volume of total sandstone in formation (table 1).

The Recapture and Westwater Canyon Members are paired in similarities of skewness and kurtosis values. This is interpreted to be a geographic difference caused possibly by the presence of a "local" source of eolian sand (p. 8); it is also an index of the amount of reworking the sediment has received.

Table 24 summarizes the averages of the statistical measure of the grain-size distributions of the siltstone and claystone samples from the Brushy Basin and Salt Wash Members. The fine sediments of the Brushy Basin are generally finer grained than those of the Salt Wash, but they show approximately the same degree of sorting. Kurtosis falls in the "normal" range for both members; skewness is classified as symmetrical for the Brushy Basin and slightly skewed for the Salt Wash.

TABLE 24.—*Summary of average statistical measures of the grain-size distributions in siltstones and claystones of the Salt Wash and Brushy Basin Members*

[From table 21 and Cadigan (1967, table 9)]

Member	Median (mm)	Mean	Standard deviation	Skewness	Kurtosis
		Phi notation			
Brushy Basin	0.011	7.151	2.37	−0.033	−0.46
Salt Wash	.022	5.93	2.33	.78	.89

RELATIONSHIPS BETWEEN SIZE AND COMPOSITION IN THE LIGHT DETRITAL MINERAL FRACTION

FELDSPAR

A study of relations between size and composition in the light detrital minerals of the Morrison Formation was made to determine the mathematical nature

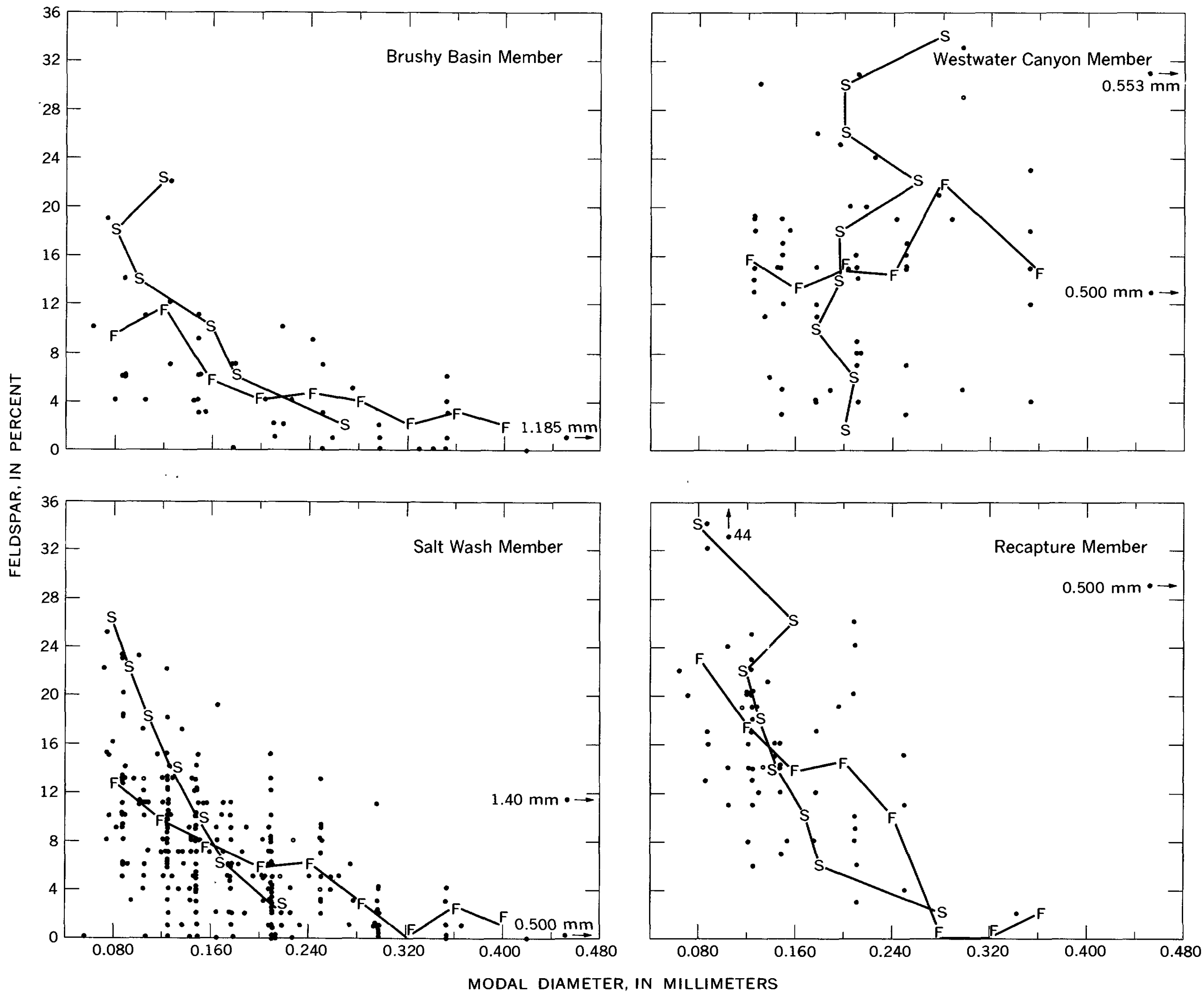

FIGURE 62.—Scatter diagrams of percentage of feldspar grains in disaggregated sandstone samples plotted over the modal grain diameters of the grain-size distributions in samples from the Morrison Formation. F, mean percent feldspar at midpoints of size classes; S, mean size at midpoints of percent feldspar classes. Data from Cadigan (1967).

of the relations, and to see if valid information on the regional variation of the feldspar content of the detrital grains, independent of the known size factors, could be obtained.

Scatter diagrams of percent feldspar grains plotted over grain-size distribution modal diameters for each of the four members are shown in figure 62. Two broken-line graphs have been constructed in each diagram which connect, respectively, correlation points which are the mean values of feldspar in each size class and mean values of modal size in each feldspar percentage class. The nearness to coincidence of the set of graphs in each scatter diagram is an indication of the degree of correlation of the two sets of means, and an indication of the validity of the mathematical relationship. The broken-line graphs for the Brushy Basin, Recapture, and Salt Wash Members descend from left to right, a fact which suggests that the mathematical correlation is negative. The persistent tendency of the graphs to curve suggests that the relationship is curvilinear rather than linear.

Fisher's test (1950, p. 147), as described by Snedecor (1956, p. 461–471), was utilized to determine the best fit of orthogonal polynomials to the correlation points. A curvilinear relationship exists in the Salt Wash Member, and the correlation points were found to best fit a fourth-degree polynomial curve. A test for curvilinear correlation of grouped data described by Davies and Yoder (1941, p. 559, 560) was applied to the mean values in the scattergrams and yielded eta coefficients of

−0.614, −0.562, −0.549, and 0.317 for the Brushy Basin, Salt Wash, Recapture, and Westwater Canyon Members, respectively. The eta coefficients are significant at the $p=0.01$ level for the Brushy Basin and Salt Wash Members, at the $p=0.05$ level for the Recapture Member, and not at the $p=0.05$ level for the Westwater Canyon Member. Thus, in the first three members, coarser grained sandstone samples tend to contain significantly less feldspar than finer grained sandstone. In the Westwater Canyon Member, although the relationship is not mathematically significant, the data suggest that coarser grained sandstone tends to contain more feldspar than finer grained sandstone. This is in accord with the observation that the Westwater Canyon is the most arkosic member and contains pebbles of granite in many localities. The Recapture, to a much lesser extent, also contains arkosic facies, which may account for the lower level of significance of the negative correlation coefficient.

The implication is that orthoquartzitic sandstones tend to show an inverse relation between grain size and feldspar content, whereas arkoses tend to show a direct relation between grain size and feldspar content. Thus, regional variation of feldspar in orthoquartzitic sandstones is, to an unknown extent, dependent upon the regional variation in grain size. In arkoses, the regional variation in grain size apparently has negligible effect on regional variations in detrital feldspar content.

In comparing the detrital feldspar grain data for the orthoquartzitic members of the Morrison Formation, only sample data from samples with approximately the same grain size could be used. Accordingly, for the analysis of regional variation in percent detrital feldspar, samples used were selected from a small range of grain sizes—samples with grain-size distribution modes of 0.160–0.220 mm, inclusive. This range was chosen because, from figure 62, the curvilinear relationship tends to flatten in this size range, and there are an adequate number of samples to be representative. The arkosic Westwater Canyon Member samples from the upper part of the Morrison were all used regardless of grain size because of the indicated lack of significant relation between size and composition of the detrital grains.

Trend-surface analysis of percentages of detrital grains of feldspar in selected samples of lower sandstone of the Morrison based on 45 data points, yielded a computed linear surface (fig. 63*A*) which strikes N. 88° E. and dips northward. The computed surface decreases the total sum of squares by 23.4 percent, evidence of a strong trend of percent detrital feldspar decreasing from south to north. The orientation of the computed trend of detrital percentage diverges from, but is similar to, that of percentage of feldspar determined in thin sections, which strikes N. 41° E. and dips northwestward.

On the linear residual map (fig. 63*B*) highs are present in southeastern and northwestern marginal areas. Two principal source directions are indicated for the feldspar, one south to south-southwest of the center of the region and one west to west-northwest of the center. The northward dip of the trend surface suggests that the southern source exerted the greatest effect on the sediments and therefore was the major source of detrital feldspar during deposition of the lower part of the Morrison Formation.

Trend-surface analysis of percentages of detrital grains of feldspar in selected samples of sandstone from the upper part of the Morrison, based on 27 data points, yielded a computed linear surface (fig. 63*C*) which strikes N. 51° E. and dips northwestward. The computed surface decreases the total sum of squares by 59.2 percent, evidence of a very strong trend of percentage of detrital feldspar decreasing from southeast to northwest. The computed trend of percentage of detrital feldspar is similar to and almost parallel to the trend of percentage of feldspar determined in thin sections, which strikes N. 55° E. and dips northwestward.

The linear residual surface (fig. 63*D*) shows high values in southeastern to southwestern and northwestern marginal areas. The northwestern high is probably the result of hypothetical zero values of the linear surface; the other highs suggest the effects of sources of feldspar, south, southwest, and west of the center of the region. The orientation of the dip of the computed trend surface suggests that the southern source was also the major source of detrital feldspar during deposition of the upper part of the Morrison Formation.

The degree of coincidence of the regional trend of percentage of detrital feldspar grains with the regional trend of percentage of modal feldspar in thin sections suggests that both methods of determining relative feldspar content yield valid and comparable results. Most of all, the coincidence indicates that the trend of regional variation of feldspar is very strong and probably mathematically highly significant.

SILICIFIED-ROCK FRAGMENTS

Study of the possible relation between size and composition in silicified-rock fragments in the members of the Morrison yielded no significant correlations between modal grain size and percentage of silicified-rock fragments. Certain averaged data, however, suggest that throughout the Morrison there is a weak pos-

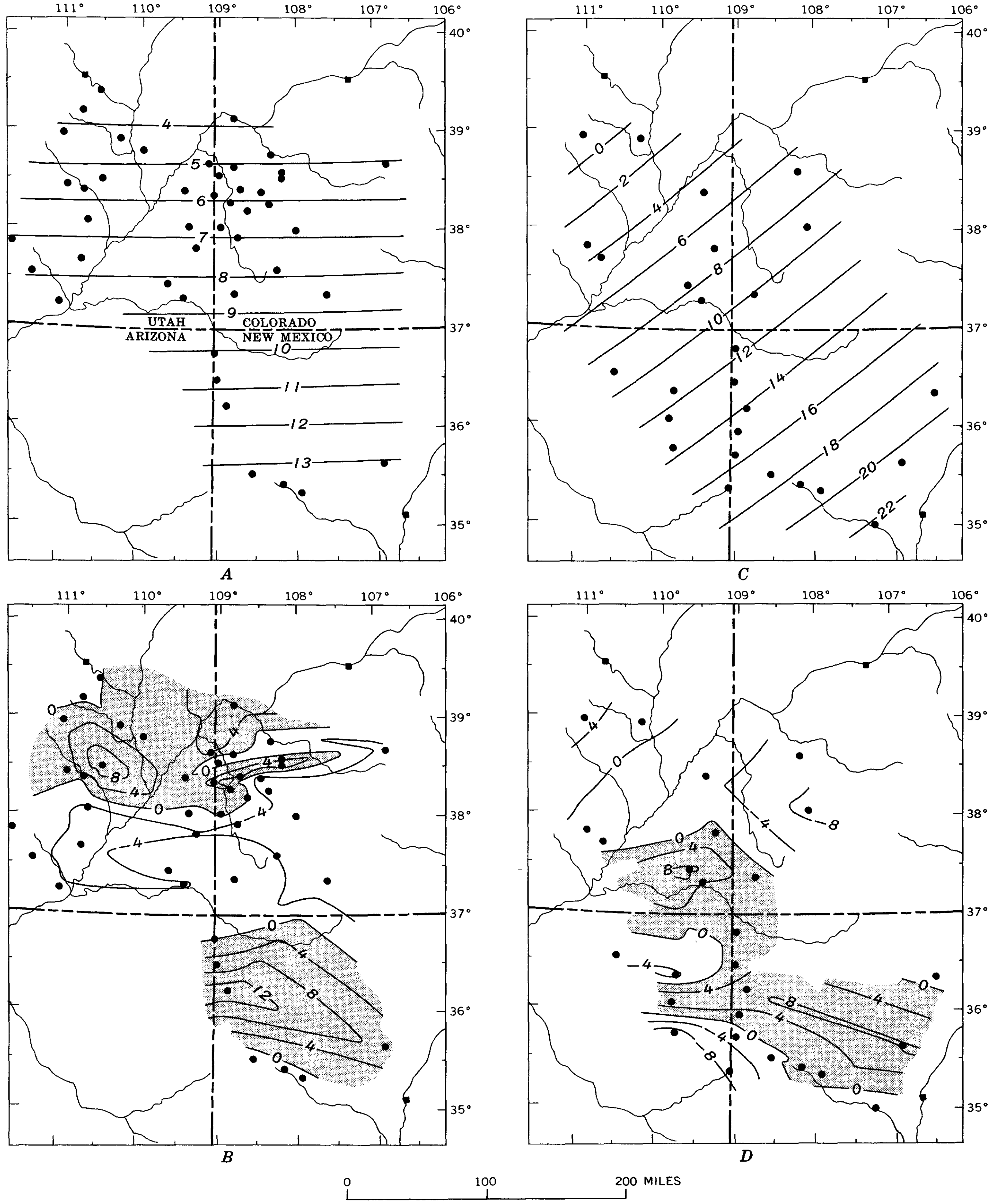

Figure 63.—Trend-surface analysis of detrital feldspar grain data, Morrison Formation. *A*, Linear surface computed from locality data on percentage of detrital feldspar grains, lower part of the Morrison Formation. *B*, Residual surface computed from *A*. *C*, Linear surface computed from locality data on percentage of detrital feldspar, upper part of the Morrison Formation. *D*, Residual surface computed from *C*.

itive relationship—that is, the proportion of silicified-rock fragments tends to increase as the grain size increases. The variation seems to be the effect of a probable major source of silicified-rock fragments west of the region (p. 53, 86), which causes a strong geographic difference in proportions of the fragments. For this reason, sample data offered in table 25 to support the relation between grain size and composition are grouped geographically, samples from the Brushy Basin and Salt Wash members are treated as northwestern samples, and those from the Westwater Canyon and Recapture Members are treated as southeastern samples. Numbers of samples in each percentage class are also given. Note that both groups of samples used have the same average modal grain size, 0.179 mm, but that the northwestern group contains an average of 8.7 percent silicified-rock fragments, compared with 3.4 percent for the southeastern group. Both geographic groups show a rough trend of general increase in average modal grain size with the increase in percent of silicified-rock fragments. Such a positive trend is in accordance with accepted theories that grain size and special mineral concentrations decrease in any direction away from a source.

TABLE 25.—*Percentage of silicified-rock fragments as related to average modal grain-size data in the Morrison Formation*

Percentage classes	Northwestern area—Brushy Basin and Salt Wash Members		Southeastern area—Westwater Canyon and Recapture Members	
	Number of samples	Average modal grain size (mm)	Number of samples	Average modal grain size (mm)
0–1	39	0.148	33	0.150
2–3	61	.131	41	.192
4–5	59	.165	21	.195
6–7	41	.179	13	.174
8–9	33	.205	6	.135
10–11	16	.203	2	.324
12–13	9	.218		
14–15	14	.206		
16–17	8	.217		
18–28			1	.250
29–86	22	.302		
Total	302		117	
Average modal grain size		0.179		0.179
Average percentage of fragments		8.7		3.4

It is concluded from the preceding discussion that no corrections or modifications need be applied to the frequency data from the light mineral grain studies prior to their use to determine the regional variation of percentage of detrital silicified-rock fragments.

Trend analysis of the regional variation in percent of detrital silicified-rock fragments in sandstones of the lower part of the Morrison Formation, based on 68 data points, yields a computed linear surface (fig. 64*A*) which strikes N. 22° E. and dips southeastward. The surface reduces the sum of squares by 22.4 percent, suggesting a strong regional trend with proportions of silicified-rock fragments decreasing from northwest to southeast.

The linear residual surface (fig. 64*B*) shows high values in northwestern marginal areas. High values in eastern marginal areas are the result of negative values in the computed linear surface and have no interpretive significance. Source directions apparently were to the west and west-northwest of the center of the region. This interpretation agrees with the results of the trend analysis of modal thin section data for the lower part of the Morrison. The computed trends for the detrital grain study and the modal data are virtually parallel.

Trend analysis of the regional variation in percent of detrital silicified-rock fragments in sandstones of the upper part of the Morrison Formation, based on 42 data points, yields a computed linear surface (fig. 64*C*) which strikes N. 23° E. and dips southeastward. The surface reduces the sum of squares by 19.6 percent, evidence for a moderately strong trend of decreasing proportions of silicified-rock fragments from northwest to southeast.

The linear residual surface (fig. 64*D*) shows high values in northwestern marginal areas. High values in southwestern marginal areas are the result of negative values in the computed linear surface and have no interpretive significance.

Source directions evidently are to the west and possibly to the west-southwest of the center of the region. The trend supporting this interpretation compares closely with the results of the trend analysis of modal thin section data on the upper part of the Morrison, although the detrital grain data trend has more of an east-west vector than the modal trend. The upper part of the Morrison detrital grain regional trend, however, coincides with the lower part of the Morrison modal data trend (see p. 53 for comparison of trends), and with the lower part of the Morrison detrital grain trend.

The degree of coincidence of the regional trend of percentage of detrital silicified-rock fragments with the regional trends of percentage of modal silicified-rock fragments in thin sections suggests that both methods used to determine relative amounts of silicified-rock fragments yield valid and comparable results. Most of all, the coincidence supports a high probability that the trend of regional variation of silicified-rock fragments is strong and mathematically significant.

HEAVY MINERALS

Table 26 summarizes the data on the proportions of the heavy-mineral groups within the heavy-mineral

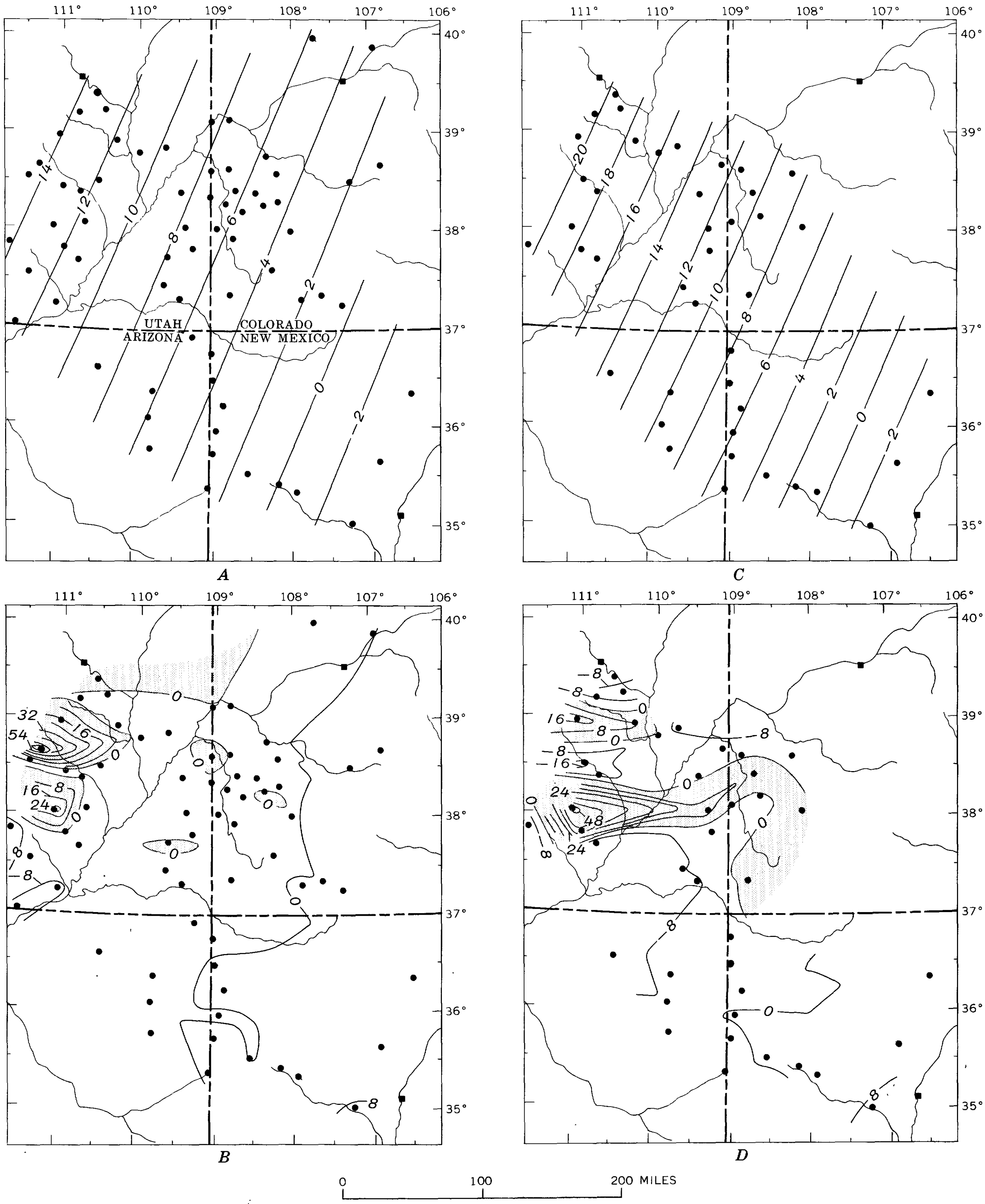

FIGURE 64.—Trend-surface analysis of detrital silicified-rock-fragment data, Morrison Formation. *A*, Linear surface com-
B, Residual surface computed from *A*. *C*, Linear surfafied-rock fragments, lower part of the Morrison Formation.
fied-rock fragments, upper part of the Morrison Formatioce computed from locality data on percentage of detrital silici-
puted from locality data on percentage of detrital silicin. *D*, Residual surface computed from *C*.

TABLE 26.—*Averages of heavy-mineral ratios and percentage of total detrital heavy minerals in 419 sandstone samples from the Morrison Formation*

[Data from Cadigan (1967, tables 5-8). Highest ratio value for each mineral group is in italics. Abbreviations: O, opaques; NO, nonopaques; Z, zircon; T, tourmaline; G, garnet; S, staurolite; R, rutile; A, apatite; E, epidote. Nonopaque minerals are listed in general order of quantitative rank]

Member	Average heavy-mineral ratios									Average percentage of total heavy minerals
	Detrital minerals		Selected nonopaque minerals							
	O	NO	Z	T	G	S	R	A	E	
Brushy Basin	63.2	36.8	60.3	19.8	14.6	2.2	2.7	0.4	0.1	0.32
Westwater Canyon	*72.6*	27.4	59.9	15.2	13.9	*7.7*	1.7	.7	.8	*.47*
Recapture	69.2	30.8	49.8	22.8	*18.7*	5.0	2.1	.2	*1.5*	.44
Salt Wash	53.6	*46.4*	*62.1*	*23.2*	8.5	1.7	*3.6*	*.8*	.1	.23

suites selected for study in the Morrison Formation. The Salt Wash Member has the highest proportions of the nonopaque minerals zircon, tourmaline, rutile, and apatite within the heavy-mineral fraction; the Recapture Member has the highest proportion of garnet and epidote; and the Westwater Canyon has the highest proportion of staurolite and the highest average total percentage of detrital heavy minerals. Some geographic differences are suggested by the rank pairing of the Recapture and Westwater Canyon Members and the Salt Wash and Brushy Basin Members in percentage of detrital heavy minerals, and in proportions of opaque minerals, staurolite, and epidote within the respective heavy-mineral fractions. No stratigraphic differences are evident. The geographic differences are interpreted as the effects of different sources.

TRENDS

The computed linear trend of a geologic variable may or may not have directional significance, depending upon the factors which control it. In regard to mineral composition, where there is a single source direction the trend of decreasing amounts of a derived mineral tends to be directly away from the source direction in the dominant direction of regional drainage; where there are two or more source directions, the trend of decreasing values is a plane which is the resultant of two or more sets of decreasing values; where other factors are involved, such as the effects of differential attrition in heavy-mineral ratios, the interpretation of trends becomes exceedingly complicated. Because of such complications, interpretation of sources is dependent to a large extent on the residual maps.

The trend directions of the same properties for the upper and for the lower parts of the formation, shown in table 27, have a highly significant degree of correlation (r=0.787). The average deviation from the resultant of each pair is 19.4°, compared with the expected average random deviation of 45°. Resultant azimuths from north of trends for the upper and lower parts of the Morrison are 14° and 19.4° respectively. From this we may conclude that a high degree of parallelism existed between the geologic factors which controlled the composition, texture, and structure of the lower part of the Morrison and those which controlled these features in the upper part of the Morrison.

Interpreted from a different viewpoint, the parallelism, despite deficiencies in the data, is strong evidence that the computed trends are not the results of random effects but have mathematical and therefore geologic significance.

TABLE 27.—*Summary of the orientation of dips of the computed linear trend surfaces of compositional and textural properties of principal sandstones in the Morrison Formation*

Variable	Trend azimuth (in degrees from north)		Deviation from resultant	Resultant
	Lower part	Upper part		
Percentage of feldspar (modal)	311	325	7	318
R_1 (p. 49, 78)	56	50	3	53
R_2 (p. 49, 78)	220	207	6.5	213.5
Percentage of tuff (modal)	31	36	2.5	33.5
Percentage of silicified-rock fragments	113	153	20	133
Median grain size	80	0	40	40
Sorting	18	43	11.5	31.5
Skewness	7	3	2	5
Kurtosis	11	3	4	7
Sphericity	135	188	26.5	161.5
Total heavy minerals	316	263	26.5	289.5
Nonopaque heavy minerals	157	98	29.5	127.5
Zircon	236	320	42	278
Tourmaline	97	150	26.5	123.5
Garnet	33	204	85.5	118.5
Staurolite	42	42	0	42
Rutile	284	310	13	297
Apatite	291	331	20	311
Percentage of feldspar grains	358	321	18.5	339.5
Percentage of silicified-rock fragments	112	113	.5	112.5
Resultant of all trend azimuths	19.4	14.0		
Average deviation from the mean azimuth				19.4

The trend azimuths themselves may be interpreted, but only with full consideration of the possible major geologic effects which control them. The overall regional orientation of bedding structures (fig. 25) lies dominantly in the range of azimuths from 15° to 105°. Of the mean azimuths in table 27, the group of trends of statistical measures of the grain-size distributions is most similiar to the bedding structures in orientation. The trends of these measures include mean azimuth orientations ranging from 5° to 40°, and individual azimuths ranging from 3° to 80°. This degree of parallelism suggests that the grain-size distribution properties are the properties of the sedimentary rocks of the Morrison Formation which were most affected by the regional pattern of erosion, transportation, and deposition. Inasmuch as this regional pattern was controlled by the regional tectonic environment, it is reaffirmed that the statistical measures of the grain-size distributions also reflect the tectonic environment.

Those groups of properties shown in table 27 which relate to composition are probably influenced to a greater extent on a regional basis by the effects of multiple sources of varied composition than the particle-size properties are. Typical of these groups are the percentage of feldspar (modal), potassic feldspar–sodic feldspar ratios R_1 and R_2, tuffaceous fragments (modal), and the silicified-rock fragments. The orientations of each of these rock components show very close parallelism in the upper and lower parts of the Morrison. The parallelism suggests persistent, significant trends and is interpreted as evidence of persistent, significant source effects.

The trends of heavy-mineral groups show wide divergence and a large range of deviations between pairs, to the extent that nearly every mineral group must be supposed to be affected by different combinations of geologic factors. For example: staurolite with highly concordant trends (figs. 42, 59) appears to have been present in nearly all sediments coming from the southern to western source directions. It had a relatively high rate of attrition, and the proportion of staurolite decreased almost uniformly in the direction of transport. The result is the absolutely parallel orientation of the trend azimuths for the upper and lower parts of the formation, and a trend orientation almost parallel to that of the modal azimuth orientation (30°–45°) of the formational bedding structures. The great strength of the staurolite linear trends is indicated by reductions of the total sum of squares of 46.5 and 57.5 percent for the lower and upper parts, respectively.

Garnet, on the other hand, shows extreme divergence of trends. Source effects (figs. 42, 59) are strongest in two widely separated areas of the region. Garnet has a high rate of differential attrition. The result of the combination of source and attrition factors is that the proportions decrease in more than one direction, only one of which is a direction of regional transport. The result is two almost oppositely oriented trends for the upper and lower parts, one of which is generally parallel to the modal orientation of the formational bedding structures. The trend generally parallel to the bedding modal orientation has a strength indicated by 26.5 percent reduction of the sum of squares, whereas the one in the opposite direction has a strength indicated by only 2.2 percent reduction of the sum of squares. Probably only the strong trend in the lower part of the Morrison is mathematically significant; the very weak trend for garnet data in the upper part is probably without either geological or mathematical significance. It is noteworthy that the insignificant trend deviates from the strong trend by nearly 180°, which suggests a seesaw effect in which the fulcrum is an axis between the garnet "highs" on the south-southeast and northwest borders of the region. The trend of garnet proportions is, thus, a resultant which for the upper part of the Morrison comes close to being a horizontal plane, owing to multiple compensating trends of source and attrition effects.

CONCLUSIONS

PETROLOGIC SUMMARY

The Morrison Formation of Late Jurassic age present in the Colorado Plateau region consisted, prior to Recent erosion, of approximately 9,200 cubic miles of continental alluvial and paludal sedimentary rock.

The Morrison in the region of study is divided stratigraphically into four members which are, from bottom to top: Salt Wash Member, Recapture Member, Westwater Canyon Member, and Brushy Basin Member. The Salt Wash is present in the northern two-thirds of the region, the Recapture and Westwater Canyon in the southern half of the region, and the Brushy Basin throughout almost the entire region. For regional study the Morrison was divided into a lower part (Salt Wash and Recapture) and an upper part (Westwater Canyon and Brushy Basin). The results of sedimentary-structure orientation study suggest that the sediments making up the formation were transported in a northward to eastward range of directions across the region of study.

The Morrison contains, by volume, 48 percent light-colored grayish, greenish, brownish, and reddish ledge-forming crossbedded irregularly lensing sandstone and conglomeratic strata. It contains 51 percent pale green, red, purple, and variegated claystone, siltstone, and mudstone strata which form relatively short nonresistant concave slopes between sandstone ledges or relatively long resistant convex weathered-bentonite-covered slopes. One percent of the Morrison consists of thin limestones and miscellaneous rocks. Half of the sandstone is in the Salt Wash Member, which composes two-fifths of the formation; 60 percent of the mudstone, claystone, and siltstone is in the Brushy Basin Member, which composes one-third of the formation.

The petrologic study of the Morrison Formation is based on 483 rock samples collected from 96 localities in the Colorado Plateau region.

Thin-section modal analysis established the sandstones as orthoquartzites, arkoses, and sedimentary tuffs. The fine-textured rocks are altered tuffs, or graywacke probably derived from tuffs. The arkoses are concentrated in the southern part of the region in the Recapture and Westwater Canyon Members; sandstones in the Recapture are less arkosic than those in the Westwater Canyon. The Brushy Basin is more tuffaceous than the other members. Chert arenites, considered part of the orthoquartzitic rock types, are concentrated in the northwestern part of the region and in the Salt Wash and Brushy Basin Members.

Rock-forming constituents of the Morrison are detrital grains of the minerals quartz, orthoclase, albite, microcline, rare sanidine, and chert; fragments of silicified rock, silicified limestone, silicified altered potassic and sodic tuff, pumice and felsite, and quartzite and granite; interstitial montmorillonite, kaolinite, mica clay, chlorite clay minerals and their physical and mineral intermixtures; interstitial calcite, optically continuous quartz overgrowths, microcrystalline silica, chalcedony, barite, dolomite, and in the Westwater Canyon Member particularly, interstitial orthoclase overgrowths on orthoclase and albite grains. Also present are the so-called heavy minerals, detrital zircon, tourmaline, garnet, staurolite, rutile, apatite, epidote, spinel, biotite, muscovite, brookite, magnetite, hematite, altered ilmenite and leucoxene, and authigenic anatase, dahlite, epidote and coarsely crystalline pennine(?).

Diagenesis, defined as post-depositional alteration of rock components, has been a determining factor in the present composition and texture of the Morrison Formation. Fine-grained detrital glassy tuff and ash components have been devitrified and silicified, or altered to even finer grained montmorillonite, mica clay, or chlorite clay minerals, or clay mineral mixtures with resulting changes in texture (grain size and sorting) of the rocks. Arkosic rocks contain recrystallized kaolinite which is probably partly detrital and partly diagenetic in origin. The clayey matrix in many rocks has been replaced by interstitial calcite, quartz overgrowths, chalcedony, or barite crystalline cements. Feldspar grains, particularly albite, have been partly or completely replaced by calcite or chlorite. Changes of the greatest magnitude occurred in the tuffaceous strata which are now the thick variegated bentonitic mudstones, claystones, and siltstones of the Brushy Basin Member.

The average grain-size distributions of the sandstones of all four members are fine grained, moderately well sorted, moderately skewed, and highly peaked. Those of the lower part of the formation are slightly finer grained and better sorted than those of the upper part. Fine-textured rocks are technically nearly all siltstones, with claystones forming a very small proportion. The siltstones may be classified as siltstones and mudstones (poorly sorted siltstones). Tuffaceous siltstones of the Brushy Basin Member are, on the average, finer grained and more poorly sorted than siltstones of the underlying Salt Wash Member.

Trend-surface analysis was done separately on data from both the lower and upper parts of the Morrison Formation. Resultant azimuths of dip directions of all composition and textural linear trend surfaces are 19.4° and 14.0° for the lower and upper parts of the formation, respectively. Paired trends for the 20 compositional and textural parameters show a highly significant degree of correlation ($r=0.787$). This evidence is a measure of the close coincidence of both the average and individual results of two independent sets of data which strongly suggests that paleotectonic conditions were similar throughout the deposition of the Morrison and that the computed regional trends are generally significant regardless of effects of localized variations.

SOURCES

Sources of sediment which composes the Morrison Formation lie in directions extending in a clockwise arc from southeast to northwest of the center of the Colorado Plateau region. Evidence of composition of the sources is derived from differences in the mineral composition of rocks which form the southeast to northwest margins of the Morrison Formation. Figure 65 summarizes the mineral component highs and the

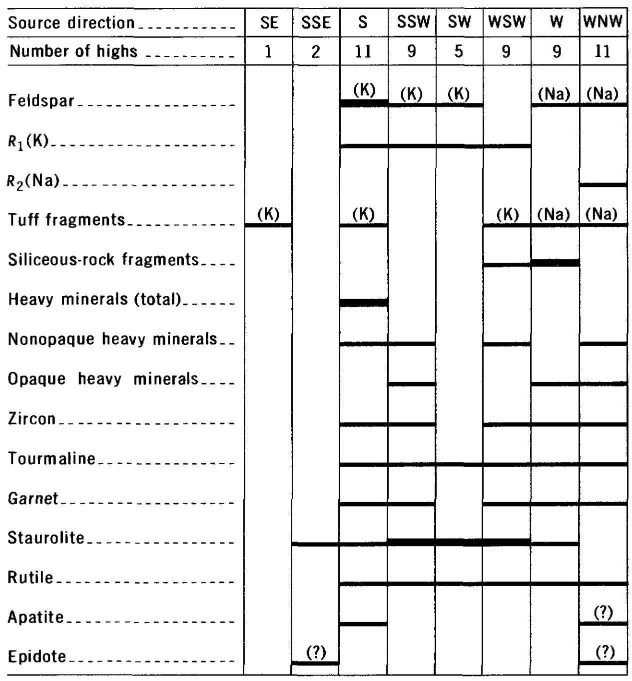

FIGURE 65.—Interpreted specific source directions of mineral groups. Heavy bar indicates major source direction. R_1, ratio of potassic feldspar to sodic feldspar; R_2, ratio of sodic feldspar to potassic feldspar; K, dominantly potassic feldspar; Na, dominantly sodic feldspar; (?), insufficient data.

source directions to which they are interpreted to be related. The actual source areas are unknown in distance, number, or continuity but are interpreted as varying in composition to such an extent that different components predominate in sediments derived from different parts of the source area or areas.

A record in figure 65 indicating that a specific mineral component is derived from a specific direction means that the mineral is present in sediment derived from that direction in relatively large proportions. Thus, for example, feldspar is present in all sediment from all source directions, but it is notably abundant in sediment from the south and at least more abundant than average in sediment from the south-southwest and southwest and from the west and west-northwest. Interpretation of the mean composition of the source terrane is also complicated by the factor of relative abundance. Granite may be present in many parts of the different source areas, but feldspar-rich pebbles and granite pebbles in sediment from the south suggest that the southern source terrane is particularly granitic. Absence of a high ratio of other definitive minerals is interpreted as indicating a highly quartzitic source.

On the basis of relative abundance, with definitive mineral components shown in parentheses, interpretations of composition source terranes which lie in the various compass-point directions (fig. 65) are as follows:

Southeastern terranes: Sedimentary quartzitic rocks and igneous rocks of rhyolitic composition (potassic tuff).

South-southeastern terranes: Sedimentary quartzitic rocks, metaquartzites (staurolite), and altered sodic rhyolitic rocks (epidote).

Southern and south-southwestern terranes: Granitic igneous (potassic feldspar, heavy minerals, nonopaque minerals, zircon, tourmaline, rutile, garnet) and rhyolitic extrusive (tuff, apatite) rocks, metaquartzites (staurolite), and other metamorphic and sedimentary rocks.

Southwestern terranes: Metaquartzites (staurolite), other metamorphic and sedimentary quartzitic rocks, and arkoses or granitic igneous rocks (feldspar).

West-southwestern terranes: Metaquartzites (staurolite), silicified limestone and other sediments (silicified-rock fragments), rhyolitic extrusive (tuff), and sedimentary quartzitic rocks.

Western terrane: Silicified limestone and other sediments (silicified-rock fragments), sodic granitic and rhyolitic igneous rocks (sodic feldspar, sodic tuff, opaque minerals, zircon, tourmaline, garnet), metaquartzites (staurolite) and quartzitic sedimentary rocks.

West-northwestern terrane: Fresh and altered sodic granitic and rhyolitic igneous rocks (sodic feldspar, sodic tuff, nonopaque and opaque minerals, zircon, tourmaline, garnet, epidote, apatite), and sedimentary quartzitic rocks.

The trends of grain-size distribution measures are generally compatible with overall direction of southwest-northeast sediment movement. Grain size decreases, and sorting improves from southwest to northeast. Skewness and kurtosis decrease from south to north; the high values for these measures are suggested as being partly the effects of contributions of sand from the eolian Cow Springs Sandstone along the south margin of the region.

The regional trend of increasing sphericity of sand grains from south-southeast to north-northwest reflects the effects of the major feldspar source south of the region.

The major source effects in Morrison Formation sediments observed and confirmed by trend analysis are the high feldspar content in sandstone in the southeastern part of the region, the high silicified-rock-fragment content in sandstone (and limestone) in the western part of the region, and the high staurolite content in sandstone in the southwestern part of the region. Minor source effects observed and confirmed by trend analysis are the relatively high proportions of sodic feldspar and generally higher total feldspar content in the northwestern and north-central parts of the region, and, the relatively higher proportions of potassic feldspar in the southern part of the region.

TECTONIC IMPLICATIONS

Interpretation or reconstruction of the tectonic environment that caused the erosion, transportation, and deposition of the sediments which make up the Morrison Formation is based on the statistical measures of the particle-size distributions, on the bedding structure orientation data, and to a minor extent on the composition of the sediments. Such reconstruction takes into account diagenetic effects which have reduced the average particle size of what were once relatively coarser tuffaceous muds, and which have also altered the particle-size distributions of nearly all the sediments, particularly those which contained significant amounts of tuffaceous or glassy detritus.

Sediments of the Morrison Formation probably were deposited in degrading alluvial, and aggrading alluvial, alluvial-paludal, and paludal-lacustrine environments. The site was a regionwide flat plain which was subsiding at different rates in different parts of the region. Variation in the aqueous environments was dependent upon the local rate of subsidence. Sediment moved by the regional alluvial system either crossed the region or was trapped and buried as the result of local and regional subsidence.

During intervals of little or no subsidence, aggrading alluvial and degrading alluvial environments were alternately dominant, and the thin strata of sediment accumulated consisted of relatively coarse sands and gravels. During intervals of low average rates of subsidence, an aggrading alluvial environment was dominant, and sediment accumulated more rapidly and consisted of sandstone and associated siltstone strata in thickness proportionate to the amount of local subsidence. During intervals of moderate to high average rates of subsidence, aggrading alluvial-paludal to paludal-lacustrine environments were dominant, sediment accumulated fastest and consisted largely of siltstone, mudstone, and claystone strata with minor sandstone.

Detailed interpretation of tectonic environment from grain-size distribution measures is based on a previous study (Cadigan, 1961, 1962b) and subsequent work which suggests that rates of tectonic uplift in source areas are related positively to the size of detrital particles, and that rates of tectonic subsidence in the areas of deposition (which are also areas of transportation in continental sedimentation) are related negatively to the degree of sorting of detrital particle distributions. The regression curve of the relation of size to sorting is V-shaped (Cadigan, 1961, p. 141).

Average grain size and sorting in sandstones of the Morrison Formation suggest a low to moderate rate of uplift in the source areas and a low to moderate rate of subsidence in areas of deposition. Low to moderate rates of subsidence suggest low to moderate rates of deposition (burial) and much reworking. This is confirmed by the moderate skewness and the high peakedness of grain-size distributions for all members. The low rate of burial is further borne out by the regionwide presence of pebbles in pebbly sandstone and conglomerate strata. These pebbles traveled hundreds of miles across a subsiding plain before being finally trapped and buried, although they must have been deposited temporarily many times.

Observed grain size and sorting in mudstones suggest a very low to low rate of uplift in the source areas, and a high to very high rate of subsidence in the areas of deposition, but these interpretations must be modified because of the effects of diagenetic changes. The breakdown of glassy particles to clay minerals by the processes of diagensis decreased the average particle size and also increased the proportion of clay-sized particles, resulting in a computed lower degree of sorting (higher standard deviation) for the present sediments as compared with the original sediments. Accordingly, the rate of subsidence in the area of deposition is interpreted as moderate to high rather than very high, and the rate of uplift in the source areas is interpreted as moderate to low rather than very low. A lack of reworking is suggested by low to insignificant average skewness and kurtosis values in Salt Wash and Brushy Basin fine-textured samples. The bedding structures of the siltstones, claystones, and mudstones are of the "floodplain" type of Craig and others (1955, p. 141) as compared with the "alluvial" type found in sandstones. The difference is due mainly to difference in rate of burial (and subsidence) and, hence, the availability of the deposits for reworking; the rate of uplift in the source areas is interpreted to be about the same for sandstone and mudstone.

The average poorer sorting and coarser grain size in sandstones of the upper part compared with those of the lower part suggest an increase in the intensity of tectonic activity during Morrison deposition. Greater abundance of feldspar and tuffaceous detritus, both commonly regarded as "tectonic" components, in the sandstones of the upper part of the formation confirms the suggestion. The thick variegated bentonitic mudstone strata of the Brushy Basin Member, derived principally from tuffaceous detritus, constitute 30 percent of the Morrison Formation in the Colorado Plateau region. These thick strata therefore, indicate an exceptional tectonic environment at the time of deposition of the uppermost part of the Morrison Formation in the Colorado Plateau region.

In summary, average grain size and sorting measures indicate that the rate of subsidence in the areas of deposition was lowest during deposition of sand. The rate was, then, generally lowest during deposition of the lower part of the Morrison Formation and highest during deposition of mudstone in the Brushy Basin. Rates of uplift in the source areas were low during deposition of the Salt Wash and Recapture but increased to moderate during deposition of the Westwater Canyon and Brushy Basin.

The complete interpretive picture of the tectonic environment which produced the sediments of the Morrison includes events of both regional and continental significance. As recognized by Emmons, Whitman, and Eldridge (1896, ch. 1), a Jurassic movement resulting in uplift of much of the North American Western Interior area of deposition in middle Late Jurassic brought to an end the tectonically quiescent environment which produced such marine, marginal marine, and continental deposits as constitute the upper part of the San Rafael Group in the Colorado Plateau region (Craig and others, 1955, p. 132–134) and the Sundance Formation in the Rocky Mountains and Great Plains regions. Lee (1915, p. 312) noted that this uplift was accompanied by continued degradation and followed by slow subsidence. Following the uplift, streams scoured and reworked the uppermost beds of the San Rafael Group in parts of the region and thus provided the first continental alluvial sediments of the Morrison Formation. As the Colorado Plateau region again began to subside, an aggrading stream system deposited sediment derived from distant rising source areas to the south, southwest, and west. In southern localities, new sediment was mixed with sediment reworked from still-exposed San Rafael Group strata near the southern border of the region. These exposures were eventually buried by upper sediments of the Morrison.

Uplift of the source areas, accompanied by volcanic activity, continued at a low rate during deposition of the lower part of the Morrison Formation. Rates of subsidence in the area of deposition ranged from low to high. The intervals of slow subsidence produced sequences dominated by moderately well sorted sandstones, and the intervals of rapid subsidence produced sequences dominated by poorly sorted mudstones. Beginning with deposition of the upper part of the Morrison, the rate of uplift in the source areas increased moderately and was accompanied by increased volcanic igneous activity. Initial low rates of subsidence in the area of deposition produced the ledgy sandstones near the base of the upper part of the Morrison; higher rates of subsidence followed and resulted in the regionwide accumulation of the thick stratified tuffaceous muds which form the uppermost sediments of the Morrison Formation in the Colorado Plateau area of deposition. The increased proportions of tuffaceous detritus deposited in and transported across the Colorado Plateau region are present in the sandstones of the Brushy Basin and Westwater Canyon Members as well as in the mudstones.

Source areas for sediments of the Morrison Formation have not been specifically identified, but their general locations have been indicated by Craig and others (1955). The source areas evidently lay in what is now the Basin and Range province of Nevada, Arizona, and New Mexico. Areas in southeastern Arizona and southwestern New Mexico became generally positive in late Paleozoic time and provided sediments to the northeast during the Triassic and Jurassic Periods (Gilluly, 1946, p. 67; 1956, p. 159; Peterson, 1952, p. 125). A low positive area that rose in south-central and southwestern New Mexico during Late Triassic and most of Jurassic time (Kottlowski, 1961), or in Late Jurassic (Kelley, 1955), is a highly probable source. Highlands southwest of the Colorado Plateau region which became tectonically active during the Late Jurassic in areas of the Peninsula Ranges and southern Sierra Nevada of California as described by Crickmay (1931, p. 57) and King (1959, p. 159, fig. 89) were also potential source areas and may have constituted part of the headwaters of the alluvial system that drained through the Colorado Plateau region. The part of the Basin and Range province which occupies what is now east-central and southern Nevada was a shallow marine basin during most of Paleozoic time but became generally positive in late Paleozoic and continued as such with periods of differential subsidence in some areas until the Middle Jurassic according to Nolan (1943, p. 141, 171), Ferguson and Muller (1949), Longwell (1950, p. 423), and Silberling (1959, p. 4). This region very probably contained rising positive areas in Late Jurassic time which contributed sediment to the Morrison Formation.

These paleotectonic relations, together with the petrographic and stratigraphic evidence of the Morrison Formation itself, suggest that the Colorado Plateau part of the subsiding area in which the Morrison Formation was deposited was bordered on the south, southwest, and west by an arc of rising positive highland areas.

The phase of continental tectonic activity which produced the Morrison Formation may have coincided in time with the beginning of the Sierra Nevada orogeny to the west.

LITERATURE CITED

Allen, P., and Krumbein, W. C., 1962, Secondary trend components in the top Ashdown pebble bed—A case history: Jour. Geology, v. 70, no. 5, p. 507–538.

Baker, A. A., Dane, C. H., and Reeside, J. B., Jr., 1936, Correlation of Jurassic formations of parts of Utah, Arizona, New Mexico, and Colorado: U.S. Geol. Survey Prof. Paper 183, 66 p.

Bowers, H. E., and Shawe, D. R., 1961, Heavy minerals as guides to uranium-vanadium ore deposits in the Slick Rock district, Colorado: U.S. Geol. Survey Bull. 1107–B, p. 169–218 [1962].

Brown, Andrew, 1961, Geologic investigations of radioactive deposits, 1942–1960, a bibliography of U.S. Geological Survey publications on the geology of radioactive deposits: U.S. Geol. Survey TEI–777, 86 p., issued by U.S. Atomic Energy Comm. Tech. Inf. Service, Oak Ridge, Tenn.

Cadigan, R. A., 1956, Lithologic studies [Colorado Plateau]: U.S. Geol. Survey TEI–640, p. 178–185, issued by U.S. Atomic Energy Comm. Tech. Inf. Service, Oak Ridge, Tenn.

——— 1959, Sedimentary petrology, *in* Stewart, J. H., and others, Stratigraphy of Triassic and associated formations in part of the Colorado Plateau region: U.S. Geol. Survey Bull. 1046–Q, p. 529–571.

——— 1961, Geologic interpretation of grain-size distribution measurements of Colorado Plateau sedimentary rocks: Jour. Geology, v. 69, no. 2, p. 121–144.

——— 1962a, A method for determining the randomness of regionally distributed quantitative geologic data: Jour. Sed. Petrology, v. 32, no. 4, p. 813–818.

Cadigan, R. A., 1962b, Geologic interpretations of grain-size distribution measurements of Colorado Plateau sedimentary rocks—A reply: Jour. Geology, v. 70, no. 3, p. 376–378.

——— 1967, Tabulated petrologic data from a study of the Morrison Formation in the Colorado Plateau region: U.S. Geol. Survey open-file report, 16 tables.

Cadigan, R. A., and Miesch, A. T., 1958, Lithologic studies [Colorado Plateau]: U.S. Geol. Survey TEI–740, p. 146–158, issued by U.S. Atomic Energy Comm. Tech. Inf. Service, Oak Ridge, Tenn.

Chayes, F. A., 1949, A simple point counter for thin-section analysis: Am. Mineralogist, v. 34, nos. 1, 2, p. 1–11.

——— 1956, Petrographic modal analysis—an elementary statistical appraisal: New York, John Wiley & Sons, 113 p.

——— 1960, On correlation between variables of constant sum: Jour. Geophys. Research, v. 65, no. 12, p. 4185–4193.

Coffin, R. C., 1921, Radium, uranium, and vanadium deposits of southwestern Colorado: Colorado Geol. Survey Bull. 16, 231 p.

Craig, L. C., 1959, Measured sections of the Morrison and adjacent formations: U.S. Geol. Survey open-file report.

Craig, L. C., and others, 1955, Stratigraphy of the Morrison and related formations, Colorado Plateau region, a preliminary report: U.S. Geol. Survey Bull. 1009–E, p. 125–168.

Crickmay, C. H., 1931, Jurassic history of North America, its bearing on the development of continental structure: Am. Philos. Soc. Proc., v. 70, no. 1, p. 15–102.

Cross, C. W., 1894, Description of the Pikes Peak sheet [Colorado]: U.S. Geol. Survey Geol. Atlas, Folio 7.

Dake, C. L., 1919, The horizon of the marine Jurassic of Utah: Jour. Geology, v. 27, no. 8, p. 634–646.

Darton, N. H., 1904, Comparison of the stratigraphy of the Black Hills, Bighorn Mountains, and Rocky Mountain front range: Geol. Soc. America Bull., v. 15, p. 379–448.

Davies, G. R., and Yoder, Dale, 1941, Business statistics: 2d ed., New York, John Wiley & Sons, 616 p.

De Lury, D. B., 1950, Values and integrals of the orthogonal polynominals up to $n=26$: Toronto, Canada, Univ. Toronto Press, 33 p.

Emery, W. B., 1918, The Green River Desert section, Utah: Am. Jour. Sci., 4th ser., v. 46, p. 551–577.

Emmons, S. F., Cross, Whitman, and Eldridge, G. H., 1896, Geology of the Denver Basin in Colorado: U.S. Geol. Survey Mon. 27, 556 p.

Fenneman, N. M., 1931, Physiography of western United States: New York, McGraw-Hill Book Co., 534 p.

Ferguson, H. G., and Muller, S. W., 1949, Structural geology of the Hawthorne and Tonopah quadrangles, Nevada: U.S. Geol. Survey Prof. Paper 216, 55 p. [1950].

Fischer, R. P., 1942, Vanadium deposits of Colorado and Utah, a preliminary report: U.S. Geol. Survey Bull. 936–P, p. 363–394 [1943].

Fisher, R. A., 1950, Statistical methods for research workers, 11th revised ed.: Edinburgh, Scotland, Oliver & Boyd, Ltd., 354 p.

Gabriel, Alton, and Cox, E. P., 1929, A staining method for the quantitative determination of certain rock minerals: Am. Mineralogist, v. 14, no. 8, p. 290–292.

Gilbert, G. K., 1897, Description of the Pueblo quadrangle [Colorado]: U.S. Geol. Survey Geol. Atlas, Folio 36.

——— 1914, The transportation of debris by running water: U.S. Geol. Survey Prof. Paper 86, 263 p.

Gilluly, James, 1946, The Ajo mining district, Arizona: U.S. Geol. Survey Prof. Paper 209, 112 p. [1947].

——— 1956, General geology of central Cochise County, Arizona: U.S. Geol. Survey Prof. Paper 281, 169 p.

Gilluly, James, and Reeside, J. B., Jr., 1928, Sedimentary rocks of the San Rafael Swell and some adjacent areas in eastern Utah: U.S. Geol. Survey Prof. Paper 150–D, p. 61–110.

Gregory, H. E., 1938, The San Juan country, a geographic and geologic reconnaissance of southeastern Utah: U.S. Geol. Survey Prof. Paper 188, 123 p.

Griffiths, J. C., Cochran, J. A., Hutta, J. J., and Steinmetz, Richard, 1956, Petrographical investigations of the Salt Wash sediments—Annual technical report [April 1, 1954–April 1, 1955]: U.S. Atomic Energy Comm. RME–3122, pt. 1, 77 p., pt. 2, 84 p., issued by Tech. Inf. Service, Oak Ridge, Tenn.

Harshbarger, J. W., Repenning, C. A., and Irwin, J. H., 1957, Stratigraphy of the uppermost Triassic and the Jurassic rocks of the Navajo country: U.S. Geol. Survey Prof. Paper 291, 74 p.

Harshbarger, J. W., Repenning, C. A., and Jackson, R. L., 1951, Jurassic stratigraphy of the Navajo country [New Mexico–Arizona], *in* New Mexico Geol. Soc. Guidebook 2d Field Conf., 1951; p. 95–99.

Hess, F. L., 1933, Uranium, vanadium, radium, gold, silver, and molybdenum sedimentary deposits, *in* Ore deposits of the Western states (Lindgren volume): Am. Inst. Mining Metall. Engineers, p. 450–481.

Hewett, D. F., 1917, The origin of bentonite and the geologic range of related materials in Big Horn Basin, Wyoming [abs.]: Washington Acad. Sci. Jour., v. 7, p. 196–198.

Inman, D. L., 1952, Measures for describing the size distribution of sediments: Jour. Sed. Petrology, v. 22, no. 3, p. 125–145.

Keith, M. L., 1939, Selective staining to facilitate Rosiwal analysis: Am. Mineralogist, v. 24, no. 9, p. 561–565.

Keller, W. D., 1958, Glauconitic mica in the Morrison formation in Colorado, *in* Swineford, Ada, ed., Clays and clay minerals: Natl. Research Council Pub. 566, p. 120–128.

——— 1959, Clay minerals in the mudstones of the ore-bearing formations, pt. 9 *of* Garrels, R. M., and Larsen, E. S., 3d, compilers, Geochemistry and mineralogy of the Colorado Plateau uranium ores: U.S. Geol. Survey Prof. Paper 320, p. 113–119.

——— 1962, Clay minerals in the Morrison formation of the Colorado Plateau: U.S. Geol. Survey Bull. 1150, 90 p.

Kelley, V. C., 1955, Regional tectonics of south-central New Mexico, *in* New Mexico Geol. Soc. Guidebook 6th Field Conf., 1955: p. 96–104.

King, P. B., 1959, The evolution of North America: Princeton Univ. Press, 190 p.

Kottlowski, F. E., 1961, Paleozoic and Mesozoic strata of south-central and southwestern New Mexico [abs.]: Southeastern Federation Geol. Socs., 4th Ann. Mtg., Program, 1961.

Krumbein, W. C., 1936, Application of logarithmic moments to size-frequency distributions of sediments: Jour. Sed. Petrology, v. 6, no. 1, p. 35–47.

——— 1941, Measurement and geological significance of shape and roundness of sedimentary particles: Jour. Sed. Petrology, v. 11, no. 2, p. 64–72.

——— 1952, Principles of facies map interpretation: Jour. Sed. Petrology, v. 22, no. 4, p. 200–211.

Krumbein, W. C., 1956, Regional and local components in facies maps: Am. Assoc. Petroleum Geologists Bull., v. 40, no. 9, p. 2163–2194.

——— 1959, Trend surface analysis of contour-type maps with irregular control-point spacing: Jour. Geophys. Research, v. 64, no. 7, p. 823–834.

Krumbein, W. C., and Pettijohn, F. J., 1938, Manual of sedimentary petrography: New York, D. Appleton-Century Co., 549 p.

Krynine, P. D., 1948, The megascopic study and field classification of sedimentary rocks: Jour. Geology, v. 56, no. 2, p. 130–165.

Lee, W. T., 1902, The Morrison shales of southern Colorado and northern New Mexico: Jour. Geology, v. 10, no. 1, p. 36–58.

——— 1915, Reasons for regarding the Morrison an introductory Cretaceous formation: Geol. Soc. America Bull., v. 26, p. 303–314.

——— 1917, Geology of the Raton Mesa and other regions in Colorado and New Mexico: U.S. Geol. Survey Prof. Paper 101, p. 9–221 [1918].

Longwell, C. R., 1950, Tectonic theory viewed from the Basin Ranges: Geol. Soc. America Bull., v. 61, no. 5, p. 413–433.

Lupton, C. T., 1914, Oil and gas near Green River, Grand County, Utah: U.S. Geol. Survey Bull. 541–D, p. 115–133.

McEwen, M. C., Fessenden, F. W., and Rogers, J. J. W., 1959, Texture and composition of some weathered granites and slightly transported arkosic sands [Texas and Colorado]: Jour. Sed. Petrology, v. 29, no. 4, p. 477–492.

McKnight, E. T., 1940, Geology of area between Green and Colorado Rivers, Grand and San Juan Counties, Utah: U.S. Geol. Survey Bull. 908, 147 p. [1941].

Mandelbaum, Hugo, 1963, Statistical and geological implications of trend mapping with nonorthogonal polynomials: Jour. Geophys. Research, v. 68, no. 2, p. 505–519.

Milner, H. B., 1952, Sedimentary petrography—with special reference to petrographic methods of correlation of strata, petroleum technology and other economic applications of geology: 3d ed., London, Thomas Murby & Co., 666 p.

Mook, C. C., 1915, Origin and distribution of the Morrison formation: Geol. Soc. America Bull., v. 26, p. 315–322.

——— 1916, A study of the Morrison formation: New York Acad. Sci. Annals, v. 27, p. 39–191.

National Research Council, 1947, Report of the subcommittee on sediment terminology, Lane, E. W., chm.: Am. Geophys. Union Trans., v. 28, no. 6, p. 936–938.

Newman, W. L., 1962, Distribution of elements in sedimentary rocks of the Colorado Plateau—a preliminary report: U.S. Geol. Survey Bull. 1107–F, p. 337–445.

Nolan, T. B., 1943, The Basin and Range province in Utah, Nevada, and California: U.S. Geol. Survey Prof. Paper 197–D, p. 141–196.

Osborn, H. F., 1915, Close of Jurassic and opening of Cretaceous time in North America: Geol. Soc. America Bull., v. 26, p. 295–302.

Page, H. G., 1955, Phi-millimeter conversion table: Jour. Sed. Petrology, v. 25, no. 4, p. 285–292.

Peterson, N. P., 1952, Structural history of the Globe-Miami district, *in* Arizona Geol. Soc. Guidebook, 1952: p. 123–127.

Pettijohn, F. J., 1949, Sedimentary rocks: New York, Harper & Brothers, 526 p.

Pettijohn, F. J., 1957, Sedimentary rocks: 2d ed., New York, Harper & Bros., 718 p.

Pettijohn, F. J., and Ridge, J. D., 1933, A mineral variation series of beach sands from Cedar Point, Ohio: Jour. Sed. Petrology, v. 3, no. 2, p. 92–94.

Pye, W. D., 1943, Rapid methods of making sedimentational analyses of arenaceous sediments: Jour. Sed. Petrology, v. 13, no. 3, p. 85–104.

Rittenhouse, Gordon, 1943, A visual method of estimating two-dimensional sphericity [abs.]: Jour. Sed. Petrology, v. 13, no. 2, p. 79–81.

Ross, C. S., and Hendricks, S. B., 1945, Minerals of the montmorillonite group, their origin and relation to soils and clays: U.S. Geol. Survey Prof. Paper 205–B, p. 23–79 [1946].

Ross, C. S., and Kerr, P. F., 1931, The kaolin minerals: U.S. Geol. Survey Prof. Paper 165–E, p. 151–176.

Russell, R. D., 1936, The size distribution of minerals in Mississippi River sands: Jour. Sed. Petrology, v. 6, no. 3, p. 125–142.

——— 1937, Mineral composition of Mississippi River sands: Geol. Soc. America Bull., v. 48, no. 9, p. 1307–1348.

Silberling, N. J., 1959, Pre-Tertiary stratigraphy and Upper Triassic paleontology of the Union district, Shoshone Mountains, Nevada: U.S. Geol. Survey Prof. Paper 322, 67 p. [1960].

Snedecor, G. W., 1956, Statistical methods: Iowa State Coll. Press, 534 p.

Stanton, T. W., 1905, The Morrison formation and its relations with the Comanche series and the Dakota formation: Jour. Geology, v. 13, no. 8, p. 657–669.

Stokes, W. L., 1944, Morrison formation and related deposits in and adjacent to the Colorado Plateau: Geol. Soc. America Bull., v. 55, no. 8, p. 951–992.

Stokes, W. L., and Phoenix, D. A., 1948, Geology of the Egnar-Gypsum valley area, San Miguel and Montrose Counties, Colorado: U.S. Geol. Survey Oil and Gas Inv. Prelim. Map 93.

Sujkowski, Z. L., 1958, Diagenesis: Am. Assoc. Petroleum Geologists Bull., v. 42, no. 11, p. 2692–2717.

Udden, J. A., 1914, Mechanical composition of clastic sediments: Geol. Soc. America Bull., v. 25, p. 655–744.

Wadell, H. A., 1932, Volume, shape, and roundness of rock particles: Jour. Geology, v. 40, no. 5, p. 443–451.

——— 1934, Some new sedimentation formulas: Physics, v. 5, no. 10, p. 281–291.

——— 1935, Volume, shape, and roundness of quartz particles: Jour. Geology, v. 43, no. 3, p. 250–280.

Waters, A. C., and Granger, H. C., 1953, Volcanic debris in uraniferous sandstones, and its possible bearing on the origin and precipitation of uranium [Colorado Plateau]: U.S. Geol. Survey Circ. 224, 26 p.

Weeks, A. D., 1953, Mineralogic study of some Jurassic and Cretaceous claystones and siltstones from western Colorado and eastern Utah: U.S. Geol. Survey TEI–285, 22 p., issued by U.S. Atomic Energy Comm. Tech. Inf. Service, Oak Ridge, Tenn.

Wentworth, C. K., 1922, A scale of grade and class terms for clastic sediments: Jour. Geology, v. 30, no. 5, p. 377–392.

Whitten, E. H. T., 1959, Composition trends in a granite; modal variation and ghost stratigraphy in part of the Donegal granite, Eire: Jour. Geophys. Research, v. 64, no. 7, p. 835–848.

INDEX

[Italic page numbers indicate major references]

U. S. GOVERNMENT PRINTING OFFICE : 1967 O - 232-378